PHYSIOLOGICALLY BASED PHARMACOKINETIC MODELLING OF ANTIMALARIAL AGENTS

OLUSOLA OMOLOLA OLAFUYI

Doctor of Philosophy

ASTON UNIVERSITY

June 2019

THESIS SUMMARY

The usefulness of physiologically based pharmacokinetic (PBPK) modelling in antimalarial drug research is evolving. Antimalarial agents are subject to drug-drug interactions (DDIs) and the resultant pharmacokinetics in special population groups is not well understood. To optimise antimalarial dosing in special population groups, the application of PBPK modelling has significant advantages towards improving clinical efficacy. This thesis addresses some of the drug therapy issues associated with antimalarial treatment in special populations using PBPK modelling. Firstly, it addresses the problem of the impact of DDI interaction between artemether and lumefantrine and rifampicin based anti-tuberculosis agent in children, then the effect of DDI perpetrated by efavirenz and ritonavir on the pharmacokinetics of piperaquine during pregnancy was evaluated. Finally, PBPK modelling was used to optimise the dose of chloroquine for the treatment of ZIKV disease during pregnancy.

The fixed dosed combination of artemether and lumefantrine (AL) is widely used for the treatment of malaria in adults and children in sub-Sahara Africa, with lumefantrine day 7 concentrations being widely used as a marker for clinical efficacy. Both are substrates for CYP3A4 and susceptible to drug-drug interactions (DDIs) but the knowledge of the impact of DDIs is currently sparse in paediatric population groups therefore complicating the treatment of malaria in patients co-infected with other infectious diseases like tuberculosis. The concomitant treatment of AL with tuberculosis chemotherapy, which includes the CYP3A4 inducer rifampicin, increases the risk of parasite recrudescence and malaria treatment failure. This study developed a population-based PBPK model for AL in adults capable of predicting the pharmacokinetics of AL under non-DDI and DDI conditions, as well as predicting AL pharmacokinetics in paediatrics of 2–12 years of age. The validated model was utilised to assess the concomitant treatment of rifampicin and lumefantrine under standard body-weight based treatment regimens for 2–5 year olds, and demonstrated that no subjects attained the target day 7 concentration (C_{d7}) of 280 ng/mL, highlighting the importance of this DDI and the potential risk of malaria-TB based DDIs. An adapted 7-day treatment regimen was simulated and resulted in 63% and 74.5% of subjects attaining the target C_{d7} for 1-tablet and 2-tablet regimens respectively.

Antimalarial therapy during pregnancy poses important safety concerns due to potential teratogenicity and the impact of maternal physiological and biochemical changes during gestation. Piperaquine (PQ) has gained interest for use in pregnancy in response to increasing resistance towards sulfadoxine–pyrimethamine in sub-Saharan Africa. Coinfection with HIV is common in many developing countries; however, little is known about the impact of antiretroviral (ARV) mediated drug–drug interaction (DDI) on piperaquine pharmacokinetics during pregnancy. This study applied mechanistic pharmacokinetic modelling to predict pharmacokinetics in non-pregnant and pregnant patients, which was validated in distinct customised population groups from Thailand, Sudan and Papua New Guinea. In each population group, no significant differences in day 7 concentrations were observed during different gestational weeks (GW) (weeks 10–40), supporting the notion that piperaquine is safe throughout pregnancy with consistent pharmacokinetics, although

possible teratogenicity may limit this. Antiretroviral-mediated DDIs (efavirenz and ritonavir) had moderate effects on piperaquine during different gestational weeks with a predicted AUC_{ratio} in the range 0.56–0.8 and 1.64–1.79 for efavirenz and ritonavir, respectively, over GW 10–40, with a reduction in circulating human serum albumin significantly reducing the number of subjects attaining the day 7 (post-dose) therapeutic efficacy concentrations under both efavirenz and ritonavir DDIs. This present model successfully mechanistically predicted the pharmacokinetics of piperaquine in pregnancy to be unchanged with respect to non-pregnant women, in the light of factors such as malaria/HIV co-infection. However, antiretroviral-mediated DDIs could significantly alter piperaquine pharmacokinetics. Further model refinement will include collation of relevant physiological and biochemical alterations common to HIV/malaria patients.

The treatment of tropical diseases is often faced with the problem of appropriate drug therapy. While researchers work to isolate new molecules that might be used to treat them, the benefits of using PBPK modelling for repurposing molecules with potentially efficacious and safe profiles against these diseases is yet to be explored. The insidious nature of Zika virus (ZIKV) infections can have a devastating consequence for foetal development. Recent reports have highlighted that chloroquine (CQ) is capable of inhibiting ZIKV endocytosis in brain cells. We applied pharmacokinetic modelling to develop a predictive model for CQ exposure to identify an optimal maternal/foetal dosing regimen to prevent ZIKV endocytosis in brain cells. Model validation used 13 non-pregnancy and 3 pregnancy clinical studies, and a therapeutic CQ plasma window of 0.3-2 μM was derived. Dosing regimens used in rheumatoid arthritis, systemic lupus erythematosus, and malaria were assessed for their ability to target this window. Dosing regimen identified that weekly doses used in malaria were not sufficient to reach the lower therapeutic window, however daily doses of 150 mg achieved this therapeutic window. The impact of gestational age was further assessed and culminated in a final proposed regimen of 600 mg on day 1, 300 mg on day 2 and 3, and 150 mg thereafter until the end of trimester 2, which resulted in maintaining 65% and 94% of subjects with a trough plasma concentration above the lower therapeutic window on day 6 and at term, respectively.

This thesis demonstrates that PBPK modelling may be used to optimise drug treatment in special population groups and in the case of complex drug therapy problems.

ACKNOWLEGDEMENTS

I would like to give my utmost praise to my Lord and my God Almighty for the grace to start and finish my PhD programme.

My deepest appreciation goes to my supervisor Dr. Raj K. S. Badhan for your tireless efforts and guidance throughout these years. You have all the element of an excellent supervisor and teacher and I salute you for every effort you have put into ensuring that my PhD programme was successful.

To my associate supervisor, Professor Mike Coleman thank you for your advice and inputs you made towards my successful completion of my PhD degree.

Thank you so much my husband, Olasunkanmi Samuel Olafuyi for always being there to encourage, support, advice and pray with me through both the easy and though times in these past years. You are absolutely the best! and I love you dearly. To my son and daughter, Mofeyifoluwa John Olafuyi and Moboluwarin Deborah Olafuyi, I want to thank you both for your patience through this period. I love you both so much.

To both my parents, I am proud to be your daughter. I appreciate all your words of encouragement and prayers when things were tough. And to my siblings who were always there to encourage me in every way they could, I am sincerely grateful to you for all you did to support me. I love you all.

To my mentors, John and Jane Ogar, I am grateful for all the moral support, prayers and encouragement that you gave me throughout this period of study. Thank you so much.

TABLE OF CONTENTS

LIST OF ABBREVIATIONS

AA	Artesunate-amodiaquine
AAG	Alpha 1-acid glycoprotein
ABC	ATP-binding cassette
ACT	Artemisinin combination therapy
ADAM	Advanced dissolution, absorption and metabolism
ADH	Alcohol dehydrogenase
ADME	Absorption, distribution, metabolism and elimination
ADR	Antimalarial drug resistance
AKR	Aldo-keto reductase
AL	Artemether/lumefantrine
ALDH	Aldehyde dehydrogenase
AMT	Antimalaria treatment
ANOVA	Analysis of variance
API	Active Pharmaceutical Ingredient
ART	Artemether
ARV	Antiretrovirals
AST	Artesunate
ATP	Adenosine triphosphate
AUC	Area under the concentration time profile curve
AUMC	Area under the moment curve
BOV	Between occasion variability
BSA	Basal surface area
BSV	Between subject variability
C	Concentration
CDC	Centers for Disease Control and Prevention
CL	Clearance
CL_b	Blood clearance
CL_h	Hepatic clearance

CL_{int}	Intrinsic clearance
CL_{iv}	Systemic clearance following intravenous drug administration
CL_{other}	Clearance through other routes
CL_p	Plasma clearance
Cl_{po}	Systemic clearance following oral drug administration
CL_T	Total clearance
C_{max}	Maximum concentration
CQ	Chloroquine
Cs	Solubility concentration
CYP	Cytochrome P450
DDI	Drug-drug interaction
DHA	Dihydroartemisinin
DHA-PQ	Dihydroartemisinin- piperaquine
DP	Dihydroartemisinin- piperaquine
EC_{50}	Concentration of a drug that gives half-maximal response
ECW	Extracellular water
EFV	Efavirenz
ER	Extraction ratio
F	Bioavailability
Fa	Fraction of dose absorbed
FDA	Food and Drug Administration
FDC	Fixed dose combination
F_g	Fraction of dose escaping gut metabolism
F_{gut}	Fraction of dose escaping gut metabolism
FIH	First in human
F_{max}	Maximum bioavailability
Fu	Fraction of unbound drug
$F_{u,mic}$	Fraction of unbound drug in microsomal incubation

GFR	Glomerular filtration rate
GIT	Gastrointestinal tract
GST	Glutathione S-transferase
GW	Gestational week
HAS	Human serum albumin
HBA	Hydrogen bond acceptor
HBD	Hydrogen bond donor
hBMEC	Human brain microvascular endothelial cells
HIV	Human immunodeficiency viruses
HIV/AIDs	Human immunodeficiency virus/acquired immune deficiency syndrome
hNSC	Human neural stem cells
ICH	International conference on harmonisation
ICW	Intracellular water
IgG	Immunoglobulin G
IPT	Intermittent preventive treatment
IPTp	Intermittent preventive treatment in pregnancy
IRS	Indoor Residual Spraying
ISEF	Inter System Extrapolation Factor
ITN	Insecticide-treated nets
IV	Intravenous
IVIVE	In vitro - in vivo extrapolation
J	Flux
K	Elimination rate constant
Ka	Absorption rate constant
Km	Michaelis-Menten constant
Kp	Tissue plasma partitioning coefficient
LPV/r	Lopinavir/ritonavir
MDCK-II	Madin-Darby Canine Kidney
MDR	Multidrug resistance
Mech KiM	Mechanistic kidney model

MRP	Multidrug resistance-associated protein
MRT	Mean residence time
MW	Molecular weight
NAD(P)H	Nicotinamide adenine dinucleotide phosphate
NATs	N-Acetyl transferases
NCA	Non compartmental analysis
NLME	Non-linear mixed effect
NPC	Neural progenitor cells
OAT	Organic anion transporter
OCT	Organic cationic transporter
OCTN	Organic cationic transporter
PAHO	Pan American Health Organisation
Papp	Apparent permeability
PBPK	Physiologically based pharmacokinetic modelling
PCR	Parasite clearance rate
P_{eff}	Effective permeability
P-gp	P-glycoprotein
PK	Pharmacokinetics
pKa	Dissociation rate constant
PNG	Papua New Guinea
Po:w	Octanol to water partitioning
popPK	Population pharmacokinetics
PQ	Piperaquine
PQP	Piperaquine phosphate
PSA	Polar surface area
Q	Blood flow
Qh	Hepatic blood flow
RA	Rheumatoid arthritis
RDT	Rapid Diagnostic Tests
rhCYP	Recombinant cytochrome P450

RNA	Ribonucleic acid
RTV	Ritonavir
SAC	Single adjustment compartment
SLC	Solute carrier
SLE	Systemic lupus erythematosus
SP	Sulphadoxine/pyrimethamine
SP-IPTp	Sulphadoxine/pyrimethamine- Intermittent preventive treatment in pregnancy
SULTS	Sulfotransferases
T	Time
$t_{1/2}$	Half life
TB	Tuberculosis
t_{max}	Time to reach maximum concentration
UGT	Uridine 5'-diphospho-glucuronosyltransferase
US	United States of America
V	Volume of distribution
V_c	Volume of central compartment
V_{max}	Maximum velocity of reaction
VPC	Visual predictive check
V_{ss}	Steady state volume of distribution
V_T	Tissue volume
WHO	World Health Organisation
ZIKV	Zika virus disease

LIST OF FIGURES

LIST OF TABLES

LIST OF PUBLICATIONS

Peer reviewed published articles:

1. Olusola Olafuyi, Raj K.S Badhan. Dose Optimization of Chloroquine by Pharmacokinetic Modeling during Pregnancy for the Treatment of Zika Virus Infection. **Journal of Pharmaceutical Sciences**. 2019;108 (1):661-673
2. Badhan R, Zakaria Z, Olafuyi O. The repurposing of ivermectin for malaria: a prospective pharmacokinetics-based virtual clinical trials assessment of dosing regimen options. **Journal of Pharmaceutical Sciences**. 2018;107(8):2236-2250.
3. Olusola Olafuyi, Michael Coleman, Raj K.S. Badhan. The application of physiologically based pharmacokinetic modelling to assess the impact of antiretroviral-mediated drug–drug interactions on piperaquine antimalarial therapy during pregnancy. **Biopharmaceutics and drug disposition**. Volume 38, Issue 8 November 2017; Pages 464-478.
4. Olusola Olafuyi, Michael Coleman, Raj K.S.Badhan. Development of a paediatric physiologically based pharmacokinetic model to assess the impact of drug-drug interactions in tuberculosis co-infected malaria subjects: A case study with artemether-lumefantrine and the CYP3A4-inducer rifampicin. **European Journal of Pharmaceutical Sciences**. Volume 106, 30 August 2017, Pages 20-33.

Conference Proceedings:

1. Olusola Olafuyi, Michael Coleman, Raj K.S.Badhan. 2016. A population physiological based pharmacokinetic study of drug-drug interactions for orally dosed artemether and lumefantrine in paediatrics. LHS PG Research day, Aston University, Birmingham, UK.
2. Olusola Olafuyi, Michael Coleman, Raj K.S.Badhan. 2016. A population physiological based pharmacokinetic study of drug-drug interactions for orally dosed artemether and lumefantrine in paediatrics. MathSys Summer School, University of Warwick, UK.

3. Olusola Olafuyi, Michael Coleman, Raj K.S.Badhan , 2016. The use of modelling and simulation to assess the risk of drug-drug interactions in paediatrics: Antimalarial treatment in pediatrics. 7th APS International PharmSci Conference, University of Strathclyde, Glasgow, UK. (Oral presentation)
4. Olusola Olafuyi, Michael Coleman, Raj K.S.Badhan , 2016. The use of modelling and simulation to assess the risk of drug – drug interactions associated with antimalarial treatments in paediatrics. PKUK Conference, London UK.
5. Olusola Olafuyi, Michael Coleman, Raj K.S.Badhan, 2017. Assessing Drug–drug Interactions Associated with Antimalarial Treatment in Paediatrics Co-infected with Tuberculosis: A PBPK Case Study with Lumefantrine and Rifampicin. 26th PAGE Meeting, Budapest, Hungary.
6. Olusola Olafuyi, Michael Coleman, Raj K.S.Badhan, 2017. Predicting drug-drug interactions of antimalarials in children with tuberculosis co-infected with malaria: a case study with artemether-lumefantrine. LHS PG Research day, Aston University, Birmingham, UK.
7. Olusola Olafuyi, Michael Coleman, Raj K.S.Badhan, 2017. PBPK modelling as a useful tool in studying piperaquine pharmacokinetics in pregnant women PKUK Conference, Great Malvern, UK (Oral presentation).
8. Olusola Olafuyi, Michael Coleman, Raj K.S.Badhan, 2018. Malaria treatments in special populations – the role of population PBPK modelling Certara (Simcyp®) virtual Seminar, 2018. (Webinar presentation).

CHAPTER 1
Introduction

1.1 Malaria and its prevalence

Malaria is a deadly parasitic disease spread by the female anopheles mosquitoes infected with *Plasmodium falciparum* (1, 2). Derived from the Italian word "mal' aria" meaning bad "air", the disease might have been in existence as far back as 1550 B.C. The World Health Organisation's (WHO) target to eliminate malaria in 35 countries by 2030 has led to several measures being taken over the past few decades directed towards malaria prevention and treatment in order to reduce its prevalence and mortality rate (2). The transmission of malaria is extensive, affecting over 219 million people across 90 countries in 2017 (2, 3). The sub-Saharan Africa region carries 80% of the global malaria burden as 90% of the malaria cases reported in this period were in this region, while in the South-East Asia and Eastern Mediterranean region, 7% and 2% of the overall cases respectively were reported. Between 2010 and 2017, the World Health Organisation (WHO) reported a 20% reduction in malaria cases in sub-Saharan Africa compared to South East Asia and the Americas, who recorded a 48% and 22% reduction in malaria related cases respectively. In 2017, 435,000 cases of malaria reported resulted in death, with 91% of the malaria deaths occurring in sub-Saharan Africa. Children younger than 5 years of age are one of the most vulnerable to the disease. In 2015, they accounted for about 70% of all reported malaria deaths (2).

1.1.1 Life cycle of the malaria parasite

The life cycle of the malaria parasite is summarised in Figure 1.1. An infected female anopheles mosquito injects the sporozoite of a *P. falciparum* parasite through a bite on its human host, the sporozoites migrates to the liver to undergo its exoerythrocytic part of its life cycle also known as the exoerythrocytic schizogony. There it matures into schizonts. A fully mature schizont then ruptures to release merozoites. While some parasites are asexually replicated, the others undergo sexual replication. The asexually replicated parasites become trophozoites while the sexually replicated parasites become the gametocytes. The trophozoites and gametocytes are taken up by the red blood cells to begin their erythrocytic stage of their lifecycle called erythrocytic schizogony. The trophozoites mature schizonts again, release merozoites and then become trophozoites to keep the cycle going while the gametocytes are ingested during a mosquito bite to continue their life cycle in the

mosquito host. The erythrocytic schizogony stage of the *P. falciparum* life cycle is said to be responsible for the clinical signs associated with malaria. In the mosquito host, the ingested gametocytes become macrogametocytes, then become exflagellated microgametocytes, they transform into ookinetes and rupture into oocysts which then release the sporozoites that may be injected again into human to continue the life cycle (4).

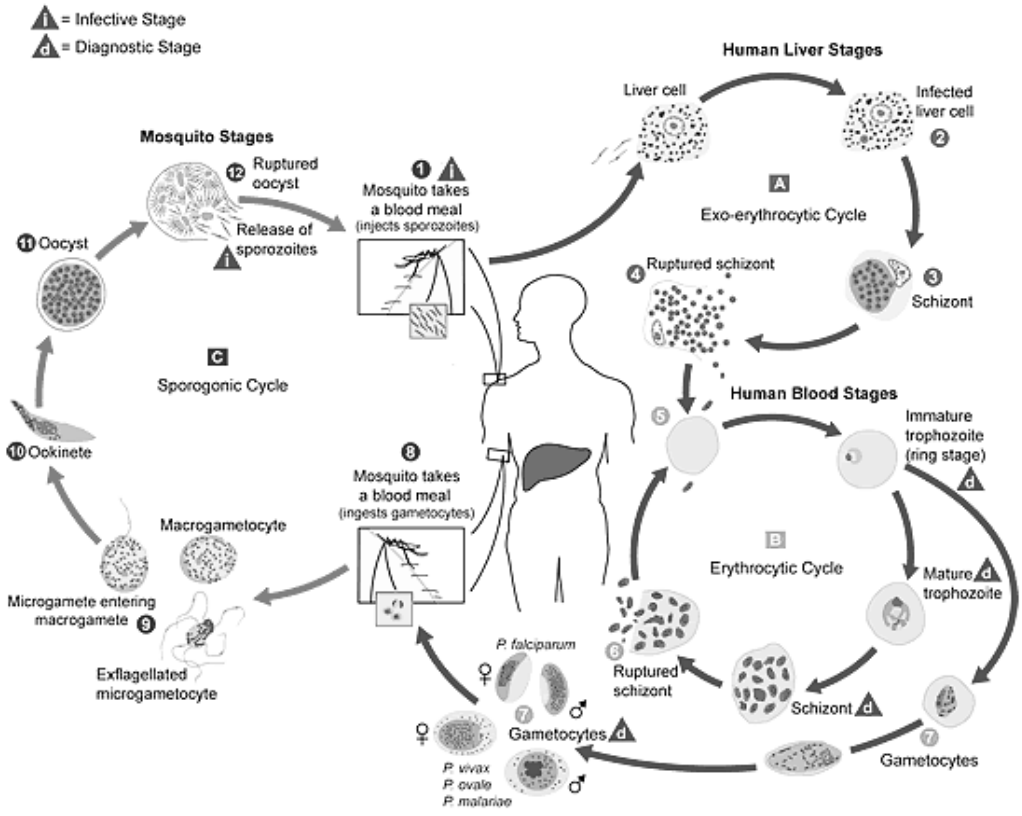

Figure 1.1: Lifecycle of the malaria parasite.

(Adapted from https://www.cdc.gov/malaria/about/biology/index.html) (4)

1.1.2 Malaria symptoms and development of immunity

The incubation period of *Plasmodium* parasite, that is, the time from infection until the time of onset of symptoms, depends on species of plasmodium parasite, immunity status of individual, use of pharmacological preventive methods and the density of parasite innocula. Incubation can vary from about one week to a month, though *P. falciparum* has the shortest incubation period of about 10 days. Malaria infection can be uncomplicated or severe. Typically, symptoms of malaria vary from one individual to the other. Some symptoms include febrile events which may be associated with sweating, chills, and rigours. More generally, malaria infection presents as pyrexia, body ache, headache, joint ache and general weakness. Clinically, complicated malarial infection can result in severe anaemia and end-organ damage affecting the kidney, liver, brain and lung leading to life threatening conditions.

Immunity against malaria may have both mortality and morbidity implications. Immunity may occur as a result of human exposure to the parasite after a few occasions and this is thought to decrease the likelihood of death resulting from an infection. Also, immunity may result from more frequent exposures to the parasite, which may lead to reduced susceptibility to the clinical manifestation of the disease (5-7). In acquired immunity, the human may be protected against the sporocytes and their maturation in the liver and, therefore, this protects the human from an infection in the first place. This type of immunity may result from prolonged exposure to the transmitted parasite but may not be noticed at the early or later stages of exposure to the parasite. Furthermore, a non-protective form of immunity occurs when an individual spontaneously produces antibodies after the expression of a gametocyte and becomes immune against the gametocytes, the form of the parasite that is ingested by the anopheles mosquito during a blood meal (8-10). The body requires immunity against the asexual form of parasite life cycle; that is, the trophozoites in order to stay protected from future infections. The process involved in the body's development of immunity against this form is intricate as there is evidence to suggest that the body needs to defend itself against each strain of malarial parasite it is exposed to (7, 9). The consequences of not attaining sufficient immunity is more severe in the very young children due to underdeveloped processes involved in building their immunity, so children are more susceptible to the life-threatening

conditions of malaria, such as severe anaemia and cerebral malaria (7, 11, 12). Another important population to consider are the pregnant women. Although this cohort may have well developed immunity against malaria prior to pregnancy, gestation may suppress their immunity and therefore expose them and their unborn child to threatening conditions such as still births, miscarriages, low birth weight and infant mortality (7).

1.1.3 Malaria parasites

There are five species the *Plasmodium* parasite known to cause malaria infection in humans. These are *P. falciparum, P. vivax, P. ovale, P. malariae, P. knowlesi*. Of these, *P. falciparum* is known to cause the highest incidence of malaria cases in sub-Saharan Africa accounting for 99% of all reported malaria cases in this region and results in the majority of deaths globally (2). *P. vivax* is prevalent in the Americas accounting for 64% of all malaria cases in that region while in South-East Asia, the malaria incidences resulting from *P. vivax* account for over 30% of cases and 40% of cases in the Eastern Mediterranean regions.

1.1.4 Malaria prevention and management

Interventions to curb the spread and consequences of malaria infections have been widely studied and may be preventive or curative. These range from non-pharmacological methods such as the use of diagnostic testing, vector control measures such as insecticide treated nets (ITN) and indoor residual sprays (IRS) to pharmacological methods involving intermittent preventive treatments (IPT) and the use of effective antimalarial treatments (13-16). Both non-pharmacological and pharmacological approaches have drawn global attention in recent years as these have shown different degrees of effectiveness towards the overall goal to eradicate malaria (17).

1.1.4.1 Non-pharmacological methods of combating malaria

ITN is a vector control method of controlling malaria infection and a few studies have been carried out to ascertain the effectiveness of this approach in the fight against malaria. A study carried out among residents of a malaria endemic region in Senegal between 2010 and 2011, found that the use of long-lasting ITN

provided a significant level of protection against malaria infection (18). Another study conducted in Lake Victoria, Kenya found that there was reduced malaria burden in school children who used long-lasting ITN (19). However, a study carried out among under five-year olds in Nigeria identified that despite having ITN in their possession, there was no significant decline the incidence of malaria parasite burden among them. They acknowledged that despite the known effectiveness of ITN, the majority of their study population did not utilise the ITN in their possession, this was attributed to poor public health education (20).

Rapid diagnostic treatments (RDT) have the potential to reduce the use of antimalarial drug therapy. Yukich *et al* (2012) (21) showed that malaria management after implementation of RDT in Zambia was lower than before its implementation and suggested that RDT contributed toward justifying a need for antimalarial therapy in Zambia. Furthermore, Murray *et al* (2008) (22) reported the effectiveness of RDT across different healthcare facilities.

Indoor residual sprays are another vector control method. They have been found to effectively reduce the incidence of mosquito bites. In one study, it was argued that their ability to reduce incidence of mosquito bites does not imply its effectiveness in reducing malaria prevalence (23). In other studies, IRS used in combinations of one or more preventive measures reduces the prevalence of malaria (24).

1.1.4.2 Pharmacological methods of combatting malaria

1.1.4.2.1 Intermittent preventive treatment

Intermittent preventive treatment (IPT) is the recurrent use of pharmacological antimalarial agents to prevent malaria. The use of IPT has been suggested in certain populations such as pregnant women and children (25). Used in combination with ITN, sulphadoxine and pyrimethamine (SP) is the first choice IPT choice by the WHO to be used in pregnant women in the high transmission areas in sub-Saharan Africa (26).

Concerns have grown about the effectiveness of SP because of the issue of antimalarial resistance. Harrington *et al* (2016) (27) argued that resistant strains developed from SP use may put pregnant women and their infants at a risk of malaria infection and suggested a newer approach to malaria prevention, however, Gutman *et al* (2016) maintained that SP is efficacious for malaria prevention in pregnant women in most parts of Africa (28). A recent study suggests the use of dihydroarteminisin-piperaquine (DP) may be a suitable alternative to this in pregnancy (29). The beneficial effect of IPT in children has been studied and though the use of IPT may offer some preventive measure against malaria, there are concerns about the impact of the side effects that may result from its use (25).

1.1.4.2.2 Quinine

The treatment of malaria was discovered three centuries before there were scientific breakthroughs on the knowledge of its cause and its mode of transmission (30). The history of malaria treatment cannot be discussed without the mention of a tree native to the tropical Andes forests of South America – the cinchona tree. In the 1600s, it was believed that the wife of a viceroy of Peru, the Countess of Chinchon had recovered from malaria after immersing herself in a pond underneath a cinchona tree, as a result cinchona tree was derived from her name. First found by the Quichuans, they used the bark of cinchona for the treatment of fevers and shivering and the Spanish Jesuit missionaries were the first Europeans to benefit from the healing power of the cinchona bark (30). In the early 1800s, Joseph Pelletier and Jean Binenaime Caventou successfully isolated a bitter alkaloid they called quinine from the cinchona bark to which the healing potential of the cinchona bark is attributed. (31). Quinine may be administered in oral or parenteral dosage forms and following oral administration, quinine exhibits fast absorption and an extensive distribution in the body. It is metabolised in the liver by mainly CYP3A4 and to a lesser extent by CYPs 1A2, 2C9 and 2D6. Approximately 20% of administered quinine is not metabolised but excreted unchanged kidney, bile and saliva (32).

1.1.4.2.3 Chloroquine

Chloroquine was an essential component of the WHO's fight against malaria after World War II (33, 34). Unfortunately, sometime in the 1950s, resistance to chloroquine developed, first in the Thia-Cambodian border, and spread to some

regions in Colombia and Venezuela in the 1960s. Following this, more chloroquine resistance cases were reported in Papua New Guinea around 1975, in Kenya and Tanzania around 1978 and by the early 1980, in Sudan, Uganda, Zambia and Malawi (33, 34). The emergence of chloroquine resistance to *falciparum* malaria has led to a focus on its efficacy for other forms of malaria infection as chloroquine efficacy on *P. vivax, P. ovale, P. malariae, P. knowlesi* has been robustly reported though a recent study suggest *P.malariae* might be resistant to chloroquine (32, 35). Chloroquine undergoes quick and nearly complete absorption following an oral administration. It is about 55% bound to plasma protein and it is widely distributed into body tissues. It undergoes hepatic metabolism through cytochrome 2C8 and 3A4 metabolic pathways which contributes to about half of its elimination from the body leaving the other half to the kidney elimination (32).

1.1.4.2.4 Antifolates

Antifolates undergo their antimalarial effect by competitively inhibiting the dihydrofolate reductase enzyme in the parasite while the sulpha antifolates competitively inhibits the effects of the dihydopteroate synthase enzyme. Proguanil was the first antifolate antimalarial agent to be discovered and the discovery of other antifolate antimalarial agents, such as pyrimethamine and clociguanil followed. However, many antifolates are faced with similar problems associated with antimalarial resistance.

To reduce the potential for resistance, many antifolates are used in combination therapies with sulphone or sulphonamides to give an additive antimalarial effect. These agents are still in use in some parts of the world where malaria is endemic either as monotherapy or as combination treatment as atovaquone/proguanil and sulphadoxine/pyrimethamine (SP) but mainly as preventive therapies (36-38). The efficacy of atovaquone/proguanil (AP) in treatment of uncomplicated malaria has been demonstrated in a few studies. Krudsood *et al* (2007) showed that in Thailand-Myanmar patients with uncomplicated malaria, 97.8% of patients administered atovaquone/proguanil were cleared of parasitaemia, however, there was a report of treatment failure in three patients which was attributed to antimalarial resistance (39). This finding was supported by Cottrell *et al* (2014) where they concluded that

resistance to atovaquone had resulted in poor AP eradication of the malaria parasite (40).

The efficacy of SP was demonstrated in a 2003 Sudan study where SP was showed to proffer satisfactory clinical and parasitological responses following treatment of 102 Sudanese patients with 25mg/kg and 1.25mg/kg SP respectively (41). Conversely, Pitmang *et al* (2005) argued that SP is not as efficacious as its comparators in clearing malaria parasites. They showed that in Nigerian patients, by day 3 and day 7, parasite clearance rate was 52% and 67% respectively in patients with uncomplicated malaria treated with standard doses of SP (42). Similarly, Basco *et al* (2002) reported that the therapeutic failure of SP was highest (13.6%) compared to amodiaquine (10.2%) and SP+amodiaquine (0%) among the patients they studied in that trial (43).

Atovaquone is lipophilic in nature and its oral absorption is poor with an oral bioavailability of 20% that varies widely from person to person but proguanil is quickly absorbed in the GIT. The absorption of atovaquone is enhanced with food hence AP should not be taken on an empty stomach (32). Atovaquone is 99% bound to plasma proteins and slowly cleared from the body with a half-life of about three days and excreted mainly in the faeces chemically unaltered. Proguanil shows 75% protein binding and is metabolised in the liver by CYP2C19 and perhaps, 3A4 and about 50% of the drug is eliminated by the kidneys (44). Sulfadoxine and pyrimethamine share similar pharmacokinetic characteristics. They both undergo quick absorption following enteric administration and are both approximately 90% bound to plasma proteins and have half-lives ranging from two to nineteen days, however, pyrimethamine has a volume of distribution that is larger than sulphadoxine. Both are metabolised by the liver and undergo kidney excretion (32, 45).

1.1.4.2.5 Artemisinins

In 2006, artemisinin derivatives used as a combination with other antimalarial agents were recommended by the WHO for the first line treatment of malaria in endemic areas (3). Though there are concerns about resistance to these agents, they

have emerged as antimalarial agents with a relatively satisfactory efficacy and less worrisome resistance profile when used as a combination therapy with other antimalarial agents (3).

Artemisinin was first identified in China in 1972 from a plant *Artemisia annua*, locally called Qinghao, several centuries after the same had been discovered by Chinese natives to have medicinal properties (31, 46). Around this time, the extracts from the plant were tested on malaria infected mice and found to be efficacious and were later tested by Mao Tse Tung in humans and also found be efficacious. This finding was published in 1979 (31, 46). Though potent, artemisinin was found to be unstable *in vitro* and this led to discovery of more stable forms of artemisinin namely artemether and artesunate. The process of synthesising these derivative requires the formation of dihydro-artemisinin (DHA) which is in itself a potent antimalarial agent but is less stable. It has been found that in the body, both artemether and artesunate are converted to DHA (31, 46).

These drug compounds are not recommended for use in uncomplicated malaria as lone oral treatments, though intravenous or intramuscular AST or intravenous ART when AST is not available is recommended in the treatment of severe malaria in adults, children and pregnant women for at least 24 hours depending on response to the treatment (32). In 2012, Sinclair *et al* published a systematic review of eight randomised controlled trials that compared parentally administered artesunate (AST) to quinine in subjects from different Asian and African countries who were treated for malaria between 1989 and 2010 (47). This research demonstrated that malaria related death among these subjects was significantly reduced by 40% in adults and 25% in children with administration of intravenous AST when compared to intravenous quinine (48).

The lipophilicity of artemether (ART) is higher than other artemisinin derivatives and it has a fast onset of action with a good oral absorption profile. Time to reach maximum plasma concentration after an oral administration is about two hours. Studies show that following the consumption of a fat rich meal, the bioavailability of artemether is more than doubled (49). ART undergoes rapid and

significant hepatic metabolism by the CYP3A4/5, and to a lesser extent by CYP2B6, CYP2C9/19. Dihydroartemisinin (DHA) is an active metabolite formed after a CYP3A4 metabolism of ART or AST. This active metabolite has been said to potentiate its antimalarial effects. Artesunate is rapidly absorbed through oral intramuscular or rectal routes of administration. When administered orally, it is metabolised into active DHA by CYP2A6. DHA, when administered orally is quickly absorbed from the GIT. It exhibits up to 93% plasma protein binding following absorption after oral administration or as a product of artemether or artesunate metabolism and it is rapidly eliminated with half-life of about one hour (32). Some artemisinin based combination treatment available for uncomplicated malaria include (32):

- Artemether/lumefantrine (AL)
- Dihyrdoartemisinin (DHA)-piperaquine (DP)
- Artesunate-amodiaquine (AA)
- Artesunate-mefloquine (AM)
- Artesunate-sulphadoxine/pyrimethamine (ASP)

1.1.4.2.6 Lumefantrine

Developed by Chinese scientists in 1967 (46) lumefantrine is a racemic product of fluorine with its chemical structure related to the arylaminoalcohol group of antimalarials such as quinine, halofantrine and mefloquine. During the haemoglobin break down by *P. falciparum,* heme, a toxic product of haemoglobin is changed to a non-toxic form called hemozoin. It has been proposed that *P.falciparum* death occurs when there is a build-up of heme as a result of a lumefantrine mediated disruption of the transformation of heme to hemozoin (50, 51). Lumefantrine is also well absorbed orally and with fat rich food, its bioavailability has been shown to increase by approximately 16-fold (49). A study which compared the impact of meal and milk consumption on the absorption profile of lumefantrine found that children who consumed a meal and were administered a crushed tablet of a lumefantrine based antimalarial agent had a 100% rise in plasma lumefantrine levels while those administered dispersible tablets had a 55% rise in plasma lumefantrine concentrations (49). Consumption of milk also increased the plasma lumefantrine

concentrations by 57% and 65% for crushed and dispersible tablets respectively (49). Lumefantrine has a relatively slow onset of action of around 6-8 hours after oral administration and is also slowly cleared from the body having a terminal half-life of about 4 to five days (49, 52).

1.1.4.2.7 Piperaquine

First synthesised by the Shanghai Research Institute of Pharmaceutical Industry in 1966, the use of piperaquine a 4-aminoquinoline for malaria dates to the late 1970s. It effectiveness against *falciparum* malaria resistant and non-resistant to chloroquine has been demonstrated in several studies (53). A number of studies have demonstrated the high cure rates for PQ combination with dihydroartemisinin (DHA). In 2007, Janssens *et al* in a randomized open-label study in Cambodia showed that a 97.5% cure rate on day 63 post treatment was observed following a standard 3-day regimen with about 62% parasite clearance on day one of treatment (54). In a more recent study in 2016, Kakar *et al* reported a 100% cure rate for DHA-PQ in Pakistani patients with mutant *falciparum* infection after 42 days from the first treatment dose (55). However, another recent report in 2016 has raised concern about a DHA-PQ treatment failure observed in Europe following infections with falciparum strains from Ethiopia. In the report, a failed DHA-PQ treatment case was reported at 32 days post treatment in an elderly Italian woman. Also, there are indications that DHA-PQ might be insensitive to *falciparum* strains in Cambodia due to resistance (56, 57). Used as a monotherapy, Pasay *et al* (2016), demonstrated that piperaquine is not as effective for malaria treatment as its use was associated with gametocytemia in subjects treated with it even at high doses (58). Piperaquine is rapidly absorbed in the GIT when administered orally with time to achieve peak concentrations at about 3 to 6 hours. It is widely distributed in the body and has a high protein binding of about 99%. It has a long elimination half-life of about two to four weeks (32).

1.1.4.2.8 Mefloquine

In the early 1970s, mefloquine was discovered to help combat the threat of malaria. In 1974, mefloquine, which was a joint discovery of the US Army medical and research command and the Hoffman La Roche, Inc. was shown to be effective as a preventive antimalarial agent ; it was later shown to be also useful to treat malaria

as well (38). However, in 1985 after the drug became available to the public, resistance to mefloquine was reported in Asia (38). In order to combat the challenge of resistance, around the mid-90s, it was combined with ACTs and found effective in some parts of Asia as well as Southern parts of America. The neuropsychiatric and gastrointestinal adverse effects of mefloquine may have impeded its use as a choice antimalarial in regions where malaria is prevalent though these side effects are thought to be related to dosing amount (59, 60). Mefloquine monotherapy is now commonly used as a chemoprophylactic measure to foreigners travelling to malaria endemic regions (61). Due to its ineffectiveness, the WHO discourages its use as monotherapy for treating both acute and severe forms of malaria. Mefloquine in combination with artesunate (an ACT) is recommended as one of the choices for treatment of uncomplicated malaria in malaria-endemic regions, but it is contraindicated in subjects with neuropsychiatric problems. The pharmacokinetics of mefloquine are thought to be altered in patients with malaria compared to patients without malaria as it has been shown that its concentration in the plasma is higher and it has higher elimination rates in patients with malaria compared with those without the disease. It exhibits wide inter-individual variation in absorption rates, it is widely distributed in the body and has a plasma protein binding of about 98%. It is primarily metabolised by hepatic CYP3A4 and has an elimination half-life of about 3 weeks. It is mainly excreted in the faeces as metabolites and unaltered drug and a small amount is excreted in the urine (32).

1.1.4.2.9 Amodiaquine

Amodiaquine is a 4-amino quinoline and its use for both malaria treatment and prophylaxis has been hit by several ups and downs in history. In 1977, it was first included the WHO essential drug list but due to its comparativeness with chloroquine, it was removed in 1979 but this decision was reversed that year. Since then, there have been modifications to its indications, and deletions from several national malaria control guidelines, mainly due to the adverse drug events associated with its use (62). However, based on evidence from several studies, amodiaquine as a combination therapy is used for treatment and prevention of malaria but due to drug resistance, monotherapy is not encouraged (32, 63). A 2017 study showed that artesunate-amodiaquine was well tolerated among Cote d'Ivoire subjects with uncomplicated malaria who were treated with this combination (64). Amodiaquine

is quickly absorbed from the GIT and undergoes biotransformation to it active metabolite, desethylamodiaquine which is mainly responsible for its antimalarial activity. Desethylamodiaquine is slowly cleared from the body compared to amodiaquine, having an elimination half-life up to 10 days (32).

1.1.5 Challenges with AMT therapy and the role of pharmacokinetics research

Malaria parasite resistance to antimalarial therapy is perhaps one of the most significant concerns of antimalarial (AMT) treatment currently (65). The main cause of this has been linked to the mutation of the parasite strains following exposure to antimalarial treatment (65). It has been showed that there is a link between malaria parasite mutation and subtherapeutic antimalarial concentrations and many studies have shown that subtherapeutic concentrations of antimalaria treatment has led to treatment failures and recrudescence of malaria infection (66). The attainment of subtherapeutic systemic concentrations of AMTs may be due to a poor understanding of the pharmacokinetics of many AMTs in subjects especially special populations like children and pregnant women as these are not routinely recruited into clinical trials. This may further be confounded by drug to drug interaction (DDIs) as many of AMT are likely to be administered with other medicinal agents capable of reducing their systemic concentration.

In a review by White *et al* (2004) on antimalarial drug resistance, the authors provided an explanation on how the pharmacokinetics of an antimalarial may be linked to antimalarial drug resistance (ADR) (67). In the review, the author explained that pharmacokinetic properties such as the oral bioavailability, volume of distribution and elimination half-life are important in ADR and explained that most antimalarials are highly lipophilic, hence their absorption is prone to high variability leading to erratic peak plasma concentrations which may favour ADR. They also explained that due to very long half-life of some slowly eliminated antimalarials, these antimalarials offer sufficient time for selection of resistance among sensitive parasites but selection for resistance may not occur at the terminal elimination phase when resistance might have occurred due to sub-inhibitory concentration of antimalarial agent towards the resistance strains (67).

Despite the fact there are many pharmacokinetic studies involving the antimalarials, these studies depend hugely on the availability of clinical data in the subjects involved, which in most cases do to not entirely represent the real therapeutic challenges that may be found in practice. Clearly, ethical constraints may hinder the ability to obtain data involving such “real” therapeutic situations, therefore, there is a need to find alternative methods of mechanistically analysing the pharmacokinetics of antimalarial concentration data, especially in population groups wherein ethical policies might hinder the collection of useful clinical data.

1.2 Basic principles of pharmacokinetics

Pharmacokinetics is the field of pharmacology which studies the "kinetics" or movement of drugs in the body. This involves the study of the processes of drug absorption, distribution, metabolism and excretion (68, 69).

1.2.1 Pharmacokinetic parameters

These are parameters derived during plasma drug concentration versus time analysis. They are used to quantify the manner in which the body alters the concentration of drugs following administration and may be classified as primary or secondary pharmacokinetic parameters (70).

1.2.1.1 Primary pharmacokinetic parameters

Primary pharmacokinetic parameters are those parameters that depend on the physiology of the species and may not be derived from other parameters. These are clearance and volume of distribution (70).

1.2.1.1.1 Clearance

The clearance of a drug describes the process of elimination from the body as it is defined as the 'volume of body fluid from which the drug is eliminated per unit time' (70, 71). Typically, clearance is measured in either plasma or blood, giving rise to the plasma clearance (CL_p) or blood clearance (CL_b).

The main sites of drug clearance are the liver and the kidney; however, drugs may be eliminated from other sites in the body, e.g. from the sweat or from the saliva (71) . The total body clearance (CL_T) of a drug is the sum of the clearances from all organs where drug elimination occurs, and may be expressed as (70):

$$CL_p + CL_b + CL_{other} = CL_T \qquad (1)$$

The ratio between the amount of drug being excreted from an organ to the amount of drug entering is called the extraction ratio (ER) (70). The product of the blood flow to an organ and the extraction ratio of a drug is defined as the clearance

from that organ (Equation 2) (70). The clearance of a low extraction drug is restrictive, that is, only unbound drug is cleared while the clearance of a high extraction drug is non-restrictive whether or not the drug is highly bound to protein (70, 71).

$$Q_{organ} . ER = CL_{organ} \quad (2)$$

The clearance of drug in a particular organ is dependent on the organ blood flow and the eliminating capacity of the organ – the intrinsic clearance (CL_{int}), that is the ability of the organ to eliminate drug without any influence of blood flow (Q) or protein binding (fu). The CL_{int} is obtained from *in vitro* studies that involve primary hepatocytes, subcellular liver fractions or transfected cell lines. Furthermore, as drugs are often bound to plasma proteins or partitioned into the blood, only the free fraction (unbound) drug is available for elimination and therefore the plasma protein binding capacity of a drug may also affect its clearance (70).

In the 1970s, Pang and Rowland (72-74) described a model that may be used for the prediction of human *in vivo* drug clearance from *in vitro* intrinsic clearance. This model was called the well-stirred model and it assumes that the eliminating organ, for instance the liver, is a one compartment and well-stirred system and there is equilibrium between unbound drug concentration in the exiting blood and unbound drug concentration in the organ (75). The well-stirred model for estimating hepatic clearance CL_h, is represented in equation 3:

$$\boldsymbol{CL_h = \frac{Q_h \times f_u \times CL_{int}}{Q_h + f_u \times CL_{int}}} \quad (3)$$

1.2.1.1.2 Volume of distribution

The volume of distribution of a drug is the volume of body fluid in which a drug must be present to reflect a particular body concentration. It is a proportionality factor that relates the amount of drug in the body to the concentration of drug present in the blood, and therefore it is not a 'real' volume but an 'apparent volume'. Drugs

that are lipophilic in nature will tend to distribute to adipose tissues, with hydrophilic drugs distributing into more of the water fractions of tissue and organs (70, 71).

The volume of distribution depends upon the drug's binding capacity to the blood (erythrocytes), plasma proteins and tissue (non-specific) binding, as only the unbound drug is available to be distributed to different parts of the body such that drugs with high binding capacity are likely to exhibit low volumes of distribution and *vice versa* (70, 71). Assuming a non-exponential decline in drug concentration in the body, the volume of distribution may therefore be expressed with respect to the administered dose and expected plasma/blood concentration (C) using equation 4 (70, 71).

$$V = \frac{Dose}{C} \qquad (4)$$

1.2.1.2 Secondary pharmacokinetic parameters

Secondary PK parameters are those PK parameters derived from the primary PK parameters, they do not directly depend on changes in physiological parameters in the organism but are directly dependent on the changes in the primary PK parameter. There are several of them but half-life, AUC and bioavailability will be discussed. (70, 71).

1.2.1.2.1 Half-life

The time taken for the plasma concentration of a drug to be reduced by 50% is called its half-life ($t_{1/2}$). This parameter is important for making drug dosage decisions as it gives an indication of drug disposition, but it is not the sole measure of drug disposition because it depends on the clearance and the volume of distribution. Alterations in protein binding can impact both the clearance and the volume of distribution of a drug and these may erratically affect the half-life of the drug. The relationship between these parameters can be represented equation 5 (70).

$$t_{1/2} = (0.693) . \frac{V}{CL} \qquad (5)$$

1.2.1.2.2 Area under the concentration versus time curve (AUC)

The measure of systemic (plasma/blood) drug exposure following drug administration through any route of administration is called the AUC (70, 71). It is determined by calculation of the area under the concentration-time curve using the trapezoidal rule (70) (Figure 1.2). Assuming a drug undergoes complete oral absorption and is completely eliminated, the AUC may be estimated with respected to the oral dose ($Dose_{oral}$) and the clearance (CL_T) as (70):

$$AUC_{oral,max} = \frac{Dose_{oral}}{CL_T} \qquad (6)$$

1.2.1.2.3 Bioavailability (F)

The is the fraction of the dose administered that enters the systemic circulation intact (70). For drug administered intravenously, F = 1 since all the drug is immediately available for systemic circulation. However, drugs that are administered through other routes of administration typically have a $F < 1$ (70, 71). The oral route of administration is the most common route of drug administration, however drug given through this route may be subject to chemical degradation due to pH changes along the GIT; secretion due to the effect of efflux proteins or enterocyctic metabolism due to the impact of drug metabolism enzymes (70, 71). Drugs may also be metabolised in the liver before they reach the systemic circulation. The metabolism of drugs either in the enterocyte or the liver the first time they come into contact with these organs is known as the "first pass effect" (70, 71). The oral bioavailability after the first pass effect can be determined using the equation 7 or 8 (70, 71):

$$F = \frac{AUC_{oral}}{AUC_{iv}} \qquad (7)$$

or

$$F = \frac{AUC_{oral}}{AUC_{IV}} \; X \; \frac{Dose\ IV}{Dose\ Oral} \qquad (8)$$

However, if the oral absorption of drug is complete, the maximum F(F_{max}) if the drug is metabolised by the liver may be calculated using equation (9) (70, 71):

$$F_{max} = 1 - ER_{hepatic} \quad (9)$$

1.2.2 Pharmacokinetic processes

1.2.2.1 Absorption

The therapeutic effects of drug are only expected if an administered drug can move from its site of administration to the systemic circulation where it will be circulated to the site of action (76). The process involved in drug molecules transferring from the site of administration into the blood is called absorption. Absorption does not occur for drugs administered intravenously (IV) since all the drug reaches the bloodstream immediately after administration. For drug absorption to take place after oral administration of a solid drug formulation, the release of active ingredient in the dosage form must be preceded by disintegration and dissolution processes in the gastrointestinal fluid (76).

Disintegration is the process whereby solid dosage forms disintegrate to release the active pharmaceutical ingredients (APIs). In order to ensure that the highest possible amount of API is absorbed from the solid dosage form, the disintegrating capability of the dosage form need to be carefully considered (76). Dissolution is the process whereby the API is dissolved in the dissolution medium of the gastrointestinal tract for absorption to take place. The dissolution rate is affected by manufacturing processes, water solubility, particle size and the excipients added to the formulation. Arthur Noyes and Willis Rodney Whitney (77) described the formulation and drug-specific properties which influence the rate of *in vitro* dissolution in equation 10:

$$\frac{dC}{dt} = k.(C_s - C) \quad (10)$$

where C_s is solubility concentration of the drug, C is the concentration of the drug in bulk media and k is the dissolution rate constant of the drug.

Following dissolution, the released drug will then permeate through the cell lining of the gastrointestinal tract, to be absorbed. As illustrated in Figure 1.2, absorption through this physiological barrier typically occurs either by through passive diffusion or active transport in the small intestine.

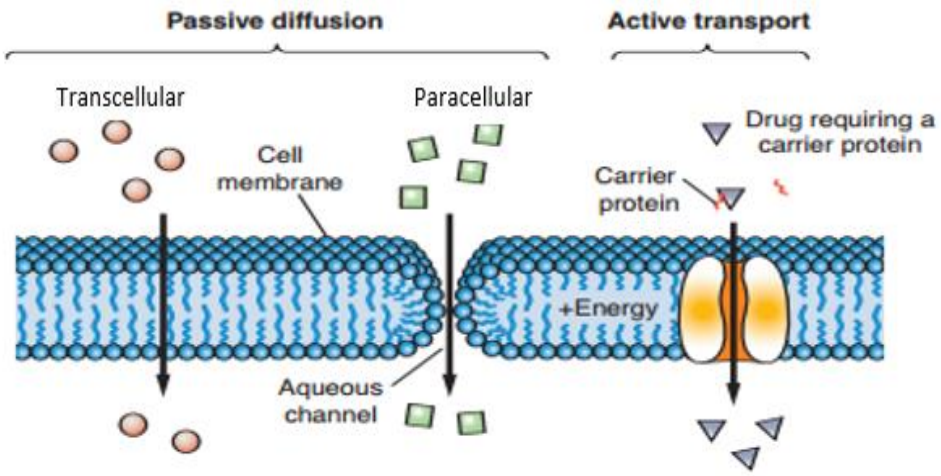

Figure 1.2: Processes of molecular drug transport across a cell membrane

Molecules with low molecular weight are usually absorbed by passive diffusion. Passive transport involves diffusion of drug molecules from a region of higher concentration to a region of lower concentration across the epithelial cells membrane until equilibrium is reached. Most drugs are absorbed passively from the enterocytes present in the duodenum or the jejunum of the GIT. The main routes of passive absorption in the GIT is transcelluar routes for lipophilic drugs and paracellular routes for hydrophilic drugs. In drug transport involving the paracellular route, the drug molecules move across the cell through aqueous membrane pores while drug transport through the transcellular route involve drug permeating through the cell membrane as shown in Figure 1.2 (78).

The ideal absorption site are the enterocytes located at the villi of the duodenum or jejunum, however the epithelial cells that form an anatomical barrier to the GI lumen may possess certain metabolising enzymes capable of oxidative, conjugative or hydrolytic metabolic reactions. This implies that drug which pass through the luminal plasma membrane will be exposed to metabolising enzymes and this might result in some form of extra-hepatic metabolism of the drugs even before the drug reaches the hepatic system. The portion of drug that escapes the intestinal enterocytes intact is typically expressed as F_g (78).

Passive diffusion exhibits direct proportionality to concentration gradient across the membrane, lipid to water partitioning coefficient of the drug and the surface area of the cell. Un-ionised drug forms have higher lipid solubility compared to the ionised forms; hence these diffuse with ease across the cell membrane. Hence the extent of drug ionisation (pKa) and gastric pH will also affect drug absorption through passive diffusion across the cell membrane. The Lipinski Rule-of-5 describes the properties of drug that makes it likely absorbable through transcellular route in the gastrointestinal tract (GIT). The properties include: presence of at most 5 hydrogen bond donors, that is oxygen or nitrogen atoms with at least one hydrogen atom; drug molecule should have not more than 10 hydrogen bond acceptors, that is nitrogen or oxygen atoms; drug molecular weight should be not more than 500g/mol and octanol-water partition coefficient (log P_{ow}) should be less than 5 (79-81).

In active transport, also known as the carrier-mediated transport, drug moves through the barrier against a concentration gradient with the aid of membrane localised drug transporter proteins, in a process which requires energy. Key transporter categories include those belonging to the adenosine triphosphate (ATP) binding cassette (ABC) and the solute carrier (SLC) group of transporters, which are present at the apical and basolateral membranes. Active transport through ABC transporters depend on energy released from the hydrolysis of ATP, whereas drug transport through SLC occurs through H^+, Na^+ and Ca^{2+} gradients by Na^+/K^+-ATPase, Na^+/H^+- ATPase.

1.2.2.2 Drug Distribution

Distribution of the drug molecule to different parts of the body starts after absorption has taken place. During distribution, drug molecules which are unbound to the plasma proteins distribute into the tissues and organs, some of which might possess high tissue binding capacity. For drugs to reach the site of action from the blood, organ perfusion, organ permeability, drug-to-plasma and drug-to-tissue binding, and the lipid nature of drug are all important factors to consider (82, 83).

1.2.2.2.1 Tissue perfusion

The extent of blood flow to different body organs may determine the extent to which a drug is capable of being distributed into that tissue. Rapidly perfused organs such as the liver, brain and kidney receive the rich supply of drugs carried in the blood or plasma while slowly perfused tissues such as the skeleto-muscular system and the adipose tissues have limits to the rate and extent to which a drug distributes into them and may lead to a delayed clinical effect (82, 83).

1.2.2.2.2 Tissue partitioning

Tissue partitioning is dependent on tissue composition. Lipophilic drugs are partitioned into high fat organs/tissues such as adipose, liver, brain, and kidney, while hydrophilic drugs are preferentially partitioned into water rich organs such as muscle (82, 83).

1.2.2.2.3 Plasma and tissue drug binding

In addition to tissue perfusion and tissue partitioning, distribution of drug to its site of action also depends on drug binding to plasma protein. Drugs will not produce a therapeutic response in a bound state as it is the unbound drug that distributes into circulation to elicit a clinical effect at target sites. The plasma proteins to which most drugs are bound are human serum albumin (HSA) and alpha-1 acidic glycoprotein (AAG) (82, 83).

1.2.2.3 Metabolism

Occurring primarily in the liver, drug metabolism is the process in which the chemical structure of a drug is altered to enhance its eventual elimination and this

process is mediated by enzymatic processes. Drug metabolism in the liver occurs in two phases – phase I and phase II and may be mediated by cytochrome P450 (CYP) enzymes or through non-CYP enzyme pathways. Metabolism may also occur outside the liver (84-87).

1.2.2.4 Phase I

CYP enzymes are typically located within the mitochondria or the endoplasmic reticulum and at least 57 functional CYPs genes and 58 pseudogenes have been identified and classified into 18 families and 43 subfamilies (88). Of these, CYP1, CYP2, CYP3 subfamilies are largely responsible for the metabolism of about 75% of drugs and xenobiotics (88). Of all the human CYP which have been characterised, the CYP3A4 is most abundant and has relatively greater number of drug substrates, inhibitors and inducers compared to the other human CYP enzymes (88). Table 1.1 summaries the abundance of some CYP enzyme expressed and their typical substrates, inducers and inhibitors.

Table 1.1 Human Cytochrome P450 enzymes, abundance, relevance in metabolism, substrates, inhibitors and inducers.

Family	Isozyme	Hepatic abundance (pmol/mg)	Amount of liver P450 pool (%)	Involvement in drug metabolism (%)	Example of substrate	Example of inhibitor	Example of inducer
CYP1	1A2	17.7 – 65	4.4 - 16.3	8.9	Caffeine, Naproxen, Acetaminophen	Cimetidine, Ciprofloxacin,	Carbamazepine, Omeprazole, Phenytoin
CYP2	2A6	14 – 56	3.5 – 14	3.4	Efavirenz	Selegiline, Tranylcypromine	Rifampicin, Phenobarbital, Artemisinin
	2B6	6.9 – 21	1.7 - 5.3	7.2	Artemether, Bupropion, Efavirenz	Clopidrogrel, Clotrimazole,	Carbamazepine, Artemisinins,
	2C8	29.3 – 30	~7.5	4.7	Amodiaquine, Rosiglitazone	Montelukast, Gemfibrozil	Dexamethasone, Phenytoin
	2C9	18 – 116	4.5 – 29	12.8	Diclofenac, Warfarin, Irbesartan, Ibuprofen	Fluconazole, Amiodarone	Rifampicin, Prednisolone, Ritonavir
	2C19	3.6 – 15	0.9 - 3.8	6.8	Omeprazole, Clopidrogrel,	Clopidogrel, Fluoxetine, Ticlopidine	Artemisinins derivatives, Carbamazepine, Efavirenz
	2D6	5 – 17	1.3 - 4.3	20	Amitriptyline, Codeine, Carvedilol	Quinidine	Induction by prototypical P450 inducers not significant
	2E1	22 – 66	5.5 - 16.5	3	Chlorzoxazone	Disulfiram, Orphenadrine	Isoniazid, Ethanol
	2J2	1 – 2	< 1	3	Albendazole, Amiodarone, Cyclosporin	Danazol	
CYP3	3A4	58 – 146	14.5 -37	30.2*	Clindamycin, Artemether, Lumefantrine, Midazolam, Tramadol, etc.	Ketoconazole, Isoniazid, Clarithromycin, Ritonavir, Diltiazem	Rifampicin, Ritonavir, Statins, Phenytoin, Valproic acid
	3A5	3.5 – 4	~1				

Data obtained from Zanger *et al* (2013) (88).

1.2.2.5 Phase II

Phase II metabolism is typically mediated by non-CYP enzymatic degradation, wherein the products of phase I metabolism are conjugated through glucuronidation, sulphation, acetylation, glutathione, Acyl Co-enzyme A conjugation and methylation to form inactive metabolites (85).

Uridine 5'-diphospho-glucuronosyltransferase (UGT) is a common phase II enzyme which mediates glucuronidation with hydroxyl, carboxylic acid and amine groups. Products of glucuronidation are generally nontoxic, though some carcinogenic glucuronides has been described in some studies. Sulphotransferases (SULTS) are responsible for sulphation metabolic reactions that lead to inactivation of some drugs. However, some studies have shown that this reaction could produce metabolites that are toxic to the genes (89, 90).

Acetylation reactions involve the catalytic effect of N-Acetyl transferases (NATs) present within the cytosol whereby amino groups take up the acetyl released from acetyl-coenzyme A to form inert metabolites. NAT exhibits polymorphs characterised as NAT1 found throughout the body and NAT2 is mainly located in the liver and gut. Glutathione conjugation is another metabolism pathway in the phase II metabolism involved in the biotransformation of many drugs. This pathway involves a glutathione S-transferase (GST) mediated catalysing reaction between nucleophilic glutathione and the electrophilic epoxide, ester, ketone, sulfoxide, peroxide and hydrocarbon groups on drugs undergoing metabolism (85, 87).

Further conjugation steps occur for some drug that have carboxylic acid groups after their glucuronide formation to produce acyl CoA thioesters. These conjugates may form taurine, glycine and carnitine conjugates following a reaction with amino acids. Finally, methylation occurring in phase II metabolism is not a common drug metabolism pathway and involves methyl substitution catalysed by methyl transferase (85, 87).

1.2.2.6 Non-CYP metabolism

Non-CYP oxidative reactions may involve the flavin-containing monoxygenases (FMOs); alcohol and aldehyde dehydrogenase (ADH and ALDH); peroxidases; monoamine, xanthine and aldehyde oxidases (MAOs, XO and AOs) (91-95). Non-CYP

reduction reactions involve nitro-, aldehyde, ketone and nitro reduction of drug entities; these reactions may involve NAD(P)H-quinone reductase (DT-diaphorases); NADPH-cytochrome P450 reductases; isoxazole reduction and aldo-keto reductase (AKR) (85, 96). Hydrolysis mainly involves non-CYP enzyme reactions where esters and amides and non-polar components of alkyl groups are subject to catalytic reactions of amidases and esterases (85).

1.2.2.7 Extra hepatic metabolism

Though the liver is the main site of metabolism in the body, metabolism may also occur in other organs or systems in the body. This is because metabolising enzymes may be expressed in varying degrees in any one organ. In 1994, Krishna *et al* reported different CYP P450 expressions in different parts of the brain, where the brain stem and cerebellum had the greatest CYP enzyme expression. Table 1.2 summarises the expression of CYP enzymes in different body systems (86, 87).

Table 1.2: Extrahepatic Cytochrome P450 enzyme expression

Body Systems	Cytochrome P450 enzyme genes								
Gastrointestinal	2A6	2C8	2C19	2D6	2E1	2J2	3A4		
Pulmonary	1A2	2A6	2B6	2C8	2C19	2D6	2E1	2J2	3A4/5
Urinary	2D6	2J2	3A4/5						
Central nervous	1A2	2A6	2C8	2D6	2E1	2J2	3A4/5		
Cardiovascular	1A2	2A6	2B6	2C9	2C19	2D6	2E1	2J2	3A4/5
Skin	1A2	2B6	2C9	2C19	2D6	2E1	2J2	3A4/5	

Data adapted from Jhajra *et al* (2012) and Krishna *et al* (1994) (86, 87)

1.2.2.8 Excretion

Excretion is the process whereby products of metabolism are irreversibly removed typically through the kidneys or through biliary excretion into the faeces. The kidney is the primary route of drug excretion and the process of excretion involves filtration, secretion and reabsorption. Blood flow to the kidney undergoes glomerular filtration driven by hydrostatic pressure in the glomerular capillaries. The rate at which filtration occurs per time is expressed as glomerular filtration rate (GFR). The GFR is an indicator of renal function and it describes the elimination of drug which does not undergo secretion or reabsorption. Creatinine is the marker used for measuring the GFR in humans and the normal GFR is 100 – 125 ml/min. The size and charge of the molecule determines whether they will be excreted through filtration. Molecules with size less than 500 g/mol are easily filtered by the kidney while molecules with negative charges are not readily filtered in the kidney (75).

Tubular secretion is an active process that occurs mainly at the proximal tubules where organic acids are transported against a negative membrane potential in the basolateral and luminal membranes through protein transporters. This process is saturable and it may have the potential to cause drug to drug interactions (75). Factors such as plasma binding, renal blood flow and intrinsic clearance can affect the secretion of drug compounds in the proximal tubules.

Tubular reabsorption in the kidney opposes the action of filtration and secretion, in that it involves transporting drugs from the kidney back into the blood. This process occurs at the proximal tubules; and is largely thought to be a passive process though some research has shown that some renal transport proteins are involved in tubular reabsorption. Rate of urine flow may influence reabsorption processes, a high urine flow rate reducing reabsorption by reducing contact time, and concentration gradient. The reverse happens with a low flow rate. Molecules that are large or ionised or hydrophilic in nature are not likely to be reabsorbed (75).

Equation 11 describes the estimation of renal clearance incorporating all three processes involved:

$$CL_{renal} = CL_{filtration} + CL_{secretion} - CL_{reabsorption} \quad (11)$$

where CL_{renal}: Overall renal excretion, $CL_{filtration}$: filtration clearance, $CL_{secretion}$: secretion clearance, $CL_{reabsorption}$: reabsorption clearance.

However, renal $CL_{reabsorption}$ is more accurately expressed in relation to fraction of filtered and secreted drug that is reabsorbed indicated by R. The Equation 12 is generally used to estimate renal excretion:

$$CL_{renal} = [f_u \times GFR + (CL_{sec})] \times (1 - R) \quad (12)$$

where CL_{sec} is the secretion clearance

Protein transporters involved with tubular secretion are the organic anionic transporters (OAT) 1, 3, 4. There is an overlap between substrates transported by *OAT1* and *OAT3*. *OAT3* also transports sulphate and glucuronide conjugates. *OAT4* participates in digoxin elimination. Those responsible for transport of basic compounds are the organic cationic transporters and these include *OCT1*, *OCTN1* and *OCTN2*. Other transporters are the multi-drug resistance-associated proteins (MRPs). *MRP1*, *MPR3* and *MRP5* are found in the basolateral membrane and *MRP2* is thought to be involved in renal secretion. Also, the multidrug resistance (MDR) proteins, P-glycoproteins (*P-gp*) interact with many drug compounds and are found in the brush border membrane and are involved in drug efflux from the cells into the lumen (97).

1.3 Pharmacokinetic modelling analysis in antimalarial drug research.

In order to appropriately quantify the pharmacokinetic (PK) parameters described above, proper analysis of drug concentration data is required. In practice, non-compartmental analysis (NCA), compartmental modelling, population pharmacokinetic modelling (popPK) and physiologically based pharmacokinetic modelling are the common PK analysis methods and these will now be discussed.

PK modelling studies involving compartmental, non-compartmental analysis (NCA) and population PK have been previously conducted to understand the PK of antimalarials in different population groups. For instance, Moore *et al* (2014), used compartmental PK modelling to determine the impact of fatty meal on the pharmacokinetic properties of DHA and PQ among children in Papua New Guinea (PNG) with uncomplicated malaria. In their model development, the researchers sought to determine how food intake affects the PK of PQ and DHA and they found that there were no significant impacts from the intake of food on the systemic exposure of PQ and DHA in children (98).Tarning *et al* (2008) using pop-PK modelling found that the clearance; volume of distribution and therefore the day 7 concentration of PQ was significantly affected by body weight (99). Salman *et al* (2015), used pop-PK to show that number of doses was a significant covariate that impacted on the PK of ART. They demonstrated that a subsequent dose of ART resulted in almost 70% increase in ART clearance in children. This was the only covariate they found that impacted on the PK of ART in children (100).

1.3.1 Non-compartmental analysis (NCA)

In NCA, statistical moment analysis is conducted such that the area under the drug concentration time profile ($AUC_{0\text{-}inf}$) and the mean residence time (MRT) are indicative of the overall drug exposure after drug is administered via the intravenous or extravascular routes (68, 101).

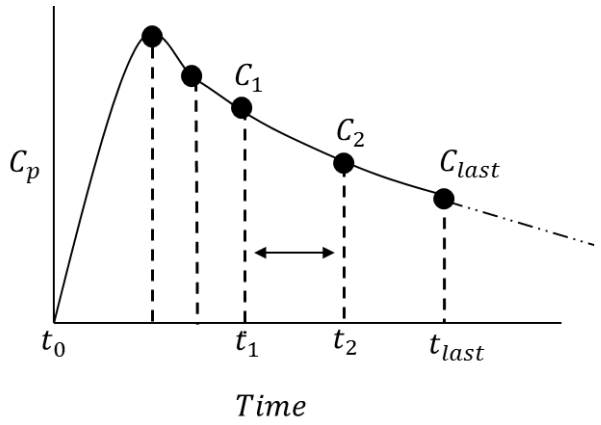

Figure 1.3 Linear trapezoidal method of estimating pharmacokinetic parameters

The AUC is often estimated using the linear trapezoidal or log trapezoidal methods whereby the concentration of the drug is multiplied by time. If AUC over two adjacent time points t_1 and t_2 are to be estimated (Figure 1.3), the $AUC_{t1\text{-}t2}$ may be estimated using the linear trapezoidal method in equation 13 or the log trapezoidal method in equation 14 (68, 101).

$$AUC_{t1-t2} = \frac{(t_2 - t_1) \times (C_2 - C_1)}{2} \qquad (13)$$

$$AUC_{t1-t2} = \frac{(t_2 - t_1) \times (C_2 - C_1)}{In\,(\frac{C_2}{C_1})} \qquad (14)$$

When the concentration time profile curve is either slowly ascending or descending, the linear trapezoidal equation can be expected to give an accurate estimation of the AUC, however, when the curve is exponentially descending, the log trapezoidal equation gives a more accurate estimation of the AUC (101). The overall AUC for from time zero (t_0) to last sampling time (t_{last}) may be estimated by summing up the AUCs from all the trapezoids in the concentration time profile. The AUC from the last time of sampling (t_{last}) to infinity, when it is assumed that the concentration at that time (C_{last}) is not null may be calculated using the equation below (68, 101).

$$AUC_{t_{last-\infty}} = \frac{C_{t_{last}}}{\lambda_Z} \quad (15)$$

where λ_Z is the terminal rate constant derived by non-linear regression analysis of concentration time profile plotted on a semi-logarithmic scale using time points that are not farther than the last sampling time. Where it is impossible to measure the Ct_{last}, as in the case when this concentration is below the quantifiable limit, the linear regression line fitted to the last three data points on the concentration time profile may be used to estimate the terminal rate constant (68, 101).

The MRT describes the mean (arithmetic) time taken for the drug compound to reside in the body before it is eliminated. It is estimated by dividing the $AUC_{0-\infty}$ by the area under the first moment curve ($AUMC_{0-\infty}$). The $AUMC_{0-\infty}$ is AUC obtained when each AUC_{t1-t2} point is plotted against the corresponding time and may also obtained using the trapezoidal method. The unit of AUMC is concentration x time^2 and $AUMC_{tlast}$ from t_{last} to infinity is calculated using the equation 16 (68, 101):

$$AUMC_{t_{last-\infty}} = \frac{C_{t_{last}}.t}{\lambda_Z} + \frac{C_{t_{last}}}{\lambda_Z^2} \quad (16)$$

In NCA, the total body clearance (CL_T) which may also be referred to as the systemic clearance following intravenous drug administration, the steady state volume of distribution (*Vss*) and oral bioavailability (*F*) of a drug may be estimated using equations 17, 18 and 19 respectively (68, 101):

$$CL_T = \frac{Dose^{iv}}{AUC^{iv}_{0-\infty}} \quad (17)$$

$$V_{ss} = MRT^{iv} \times CL_s \quad (18)$$

$$F^{po} = \frac{AUC^{po}_{0-\infty}}{AUC^{iv}_{0-\infty}} \times \frac{Dose^{iv}}{Dose^{po}}$$

During NCA, fewer assumptions are made compared to a compartmental analysis. But the disadvantage of NCA compared to compartmental analysis is that with NCA, PK profiles cannot be predicted when a dosing regimen is changed because it cannot predict compound concentration at any time (68, 101).

1.3.2 Compartmental pharmacokinetic analysis

Unlike NCA, in compartmental analysis the body is represented by one or more compartments that possess no real anatomical or physiological meaning and the movement of drugs in and out of the compartments is described by rate constants (68). Each compartment is a discrete pharmacokinetic compartment and is symbolic of a combination of tissues or organs in the body. Drug distribution between compartments are assumed to be rapid and at equilibrium with each other in one compartmental model but not so in multi-compartmental models (68). Multi-compartmental models are used to describe the shape of the concentration time profile. When plotted on a semi-log scale, if the concentration time profile produces a straight line, the drug is said to distributed into one compartment and follows a mono-exponential decay, but if lines on the semi-log scale appears to be in more than one phase, the drug is said to be distributed into multiple compartments depending on the number of phases observed in the semi-log profile (68).

1.3.2.1 One compartmental pharmacokinetic model

In one compartmental PK analysis, the body is assumed a homogenous compartment whereby the distribution of the drug in the body is instantaneous and in a single compartment (Figure 1.4) (68).

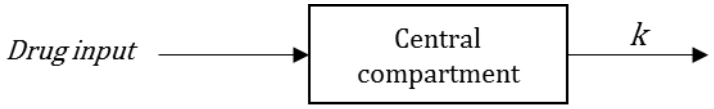

Figure 1.4: A one-compartment model

k: elimination rate constant

In a one compartmental model, the decline of a drug compound from the body is mono-exponential and the concentration of the drug in the plasma or in the blood (C(t)) at a given time *t*, is calculated using equation 20 (68):

$$C(t) = \frac{Dose^{iv}}{V} \cdot e^{-kt} \qquad (20)$$

where *V* is the volume of distribution, *k* is the first order elimination rate constant and *t* is time.

The one compartmental model for a drug administered through the extravascular routes will require incorporation of the absorption component into the model as depicted in Figure 1.5.

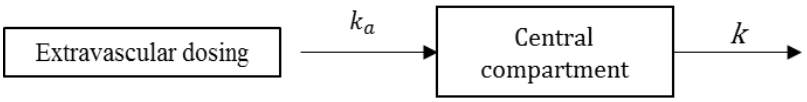

Figure 1.5: A one-compartment model including extravascular absorption component

k_a: absorption rate constant

This will involve the estimation of an absorption rate constant k_a, using the curve fitting or residual method and concentration at any time *t*, may be calculated using the equation 21 (68):

$$C(t) = \frac{K_a .F. Dose^{po}}{V \cdot (k_a - k)} \cdot (e^{-kt} - e^{-k_a t}) \qquad (21)$$

1.3.2.2 Multi-compartmental pharmacokinetic modelling

Multi-compartmental models are used to analyse the PK of drugs undergoing bi- or tri- exponential decay, in that their concentration time profile following will show a bi- or triphasic declines respectively. The body is assumed to be comprised of a central and

one or more peripheral compartments (Figure 1.6) whereby the central compartment is a lumped up compartment making up the highly perfused tissues such as the lungs, heart and kidneys while the peripheral compartment comprises the poorly perfused tissues like the fat, skin or muscles (68).

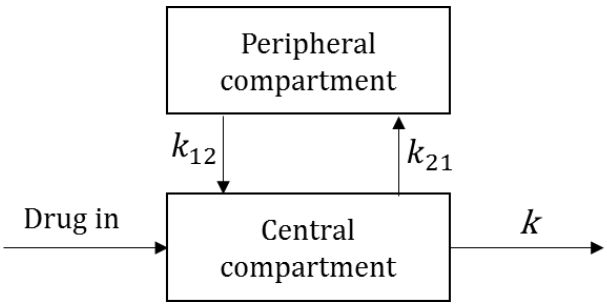

Figure 1.6: Two-compartment model.

k_{12}, k_{21} and k are first-order rate constants: k_{12}: rate of transfer from central to peripheral compartment; k_{21}: rate of transfer from peripheral to central compartment; k: rate of elimination from central compartment.

The assumption in a multi-compartmental model is that, after drug administration into the central compartment, drug is transferred between the central and peripheral compartments but the distribution of drug between the central compartment and the peripheral compartments is not instantaneous. The two compartmental model can be described as follows (68):

$$C(t) = A \,.\, e^{-\propto.t} + B \,.\, e^{-\beta.t} \qquad (22)$$

where A, B, are Y-intercepts while α and β are slopes (rate constant) following curve fitting of the plasma concentration time curve using the residual or nonlinear regression analysis methods such that A and α are the Y-intercepts and slopes of the distribution phases while B and β are the Y-intercept and slope of the elimination phase.

The concentration at time zero C_0 equal the sum of A and B while the volume of central compartment the V_c is the $Dose_{iv}/C_0$ (68). A steeper distribution phase occurring after administration depicts a rapid distribution and elimination of drugs from plasma to the

well perfused organs while a less steep phase depicts the elimination of the drug from the body (68). A three compartmental model comprising of a tri-phasic concentration time response may be expressed as equation 23 (68):

$$C(t) = A \,.\, e^{-\propto.t} + B \,.\, e^{-\beta.t} + \, C \,.\, e^{-\gamma.t} \qquad (23)$$

where the C and γ are the Y intercept and slope of the extra phase which may be an additional distribution phase or an additional elimination phase.

1.3.3 Population pharmacokinetic modelling

Under the same dosage scheduling conditions, the concentrations of a drug may vary from person to person within a similar population group due to different manners in which individuals handle the drug (102). Population PK (popPK) studies the inter-individual variabilities (or between subject variability (BSV)) and intra-individual variabilities (or between occasion variability (BOV)) in PK of drugs and the demographic, pathophysiological or therapeutic factors (or covariates) that are responsible for the variations within a given population (102, 103). Population PK modelling requires a thorough assessment of many models with varied amount of compartments, elimination methods and variabilities. In popPK analysis, drug concentration samples from representatives of the target population are collected and the variabilities in PK of the drug between the subjects or within the subjects are identified, explained and quantified (102). This process informs the optimisation of dosing strategies for the drug in the population of interest (102, 103). Population PK analysis may be carried out using the traditional "two-stage" approach or the non-linear mixed effect (NLME) method, the latter being more reliable and now more commonly used (102, 103).

The two-stage method requires first, the estimation of the PK using the non-linear regression analysis of the individual patient concentration time profiles when there is rich concentration time data (102, 103). The individual PK parameters estimated from the non-linear analysis are then used as input parameters in the second stage which involves a statistical analysis of individual PK parameters. During the second stage, linear stepwise regression, covariance analysis and cluster analysis may then be used to analyse whether parameters depend on covariates and the magnitude of the dependency (102, 103). The two-stage approach may yield accurate and unbiased estimation of population

characteristic but it requires large data sets of concentration-time points and may overestimate the random effects (that is, effects due to sampling times or methods) (102, 103). The NLME approach does not require strict or restrictive sample collection designs, hence may be used to analyse sparse, fragmented and unbalanced data (102, 103). It uses the available drug concentration time data for assessing the distribution of parameters and combines these with PK data from rigid and well-sampled PK studies to analyse the distribution of PK parameters across the population and estimate how these relate with covariates (102, 103).

Population PK is widely used to determine the covariates that influence the systemic exposure of antimalarial agents across different population groups. One of such studies showed that body size and age were the main covariates which influenced the clearance of amodiaquine in 261 patients which included children younger than 5 years old and pregnant women (104). Another study showed that body weight and malaria infection are significant covariates that affect the systemic disposition of mefloquine in 43 patients who were being treated for malaria infection (105). Also, population PK has been used in dosage optimisation studies especially for the optimisation of antimalarial dosage strategies in children. For example, Hoglund *et al* (2017) constructed an optimised dosing strategy of piperaquine across age groups as age was found a significant covariate which affected the systemic exposure of piperaquine in children (106).

1.3.4 Mechanistic pharmacokinetic modelling

In mechanistic PK modelling, the body is divided into organs which are represented by physiologically important compartments with precise blood flows rates and organ size such that changes in drug concentrations in these organs can be estimated using mathematical equations (107-110). Physiologically based-pharmacokinetic (PBPK) modelling is a modelling approach whereby the PK of drugs can be studied mechanistically. One of such studies used a PBPK modelling technique to describe the pharmacokinetics of artemether in adults and paediatric patients (111). More recently Johnson *et al* (2019) developed a PBPK model for mefloquine in children and used their model for a dose selection study in Caucasian patients weighing between 5 and 10 kg (112).

1.4 Physiologically based pharmacokinetic modelling

Initially developed as a predictive safety tool to address toxicity associated with environmental pollutant exposure to humans, physiologically based pharmacokinetic (PBPK) modelling has emerged as a promising technique to circumvent many challenges faced within drug development (113, 114). In 1937, Teorell first introduced the concept of simulating pharmacokinetic parameters in different types of compartmental models using physiological and biological mechanisms of species (109). Physiologically based pharmacokinetics (PBPK) is a branch of systems biology which utilises a mechanistic or "bottom up" method to make pharmacokinetic estimations. Mathematical models are used alongside drug specific properties such as the physicochemical, metabolic and pharmacogenomic data obtained from preclinical or *in vitro* biochemical, chemical or pharmaceutical experiments and species specific anatomical, physiological and pathophysiological parameters to describe the best pharmacokinetic (PK) estimates of drugs in the body (109).

In PBPK modelling, different organs of the body are represented by smaller compartments and different processes affecting drug concentrations in the body are modelled in mathematical expressions to quantify the drug concentrations in a particular tissue or organ (113, 114) (109). In a typical PBPK model, the physiology of the main organs or tissues impacting upon the pharmacokinetics of the drug needs to be properly modelled, for instance, for a drug administered orally, factors influencing the release of drug molecule from its delivery system into the systemic circulation need to be accounted for in the model(109). These factors can include gastric emptying and intestinal transit time; intestinal pH and geometry; regional variations of drug; metabolising enzymes and transporter protein along the small intestine. Other pharmacokinetic processes such as absorption, drug permeability, tissue partitioning, metabolism and clearance of the drug are modelled as well to describe how each of these affect drug concentrations in plasma/blood or tissue (109, 113, 114). Figure 1.7 shows the structure of a minimal model and a generic whole body PBPK model.

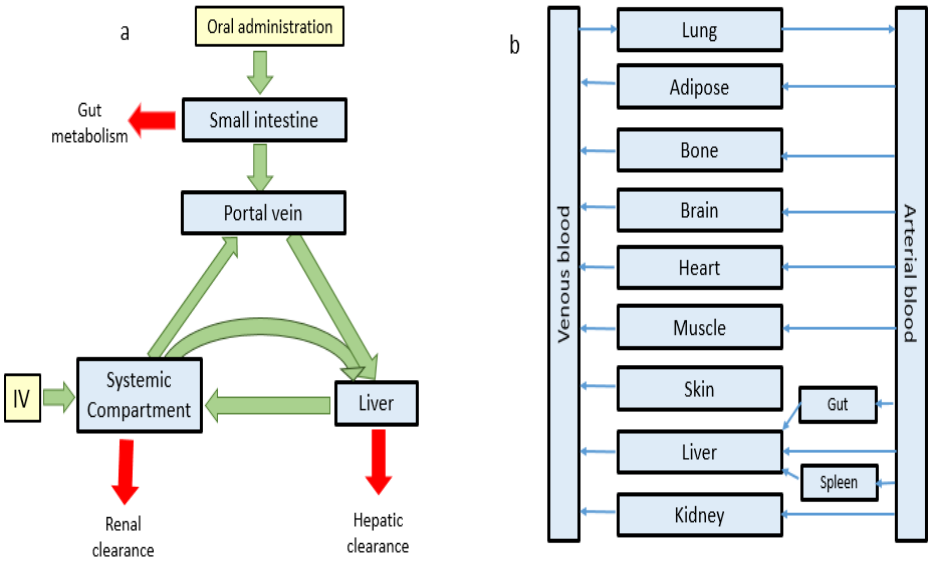

Figure 1.7: Minimal PBPK models (a) and generic whole body PBPK model (b) adapted from (109, 115)

1.4.1 Input parameters

In PBPK models, input parameters required for simulations may be classified as either system-related parameters or compound-related parameters.

1.4.1.1 System dependent parameters

These are the species physiological or biochemical characteristics that affect the disposition of drug and these vary across species. The mechanistic nature of PBPK allows for characteristics such as organ blood flows, CYP450 enzymes, transporter protein expression, haematocrit, liver and kidney functions to be incorporated into the model (109). Other system-related parameters used in PBPK simulations are organ volume, glomerular filtration rates, body weight and adipose content (107).

1.4.1.2 Drug-related parameters

These parameters depend on drug molecule characteristics. These parameters are determined from prior *in vivo* or *in vitro* experiments or may be predicted and have an effect on the absorption and disposition of the drug in the body. They generally include the physicochemical properties of the drug such as pKa, molecular weight, tissue partition coefficients, permeability properties such as *in vivo* or *in vitro* permeability values

(effective permeability P_{eff} and apparent permeability P_{app}), active transport, or metabolic properties such as the intrinsic clearance or the *in vitro* enzymatic clearance, which may be based on the Michaelis-Menten kinetics.

1.4.2 Developing a model

A whole body PBPK model incorporates the kinetic processes occurring in different tissues to determine the changes in drug concentrations over time in the body. The drug distribution processes are influenced by perfusion or permeability of the tissue. Most tissues in the human body exhibit mainly perfusion limited distribution. Conversely, some tissues have significant drug permeability problems making them permeability limited. In such tissues, permeability limited models will best describe the changes in drug concentration over time (107).

In the perfusion-limited and permeability-limited models, tissue compartments are defined by the volume (V_T) which are actual tissue volumes. These tissue compartments may be vascular or extravascular with volumes and composition characteristics readily available from published literature (116-119). In Figure 1.8 and 1.9, perfusion and permeability limited models for a one compartment tissue models are illustrated. Also, the rate of change of drug concentration in a perfusion limited organ can be determined using equation 24 while in a permeability limited organ, the rate of change of drug can be determined using the equations 25 and 26 (110, 120).

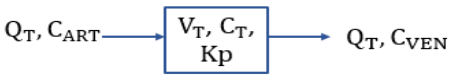

Figure 1.8: A one-compartment perfusion limited model

$$V_T \frac{dC_T(t)}{dt} = Q_T . C_{ART(t)} + \frac{(Q_T \, . \, C_T)}{Kp} \qquad (24)$$

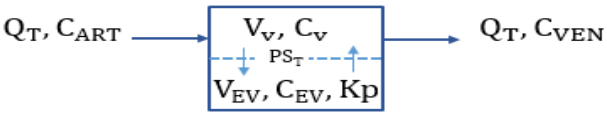

Figure 1.9: A two-compartment vascular membrane permeability limited model

$$V_T \frac{dC_V(t)}{dt} = Q_T . C_{ART(t)} + \frac{PS_T . C_{EV}}{Kp} - (Q_T + PS_T) . C_{V(t)} \qquad (25)$$

$$V_{EV} \frac{dC_{EV}(t)}{dt} = PS_T . C_{v(t)} - \frac{PS_T . C_{EV(t)}}{Kp} \qquad (26)$$

where *Q*: blood flow; *C*: concentration; *V*: volume; *Kp*: tissue: plasma partition coefficient; *PS*: permeability surface area coefficient; Subscripts *T*, *ART*, *VEN*, *V*, and *EV* present tissue, arterial, venous, vascular compartment, and extravascular compartment, respectively.

1.4.3 Mechanistic prediction of pharmacokinetic parameters

Prediction of the pharmacokinetic parameters of drugs can be conducted mechanistically even without prior knowledge of the drug is *in vivo* pharmacokinetics in the species of interest (109). This is possible because drug specific parameters obtained from *in vitro* studies can be scaled to predict their pharmacokinetic parameters through a process termed '*in vitro-in vivo* extrapolation' (IVIVE) (109). This technique provides a mechanistic framework which relies heavily of the availability of *in vitro* drug data that are used to extrapolate the *in vivo* PK characteristics of the drug (109). Pharmacokinetic processes of drug disposition and elimination have been mechanistically described with several mathematical models to enable adequate prediction of pharmacokinetic parameters, some of which are now discussed.

1.4.3.1 Dissolution

Mathematical models for dissolution was first proposed by Noyes and Whitney in 1897 (77) following an *in vitro* dissolution experiment. Brunner and Nernst in 1904 (121, 122) expanded Noyes and Whitney's equation by including the surface area (*A*) of the drug particle available for dissolution in the equation 27:

$$\frac{dC}{dt} = k . A . (C_s - C) \qquad (27)$$

Brunner and Nernst considered the impact of diffusion coefficient (*D*) of drug through diffusion and volume of the media (V_m) wherein the drug is to be dissolved and the thickness (*h*) of the diffusion layer may be incorporated into the equations by relating these variables to *k* using Fick's second law as shown in equation 28 and 29 (121, 122):

$$\frac{D}{V_m h} = k \qquad (28)$$

therefore, they expanded the dissolution model equation as follows

$$\frac{dC}{dt} = \frac{D.A}{V_m h}.(C_s - C) \qquad (29)$$

Other *in vitro* dissolution models have been described apart from the Brunner and Nerst equations. These include the widely known Weibull model and other models like the Higuchi model, Korsmeyer–Peppas model and the Baker–Lonsdale models have been proposed (123).

1.4.3.2 Drug permeability

The flux (*J*) of drug molecules passively moving across a membrane can be expressed by equation 30 to incorporate the *in vitro* permeability (P_{eff}), intestinal surface area S, and the change in concentration across the membrane, ΔC (107):

$$J = P_{eff} \times S \times \Delta C \qquad (30)$$

For preclinical studies, however, the P_{eff}, may not be obtained easily, therefore an apparent permeability (P_{app}) obtained by *in vitro* methods using cell culture based permeability studies with either human epithelial colorectal adenocarcinoma cells (Caco-2) or Madin-Darby canine kidney (MDCK-II) cells, with Caco-2 being the method more predominantly used. A regression relationship has been determined to correlate P_{eff} values for some drugs to their P_{app} values and the resultant correlation relationship (equation 31) can be used to estimate the P_{eff} value from P_{app} values for other drug compounds (107).

$$Log(P_{eff}) = 0.6532\ Log\ (Papp) - 0.3036 \qquad (31)$$

Where there is active transportation of drugs due to membrane bound proteins, the flux of drug across the intestinal mucosa is affected. Caco-2 studies are able to detect this and such compounds will be subject to further studies to determine the kind of transporter proteins that influences their transport (107). The determination of drug-transporter interactions using the Michaelis-Menten equation may appropriately express the relationship between drug and transporter; this is due to saturation of enzyme binding sites, however, when protein transporter abundance is known, the determination of specific transporter pathways has been developed using insect-derived membrane fractions which allow for more specificity. The flux of active transporter substrates can be determined by the equation 32 (107).

$$J_{transporter} = \frac{J_{max} \cdot C_{lumen}}{Km + .C_{lumen}} \qquad (32)$$

where $J_{transporter}$ is flux of transporter; J_{max} is maximum velocity of flux, C_{lumen} is the concentration at the lumen and K_m is the Michaelis-Menten constant. Since J_{max} and K_m are obtained from *in vitro* cell lines, *in vivo* scaling is accomplished by accounting for the segmental protein abundances along the small intestine (107).

1.4.3.3 Drug metabolism and renal excretion

Modelling of drug metabolism involves estimation of *in vivo* human clearances from clearance determined from *in vitro* experiments. Experimental *in vitro* hepatic intrinsic clearance CL_{int}, are converted to *in vitro* unbound intrinsic clearance ($CL_{int,u}$) by accounting for CYP enzyme or UGT protein concentrations and non-specific binding. The $CL_{int,u}$ is then converted to human unbound *in vivo* intrinsic clearance ($CL_{int\ invivo}$) by accounting for microsomal recovery, hepatocellularity and liver weight (equation 33). In equation 34, the fraction of unbound drug in the plasma and the blood to plasma ratio are incorporated in an equation together with the $CL_{int\ invivo}$ to determine the hepatic clearance, assuming a well stirred mechanistic liver model.

$$CLint_{\ in\ vivo} = CLint_{\ in\ vitro} \cdot \frac{milligram\ of\ microsomal\ protein\ (mg)}{gram\ of\ liver\ (g)} \cdot \frac{Liver\ weight\ (g)}{Body\ weight\ (kg)} \quad (33)$$

$$CL_H = Q_H \cdot \left[\frac{(f_{up}/B{:}P).\ CLint_{\ in\ vivo}}{Q_H + (f_{up}/B{:}P)\ .\ \ CLint_{\ In\ vivo}}\right] \quad (34)$$

Modelling the renal clearance has not been extensively explored. Presently, animal *in vivo* renal clearances are extrapolated to determine human adult clearance or estimation of clearance by calculation of glomerular filtration rates may be used to estimate human *in vivo* clearance. Only a few studies describe the processes of glomerular filtration, passive and active secretion/re-absorption occurring in the kidney from the mechanistic viewpoint, one of such is by Neuhoff *et al* (2013) where they developed a mechanistic kidney model (Mech KiM) that was able to account for the effect of both active and passive transport processes occurring in the kidney during the excretion of drugs (124) (107).

1.4.3.4 Drug-tissue partitioning

For drugs to elicit the desired therapeutic outcome, they need to be distributed to the primary site of action. The factors affecting drug tissue partitioning (drug distribution into the tissues) are the rate and extent of drug partitioning into a tissue. This may be affected by tissue composition, and the lipophilic property of drug molecule (107). Modelling partitioning of drug into the tissue involves determining the ratio of the concentration of drug in the tissue to its concentration in the plasma at steady state through *in vitro* or *in vivo* methods. This ratio is termed the partition coefficient *Kp* and calculated using equation 35 (107).

$$Kp = \frac{C_{tissue}}{C_{plasma}} \quad (35)$$

where C_{tissue} is the concentration of drug in the tissue; C_{plasma} is the concentration of drug in the plasma. When the fraction of unbound drug in the tissue and plasma is determined through *in vitro* equilibrium dialysis methods, the *Kp* can be is calculated by dividing the fraction of unbound drug in the tissue f_{ut} by the fraction of unbound drug in the plasma f_{up} as shown in equation below (107):

$$Kp = \frac{f_{ut}}{f_{up}} \quad (36)$$

In practise however, unbound tissue-to-plasma concentration ratio (Kp_u) which accounts for the fraction unbound in the plasma fup is employed rather than the Kp. Therefore, the equation can be expanded to:

$$Kp = f_{ut}.Kp_u \quad (37)$$

therefore,

$$Kp = \frac{Ctissue}{Cplasma} = f_{ut}.Kp_u \quad (38)$$

It is normally difficult and costly to experimentally determine these values, so Poulin and Theil first developed a model to predict the *Kp*. Their model was later expanded in 2005 by Rodgers and Rowland (125, 126) to account for the ionisation properties of the drugs as well as the composition of the tissue the drug is partitioning into. Based on the Rodgers and Rowland tissue partitioning model, the *Kp* of moderate-to-strong basic drugs:

$$Kp_u = \begin{bmatrix} \left(\frac{1+X.f_{IW}}{1+Y}\right) + F_{EW} + \left(\frac{Ka_{AP}.\,[AP]_T.\,X}{1+Y}\right) + \\ \left(\frac{P.f_{NL}+(0.3P+0.7).F_{NP}}{1+Y}\right) \end{bmatrix} \quad (39)$$

An equivalent model was developed for *Kpu* drugs which are not moderate-to-strong basic as shown below:

$$Kp_u = \begin{bmatrix} \left(\frac{1+X.f_{IW}}{1+Y}\right) + F_{EW} + (Ka_{PR}.[PR]_T) + \\ \left(\frac{P.f_{NL}+(0.3P+0.7).F_{NP}}{1+Y}\right) \end{bmatrix} \quad (40)$$

where *P*: n-octanol:water partition coefficient for unionised compound for all tissues besides the adipose, *F*: fractional tissue volume, *IW*: intra-cellular tissue water, *EW*: extra-

cellular tissue water *NL*: tissue neutral lipids, *NP*: tissue neutral phospholipids, $[AP]_T$: tissue concentrations of acidic phospholipids and extra-cellular albumin (for acids and weak bases), $[PR]_T$: tissue concentrations of lipoprotein (for neutrals), Ka_{AP}: the affinity constant of the drug for acidic phospholipids which can be derived by equation 41, Ka_{PR}: either extra-cellular albumin or lipoprotein, respectively which can be derived by equation 42, *X*, *Y* and *Z*: drug ionisation as shown in Table 1.3 below:

$$Ka_{AP} = \left[Kpu_{BC} - \left(\frac{1+Z}{1+Y} \cdot f_{IW,BC}\right) - \left(\frac{P.f_{NL,BC} + (0.3P+0.7).F_{NP,BC}}{1+Y}\right) \right] \cdot \left(\frac{1+Y}{[AP]_{BC}.\ Z}\right) \qquad (41)$$

$$Ka_{PR} = \left[\frac{1}{fu} - 1 - \left(\frac{P.f_{NL,P} + (0.3P+0.7).F_{NP,P}}{1+Y}\right) \right] \cdot \frac{1}{[PR]_P} \qquad (42)$$

Table 1.3: Drug Ionisation

	X	Y	Z
Monoprotic base	$10^{pKa-pHiw}$	$10^{pKa-pHp}$	$10^{pKa-pH_{BC}}$
Diprotic base	$10^{pKa2-pH_{iw}} + 10^{pKa1+pKa2-2pH_{iw}}$	$10^{pKa2-pH_p} + 10^{pKa1+pKa2-2pH_p}$	$10^{pKa2-pH_{BC}} + 10^{pKa1+pKa2-2pH_{BC}}$
Monoprotic acid	$10^{pH_{iw}-pKa}$	10^{pH_p-pKa}	NA
Diprotic acid	$10^{pH_{iw}-pKa} + 10^{2pH_{iw}-pKa1-pKa2}$	$10^{pH_p-pKa1} + 10^{2pH_p-pKa1-pKa2}$	NA
Zwitterion	$10^{pKa_{BASE-pH_{IW}}} + 10^{pH_{iw}-pKa_{ACID}}$	$10^{pKa_{BASE-pH_p}} + 10^{pH_p-pKa_{ACID}}$	$10^{pKa_{BASE-pH_{BC}}} + 10^{pH_{BC}-pKa_{ACID}}$
Neutral	0	0	NA

1.4.4 Software based PBPK modelling approaches

As a result of computational advancement in PK modelling, PBPK models are now being built into computer software programs to enhance the predictability capacity of the models. The use of computer software programs to predict PK parameters using PBPK modelling is known as *in silico* PBPK modelling. *In silico* PBPK modelling particularly addresses challenges such as cost at preclinical drug development stages when no clinical drug data exist so that potentially harmful drugs can be excluded at early stages of drug development. Some software programs have as a result emerged on a commercial scale such as GastroPlus (Simulation Plus: www.simulations-plus.com); Simcyp® (Simcyp® Ltd: www.simcyp.com); PK-Sim (Bayer: www.systems-biology.org). Some mathematical and statistical software are available like Simbiology (MATLAB, MathWorks, Inc., Natick, Mass., USA) and R (R Development Core Team) where desired models can be inputted to run PK simulations.

Thus, PBPK may not only be useful for predicting PK parameters in single adult but can be employed for population PK simulation even prior to availability of clinical data in contrast to conventional population PK analysis where prior clinical data is analysed to describe PK of drugs.

1.4.5 Modelling population variabilities in PBPK modelling

The significance of population variability of pharmacokinetic parameters and the cause of this in a given population group cannot be overemphasised as the understanding of this guides researchers on dosing recommendations especially in special populations(127). As the PBPK modelling technique is mechanistic in nature, covariate models which are based on the extrapolation of clinical pharmacokinetic parameters of the drug are therefore important. The clinical pharmacokinetic parameters are obtained from well explained interindividual variabilities in parameters that are influenced by variation in physiological or anatomical characteristics within a population group (128). Huisinga *et al* (2012) demonstrated how mechanistic covariate models may be used to determine the population variabilities of different pharmacokinetic parameters (128). They showed that variation in tissue partition coefficients significantly influenced the variabilities of the predicted blood concentration time profile of a drug. They further explained that the influence of variable tissue/plasma partitioning coefficients on predicted blood drug concentrations was possibly more significant than might be

expected in the case of inter-individual variations in tissue volumes and blood flows (128). They also proposed a mechanistic covariate model which agreed with the principles of PBPK modelling that was able to mechanistically predict the expected inter-individual variabilities in pharmacokinetic parameters from variations in anatomical and physiological characteristics relevant to drug disposition. Their model was able to predict the inter-individual variation in plasma concentration of several drugs in a paediatric population group aged 5 years old and older using the allometric scaling technique and the PBPK modelling technique. They found that in this population group there is no significant difference in the predicted volume of distribution and blood clearance using both methods (128). Also, prediction of factors influencing variability of drug disposition within a specific population can be performed using covariate models from multiple species, and this may be done through virtual population simulations (114).

1.5 PBPK modelling in special populations

Clinical studies are often conducted in individuals with normal physiological, and biochemical body compositions. The recruitment of special populations, such as paediatrics, pregnant women, geriatrics and patients with renal/liver impairment into clinical trials still remains challenging. Unfortunately, the lack of adequate clinical PK studies in these population group results in poorly made clinical decisions relating to doses of drugs. The uniqueness of PBPK modelling in incorporating physiological and biochemical variations across populations makes it a powerful tool in describing population specific PK parameters of drugs where there is sparse clinical data (129).

Over the past decade, several studies have been used to reiterate the importance of PBPK modelling in improving drug treatments in special populations. In 2014, Khalil *et al* (130) used PBPK modelling to predict drug exposure of sotalol following oral administration in children from neonatal age till adolescence. Following a validation of model predictions with adult sotalol plasma concentration data, they scaled down simulations in paediatrics and their model-predicted PK parameters of sotalol were acceptable across all paediatric age groups except in neonates. They concluded that PBPK modelling was useful to guide the paediatric clinical data and help with clinical decisions with respect to sotalol therapy. Walsh *et al* (2016)(131) also discussed the usefulness of PBPK simulations in guiding actinomycin D dosing in young patients as they found that their model gave good actinomycin D predictions in this age group. Also Batchelor *et al*

(2015) (132) used PBPK modelling to show that there may be a marginally higher risk for supra-therapeutic phenytoin systemic exposure in children receiving 20 mg/kg IV loading dose, necessitating therapeutic drug monitoring when phenytoin is used in this group.

In pregnancy PBPK studies, Mendes *et al* (2015) (133) showed that PBPK models can be used to predict systemic drug exposure of antiretroviral (ARV) drugs excreted through the kidney. They proposed their models for optimizing ARVs in pregnant women. Again, Alqahtani *et al* (2015) (134) developed a PBPK model which adequately predicted the PK of indomethacin in women in their second trimester. PBPK also has been successfully applied to predict clinically observed plasma concentrations of 151 compounds in patients with chronic kidney disease and another study showed its usefulness in predicting the altered plasma profiles of 7 drugs in patients with diabetes (135, 136).

Finally, Polasek *et al* (2013) (137), showed that in the elderly, PBPK models predicted reduced metabolic clearance as they showed good model predictability with the four drugs used in their research. There is more room to explore the potential of PBPK modelling in special populations as there are several drugs whose PK parameters are not well described in special populations.

1.6 Best practice in the use of PBPK modelling

The increase in popularity in the use of PBPK modelling techniques during early and late drug development stages has prompted the requirement to follow a "standardised" approach during the development and application of PBPK models to ensure model validity, hence there has been a consensus among regulatory bodies, industries and the academia on the best ways to carry out and report PK analysis using PBPK modelling (138). Depending on the purpose of the PBPK study, there are stages that should be followed during modelling in order to increase reliability on the resultant PK predictions (139-141). PBPK modelling techniques follow a 'predict-learn-confirm' approach (Figure 1.10) whereby initial model development is followed by a validation process to identify possible faults in the initial model prediction and subsequent optimisation of the model which will then be followed by a validation of final model to ensure reproducibility across different dosing conditions (142).

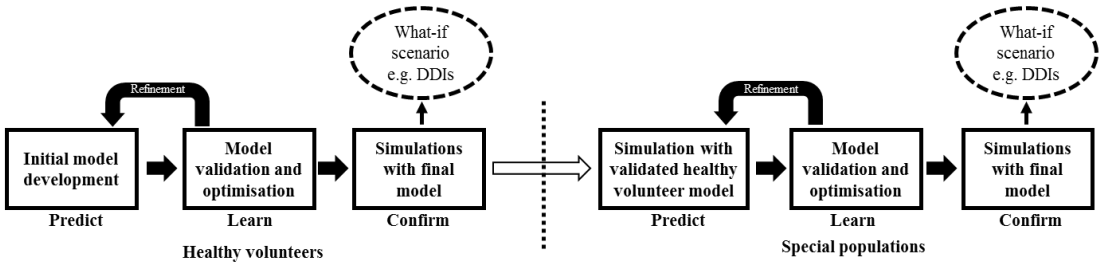

Figure 1.10: Predict-learn-confirm procedures in PBPK modelling

1.6.1 Predict

This stage involves parameterising PBPK models by gathering relevant drug related data from *in vitro* or *in vivo* studies such as physiochemical drug data and pharmacokinetic data to create an initial model to simulate the concentration profile and/or predict the PK of the drug. At preclinical stages of drug development, there may be sparse PK drug data and more physicochemical data available for use during initial model development. These physicochemical data might be used to predict the necessary PK data that are required during simulations that guide first in human (FIH) clinical trials (109, 142, 143).

1.6.2 Learn

At this stage, validation and optimisation of the initial model is done using retrospective clinical data. Where the initial model is not able to recover the clinically observed concentration time profiles or adequately predict the PK of the drug, the sources of these inconsistencies are identified and refined. This may require sensitivity analysis of parameters to determine what impact changes in these parameters might have on the predicted output. In preclinical studies, this stage involves refining preclinical models with clinical ADME data (109, 142, 143)

1.6.3 Confirm

This stage requires the application of the optimised model under different scenarios in other to further affirm the predictability of the model. During latter phases of drug development, this stage may guide drug dosage design in special populations or in

different disease states. It may also involve designing DDI studies or drug-food interaction studies (109, 142, 143).

1.7 Opportunities for PBPK modelling in antimalarial drug research

The pharmacokinetics of the pharmacological agents has a direct impact on their efficacy. There is sparse data available to describe the pharmacokinetics of antimalarials in children and pregnant women; this affects the quality of clinical decisions made during antimalarial treatment in these populations. In previous sections, the use of PBPK modelling has been elaborated and the fact that clinical data is not a prerequisite for developing models to describe the PK of a drug makes it an excellent tool for better understanding of uncertainties in the PK of antimalarial treatment in paediatrics and pregnant women. So far, there are only a few studies that used PBPK modelling to identify, explain or solve challenges that have PK implications in paediatric and pregnancy antimalarial drug treatment. Due to several physiological changes occurring in these such as the ontogeny of metabolising enzymes in children and changes in CYP enzyme activity in pregnancy, it may be erroneous to assume that healthy adults will handle drugs in the same manner, and bearing in mind that they are at a higher risk for malaria induced mortality, there is a need to find alternative ways to optimise current treatments for them. Some areas wherein PBPK modelling can be used to improve antimalarial therapy in these populations are in assessing drug-drug interaction (DDIs) and dose optimisation of currently existing adult based dosing regimens (144-146).

In children for example, an understanding of the metabolic pathways responsible for the biotransformation of drugs coupled with knowledge of the ontogenesis of the enzymes involved in these pathways are important (147), to determine the nature of DDI expected in children using antimalarials. As DDIs are mainly related to drug metabolism, in adults, the DDI between victim drug and interacting drug may be known, but the difference in pattern of expression of CYP enzymes in children may alter the way drugs are metabolised in them especially from birth till about 3 years of age (148). Therefore, the ontogeny of CYP needs to be considered when predicting DDI in children as this may affect the amount of drug metabolised in children compared to adults. An interacting drug that is a competitive inhibitor of the CYP (say 3A4 for instance) may increase the expected DDI between the drug and the victim drug in children about a month old since there is not sufficient 3A4 for binding to the substrate in the first place (148, 149).

Conversely, the induction effect of an inducer may not be sufficient to result in a DDI between and inducer and victim drug in child below one month old as there may not be sufficient enzymes to induce in the first place (148, 149).

The DDI interactions between antimalarials and other drugs in paediatrics and during pregnancy are not well studied and this may impact on the clinical efficacy, and safety of the antimalarial drug therapy. PBPK modelling has been used in adult DDI studies (150, 151) and therefore its seems promising to study the DDI of antimalarials in children and pregnancy as well since it captures the dynamic nature of paediatric and pregnancy physiology and helps better understanding how drug metabolism is changed in these. Table 1.4 illustrates the main metabolic pathways of antimalarials used in these populations as well as possible inhibitors and inducers of their metabolic pathways and the drugs may inhibit or induce them.

Table 1.4: Some antimalarials, enzymes involved in their metabolism, inhibitors and inducers of their metabolism pathway

Antimalarials	Main metabolising enzyme[152]	Inhibitor[88]	Inducer[88]
Artemether, lumefantrine, mefloquine, piperaquine	CYP34A	Ritonavir, clarithromycin, itraconazole, ketoconazole	rifampicin, efavirenz, nevirapine, carbamazepine
Artesunate	CYP2B6	Clotrimazole	Rifampicin, nevirapine, ritonavir, efavirenz, carbamazepine
Amodiaquine	CYP2C8	Trimethoprim, montelukast	Rifampicin, ritonavir

1.8 Aims and Objectives

The general aim of the thesis is to demonstrate the application of PBPK modelling in the assessment of the pharmacokinetics and the optimisation of antimalarial agents in special population groups, precisely in children and pregnant women.

The thesis addresses three specific applications of PBPK modelling:

1. *Prediction of artemether and lumefantrine pharmacokinetics in absence and presence of DDIs with rifampicin in children using PBPK modelling*

   This section of the thesis focusses on assessing the pharmacokinetic impact of DDIs in the treatment of malaria in children co-infected with tuberculosis. Artemether and lumefantrine (AL) are the first line treatment options for the treatment of malaria in malaria endemic regions but the challenge of using this medication to treat malaria in children who are also being treated with rifampicin based anti-tuberculosis (anti-TB) medication is yet to be addressed. This was addressed by developing a PBPK model for AL and validating it in adult and in children. The model was then validated in the presence of potential drug-drug interactions (DDIs) in adults and scaled down to children. The developed models were used to optimise the already existing dosing schedule of AL for the treatment of malaria in children who are co-administered rifampicin-based anti-TB medications.

2. *Assessment of the pharmacokinetics of piperaquine in the presence of drug-drug interaction with efavirenz and ritonavir during pregnancy.*

   This section of the thesis aimed to assess the impact of DDIs on the pharmacokinetics of piperaquine during pregnancy. Though the pharmacokinetics of piperaquine is widely studied in the absence of DDIs during pregnancy, the effect of potential DDIs when it is administered with antiretroviral agents like ritonavir or efavirenz on its pharmacokinetics is not well known. This knowledge is important because pregnancy is known to alter certain physiological and biochemical properties in women, and this may have implications on the pharmacokinetics of AL. It is also known that there may be ethnic variation in physiological and biochemical parameters relevant to the understanding of the PK of piperaquine. DDIs between piperaquine, an antimalaria agent used during

pregnancy to prevent and treat malaria, and drugs that may be used to treat HIV/AIDs, e.g. ritonavir and efavirenz is highly likely since these co-morbidities are prevalent within the same ethnicity. In this study, a PBPK model for piperaquine was developed and robustly validated in non-pregnant population groups across different ethnic groups and then in pregnant population. Then the effect of changes in human serum albumin and gestational age was simulated in the presence of DDI interactions with ritonavir and efavirenz.

3. *Optimisation of chloroquine dosing for repurposing in the treatment of Zika Virus disease during pregnancy using PBPK modelling*

This section of the thesis aimed to optimise the dosing of chloroquine (CQ) for the treatment of Zika virus disease (ZIKV). The prevalence of ZIKV is becoming worrying and while scientists are racing against time to develop new drugs or vaccines to combat this infection, the potential for chloroquine to be repurposed for the prevention and/or treatment ZIKV has been reported. With well-defined effective dosing strategies for its use in the treatment of malaria and management of rheumatoid arthritis (RA) and systemic lupus erythematosus (SLE) in pregnant women, a clinically viable dosing regimen of CQ for the inhibition of ZIKV is yet to be determined. In this study, PBPK modelling techniques were used to optimise the dosing of CQ for treatment of ZIKV during pregnancy. A PBPK model was developed for CQ and robustly validated in non-pregnant and pregnant subjects. This was followed by the determination of safe and effective dosing strategies of CQ in pregnant subjects.

CHAPTER 2

PBPK prediction of artemether and lumefantrine pharmacokinetics in the absence and presence of DDIs with rifampicin in children

Disclaimer

Elements of this chapter have been published as follows:

Olusola Olafuyi, Michael Coleman, Raj K.S. Badhan. Development of a paediatric physiologically based pharmacokinetic model to assess the impact of drug-drug interactions in tuberculosis co-infected malaria subjects: A case study with artemether-lumefantrine and the CYP3A4-inducer rifampicin. **European Journal of Pharmaceutical Sciences**. 2017 Aug;106:20-33.

DOI: 10.1016/j.ejps.2017.05.043

2.1 Introduction

2.1.1 Malaria in paediatrics

A new born baby living in a malaria endemic region has a high risk of contracting malaria infections before they are five years old. The WHO reported that in 2015, approximately 70% of malaria death occurred in children under 5 years of age (153). Contrary to adults who possess naturally acquired immunity, children lack this acquired immunity and this puts them at risk of succumbing to the infection (154). In addition to the transmission mode discussed in section 1.1.1, malaria may also be transferred through transplacental transmission, where an unborn child may develop congenital malaria from its mother. In this case the mother may be asymptomatic and possess malaria parasites in her placenta or other peripheral locations. Foetal infection may lead to anaemia in the child or even death. Uncomplicated malaria may be treated successfully, however, poor recovery may result in life-threatening severe malaria. Poorly managed malaria infection in children can results in complications such as seizures, acidosis, cerebral malaria, renal impairment, severe anaemia, hypoglycaemia, respiratory distress and jaundice (155, 156). Also, frequent malaria infection in children may result in malnourishment, poor growth and development as well as chronic anaemia.

The risk of malaria infection and its complications is higher in children between the ages of 6 months and 5 years (32). It is thought that in malaria endemic regions, new-born babies possess non-specific temporary immunity conferred on them through the transfer of maternal immunoglobulin G (IgG) antibodies in the uterus around the third trimester of gestation and the levels of IgG decrease gradually after birth until around the first year of life (154). Though a study argues otherwise suggesting that humoral response to *P. falciparum* was implicated in age-related prevalence of malaria in its study subjects (157). Another study explained that malaria immunity in infants may be due to parasite growth inhibitory factors like lactoferrin and secretory IgA which are present in the breast milk, maternal sera and infant sera (158).

2.1.1.1 Drugs used for the treatment of malaria in children

Quinine is the oldest antimalarial agent known, and it has been modified structurally to produce newer antimalarials. Quinine may be used for complicated malaria especially when other agents recommended for uncomplicated malaria have failed. A major setback to malaria chemotherapy is with transmission of malaria resistance strains. Resistance to antimalarials like chloroquine and SP dated as far back as the 1970s. Unfortunately, drugs like mefloquine and atovaquone, developed with the purpose of defeating resistance, seem to have succumbed to it. New discoveries have led to the use of artemisinin based combination therapies to improve malaria treatment outcomes and possibly prevent antimalarial drug resistance. Though there are concerns resistant strains to this treatment approach has also emerged, they remain the least likely to be ineffective due to drug resistance (159). Commonly used antimalarial drugs in children will now be discussed.

2.1.1.1.1 Dihyrdoartemisinin (DHA)-piperaquine (DP)

Dihydroartemisinin (DHA)-piperaquine (DP) is an artemisinin based combination therapy (ACT) used to treat malaria in paediatrics. DHA is also available as a suppository but for the reasons discussed in section 1.1.4.2.5, it is used in combination with piperaquine. (160). The possibility of resistance to DP has been reported in Cambodia. Though in March 2016, Amaratunga *et al* reported that the use of DP in treatment of malaria in their subjects some of which were children was associated with failed therapy (161), in another study, Adjei *et al* (2016) showed that in four sub-Saharan African countries, DP was efficacious for the treatment of uncomplicated malaria (162).

2.1.1.1.2 Artemether/lumefantrine (AL)

In children, AL is given as an oral dose of 2 mg/kg of artemether and 12 mg/kg of lumefantrine for managing uncomplicated malaria, though artemether alone is available as intramuscular and sublingual dosage forms (160). An AL efficacy study in children published by Sowunmi *et al* (2016) showed that in Nigeria children with anaemia associated malaria, AL was an efficacious treatment for malaria. A similar study carried out in Togo in children between 2 -3 years by Dorkenoo *et al* (2016) showed that AL and artesunate-amodiaquine (AA) were both efficacious, however, AL gave better parasite clearance rates than AA (163, 164).

A key recommendation from the WHO for uncomplicated malaria treatment in children is artemether and lumefantrine (AL) (165) administered as a fixed dose combination (FDC) of 20mg/120mg respectively, in six doses usually over three days (commonly at 0, 8, 24, 26, 48 and 60 hours). Typical treatment regimens for children include a similar 3 day six-dose regimen stratified based on body weight: 5-15 kg 1 tablet per dose; 15-25 kg 2 tablets per dose; 25-35 kg 3 tablets per dose and >35 kg 4 tablets per dose (26), with the latter dose primarily being the default adult dose.

The safety and efficacy of AL in children has been demonstrated in a number of studies which have reported greater than 90% cure rates after a 4-week period without deleterious side effects. Falade *et al* (2005) reported a 28 days 97% malaria cure rate following an AL treatment in Nigerian children, the same study reported that when given in a six-dose regimen, the cure rate was higher than a four-dose regimen (166, 167). Another AL study in Uganda showed that when compared to the cure rate from quinine treatment, the efficacy of AL was better than quinine in children between six and 59 months of age as the 28 day cure rate of quinine and AL were reported to be 64% and 96% respectively (168). More recently, a study comparing sulfadoxine-pyrimethamine (SP), AL and artesunate-amodiaquine (AM) cure rates in children between 6 and 60 months revealed that AL gave the best efficacy profile compared to AS and SP with cure rates of 94%, 93% and 28% cure rates respectively (169).

Despite the efficacy profile of AL for uncomplicated malaria, the WHO contraindicates AL for complicated malaria and cerebral malaria (165). AL has been shown to increase the QTc interval and is therefore not recommended in subjects with congenital QTc prolongation, or where there is a family history of cardiac arrhythmias or sudden death. Adverse effects associated with AL use may include vomiting, fever, headache and cough. Since ART and lumefantrine are both substrates of CYP3A4 enzyme, AL should be used with caution when used in combination with drugs that also interact with the CYP3A4 enzyme pathway (170).

2.1.2 Therapeutic endpoint of AL

One of the key therapeutic endpoints of AL treatment is the 28-day corrected parasite clearance rate (PCR)(171). Several studies have been conducted to determine the correlation

between response to parasite clearance rates and systemic concentrations of lumefantrine. Ezzet *et al* (1998) showed that a day 7 lumefantrine concentration greater than 280 ng/ml was linked to a higher observation of 28-day PCR (172). Another study found recrudescence of malaria infection in patients with lumefantrine day 7 concentrations less than 175 ng/ml (173). Also, a meta-analysis of day 7 concentrations obtained from 21 studies with 2,782 subjects concluded that day 7 lumefantrine concentrations less than 200 ng/ml were effective to prevent recrudescence. They highlighted that certain sub-populations groups may fail to achieve this level due to unsupervised treatments or may still experience recrudescence of malaria despite achieving this level, for example in patients with high level of parasitaemia (174).

2.1.3 Drug-drug interactions (DDIs) associated with AMTs

It was reported in 2015 that there were an estimated 10 million new tuberculosis (TB) cases worldwide of which 26 % of all TB cases were reported in Africa and 10 % were in children (175). Worryingly, the mainstay treatments for tuberculosis, namely a FDC of rifampicin (10-20 mg/kg), isoniazid (10-15 mg/kg), pyrazinamide (30-40 mg/kg) and ethambutol (15-25 mg/kg), can directly affect CYP3A4 activity through rifampicin (inducer) (176, 177) or isoniazid (inhibitor) (177, 178). Thus, DDIs are commonplace in patients who present with both malaria and tuberculosis making dosing strategies in paediatrics complex. Although data is sparse and the connection between malaria and tuberculosis co-infection has not been widely investigated (in contrast to HIV and tuberculosis coinfection), one study in Angola reported that the presence of malaria in patients admitted with tuberculosis as 37.5 % (179). Furthermore, the risk of rifampicin-mediated induction in CYP3A4 expression/activity would have the potential to significantly increase the clearance of AL, as has been demonstrated in adult populations (180) and has been contraindicated when used with rifampicin (181). However, the magnitude of this induction effect on AL pharmacokinetics in children has not been investigated. DDIs between antimalarials and other drugs in paediatrics are not well studied and this may impact on the clinical efficacy, and safety of antimalarial drug therapy.

A 2016 study demonstrated that in Ugandan children when the antiretroviral drug efavirenz was co-administered with AL, there was an overall reduction in exposure of AL by

2.1 to 3.4-fold when compared with the administration of AL alone. In the same study when lopinavir/ritonavir (LPV/r) was administered with the antimalarial concomitantly, the systemic exposure of lumefantrine increased by 2.1-fold, while a DDI between AL and nevirapine was only seen in artemether. There was also a 10-fold reduction of lumefantrine day 7 concentration in children co-administered efavirenz compared to those co-administered with LPV/r. This reduction led to a fourfold higher likelihood of recurrent malaria 28 days after the start of therapy (182).This finding was supported by another Ugandan study that revealed that more than 80% of children who received efavirenz had target lumefantrine day 7 concentrations below the therapeutic level (183). Another Ugandan study showed that in children who received amodiaquine for malaria infection and who were co-administered with the recommended antiretroviral (ARV) drug, there was an incidence of prolonged neutropenia, but did not clarify the degree to which the prolonged neutropenia was caused by the ARV (184).

2.1.4 PBPK modelling in children

Ethical procedures, study size, study length, invasiveness and recruitment procedures have historically impeded paediatric drug development (113, 185). Safe drug administration in children is crucial because there are weak evidence based paediatric clinical trials to support to use of many drugs in this population (185). In practice, unapproved means of drug administration known as “off-label” methods are often employed during administration of many paediatric drugs. When drugs are used off-label, it implies that its dosage regimen are not as agreed and documented in the drug labelling and this method has potential for adverse drug reactions (114, 186).

2.1.5 Developmental physiology and pharmacokinetic processes in children

Between birth and adolescence, physiological and anatomical changes occur in the human body. The physiological changes may impact on the pharmacokinetics of drugs in this group making drug effect vary across these paediatric subpopulations. The paediatric populations have been classified into smaller groups to capture major physiological changes and according to the international conference on harmonisation (ICH) E11 classification (187), paediatrics are classified as:

- **Preterm newborn**
- **Newborn** (0-28 days)
    - **Infant and toddler** (>28 days – 23months)
    - **Infant** (>28 days – 12 months)
- **Toddlers** (>12 months -23 months)
- **Child** (2- 11 years)
- **Preschool child** (2-5 years)
- **School age child** (6-11 years)
- **Adolescents** (12 -18 years)

2.1.5.1 Body size and composition in paediatrics

Most body composition changes occur during the period between birth and three years of age. The body maturation process occurring within this period impacts on drug response, its safety profile and pattern of dosing (147, 188-190). Paediatric height doubles from the birth height by the time they are four years old (Figure 2.1). At six months, birth weight estimates are doubled and by one-year-old, their weight is three times the birth weight (Figure 2.2). Body surface area (BSA) increases two fold by one year of age and by their fourth year, BSA triples the birth BSA (Figure 2.3) (190).

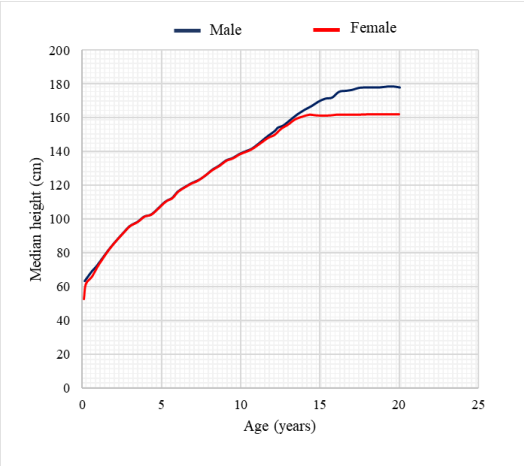

Figure 2.1: Growth chart median height in centimetres in males and females 0-20 years of age

Graph was adapted from Jong *et al (190).*

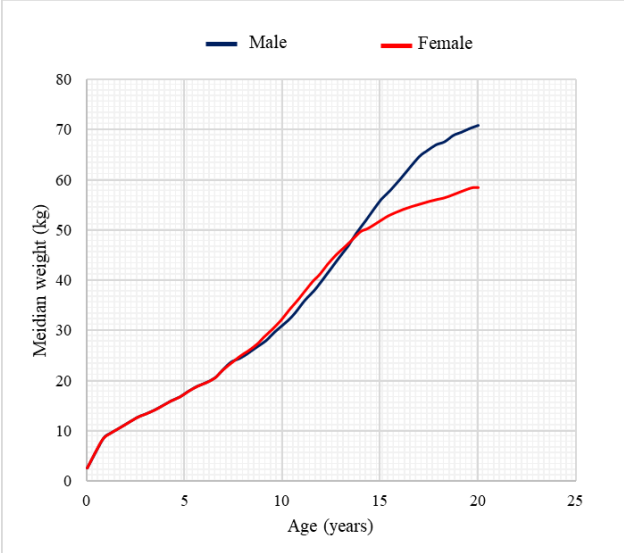

Figure 2.2: Growth chart median weight in centimetres in males and females 0-20 years of age

Graph was adapted from Jong *et al* (190)

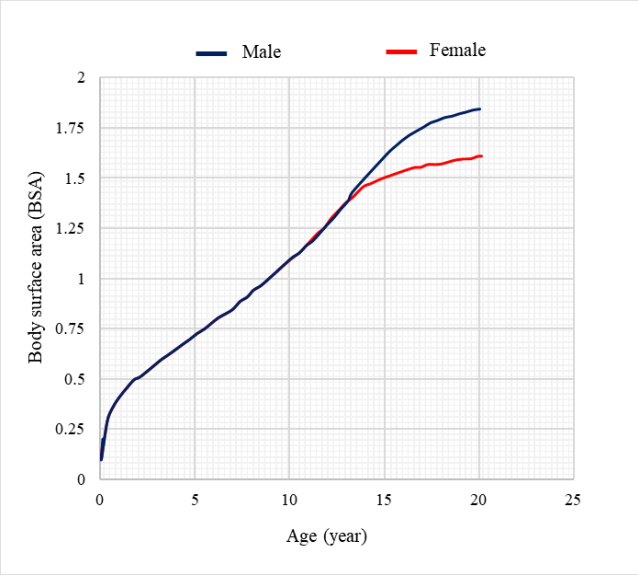

Figure 2.3: Body Surface Area (BSA) curve for males and females 0–20 years of age.

Calculation of BSA was based on the Mosteller formula (BSA = (W × H /3600) 1/2 . Graph was adapted from Jong *et al (190).*

Paediatric body proteins, intracellular water and fat undergo remarkable changes within the early years of life as highlighted in Table 2.1 (191-193). In preterm neonates, 85% of body weight comprises total body water while in term neonates; it reduces to about 75% of body weight. At four months, these estimates further reduce to about 60% and remains virtually unchanged from that age onwards, though there is a decline in extracellular water throughout childhood. By about nine months, children begin to loss their baby fat and there is a steady increase in the protein portion of their body composition (190).

Table 2.1: Percentage contribution of body composition to body weight in children

Age	Fat	ECW	ICW	Minerals	Carbohydrates	Protein
				%		
Birth	13.7	42.5	27	3.2	0.5	12.9
1 month	15.1	41.1	27.3	3.2	0.5	12.9
2 months	19.9	38	26.3	3	0.5	12.3
3 months	23.2	35.7	25.8	2.9	0.5	12
4 months	24.7	34.5	25.7	2.8	0.4	11.9
5 months	25.3	33.8	25.8	2.8	0.4	11.9
6 months	25.4	33.4	26	2.8	0.4	12
9 months	24	33	27.2	2.9	0.5	12.4
12 months	22.5	32.9	28.3	2.9	0.5	12.9
18 months	20.8	32.3	29.9	3.1	0.5	13.5
24 months	19.5	31.9	31	3.2	0.5	14
3 years	17.5	31.1	32.8	3.4	0.5	14.7
4 years	15.9	30.5	34.2	3.5	0.5	15.3
5 years	14.6	30	35.4	3.7	0.5	15.8
6 years	13.5	29.6	36.4	3.8	0.5	16.2
7 years	12.8	29.1	37.1	3.9	0.5	16.5
8 years	13	28.3	37.5	4	0.5	16.6
9 years	13.2	27.6	37.8	4.1	0.5	16.8
10 years	13.7	26.7	38	4.1	0.5	16.8

ECW: Extracellular water; ICW: Intracellular water. Data obtained from Jong *et al* (2014) (189)

2.1.5.2 Absorption in paediatrics

In children, drug absorption is influenced by the same factors as it in adults (190). The physicochemical properties of the drugs such as molecular weight, pKa and lipophilicity have some influence on absorption of drugs (189, 190). However physiological changes resulting in differences in rate and extent of absorption, pH and emptying time of the stomach, surface area and transit time of the intestine, activities of bile and pancreas, bacterial flora, transporter systems and enzymatic activities occurring throughout childhood often account for differences in rate and/or extent of absorption of drugs at different stages of growth in this population (194). Table 2.2 summarises the physiological factors that may cause variations in absorption rate and extent from birth till early childhood as compared with the adult population in Alcorn *et al*'s review of drug delivery in the new-born.

Table 2.2: Factors affecting gastrointestinal absorption and their influence on pharmacokinetic effects compared to adults

	Newborn	Neonate (one day to one month)	Infant (one month to 2 years)
Physiological factors			
Gastric pH	Neutral $\rightarrow$ 1	> 5	Adult
Gastric emptying	Reduced (variable)	Reduced (variable)	Increased
Intestinal surface area	Reduced	Reduced	Adult
Intestinal transit time	Reduced	Reduced	Increased
Pancreatic and biliary function	Very immature	Immature	Adult
Bacterial flora	Very immature	Immature	Adult
Enzyme/transporter activity	Very immature	Immature	Adult
Pharmacokinetic outcomes			
Rate and extension of absorption	Variable	Variable	≥ Adult
Gastrointestinal first-pass effect	Very reduced	Reduced	Approaching adult

Data obtained from Alcorn *et al* (2003) (195)

Gastric pH is neutral in newborns and gradually lowers to adult levels as they grow older. The implication of gastric acid pH changes is in the use of drugs that are sensitive to acidic environments like penicillin. Such medication has been shown to have a higher bioavailability in new-born infants compared with older children and adults. Drugs that are weak acids in nature are present majorly in easily absorbed non-ionic forms at the adult low stomach pH, such drugs will be poorly absorbed in new-borns (147, 196, 197).

Intestinal motor activity is generally thought to be reduced at birth and improves to adult patterns towards childhood and adulthood (189, 196). There is a reduced intestinal surface area in newborns which is gradually increased to adult levels as they mature (147, 189). It is therefore expected that orally administered drugs may achieve therapeutic plasma levels at a reduced rate compared to an adult population. Though absent at birth, biliary and pancreatic activities gradually approach adult patterns throughout infancy and childhood.

2.1.5.3 Drug distribution in paediatrics

From birth onwards, the apparent volume of drug distribution (*V*) is influenced by tissue composition, extent of plasma/tissue binding and carrier transporter maturation. (195, 196). Compared to adults, the *V* of hydrophilic drugs in neonates is higher but for hydrophobic drugs, *V* is lower owing to the high total body water and low-fat levels from birth through childhood compared with adults. Studies have shown that total plasma protein is lower in neonates and infants compared to adults. This results in an increased level of free drug concentration and consequently the bioavailability of the drug (198, 199).

2.1.5.4 Metabolism in paediatrics

The liver blood flow, protein binding and the maturation of enzymatic capacity of the liver of new-borns, infants and children influence their drug metabolism capacity (195). The change in CYP expression in children from birth to approximately 3 years of age is dynamic and CYP expression exhibits inter-individual variations in children. Generally, *in vivo* and *in vitro* data show that at birth most CYP enzymes are either not present or are at relatively low levels compared to adult levels. CYPs 2C19, 2D6, 2E1 and 3A4 are present are birth in low levels, while 2D6 and 3A4 steadily increase in their expression till about 3 years of age, there is a markedly high expression of 2C19 and 2E1 compared to the other enzymes within the

first 24 hours followed by an increase in their expression until they align with adult levels. CYPs 1A2 and 2B6 are not initially present at birth while 2C8 and 2C9 are at very minimal levels compared to adults. Studies show that 1A2 is expressed within the first day of birth, and 2B6 is not detectable at birth but may be expressed at one tenth of adult levels within one year of life while 2C8 and 2C9 increase within the first few weeks of birth and may be 30% of adult levels when they are about a year old. Conversely, high proportions of 3A7 are found in the foetus at birth reaching peak levels at about 7 days old then steadily reduces to adult levels. Of clinical therapeutic significance are 1A2, 2C9, 2C19, 2D6, 2E1 and 3A4 since these are implicated in the metabolism of many drugs (149, 200).

2.1.5.5 Elimination in paediatrics

Primarily estimated in terms of the renal clearance, the elimination of substances at birth is noticeably reduced due to immaturity of the mechanisms involved in renal excretion (195), however, renal clearance appreciably improves to adult levels by their first birthday though the efficiency of renal elimination varies from child to child owing to differences in patterns and rates of development of both the kidney tubular functions and glomerular filtration (195).

2.1.6 The role of PBPK modelling in paediatric antimalarial drug therapy

There are few PBPK studies of antimalarials in children despite the significant potential in using this technique to address antimalarial therapy problems such as DDI studies in this population group. As many antimalarials are highly lipophilic in nature, the distribution of many antimalarials is expected to be significantly altered in children at different levels of their development due to changes in fat distribution and body water (201). Similarly, as metabolic mechanism in children is premature, the clearance of antimalarials that depend on such metabolic mechanisms will be altered. Salem *et al* (2013) reported that DDI trends in children younger than two years of age were likely to be different from those in adults due to several developmental changes occurring at this age and elaborated how PBPK modelling techniques can be used to address DDI is paediatric populations (202-204).

2.2 Aim and Objectives

2.2.1 Aim

The aim of this chapter was to demonstrate the application of PBPK modelling in the prediction of DDI risks in malaria-tuberculosis co-infection paediatric population groups. Specifically, the potential for a DDI between the CYP3A4 inducer rifampicin and AL was assessed among 2-5 year old population groups and a subsequent dosing optimisation strategy of AL in the presence of rifampicin was proposed in this population group.

2.2.2 Objectives

1. To develop and validate a PBPK model to predict the pharmacokinetic parameters of AL in adults and children
2. To simulate and validate the impact of DDIs with rifampicin on the pharmacokinetic parameters of AL in adults
3. To predict the impact of DDIs with rifampicin on the pharmacokinetic parameters of AL in children
4. To optimise the dosing regimen of AL in the presence of DDIs with rifampicin in children

2.3 Methods

All population based PBPK modelling was conducted using the virtual clinical trials simulator Simcyp® (Simcyp® Ltd, a Certara company, Sheffield, UK, Version 16) using either the pre-validated in-built 'Healthy Volunteer' or 'Paediatric' population groups. The latter population group accounts for age-related changes in systems-parameters such as organ volumes, organ perfusion and ontogeny of drug metabolising enzymes (205-207) and allows for the prediction of drug behaviour in paediatric population groups. In the case of both models, population variability was accounted for by the inclusion of a variability metric (% coefficient variability) which were retrieved from public health data bases such as the US National health and Nutrition Examination Survey (https://www.cdc.gov/nchs/nhanes/).

2.3.1 Study design

A four-stage strategy was employed for model development and validation.

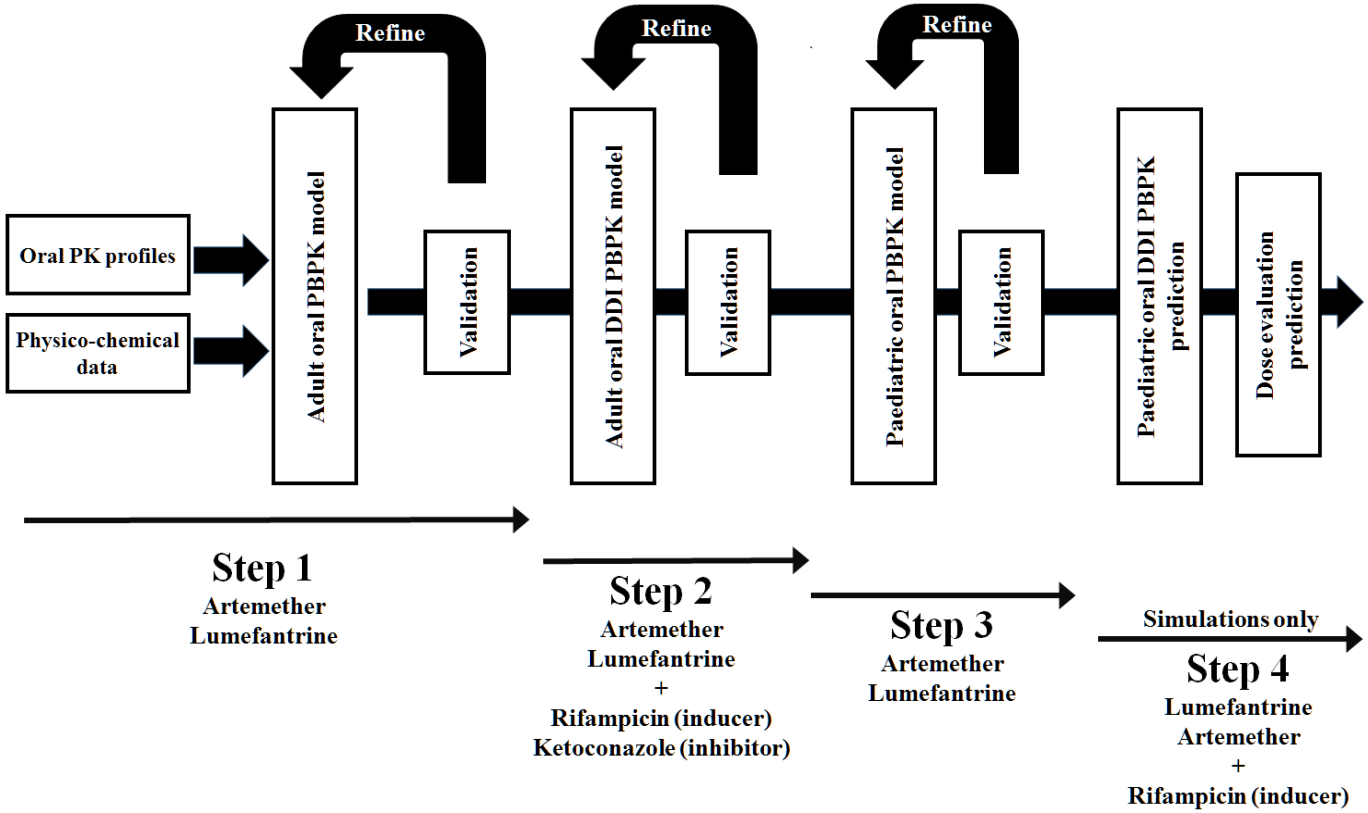

Figure 2.4: Work flow process of model development for the simulation of AL pharmacokinetics in adults and children in the presence and absence of DDIs .

The workflow was implemented for the prediction of the pharmacokinetics of artemether and lumefantrine in adults and paediatrics. The workflow also showed process involved in DDI prediction in adults and children, followed by dosage optimisation of artemether and lumefantrine in the presence of DDI with a rifampicin-based anti-tuberculosis regimen.

2.3.1.1 Step 1: Base model development and validation

This step focussed on the development of a base model on Simcyp®. The compound physicochemical properties of artemether and lumefantrine obtained from literature were used to develop a model that recovered the absorption, distribution and the elimination phases of the concentration time profiles observed from clinical studies and to simulate the key pharmacokinetic properties of artemether and lumefantrine such as the maximum concentration (C_{max}), areas under the curve (AUCs) and the lumefantrine day 7 concentration where required at different dose regimens as reported in the clinical studies.

When required, model parameters were optimised to produce parameters with better certainty, and which best recovered published clinical drug profiles. Parameter optimisation was done with the Weighted Least Square (WLS) approach and the Nelder-Mead minimisation method on Simcyp®. For artemether, literature- reported isozyme specific hepatic intrinsic clearances were utilised for the description of drug metabolism (Table 2.3). For lumefantrine, the isozyme specific hepatic intrinsic clearance (CL_{int}) was back-calculated using the Simcyp® retrograde calculator from the oral clearance and assuming CYP3A4 was the predominant isozyme for lumefantrine metabolism (208). The Simcyp® retrograde calculator is a feature on Simcyp® which permits the reverse calculation of intrinsic clearance of drug from either oral or intravenous clearance data. In certain cases, *in vitro* hepatic intrinsic clearance (CL_{int}) of a drug molecule is not available, since PBPK modelling is dependent on this parameter to mechanistically predict the elimination of the drug, this parameter may be calculated using the data from adult human *in vivo* intravenous (CL_{iv}) or oral (CL_{po}) clearance as long as the elimination pathway and hepatic uptake factor for the drug is known. The accuracy of such prediction is dependent on the accuracy of the *in vivo* intravenous (CL_{iv}) or oral (CL_{po}) clearance reported for the drug. The reverse calculation method back-calculates the CL_{int} values from the oral or IV clearance using information on additional clearance (for example, the biliary clearance), ideal renal clearance for a 20-30 year old healthy male subject, hepatocyte uptake, unbound fraction of drug in plasma and blood to plasma ratio. This model also factors in the impact of fraction of drug absorbed (f_a), fraction escaping gut metabolism (f_{gut}) and contribution to clearance from other routes like the renal or biliary clearance (115). In this case, the CL_{int} of lumefantrine (mechanistic parameter) was calculated from its CL_{oral} (non-mechanistic parameter).

Table 2.3: Input base model parameter values and predicted PBPK values for use in the simulation of artemether, lumefantrine.

Parameters	Artemether	Lumefantrine
Compound type	Monoprotic base	Diprotic base
Molecular weight (g/mol)	298.4[209]	528.94[209]
Log P	3.53[210]	8.70[211]
Fu	0.05[212]	0.003 [212]
pKa 1	3.9[209]	14.1[209]
pKa 2	-	9.80[209]
B/P	1.09[a]	0.80[213]
Vss (L/kg)	1.77[a]	0.70[a]
Peff (10^{-4} cm/s)	2.74[a]	8.3[a]
Kp scalar	1[b]	1[b]
Solubility (mg/mL)	0.012[214]	0.002[215]
CLpo (L/min)	-	0.25[172]
CL_{int3A4} (µL/min/pmol)	1.47[216]	2.61[c,d]
CL_{int2B6} (µL/min/pmol)	9.31[216]	-
ISEF CYP3A4	1[b]	-
ISEF CYP2B6	1[b]	-
Absorption model	ADAM	ADAM
Distribution model	Full	Full

[a] Simcyp® mechanistic prediction; [b] Default values in Simcyp®; [c] Parameter estimated; [d] Simcyp® retrograde calculation from population estimates of CL_{po} followed by parameter estimation (final optimised value: 0.85 µL/min/pmol for CYP3A4); MW: Molecular weight; P_{eff}: human effective permeability; B/P: blood-to-plasma ratio; CLint: *in vitro* intrinsic clearance; Vss: Steady state volume of distribution; ISEF: Intersystem extrapolation factor for scaling CYP *in vitro* kinetic data; Ki: concentration of inhibitor supporting half-maximal inhibition; K_{inact}: inactivation rate of the enzyme; K_{app}: concentration of mechanism based inhibitor associated with half-maximal inactivation rate.

Due to unavailability of published data for the human jejunal effective permeability (P_{eff}), the molecular descriptors (PSA and HBD) of AL, were predicted and optimised for artemether and lumefantrine respectively. The P_{eff} was predicted using the equation below (217):

$$logP_{eff} = 4 - 2.546 - 0.011 \times PSA - 0.278 \times HBD \qquad (43)$$

The *Kp* scalar, which is a scaling factor used to scale the tissue to plasma partitioning coefficient (*Kp*) of the drug to the expected steady state volume of distribution (Vss) (218) of the drug were further optimised for AL using a parameter estimate method within Simcyp® to yield optimal estimates of tissue distribution and *Vss* prediction.

Furthermore, for artemether, where necessary, the *in vitro* metabolic clearance was optimised through the parameter estimation of the Inter System Extrapolation Factor (ISEF) (Table 2.3). The ISEF is a scaling factor used for prediction of the human drug clearance (CL_{int}) from *in vitro* CL_{int} obtained from recombinantly expressed human cytochrome P450s (rhCYP). This is important because the intrinsic activity per unit CYP between rhCYP and human hepatic enzymes differs, therefore, the ISEF allows for IVIVE of human drug clearance from rhCYPs (219).

The published clinical studies used for the validation of artemether and lumefantrine included a study conducted in 120 adult subjects who were orally dosed the branded AL combination called Coartem®, and studies conducted in 16 subjects who were orally dosed the branded AL combination called Riamet® (220). For lumefantrine an additional study included a 6-dose study conducted in 17 subjects (221).

2.3.1.2 Step 2: Simulation and validation of drug-drug (DDI) interactions in adults

This step focussed on the validation of the adult DDI predictions. CYP3A4 inhibition and induction mechanisms were simulated using ketoconazole and rifampicin respectively. Following the successful development of and validation of the AL base model, all adult DDI simulations were, where possible, run identically to the reported clinical study with which

the validation was conducted against, and primarily included matching age ranges, male-to-female ratios and identical dose/dosing intervals. In order to validate the capability of the model to predict a broad range of DDIs, the pre-validated Simcyp® in-built compounds ketoconazole and rifampicin were directly utilised in simulations as candidates to simulate CYP3A4 inhibition DDIs (ketoconazole) and CYP3A4 induction DDIs (rifampicin). Rifampicin and ketoconazole compounds were used in simulations without modification from the library of pre-validated drug molecules within the Simcyp® simulator, using a 1st-order absorption model and assuming dosing in solution form.

Where the Simcyp® ADAM (Advanced Dissolution Absorption Model) was used, an immediate release formulation with an applied diffusion layer model was utilised for modelling with literature-reported solubility parameters included. Where simulations were performed in paediatrics, all APIs were assumed to be dosed in solution form, mimicking the dispersible/crushed application of AL in paediatric subjects (26).

A previously validated isoniazid compound file (222) was used for all rifampicin DDI simulations to account for the impact of isoniazid mediated CYP3A4-inhibition associated with TB chemotherapy. All simulations included both rifampicin (as the primary perpetrator) and isoniazid (as the secondary perpetrators), however results are presented for the key interactions between AL and rifampicin only, and reflects the clinical net effect of CYP3A4 induction with the clinical use of the combination of rifampicin and isoniazid in DDI-focussed studies (223-225).

Clinical studies demonstrating such a DDI were obtained from Lefèvre *et al* (2002) who studied AL with ketoconazole (220) (single dose of 80/480 mg of AL and 5 day treatment with ketoconazole) and Lamorde *et al* (2013) (226), who studied AL DDI with rifampicin where rifampicin was dosed at 10 mg/kg for the duration of the study with AL dosed as six 80/480 mg doses (12 hourly) on days 8, 9 and 10.

2.3.1.3 Step 3: Simulation and validation of base model in paediatric population

In this step the previously validated adult base model of artemether and lumefantrine were scaled to paediatric groups reported in clinical trials. This step focussed on the validation of artemether and lumefantrine model predictions in paediatrics. In these studies, weight bandings were simulated based on dosing strategies for AL if the clinical study did not use a weight normalised dosing method. Dosing boundaries were set at 1 tablet for 5-14.9 kg, 2 tablets for 15-24.9 kg and 3 tablets for 25-34.9 kg and trials were run to ensure, where possible, an equal proportion of subjects were included into each distribution banding based on the total number of subjects recruited within each reported trial. Simulated profiles were body weight stratified according to the corresponding clinical trial and analysed consequently.

2.3.1.4 Step 4: Prediction of drug-drug interaction between AL and rifampicin-based drug in the paediatric population

This step focussed on simulations to predict the impact of rifampicin-mediated DDIs on artemether and lumefantrine pharmacokinetics in children of 2-5 years of age over a weight boundary of 5-14.9 kg or 15-24.9 kg. In these simulations, trials of 100 subjects were simulated and analysed with appropriate weight-based dosing (see above) and under treatment of rifampicin with AL. A 100-subject simulation was run in a 10x10 trial (10 subjects per trial with 10 trials) to ensure that reasonable inter-/intra individual variability was captured within the model simulations. However, as simulations are not possible with defined age and weight ranges, pooling and post-processing of output data was conducted to match individuals to the required age-weight boundary conditions for the study.

For all validation steps, unless otherwise stated, all observed data sets were obtained from ‘supervised’ administration groups in reported clinical studies and simulated under ‘fed’ conditions. Furthermore, unless otherwise stated all simulations included subjects of ≥ 5 years.

2.3.2 Predictive performance

Whilst no agreed criterion has been suggested for an 'optimal' predictive performance range, it is generally considered that a prediction to within 2-fold of the observed data is acceptable (227). Given the wide inter-subject variability in artemether pharmacokinetics, this 2-fold range (0.5-2.0) was selected as the criterion for comparing C_{max} and AUC parameters between model predictions and those clinically reported. Where a DDI was simulated, the model performance was primarily dictated by a comparison of the AUC ratio (ratio of AUC in the absence and presence of the perpetrator agent) (AUC_r). A prediction of AUC_r within 2-fold of the reported AUC_r was considered as acceptable, an AUC_r greater than 1.25 was indicative of an inhibition reaction whereas an AUC_r less than 0.8 was indicative of an induction reaction whilst an AUC ratio of between 0.8 – 1.25 indicated no interaction.

2.3.3 Visual Predictive Checks

Model predictions were compared to existing clinical studies using visual predictive checking (VPC), an approach described at the 2012 FDA Paediatric Advisory Committee (US Food and Drug Administration, 2012) (228). In brief, the predictability of the simulations was confirmed by comparing the predicted 5^{th} and 95^{th} percentiles of predicted concentration–time profiles with the observed data for any validation data sets. When the predicted data points overlapped with those from the observed data sets, which should (normally) contain a measure of spread of observed plasma concentration data (e.g., a standard deviation for each mean concentration point), the prediction was assumed to be valid.

2.3.4 Data analysis

Unless otherwise stated, all simulations of plasma concentration-time profiles were presented as arithmetic mean and 5-95^{th} percentiles. In circumstances where reported concentration-time profiles did not provide corresponding tabulated summary data, the observed data points were retrieved using the WebPlotDigitizer v3.10 (http://arohatgi.info/WebPlotDigitizer/) (229) and superimposed onto simulated profiles for visual predictive checks. Statistical analysis was used to determine statistical difference between different sets of data where necessary.

2.4 Results

2.4.1 Base model development

Model parameters obtained from published sources were used for initial simulation of single doses of 80 mg artemether and 480 mg lumefantrine while keeping all unknown parameters as default values or values predicted based on physicochemical properties of each drug compound. The plasma concentration-time profiles of both drugs using these parameters (listed in Table 2.3) did not recover the observed plasma concentration time points on the published clinical concentration time profiles as reported in two single dose studies reported by Lefevre *et al* (2013) (Figure 2.5 A-B)(230, 231).

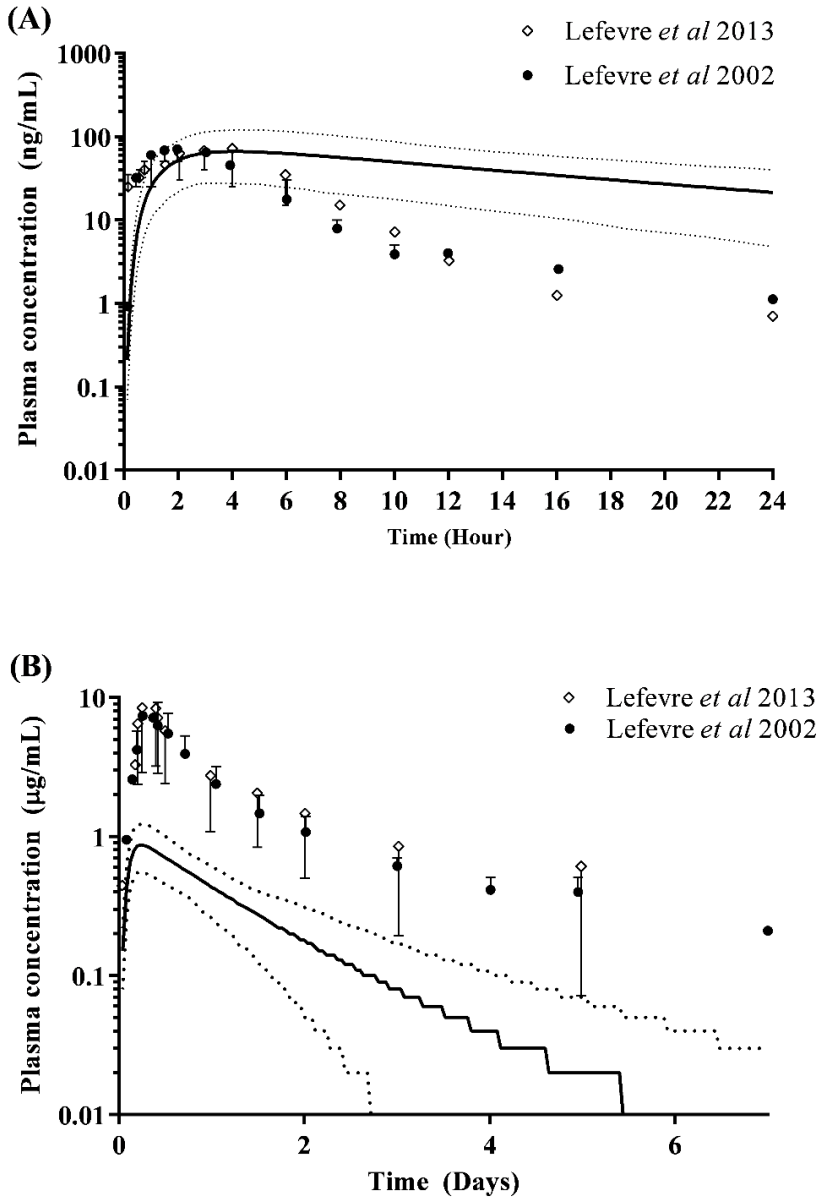

Figure 2.5: Simulation of single dose artemether (A) and lumefantrine (B) with base model

Simulation of (A) artemether and (B) lumefantrine concentration time profiles following a single oral dose of 80 mg and 480 mg respectively using the base model. For all simulations, a standard population size of 100 subjects was used. The solid line represents population mean predictions and the dash lines represent 5^{th} and 95^{th} percentiles of prediction. Mean observed plasma concentrations are represented by the solid circles (Lefevre *et al*, 2002) and diamonds. (Lefevre *et al* 2013). Error bars represent standard deviations.

2.4.2 Step 1: Optimisation and predictive performance for artemether-lumefantrine models for adults

Following optimisation of P_{eff} values obtained from the predicted PSA and HBD parameters, 3.67×10^{-4} cm/s and 0.97×10^{-4} cm/s were obtained for AL respectively. Similarly, following parameterisation of the *Kp* scalar, the simulated distribution phase of the plasma concentration-time profile for artemether and lumefantrine were adequately recovered (Table 2.4; Figure 2.6). The ISEF for scaling rhCYP *in vitro* kinetic data to human liver tissue clearance was parameterised from an initial value of 1 (Table 2.3) for the enzymatic pathways involved in artemether metabolism (CYP3A4 and CYP2B6) to 2.42 and 1.70 (Table 2.4) respectively. For lumefantrine, the retrograde calculation resulted in an estimated intrinsic clearance of 2.61 µL/min/pmol (Table 2.4) from published oral clearance data (172).

The model consistently captured the observed clinical data points for single and multiple dose studies (Figures 2.6 and 2.7) as illustrated in the predicted plasma concentration-time profiles relative to the observed clinical profile. In Figure 2.6, single dose observed clinical concentration-time points were within the 5^{th} and 95^{th} percentiles of the simulated concentration time profile after optimisation of the necessary model parameters. In Figure 2.7, the model did not only recover the clinical data points for the multi-dose study, it also reflected the inter-individual variabilities observed in clinical studies.

The optimised model parameters (Table 2.4) predicted population plasma concentration profiles for both artemether and lumefantrine that recovered the observed mean plasma concentration profiles. The model predicted C_{max} values were within 2-fold of the reported C_{max} for each clinical study for both artemether (139.1 ± 116.2 ng/mL; Table 2.5; Figure 2.6A) and lumefantrine (single dose: 6.31 ± 3.72 µg/mL; six doses: 9.56 µg/mL; range: 5.67-16.78 µg/mL; Table 2.5; Figure 2.6B and 2.7). The 24 h, 48 h, 72 h and day 7 lumefantrine concentrations were also predicted to within 2-fold of those reported by Ashley *et al* (2007) (221). Similarly, the model predicted AUC_{last} for artemether and lumefantrine were within 2-fold of the reported AUC_{last}.

Table 2.4: Final optimised model parameter values and predicted PBPK values for use in the simulation of artemether, lumefantrine.

Parameters	Artemether	Lumefantrine
Compound type	Monoprotic base	Diprotic base
Molecular weight (g/mol)	298.4[209]	528.94[209]
Log P	3.53[210]	8.70[211]
Fu	0.05[212]	0.003 [212]
pKa 1	3.9[209]	14.1[209]
pKa 2	-	9.80[209]
B/P	0.55[a]	0.80[213]
Vss (L/kg)	1.77[a]	0.70[a]
P_{eff} (10^{-4} cm/s)	3.67[b]	0.97[b]
Kp scalar	0.21[b]	0.10[b]
Solubility (mg/mL)	0.012[214]	0.002[215]
CL_{po} (L/min)	-	0.25[172]
$CLint_{3A4}$ (µL/min/pmol)	1.47[216]	2.61[b,c]
$CLint_{2B6}$ (µL/min/pmol)	9.31[216]	-
ISEF CYP3A4	2.424[b]	-
ISEF CYP2B6	1.697[b]	-
Absorption model	ADAM	ADAM
Distribution model	Full	Full

[a] Simcyp® mechanistic prediction; [b] Parameter estimated; [c] Simcyp® retrograde calculation from population estimates of CL_{po} followed by parameter estimation (final optimised value: 0.85 µL/min/pmol for CYP3A4); [d] Unless otherwise detailed data was obtained from Gaohua *et al* (2015) (232). MW: Molecular weight; P_{eff}: human effective permeability; B/P: blood-to-plasma ratio; $CL_{int:\ in\ vitro}$ intrinsic clearance; Vss: Steady state volume of distribution; ISEF: Intersystem extrapolation factor for scaling CYP *in vitro* kinetic data.

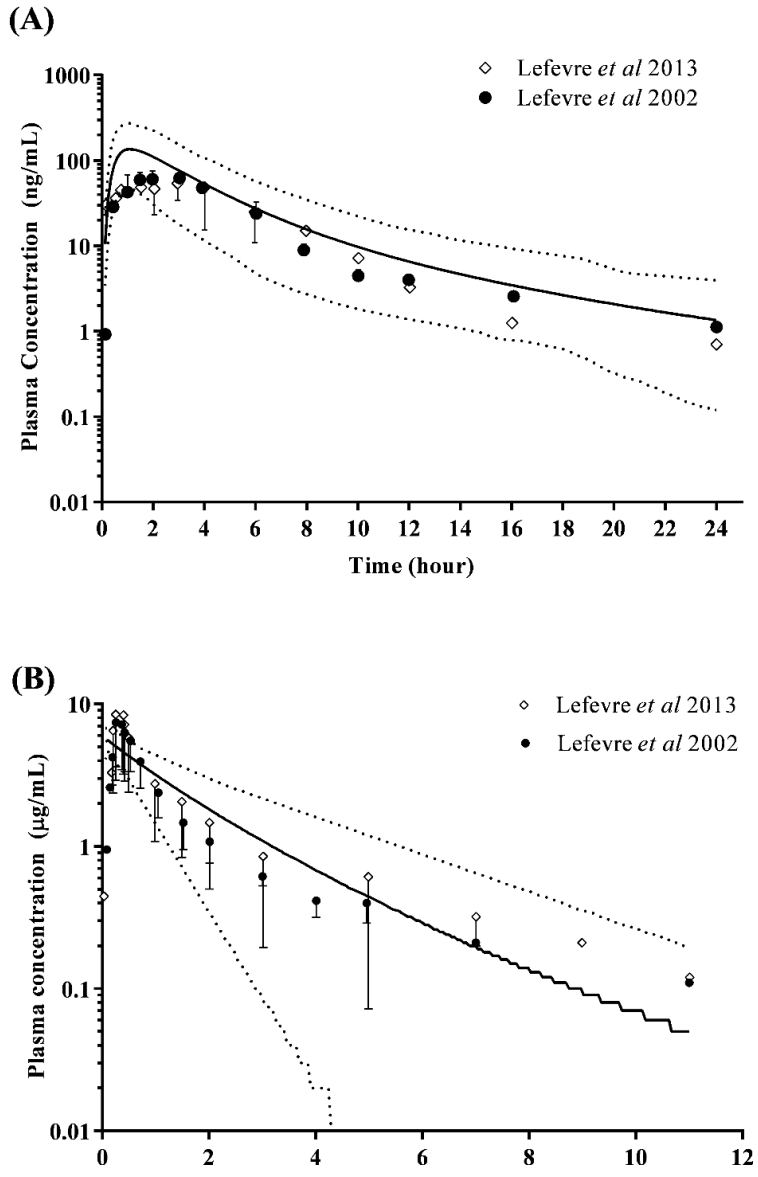

Figure 2.6: Simulation of single dose artemether (A) and lumefantrine (B) using the optimised model

Simulation of (A) artemether and (B) lumefantrine concentration time profiles following a single oral dose of 80 mg and 480 mg respectively using the optimised model. For all simulations, a standard population size of 100 subjects was used. The solid line represents population mean prediction and the dash lines represent 5^{th} and 95^{th} percentiles of prediction. Mean observed plasma concentrations are represented by the solid circle (Lefevre *et al*, 2002) and diamonds (Lefevre *et al* 2013). Error bars represent standard deviations

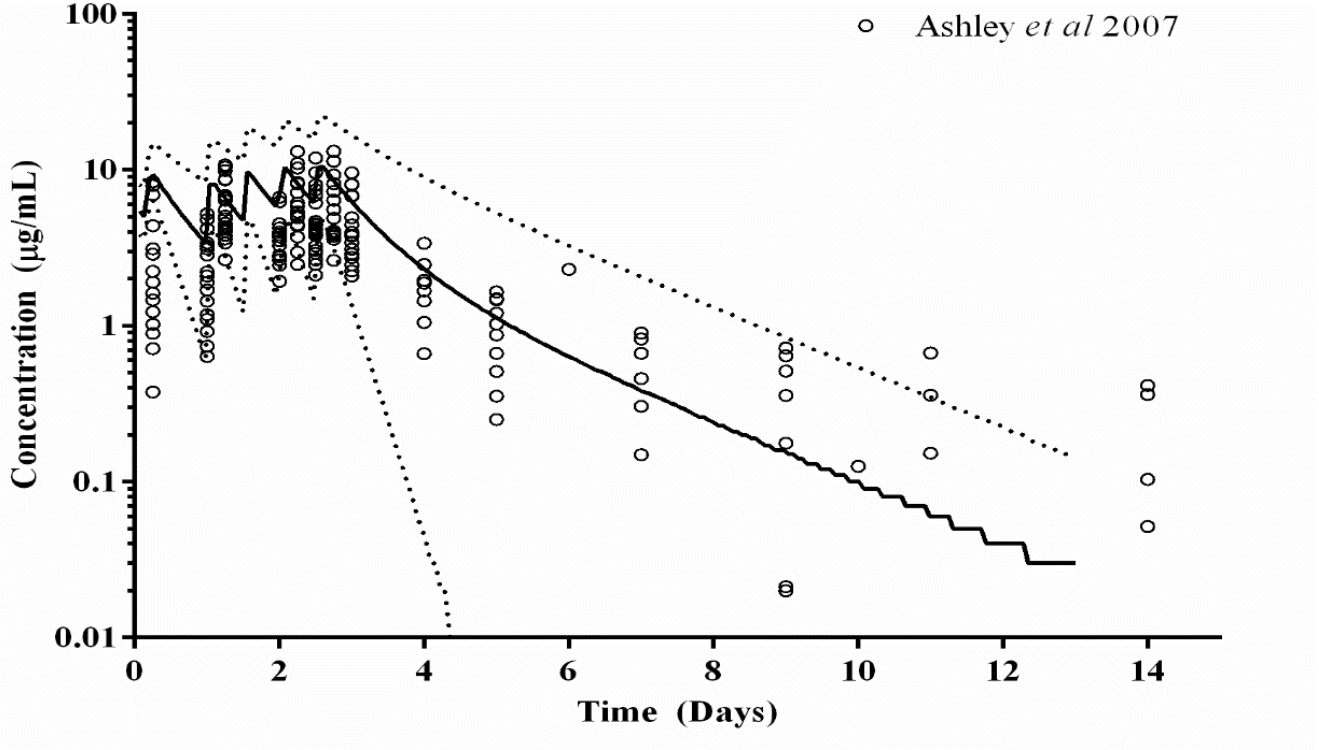

Figure 2.7: The simulated plasma concentration-time profile of multiple dose lumefantrine with the optimised model

Simulation of lumefantrine concentration time profile following a 480 mg six-dose three-day regimen using the final optimised model. A standard population size of 100 subjects was used. The solid line represents population means prediction and the dash lines represent 5th and 95th percentiles of prediction. Individual observed data obtained from Ashley *et al* 2007 (221) points are represented by open solid circle.

Table 2.5: Summary of predicted and observed pharmacokinetic parameters of artemether and lumefantrine in healthy adults

		Prediction	Lefevre *et al* 2013[230]	Lefevre *et al* 2002[220]	Ashley *et al* 2007[221]
Artemether	Dose (mg)	80	80	80	
	Population size (n)	100	58	16	
	C_{max} (ng/ml)	139 ± 116	113 ± 69.5	104 ± 40	
	AUC_{last} (ng/ml.h)	521 ± 254	408 ± 209	302 ± 135	
Lumefantrine	Dose (mg)	480	480	480	
	Population size (n)	100	58	16	
	C_{max} (µg/ml)	6.31 ± 3.72	8.92 ± 3.18	7.91 ± 3.49	
	AUC_{last} (µg/ml.h)	251 ± 112	236 ± 93	195 ± 119	
Lumefantrine[a]	Dose (mg)	6-dose regimen			6-dose regimen
	Population size (n)	100			17
	C_{max} (µg/ml)	9.6 (5.7-16.8)			6.9 (3.7-13.2)
	C_{24h} (pre-dose)	3.4 (2.0-9.3)			2.5 (0.7-9.8)
	C_{48h} (pre-dose)	5.8 (1.5-13.1)			3.8 (1.9-6.8)
	C_{72h} (pre-dose)	5.8 (1.1-12.7)			3.9 (2.2-9.6)
	C_{d7}	0.32 (0.11-0.78)			0.35 (0.20-0.87)
	$AUC_{0-\infty}$ (µg/ml.h)	387 (98-1157)			432 (308-991)

Data represent mean ± SD or mean (range). [a] Concentrations measured at 24, 48 and 72 hours immediately pre-dose are labelled by the subscript time (hour) nominals, with all concentrations units expressed as µg/ml. C_{d7} indicates the 7^{th} day concentration.

2.4.3 Step 2: Simulation of the AL DDIs following exposure to ketoconazole and rifampicin

2.4.3.1 Simulation of AL DDI with concomitant administration of ketoconazole

The artemether and lumefantrine compound files were further assessed for their ability to recapitulate the literature reported extent of DDIs on plasma concentration profiles in adults.

Predictions for inhibition-based DDIs with artemether and ketoconazole resulted in predicted plasma-concentration profiles for the simulated population within the observed range reported by Lefevre *et al* (2002) (231) (Figure 2.8). The predicted C_{max} ratio was 2.49 ± 0.51 compared with a reported ratio of 2.24 and predicted AUC_r was 2.96 ± 0.80 compared to a reported ratio of 2.51 (Table 2.6).

Predictions for inhibition-based DDIs with lumefantrine and ketoconazole, resulted in plasma-concentration profiles for the simulated population within the observed range reported by Lefevre *et al* (2002) (231) (Figure 2.9). The predicted C_{max} ratio was 1.16 ± 0.89 compared with a reported ratio of 1.26 and predicted AUC_r was 2.10 ± 0.54 compared to a reported ratio of 1.65 (Table 2.6). The C_{max} estimated under interaction and no interaction conditions were slightly under predicted, this might be due to the wide inter-individual variation in the absorption of lumefantrine. Lumefantrine is highly lipophilic and its absorption may be erratic. Its erratic absorption may be influenced by concomitant intake of lumfantrine with food (230).

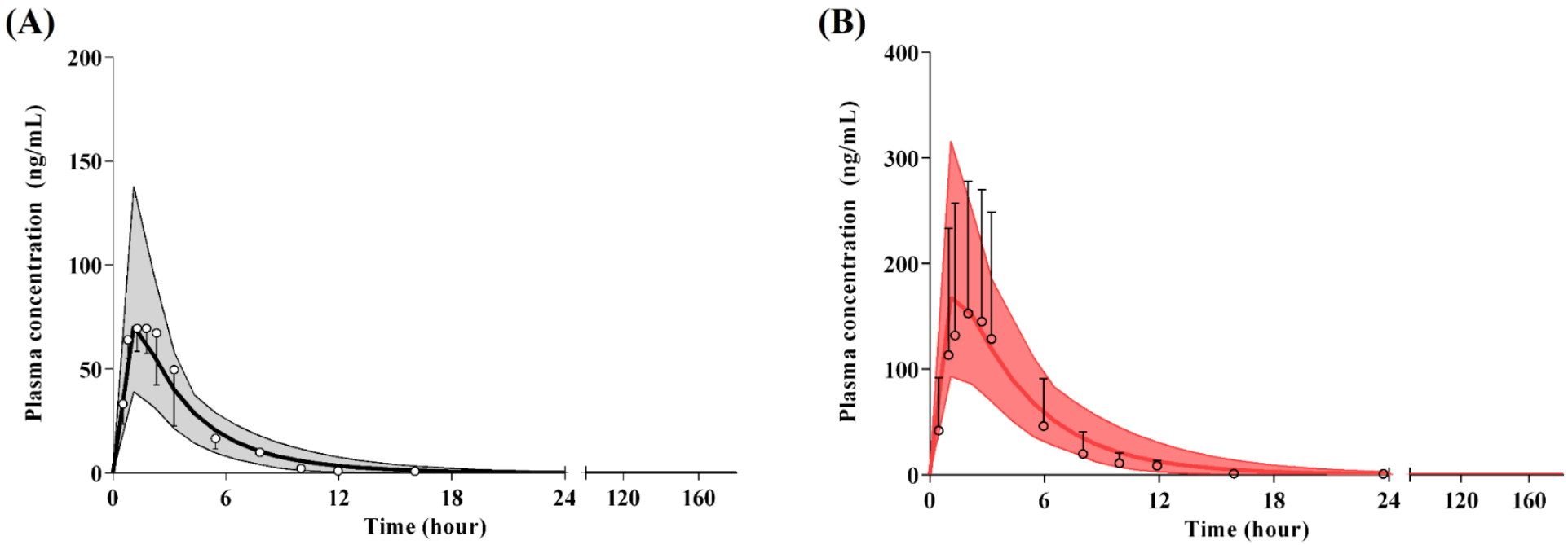

Figure 2.8: The simulated plasma concentration-time profile of artemether in the absence and presence of ketoconazole

Artemether was dosed as a single 80 mg oral dose in the absence (A) and presence (B) of ketoconazole, dosed as a single 400 mg oral dose over a 24-hour period under fed-conditions. Open circles represent observed mean data points (231)

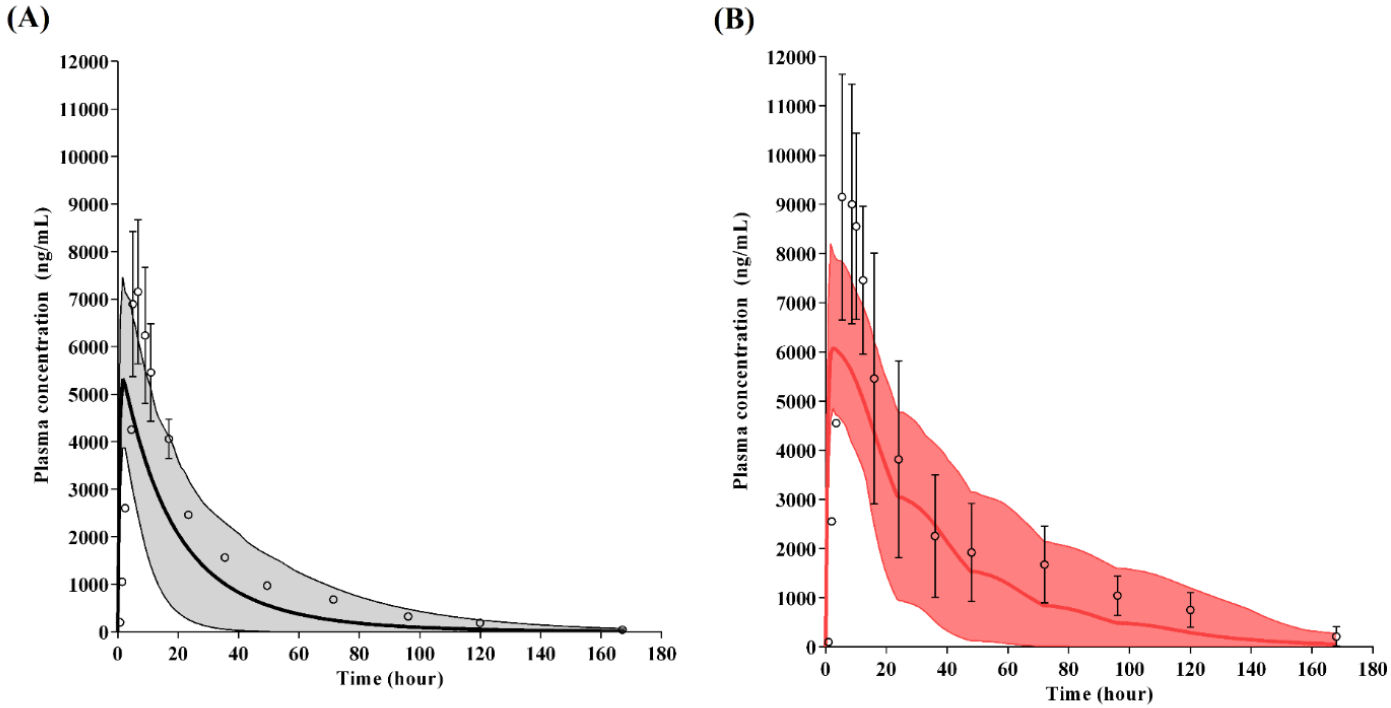

Figure 2.9: The simulated plasma concentration-time profile of lumefantrine in the absence and presence of ketoconazole

Lumefantrine was dosed as a single 80 mg oral dose in the absence (A) and presence (B) of ketoconazole, dosed as a single 400 mg oral dose over a 24-hour period under fed-conditions. Open circles represent observed mean data points (231).

Table 2.6: Summary of predicted and observed pharmacokinetic parameters of artemether and lumefantrine in the absence and presence of ketoconazole in healthy adults

		-Ketoconazole		+Ketoconazole		Ratio	
		C_{max} (ng/mL)	AUC[a] (ng/mL.h)	C_{max} (ng/mL)	AUC[a] (ng/mL.h)	C_{max}	AUC
Artemether	Predicted	71.2 ± 62.7	316.2 ± 96.05	171.39 ± 115.21	911.24 ± 324.60	2.49 ± 0.51	2.96 ± 0.80
	Observed	104 ± 40	302 ± 135	225 ± 77	718 ± 279	2.24	2.51
Lumefantrine	Predicted	5476 ± 2168	118211 ± 57079	6305 ± 2432	235041 ± 97260	1.16 ± 0.89	2.10 ± 0.5
	Observed	7910 ± 3490	195000 ± 119000	10100 ± 4740	312000 ± 181000	1.26	1.65

[a] Artemether: $AUC_{(0-\infty);}$ lumefantrine: $AUC_{(0\text{-last});}$ Data represent mean ± SD.

2.4.3.2 Prediction of AL DDI with concomitant administration of rifampicin.

For induction based DDI studies, only one clinical study was identified where the impact of rifampicin mediated DDIs on the pharmacokinetics of both artemether and lumefantrine in the same subjects was reported (180). This study was a small clinical study involving six subjects and a narrow age and weight range, therefore, a virtual clinical trial of 10 trials consisting of 10 subjects per trial within the weight and age boundaries reported by Lamorde *et al* (2013) was simulated (180). As there was no direct way to specify a weight boundary, the trials containing at least 6 subjects within the correct weight boundaries were selected for study and subsequent analysis.

Predictions for induction-based DDIs with artemether and rifampicin were validated against a single study reporting one concentration time point of artemether at 12-hours (C_{12h}) post final dose (180) in six subjects who were administered AL in the absence and presence of FDC treatment for tuberculosis which included rifampicin (180). In order to account for the net DDI effect of CYP3A4 interaction (that is the CYP3A4 interactions due to the APIs within the FDC), the simulation was conducted in the presence of isoniazid as this has an inhibitory effect on CYP3A4 using a previously validated model for isoniazid (222). The predicted C_{12h} was 3.56 ± 3.13 ng/mL (Figure 2.10) which reduced to 0.77 ± 1.14 ng/mL (Figure 2.11) in the presence of rifampicin, and was within 2-fold of the reported C_{12h} of 0.5 ± 1 ng/mL.

Predictions for induction-based DDIs with lumefantrine and rifampicin were validated against a single study reporting one concentration time point of lumefantrine on the 8th day after initiating lumefantrine dosing (C_{d8}) (7.3 days post first dose). Using this approach, the predicted C_{d8}, 59.83 ± 24.86 ng/mL, was within 2-fold of the observed reported C_{d8} of 107.75 ± 19.58 ng/mL (180) (Figure 2.12).

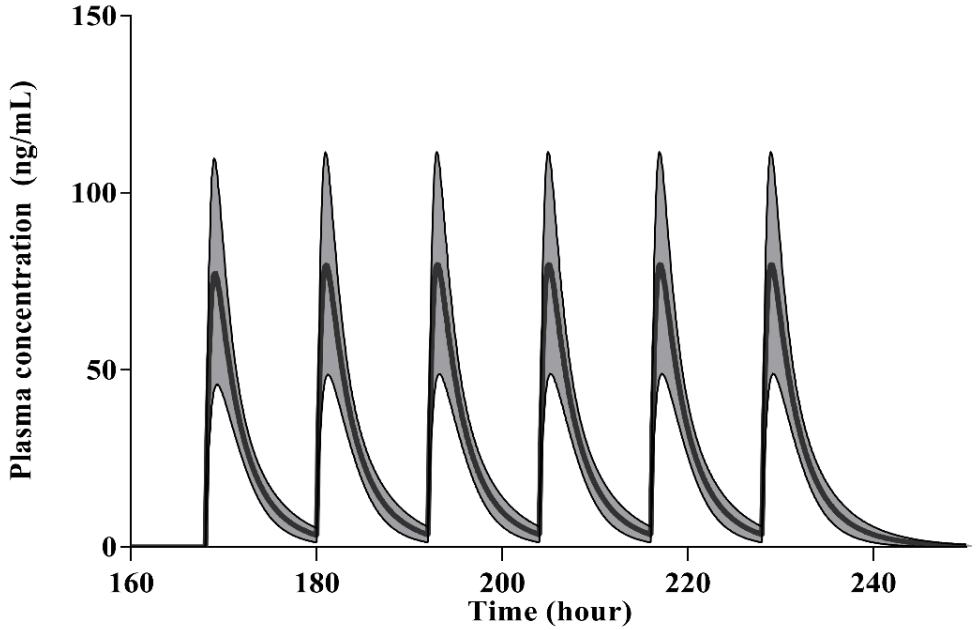

Figure 2.10: The simulated plasma concentration-time profile of artemether in the absence of rifampicin

Artemether was dosed as 6 doses (80 mg per dose) over 3 days (on days 8–10) in the absence of an interaction with a rifampicin based anti-TB medication. The solid line represents the population mean prediction with shaded regions representing the 5th and 95th percentiles of prediction

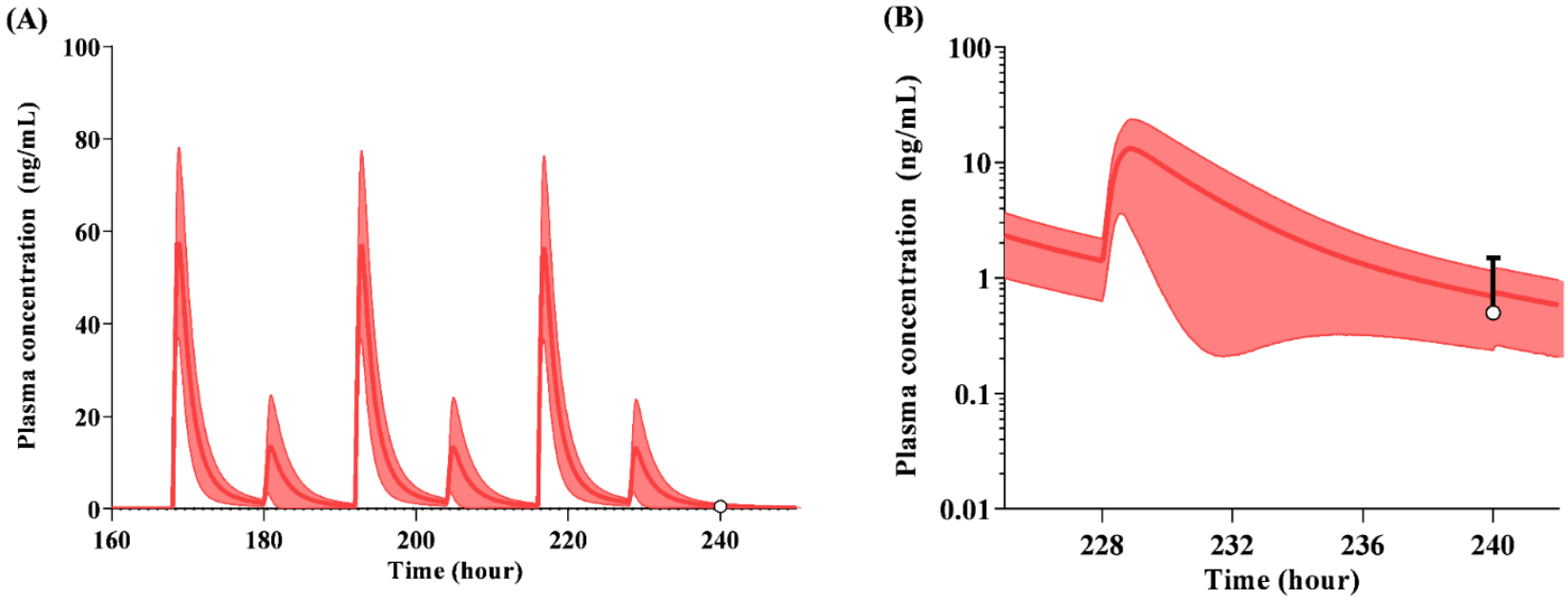

Figure 2.11: The simulated plasma concentration-time profile of artemether in the presence of rifampicin

Artemether was dosed as 6 doses (80 mg per dose) over 3 days (on days 8–10) of a 14-day trial with rifampicin dosed at 10 mg/kg once daily during the duration of the trial. Isoniazid was also dosed at 10 mg/kg and used as a secondary perpetrator considering its inclusion in anti-TB therapy. (A) represents the entire simulation period, (B) represents the last 14 hours of study and the open circle represents the observed mean 12-hour post final dose concentration ± SD. The solid line represents the population mean prediction with shaded regions representing the 5th and 95th percentiles of prediction.

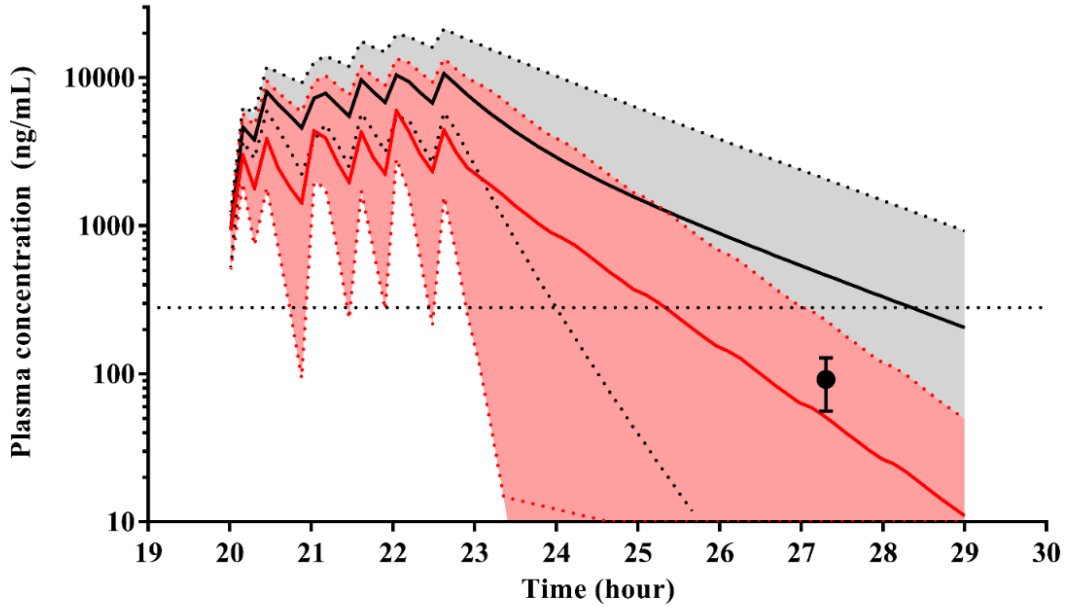

Figure 2.12: Simulated plasma concentration-time profile of lumefantrine in the absence (grey shaded area) and presence (red shaded area) of rifampicin

Lumefantrine was dosed as 6 doses (480 mg per dose) over 3 days (on days 8–10) of a 14-day trial with rifampicin dosed at a dose of 10 mg/kg once daily and isoniazid (secondary perpetrator) administered at a dose of 5 mg/kg during the duration of the trial. Solid circles represent the observed mean day 8 concentration (7.3 h after final dose) ± SD (180). The solid line represents the population mean prediction with shaded regions representing the 5th and 95th percentiles of prediction (grey: no interaction; red: interaction). The dashed line represents minimum effective parasite clearance plasma concentration for lumefantrine (280 ng/mL).

2.4.4 Step 3: Predictive performance of model for artemether and lumefantrine in children

2.4.4.1 Step 3a: Predictive performance of model for artemether

The majority of clinical studies assessing AL pharmacokinetics in children often focus on lumefantrine. Existing artemether clinical studies are sparse and include either sampling around the expected C_{max} (1-2 hours) (233, 234) or limited large population based sampling approaches (235), with dosing based on the body weight stratification. Therefore, the simulations and interpretation of the results were carried out as close as possible to the reported clinical studies.

The model predicted mean artemether plasma concentration for the lower doses (221µg/mL ± 105µg/mL) and higher doses (294 ± 97 µg/mL) were within 2-fold of the literature reported plasma concentrations for both lower (150 ± 206 µg/mL) and higher doses (196 ± 204 µg/mL) (Figure 2.13A) (233). Similarly when using a single lower dose and stratifying further for weight into 5 < 10 kg and 10 to < 15 kg, the reported concentrations for the lower and higher weight banding, 295 ± 214 µg/mL and 137 ± 111 µg/mL, were within the 5^{th} and 95^{th} percentiles of the mean predicted profiles (Figure 2.13B), with a predicted mean concentration (mean of 1 and 2 hour time points) of 226 ± 187µg/mL for the lower weight boundary and 239 ± 187 µg/mL for the higher weight boundary (234) (Figure 2.13B).

To confirm a successful model prediction of the distribution and elimination phases of artemether pharmacokinetics, Figure 2.14 illustrates that the model adequately predicted the concentration-time profiles for artemether dosing at the lowest (5-14 kg) and highest (25-34 kg) doses, where observed sampling points were obtained from a population study reported by Hietala *et al* (2010) (235). The predicted profile for each dosing band fell within the range reported by Hietala *et al* (2010) (235). However, due to the well documented variability in the absorption phase of artemether, the predicted concentrations during the absorption phases (0-4 hours) were slightly over-predicted.

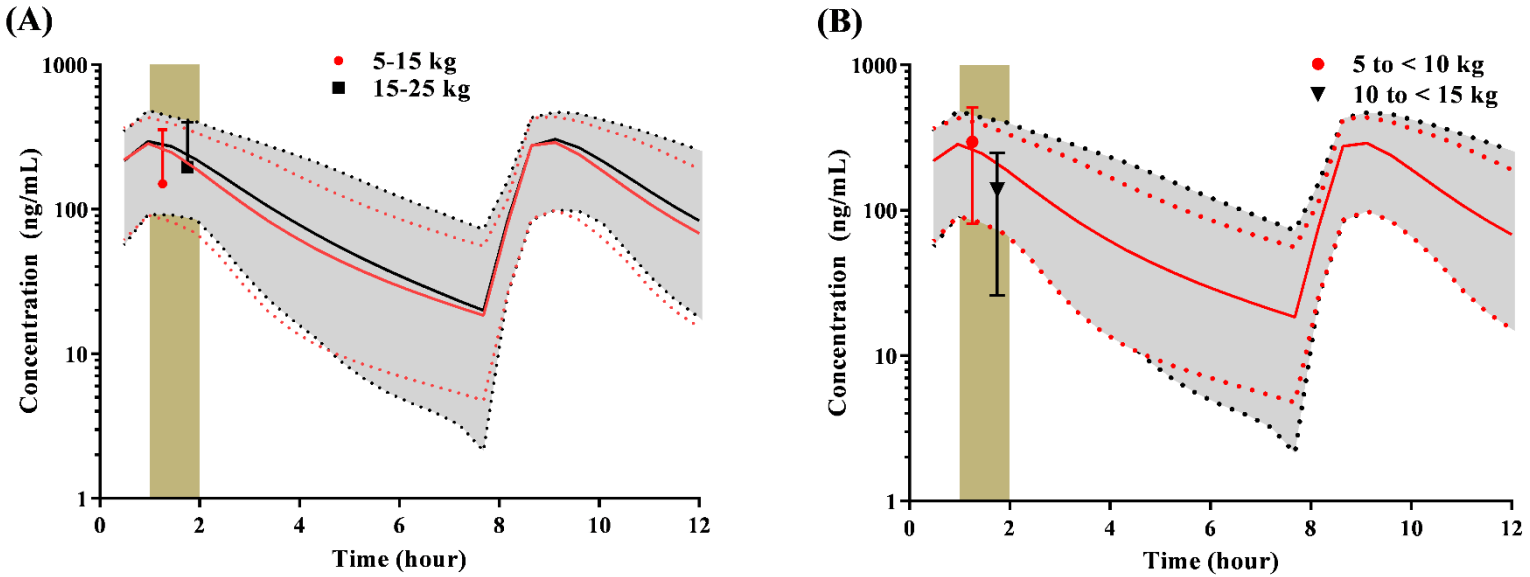

Figure 2.13: The simulated plasma concentration-time profile of artemether in paediatrics.

Six doses of artemether were administered at 0, 8, 24, 36, 48 and 60 h based on patient weight (20 mg: 5–15 kg or 40 mg: 15-25 kg). Shaded regions between 1 and 2 h indicate observed sampling times (1–2 h). Red circles, black squares, and black diamonds are observed clinical data from subjects receiving the weight-based doses. (A): Observed data from Djimde *et al* (2012) and (B): Observed data from Bassat *et al* (2011) (233, 234). The red and black solid lines indicate mean profiles for the corresponding weight-based doses while the 5th and 95th percentiles are illustrated by the corresponding coloured dash lines.

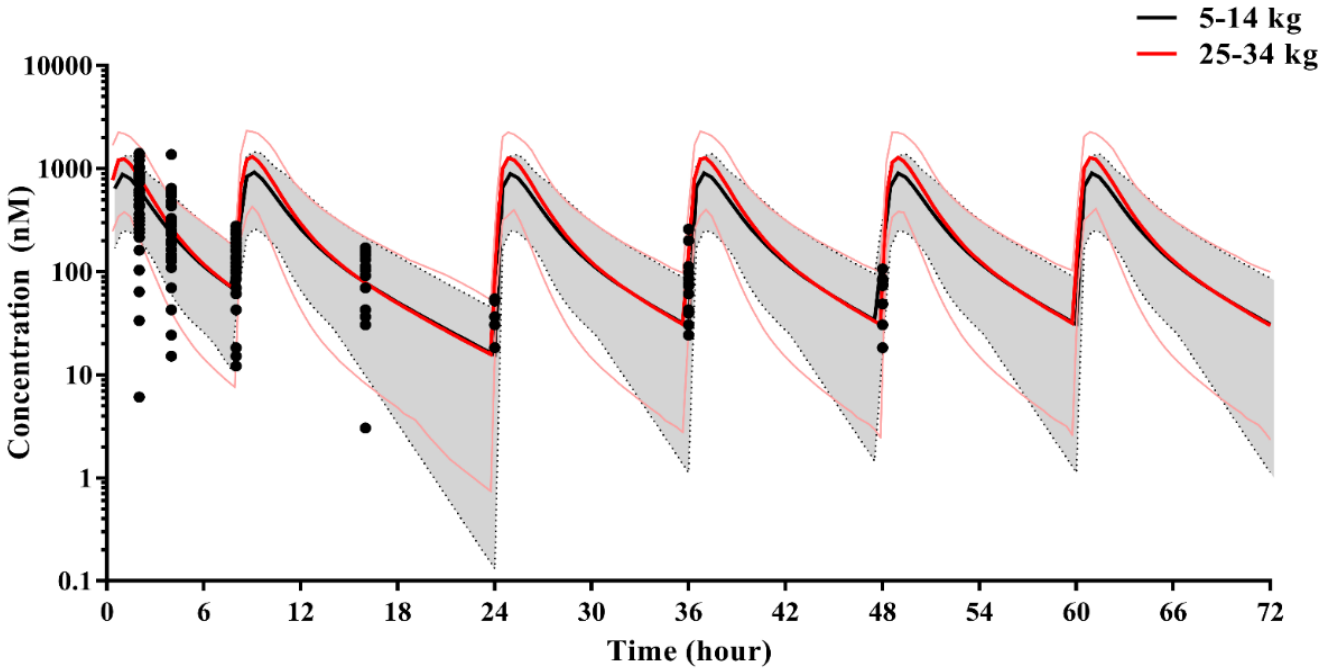

Figure 2.14: The simulated plasma concentration-time profile of artemether in paediatrics.

Six doses of artemether were administered at 0, 8, 24, 36, 48 and 60 h based on patient weight. The black line represents simulated lower doses (5–14 kg) and the red line represents the simulated highest dose (25–34 kg). Observed data points are represented by solid black circles (180) with red and black solid lines indicating mean profiles with 5th and 95th percentiles illustrated by coloured dashed lines.

2.4.4.2 Step 3b: Predictive performance for lumefantrine

Lumefantrine is often studied, in preference to artemether, in clinical trials due its longer half-life (231) (160), and a range of clinical studies are available to validate the PBPK-based model development where 7-day post-dosing concentration (~280 ng/mL (172)) is used as a marker of achieving a successful 'target' concentration to obtain parasite clearance. To validate the lumefantrine compound we first assessed the predictive performance against two studies that reportedmean plasma concentrations through the study duration period. Based on a study by Borrman *et al* (2010) (49) where mean ± SD plasma concentration data was available for 30, 54, 66, 84 and 168 hours post first dose, the $CL_{int,3A4}$ was optimised to 0.71 and K_p scalar optimised to 0.05 (Vss: 0.53 L/kg). Using this revised lumefantrine compound file, the 4 concentration time-points reported by Borrmann *et al* (2010) over the 3 doses stratification used in their study was recovered (Figure 2.15).

This optimised compound file was then applied to all subsequent simulations, and was confirmed with a second study reported by Piola *et al* (2005) (173) where the pharmacokinetics of lumefantrine in 5-14 year olds were simulated with appropriate weight-based dosing, and where observed mean ± SD plasma concentration data was available for day 3 and day 7 (Figure 2.16). Day 3 predicted concentrations were 7958 ± 2381 ng/mL and 8246 ± 5478 ng/mL for the 5-15 kg and 15-25 kg doses, and day 7 predicted concentrations were 659 ± 289 ng/mL and 719 ± 554 ng/mL for the 5-15 kg and 15-25 kg doses. The observed day 3 (7050 ± 3560 ng/mL) and day 7 (376 ± 217 ng/mL) mean plasma concentrations were within 2-fold of the predicted mean concentrations, in addition to being within the 5^{th} and 95^{th} percentiles of the mean lumefantrine predicted plasma concentration for the two weight-based doses (Figure 2.16). The optimised compound file was further utilised to assess the predictive performance for median day 3 and day 7 (predominantly) concentrations (Table 2.7) and was able to capture day 3 and day 7 concentrations to within 2-fold of those reported in clinical studies. In the observed studies, the reported lumefantrine concentrations were not segregated based on the doses taken by the children and the studies only reported median and range concentrations for all the paediatric subjects regardless of the doses they were administered. In this study however, day 7 concentrations were recorded separately based on the doses the patients were administered.

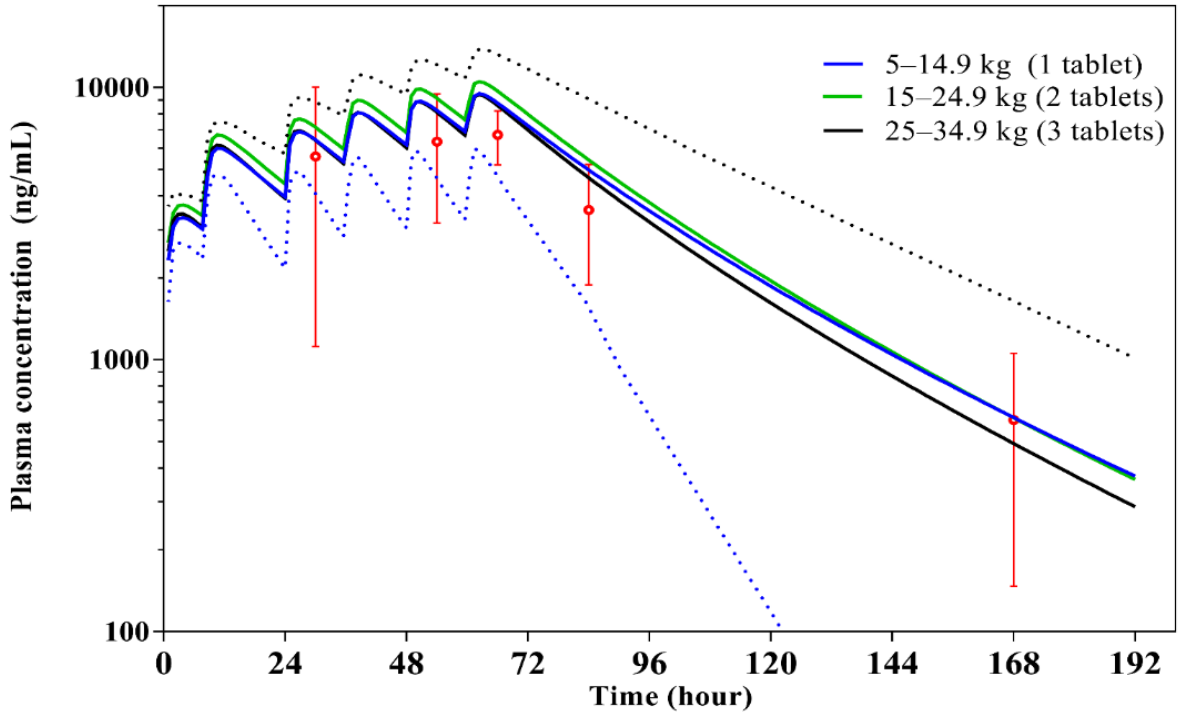

Figure 2.15: The simulated plasma concentration-time profile of lumefantrine in children.

Blue, green and black solid lines indicate 1 (5–14.9 kg), 2 (15–24.9 kg) or 3 (25–34.9 kg) tablet dosing regimens respectively. Upper and lower dashed lines represent the 95th percentile for the 360 mg (3 tablets) dose and 5th percentile for the 120 mg (1 tablet) dose, respectively. Red circles represent mean population observed concentrations reported in (49).

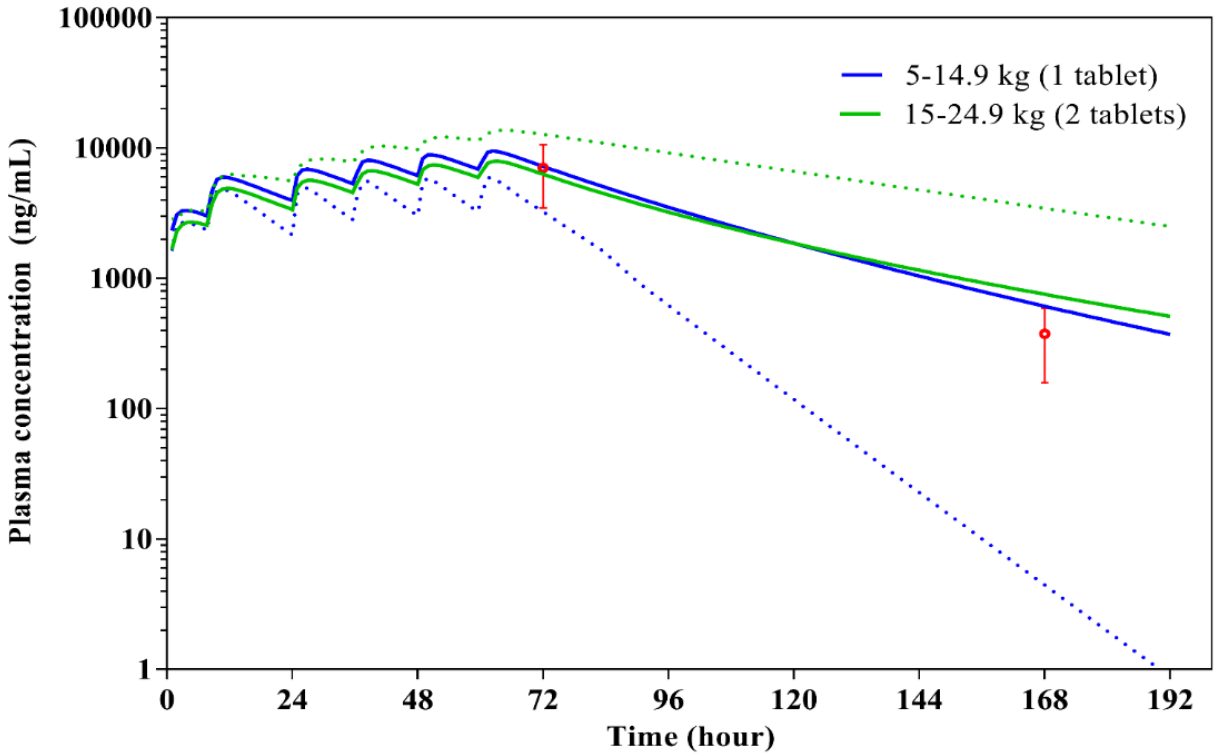

Figure 2.16: The simulated plasma concentration-time profile of lumefantrine in children.

Blue and green solid lines indicate increasing doses of lumefantrine (1 tablet: 5–14.9 kg); 2 tablets 15–24.9 kg). Upper and lower dashed lines represent the 95th percentile for the 240 mg dose and 5th percentile for the 120 mg dose, respectively. Red circles represented mean population observed concentration reported in (173).

Table 2.7: Summary of simulated and observed median day 3 or day 7 lumefantrine concentrations in children

Study	Notes	Observed Median Concentration [Range] (ng/mL)		Simulated Median Concentration [Range] (ng/mL)	
		Day 3	Day 7	Day 3	Day 7[a]
Mayxay *et al* (2004) (236)	n=77; 95% CI reported	-	520 [390–650]	-	1 tablet: 374 [0.1-2341] 2 tablets: 392 [0.1-4719] 3 tablets: 411 [0.3-4853]
Schramm *et al* (2013) (237)	n=139; IQR reported; ACRP results	-	356 [211-547]	-	1 tablets [b]: 369 [37-885]
Ngasala *et al* (2011) (238)	n=177; Range reported	-	205 [0-1887]	-	1 tablet: 392 [0.12-6785] 2 tablets: 408 [0.13-7511]
Borrmann *et al* (2011) (239)	n=15; Range reported from 2005-2006 study	-	536 [178-3270]	-	369[c] [0.1-5028]
Checchi *et al* (2006) (240)	n=70; Range reported in supervised group in under 5 years	7050 [1876-14985]	367 [0.12-768]	4877 [1678-25285]	1 tablet: 389 [0.1-7544] 2 tablets: 348 [0.3-8641]

[a] Simulated day 7 median concentrations were predicted following dosing based on body-weight stratification as a result of the lack of clear; age-weight dosing strategies detailed in the observed studies. Doses were given at the regimens stated in the studies simulated; [b] Observed study demographics required a single tablet dosing of AL based on weight; [c] Dosed as 12mg/kg.

2.4.5 Step 4: Simulating the impact of rifampicin-mediated CYP3A4 induction on artemether and lumefantrine pharmacokinetics in children

The presence of tuberculosis is thought to occur in at least 37.5 % of subjects infected with malaria (179), and given the potential for TB treatments to attenuate CYP-mediated drug metabolism (rifampicin being a CYP3A4 inducer and isoniazid a CYP3A4 inhibitor), the potential risk in paediatric patients is important to assess considering the ontogeny CYP3A4 expression during the first 5 years of life (202-204). Simulations to predict the potential impact of TB treatment on subjects who are on anti-malarial treatment were assessed to quantify the change in AL plasma concentrations in the absence and presence of dosing with rifampicin (and isoniazid) for subjects of 2-5 years of age with weight-based dosing (1 tablet: 5-14.9 kg and 2 tablets 15-24.5 kg) where rifampicin (and isoniazid) was dosed daily for 7 days prior to the initiation of AL.

2.4.5.1 Artemether

A DDI initiated with a combination of rifampicin and isoniazid significantly reduced the C_{max} for both one and two tablet regimens by approximately 80 %, with a calculated C_{max} ratio of 0.21 (Figure 2.17) (Table 2.8). Similarly, a significant reduction in the AUC following the DDI resulted in an AUC_r of 0.22 (Table 2.8) (Figure 2.17). No differences in the overall impact of the DDI between the two dosing groups was reported suggesting the magnitude of the DDI is similar across the 2-5 years' age range.

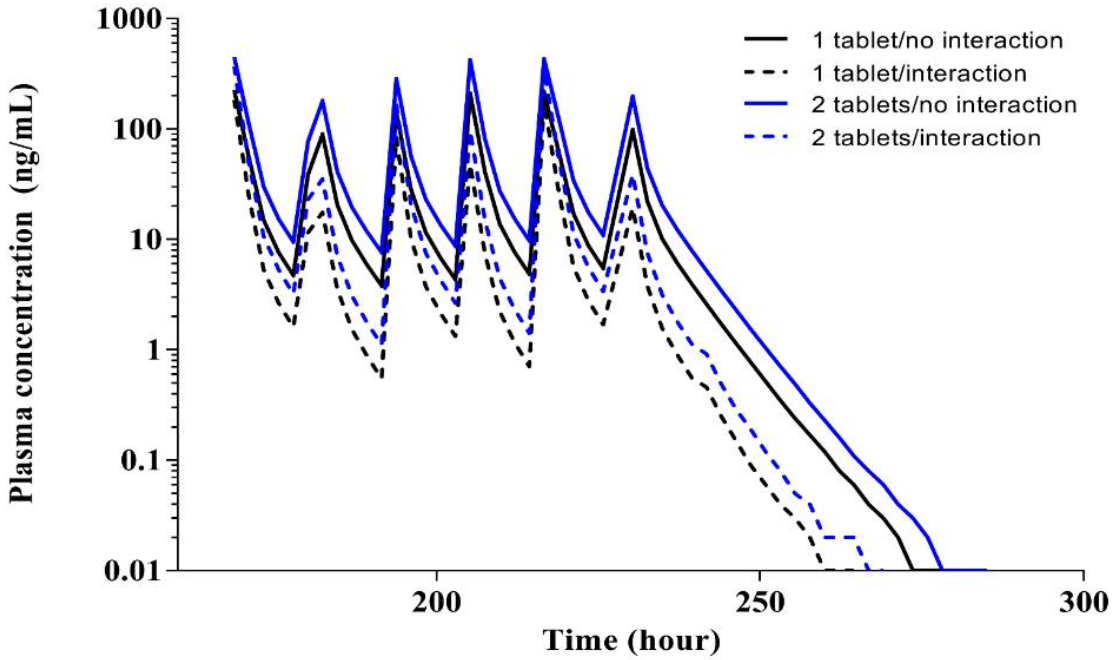

Figure 2.17: The simulated mean plasma concentration-time profile of artemether in paediatrics in the absence and presence of a DDI

Artemether plasma concentrations following a regular six-dose over three days regimen with 1 tablet (5–14.9 kg) or 2 tablets (15–24.5 kg) per dose to children (2–5 years) in a 14-day trial with rifampicin. Solid lines represent clinical trials with artemether alone. Dashed lines represented artemether dosing with rifampicin (10 mg/kg). One tablet doses are indicated in black and two tablet doses in blue. Isoniazid was also dosed at 10 mg/kg and used as a secondary perpetrator considering its inclusion in anti-TB therapy.

Table 2.8: Summary of predicted artemether pharmacokinetics in the absence and presence of a DDI in children aged 2-5 year.

	No Rifampicin		Rifampicin		Ratio	
	C_{max} (ng/mL)	AUC (ng/mL.h)	C_{max} (ng/mL)	AUC (ng/mL.h)	C_{max}	AUC
One	89.1± 78.9	564 ± 317	18.5 ± 31	121 ± 143	0.21	0.22
Two	210 ± 179	1127 ± 633	39.1 ± 136	243 ± 290	0.18	0.21

C_{max} data is from the final dose; AUC calculated from final dose to end of study period. "One": subject dosed one (20/120 mg AL) tablet; "two"; subject dosed two (40/240 mg AL) tablets.

2.4.5.2 Lumefantrine

In the absence of a DDI (i.e. malaria only patients), the predicted mean day 7 concentration was above the minimum therapeutic target of 280 ng/mL (Figure 2.18) for both the single tablet per dose (5-14.9 kg) and two tablets per dose (15-24.9 kg) strategies, 300.49 ng/mL (range: 0.1-4442 ng/mL) and 614.37 ng/mL (range: 0.14-6485 ng/mL) respectively (Table 2.9).

However, in TB co-infected patients receiving lumefantrine and rifampicin, the predicted day 7 concentration fell significantly below the therapeutic target of 280 ng/mL for both the single and two tablet regimens, with a calculated AUC_r of 0.41 and AUC_r 0.40 respectively (data not shown) and no subjects presented with a simulated day 7 concentration of > 280 ng/mL (Table 2.9). The potential risk for failure of AMT is therefore of significant concern in TB co-infected paediatric patients, particularly those falling into the lower body-weight stratification who would typically be younger in age and therefore more prone to treatment failure.

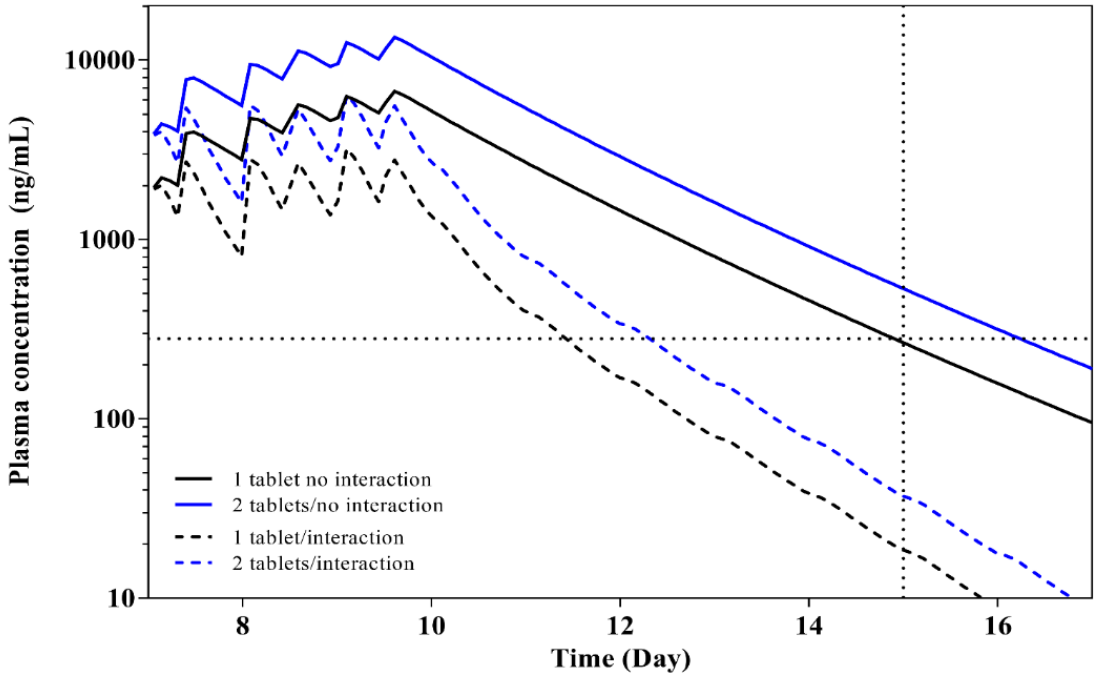

Figure 2.18: The simulated mean plasma concentration-time profile of lumefantrine in paediatrics in the absence and presence of a DDI for a standard 3-day regimen

Lumefantrine plasma concentrations following dosing with 1 tablet (5–14.9 kg) or 2 tablets (15–24.5 kg) to children (2–5 years). Solid lines represent clinical trials with lumefantrine alone. Dashed lines represent lumefantrine dosing with rifampicin (10 mg/kg). Isoniazid was also dosed at 10 mg/kg and used as a secondary perpetrator considering its inclusion in anti-TB therapy.

2.4.6 Dose optimisation

Given that orally administrated AL often shows absorption saturation kinetics, to overcome the risk of significant treatment failure increasing the dose of AL administered in each FDC would not be appropriate. We assessed the impact of increasing the duration of treatment from 3 days to 5 or 7 days on the potential impact on day 7 lumefantrine concentrations (Figure 2.19-2.20).

Increasing the duration of treatment to 5 days had a minimal impact on day 7 mean concentrations, with a modest increase for the single tablet to 63.63 ng/mL leading to a 11.1 % (n=5/46) increase in the subjects with day 7 target > 280 ng (Table 2.9) (Figure 2.19). Similarly, for the two-tablet treatment an increase in the mean day 7 concentration was simulated at 76.9 ng/mL which resulted in an overall increase in subjects with a target concentration > 280 ng of 11.3 % (n=6/53) (Table 2.9) (Figure 2.20). However, for a 7-day treatment 63 % (one tablet) and 74.5 % (two tablets) of subjects demonstrated a day 7 concentration in excess of 280 ng/mL (Table 2.9) (Figure 2.20).

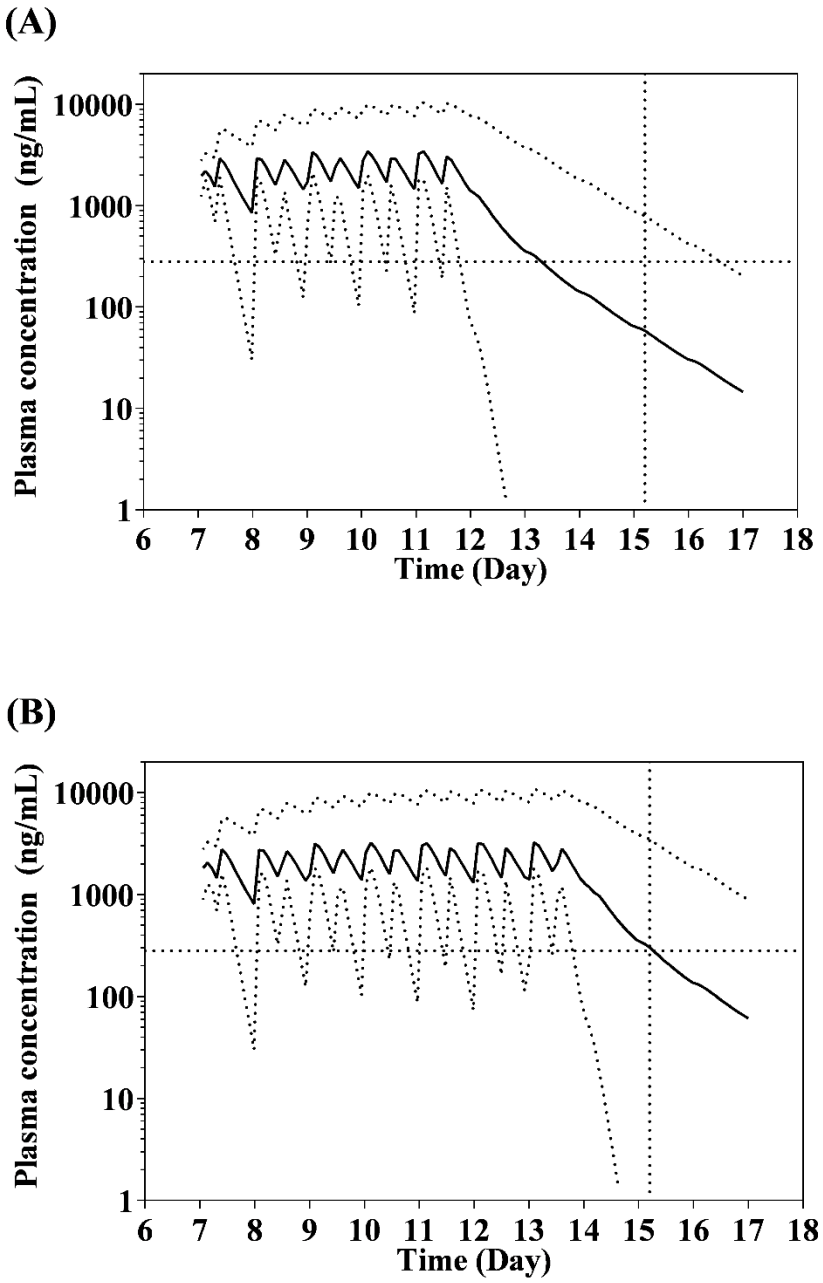

Figure 2.19: The simulated mean plasma concentration-time profile of one tablet of lumefantrine in paediatrics in the presence of a DDI for an adapted 5 (A) and 7-day (B) regimen.

Lumefantrine plasma concentrations following dosing with one tablet (5–14.9 kg) to children (2–5 years) in the presence of rifampicin (10 mg/kg) when dosed for 5 days (upper panels) or 7 days (lower panels). Solid lines represent mean and dashed line represent upper and lower ranges of predicted concentrations with shaded regions representing the range of predicted concentrations. Isoniazid was also dosed at 10 mg/kg and used as a secondary DDI perpetrator.

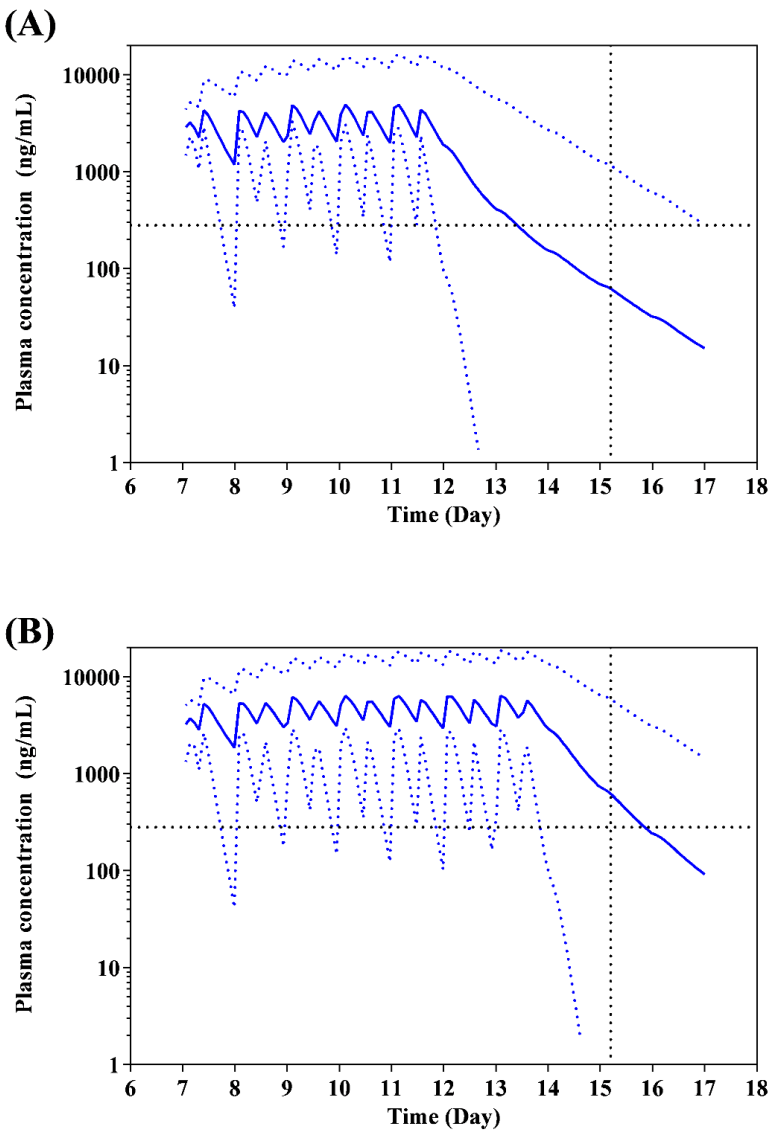

Figure 2.20: The simulated mean plasma concentration-time profile of two tablets of lumefantrine in paediatrics in the presence of a DDI for an adapted 5 (A) and 7-day (B) regimen.

Lumefantrine plasma concentrations following dosing with two tablets (15–24.5 kg) to children (2–5 years) in the presence of rifampicin (10 mg/kg) when dosed for 5 days (upper panels) or 7 days (lower panels). Solid lines represent mean and dashed lines represent upper and lower ranges of predicted concentrations with shaded regions representing the range of predictions concentrations. Isoniazid was also dosed at 10 mg/kg and used as a secondary DDI perpetrator.

Table 2.9:Summary of predicted mean day 7 lumefantrine concentrations during a 3, 5 and 7-day treatment schedule in children

Dosing	Mean C_{d7} (Range) (ng/mL)			Lumefantrine ≥ 280ng/mL[a]		
	Regimen			Regimen		
	3 day	5 day	7 day	3 day	5 day	7 day
1 tablet/NI	300.(0.1-4442)	1451 (15.2-8367)	7509 (79.7-12438)	47.8 (n=22)	86.7 (n=39)	95.6 (n=44)
1 tablet/I	18.1 (0.01-88.9)	63.6 (0.01-578)	329 (0.12-4385)	0	11.1 (n=5)	63 (n=29)
2 tablets/NI	614 (0.14-6485)	1516 (14.9-9656)	9748 (28.5-14375)	46.6 (n=21)	60.3 (n=32)	85 (n=40)
2 tablets/I	42.7 (0.01-154)	76.9 (0.02-1087)	704 (0.08-7895)	0	11.3 (n=6)	74.5 (n=35)

[a] Percentage (number) of subjects with C_{d7} ≥ 280ng/mL; 3 days: 1 tablet (n=53), 2 tablets (n=45); 5 days: 1 tablet (n=46), 2 tablets (n=53); 7 days: 1 tablet (n=46), 2 tablets (n=47). NI: no interaction; I: interaction. C_{d7}: mean day 7 concentration.

2.5 Discussion

Children are more vulnerable to the effects and complications of malaria infections than adults (153). The need for optimising the dosing strategy of antimalarials in children especially in the case where there is the risk of clinically significant DDI is very important because they are often excluded from clinical trials for ethical reasons. In the highly likely case when children are coinfected with malaria and tuberculosis, there are currently no clear guidelines on how to treat malaria infection in a child using anti-tuberculosis (anti-TB) therapy. Antimalarial drugs like AL, which are available in resource limited countries to treat malaria, significantly interact with the standard anti-tuberculosis regimens, in fact, the administration of AL and the standard rifampicin based anti-TB cocktail is contraindicated in adults (180).

The ultimate goal of this study was to address the potential risk associated with DDIs related to tuberculosis therapy in children between 2-5 years of age. This age group accommodates the lowest dosing range (age based) for use of both AL and rifampicin. Our modelling strategy included a 4-step approach commencing with the prediction of AL pharmacokinetics in adult population groups with the developed and validated compound files (Step 1 and 2) before scaling the model to paediatric subjects and validating with published non-DDI clinical studies (Step 3). Finally, potential AL DDI risks in co-infected malaria-tuberculosis children receiving a rifampicin based anti-TB regimen were simulated which was then followed by proposing dosing optimisation strategies (Step 4).

2.5.1 Model development

The development of a PBPK model which is able to predict clinically observed pharmacokinetic parameters of APIs is key in PBPK modelling and hinges on the concept of *in vitro* to *in vivo* extrapolation (IVIVE) approaches whereby mechanistic *in vitro* parameters are used in a bottom-to-top fashion to predict *in vivo* pharmacokinetic parameters of drugs (138). Since PBPK modelling is mainly dependent on mechanistic data, the challenge of unavailability of certain *in vitro* data poses a significant challenge on the ability to successfully develop the models. For example, in this study, the effective permeability (P_{eff}) values of AL, an important parameter to mechanistically predict their absorption rate constants (k_a) might have been estimated from the apparent permeability (P_{app}) value obtain in *in vitro* cell-based models like Caco-2, but due to unavailability of

published P_{app} values for AL, the molecular descriptors of AL, that is, the polar surface area (PSA) value and the hydrogen bond donor of the drug were used to predict the P_{eff} value for both compounds using equation 43. The resultant predicted P_{eff} values did not adequately recover the absorption profile of the observed clinical data of AL as seen in Figures 2.5A-B but following the optimisation of the predicted P_{eff} parameter, there was an improvement in the simulation of the absorption phases of AL in both single and multiple dose simulations (Figures 2. 6A-B, 2.7). As an example, the optimised P_{eff} value for lumefantrine (Table 2.2) resulted in estimation of k_a as 0.43 h^{-1} at a 30% coefficient of variation. This was similar to the k_a values reported in Salman *et al* (2011) and Tchaparian *et al* (2016) as 0.46 h^{-1} and 0.45 h^{-1} respectively (241, 242). While the f_a values of lumefantrine are scarcely reported, a study reported an estimate of $f_a \approx 1$ (243); again this value is close to predicted lumefantrine f_a (0.73) in this current study.

2.5.2 Simulation of AL pharmacokinetics in adults in the presence and absence of DDIs

In adults, successful AL model development (Step 1) was achieved through comparison to 3 key clinical studies quantifying both artemether and lumefantrine in each study and all predictions were within 2-fold of the reported C_{max} and AUC from clinical studies (Table 2.5). The large variability in the absorption phase of artemether and lumefantrine (Figure 2.6B, 2.7) was evident in the observed clinical data and the slight model over prediction may be as a result of the lower limit of detection for artemether in the studies reported by Lefevre *et al* (2002, 2013) (220, 230) compared to that reported by Bindschedler *et al* (2002)(244).

Following successful model development, the ability of each compound file to mechanistically predict a DDI was then assessed through the use of two inbuilt Simcyp® inhibitors, namely ketoconazole (CYP3A4 inhibitor) and rifampicin (CYP3A4 inducer) (Step 2). For CYP3A4 inhibition, the model was able to recapitulate the extent of DDIs with reported plasma concentrations within the predicted 5^{th}-95^{th} percentiles for the simulation for artemether and lumefantrine (Figure 2.8-2.9 and Table 2.6).

For the induction-based interactions of CYP3A4 with AL, very few reports have characterised rifampicin mediated DDIs and we utilised a study which reported AL concentration within the same subjects (180). Under these circumstances, the model

predicted 12-hour post final dose concentration (artemether) and day 8 concentration (lumefantrine) was similar (within 2-fold) to that reported by Lamorde *et al* (2013) (Figure 2.10-2.12) (180). Steps 1 and 2 demonstrate the ability of the developed AL models to replicate pharmacokinetic parameters reported from a range of non-DDI and DDI studies, confirming successful model development.

2.5.3 Simulation of AL pharmacokinetics in presence and absence of DDI in children.

2.5.3.1 DDI with AL in paediatrics in developing countries

Although standard regimens for malaria treatment have shown positive treatment benefits with a reduction in mortality rates (2), in many developing countries with a high burden of communicable disease such as HIV/AIDS and tuberculosis, the risk potential of DDIs with co-infected malaria patients is high (179). Such DDI issues are more apparent in children where the recruitment and inclusion of such onto antimalarial clinical trials is limited. Pragmatically assessing the risk of DDIs in paediatrics is difficult due to CYP-ontogeny observed in key drug metabolic pathways associated the AL metabolism, mainly CYP3A4, during the first 5 years of life (202-204), where maturation of CYP3A4 expression may lead to both altered plasma concentrations of CYP3A4-subtrates (such as AL) whilst also dynamically altering the magnitude of any CYP3A4-induction process. Rifampicin is a known potent CYP3A4 inducer, and therefore has the potential to lead to AL treatment failure if the antimalarial metabolic pathway favours CYP3A4-mediated transformation.

2.5.3.2 The usefulness of PBPK modelling approach in studying the pharmacokinetics of drugs in children

The study of pharmacokinetics in paediatric population groups is often neglected for many therapeutic agents because of complexities in ethical/legal and recruitment strategies coupled with the requirement for limited sample collection and often diverse population-based data analysis.

Although allometric scaling remains a useful tool for first predictions of primary pharmacokinetic parameters such as V_{ss} or clearance (245, 246) it can often fail in the prediction of clearance (247-250), when assessing dosing-optimisation strategies in paediatrics (251) and in situations where body weight may be significantly variable based

on geographical locations (252). Further, allometry often does not address the impact of maturation at early ages of childhood and can often over-predict clearance during the maturation of metabolic elimination pathways (253). However, PBPK modelling can be used to support population modelling approaches such that deviations in covariate models can be built into the model based on the mechanistic knowledge of the physiological or biochemical variation in parameters in the population under study allowing the rational extrapolation of a drug pharmacokinetics across age groups. In light of these facts, PBPK is now gaining regulatory acceptance (108, 141, 254-256) as one approach to assess pharmacokinetics in paediatric patients (257) and in complex scenarios such as DDIs (258, 259).

2.5.4 AL pharmacokinetics and interaction with rifampicin in children

To consider the potential impact of a DDI on AL pharmacokinetics in 2-5-year olds, it was important to demonstrate the capability of the developed model to predict AL pharmacokinetics in children. To this end, step 3 focussed on validation of artemether and lumefantrine in children. Artemether model predictions in children were able to capture the differences in weight-based dosing strategies on the outcome pharmacokinetic profiles, both in 'single' point concentrations centred around the C_{max} (Figure 2.13-14) and population-based sampling over a dosing period (Figure 2.11). Lumefantrine model predictions required an optimisation step and following this optimisation procedure, observed time-point data for 30, 54, 66, 84 and 168 hours (49) and the day 3 and day 7 points (173) were within 2-fold of the simulated profiles and within the 5^{th} and 95^{th} percentiles of the mean predicted profiles (Figure 2.15-16). Lumefantrine model predictions were finally further validated using median concentration data at day 3 or day 7 (Table 2.7), which were found to be well predicted and within 2-fold of the reported concentrations. The approach described in Step 3 resulted in appropriate model predictions based on existing published literature detailing either a single-time point or multiple-time point concentration data of AL in children.

Having established a working model for AL pharmacokinetics in adults and children, along with a working model for quantifying AL DDIs in adults, we addressed the major focus of this study, the prediction of potential AL based DDIs in children between the ages of 2-5 years of age. As expected, the impact of rifampicin on the pharmacokinetics of artemether was significant, reducing both the final dose C_{max} for both

one and two tablet regimens by approximately 80 % (C_{max} ratio: 0.18-0.21) (Table 2.8) along with an AUC_r of 0.21-0.22 for both dosing regimens.

2.5.5 Importance of DDIs of lumefantrine and rifampicin based anti-TB treatment in children

To infer a clinical consequence of this is difficult, given the shorter half-life of artemether compared to lumefantrine. AL is a very efficacious therapy in uncomplicated malaria patients with the recommend 6-dose treatment showing efficacy of 97.6% on day 28 and 96.0% on day 42 (260), however the efficacy of treatment reduces with patients receiving lower doses (an 8% decrease in patients for every 1 mg/kg decrease in dose received). However, the overall determinant of AL clinical efficacy is AUC of lumefantrine (208), with lumefantrine day 7 concentration of ~280 ng/mL being the primary marker for successful therapy under dosing with 3-day dosing regimen.

The DDI has a detrimental effect on lumefantrine C_{d7}, significantly reducing this below the target concentration for both one and two dose treatment (Figure 2.19-2.20). Although data on such interactions in paediatric is lacking, Lamorde *et al* (2013) (180) have demonstrated a similar effect in adults with a significant decrease (3-10 fold) in lumefantrine concentrations during TB treatment (180). Artemether and lumefantrine have been reported to show saturation in absorption pharmacokinetics and it would be expected that dose increases would have a limited impact on the resultant pharmacokinetics of lumefantrine (221) (261). Therefore, to overcome the DDI-based decrease in C_{d7}, an increase in the dose administered would not be viable for increasing C_{d7}. We then simulated the impact of an increase in dosing duration to determine how this would influence the plasma concentration of AL, and whether an increase in C_{d7} would be evident.

2.5.6 Optimisation of dosing regimen of AL in the presence of rifampicin based DDI in children

Whilst a 3-day treatment is viable for patient compliance, the day 7 concentration s in malaria-TB co-infected children receiving AL and rifampicin based anti-TB regimen were significantly lower than the target concentration. An increase in dosing duration was investigated to assess the impact on the predicted target concentration. Whilst a 5-day course resulted in some modest increase in the percentage of subjects with a C_{d7} >

280ng/mL (~11% increase), this increase was far greater for a 7-day treatment regimen with ~63-75% of subjects demonstrating C_{d7} > 280ng/mL across both dosing bandings (Table 2.9). A recent population pharmacokinetic study by Hoglung *et al* (2015) (262) assessed the potential for DDI with malaria-HIV co-infected adult patients. In prospective simulations they demonstrated a similar beneficial effect of an increase in dosing duration to counteract the induction effect of antiretroviral on malaria (AL) treatment regimens.

Whilst the impact of this will require prospective clinical analysis, it is suggested that an increase in the dosing duration for children who are co-infected with malaria and TB and receiving AL and rifampicin based anti-TB drugs from a standard 3 days AL regimen to a 7-day regimen might result in full malaria parasite clearance. Our results have demonstrated that children aged 2-5 years of age are susceptible to significant DDI when being co-treated with TB chemotherapy, which directly impacts upon the potential for AL therapy failure.

2.5.7 The effect of unbound fraction of lumefantrine on the day 7 concentrations

Malaria patients are susceptible to reduced albumin and α1-acidic glycoprotein, which can directly impact upon the extent of plasma protein binding and therefore exposure of AL to metabolic extraction as reports demonstrate a decrease of ≥ 30 % of serum albumin, (≤ 35 g/L) in malaria patients (263-265). For highly protein bound drugs, such as lumefantrine, any change in the extent of protein binding (e.g. reduced binding due to reduced serum protein) will inevitably alter the unbound drug concentration but not the fraction of unbound drug. This effect will be observed as a change in total drug concentration and potentially enhance or reduce both drug tissue distribution along with metabolic clearance.

The potential impact of such a change was assessed in 2-5 year olds (1 tablet per dose over the 7 day optimised regimen) (Figure 2.21) and demonstrated that a modest increase in $f_{u,plasma}$ from 0.003 to 0.005, results in all subjects possessing a C_{d7} of just below the target < 280 ng/mL subjects (when considering the range of simulated values). Furthermore a 10-fold increase in $f_{u,plasma}$ (0.003 to 0.03) yields C_{d7} which would be irreconcilable by dosing adjustments.

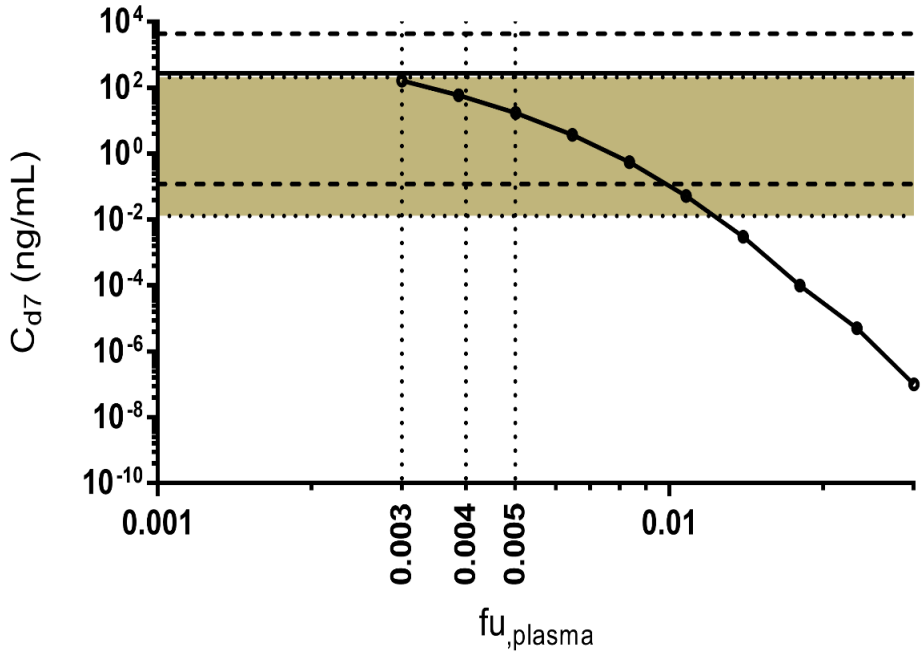

Figure 2.21: The impact of alterations in lumefantrine plasma unbound fraction on simulated C_{d7} in paediatrics in the presence of a rifampicin-mediated DDI for a 7-day regimen (one table/dose)

Day 7 lumefantrine plasma concentrations (C_{d7}) were simulated for 56 subjects within a weight range of 5–15 kg (1 tablet/dose) in the presence of rifampicin (10 mg/kg). The solid line represents the 280 ng/mL lumefantrine 'target' concentration. Dashed lines represent the simulated range (upper and lower) and C_{d7} target concentration when $f_{u,plasma}$ = 0.003. Dotted lines represent the simulated range (upper and lower) concentrations when $f_{u,plasma}$ = 0.005. Isoniazid was also dosed at 10 mg/kg and used as a secondary perpetrator in light of its inclusion in anti-TB therapy.

2.5.8 Study challenges

The impact of non-adherence to designed treatment regimens would render the impact of the induction effect variable and unpredictable (266). However, given the erratic absorption of lumefantrine (and artemether) (267), the extension of a dosing regimen from 3 to 5 days would not alter the peak concentrations significantly (Figure 2.17-2.20) and would be within this erratic absorption range. Furthermore, it should be noted that simulations were performed in healthy subjects in our simulations, and

therefore we have assumed that any physiological changes associated with malaria are negligible and do not impact upon the extent of the DDI in our simulation trials.

In children, changes in body weight (malnutrition) can potentially impact upon pharmacokinetics of antimalarials (268), our dosing range for the age selection (5-15kg and 15-25kg) is broad enough to simulate the impact on potential underweight children who are within the simulated age range (2-5 years). Interesting, a clinical trial is on-going (269) to assess the impact of an increased treatment frequency to 5 days for AL, the outcomes of which may support the requirement for an increase in dosing frequency for patients subjected to induction-based DDIs.

2.6 Conclusion

The WHO have highlighted the increased risks of mortality children face with malaria infection (2, 3) and coupled with the complications of co-infection with tuberculosis, children are at significant risk of potential drug-drug interactions in many areas of sub-Sahara Africa and this DDI may impact upon parasite clearance. Whilst clinical studies exploring this risk of DDI in co-infected paediatric population groups are sparse, mechanistic population-based PBPK modelling provides a potential approach to assess this risk-potential. The pharmacokinetics of artemether and lumefantrine has been simulated for two-body weights in children ages 2-5 years old, who would be a greater risk of mortality associated with both malaria and tuberculosis. We demonstrated that an extension of the current recommended dosing range for AL, from 3 to 7 days, would counteract the potential rifampicin-mediated induction on lumefantrine (and artemether) metabolic clearance and yields a significantly greater proportion of subjects attaining a target lumefantrine concentration thereby preventing recrudescence and potential mortality.

CHAPTER 3

Assessment of the pharmacokinetics of piperaquine in the presence of drug-drug interaction during pregnancy

Disclaimer

Elements of this chapter have been published as follows:

Olusola Olafuyi, Michael Coleman, Raj K.S. Badhan. The application of physiologically based pharmacokinetic modelling to assess the impact of antiretroviral-mediated drug–drug interactions on piperaquine antimalarial therapy during pregnancy. **Biopharmaceutics and drug disposition.** 2017 Nov;38(8): 464-478.

DOI: 10.1002/bdd.2087

3.1 Introduction

3.1.1 Malaria incidence in pregnancy

In 2009, it was reported that 25 million pregnant women were at risk of malaria infection in a WHO report and that malaria was the cause of death in 10,000 pregnant women and 200,000 neonates yearly (270). More recently, maternal death due to malaria was reported to account for up to 25% of maternal deaths due to all causes in malaria endemic regions (271).

3.1.2 Consequences of malaria in pregnancy

The problem of malaria-induced maternal morbidity and mortality in endemic areas for the disease is far reaching, particularly with respect to the unborn child. Malaria infection in pregnancy triples the maternal risk of suffering from severe diseases compared with non-pregnant women and puts pregnant women at a 50 % higher chance of dying from severe malaria (270, 272). In high transmission areas, women pregnant for the first time, adolescents, and those infected with human immunodeficiency virus (HIV) are said to be at an even greater risk of being infected with disease. The effect of malaria in pregnancy depends on immunity of the pregnant woman against malaria and malaria infection can result in debilitating complications such as maternal anaemia, miscarriage, foetal growth retardation, preterm delivery, illness and low foetal birth weight and foetal and/or maternal death (270, 273).

3.1.3 Treatment of malaria in pregnancy

The treatment of malaria during pregnancy possesses major challenges to healthcare systems. This is because antimalarial treatments (AMT) which yield satisfactory safety and efficacy profiles are often found to be unsafe during the early stages of pregnancy (274). The WHO's current recommendations for AMT chemoprophylaxis are based on intermittent preventive treatment with sulfadoxine-pyrimethamine (IPTp-SP) (165). This recommendation was based on a review (275) of seven trials which assessed the use of monthly SP administration for malaria prevention in pregnant women across six African countries. The result of the review demonstrated that there was a significant reduction in both low birth weights and placental and maternal parasitaemia following administration of no less than two doses of SP monthly during pregnancy (275).

However, with the spread of SP resistance, new interventions have been sought. In high transmission settings where there may be widespread resistance to SP-IPTp, dihydroarteminisin-piperaquine (DHA-PQ) has been demonstrated to result in a lower malaria burden (276).

In practice, other non-pharmacological methods previously discussed, and the use of other ACTs have been used for prevention of the disease. Adequate treatment of uncomplicated malaria is also encouraged during pregnancy to avoid complications.

3.1.3.1 Dihydroartemisinin/piperaquine

The effectiveness of DHA-PQ in the treatment of malaria during the second and third trimesters of pregnancy has been robustly demonstrated. In more than 2000 pregnant women in Thailand and Indonesia in either the second and third trimesters of their pregnancy, the administration of DHA-PQ resulted in successful antimalarial treatment and safety outcomes. The safety of DHA-PQ in pregnancy has been demonstrated in many studies. In 2015, a randomised controlled superiority trial showed that in addition to the observed efficacy of DHA-PQ for preventing malaria in pregnancy, DHA-PQ resulted in fewer detrimental maternal and infant side effects compared with SP-IPTp (277). Also, another study revealed that compared to quinine, DHA-PQ used for the treatment of multi-resistant malaria in the second and third trimester of pregnancy resulted in less perinatal mortality, though in the first trimester, quinine appeared to be safer (278).

In high malaria transmission settings with the possibility of widespread resistance to SP-IPTp, dihydroarteminisin-piperaquine (DHA-PQ) has been shown to result in reduced malarial burden (276). This is evident in a study which showed that the administration of DHA-PQ gave significantly higher protection against placental malaria, significantly lowered maternal parasitaemia and reduced prevalence of composite adverse birth consequences when compared to the use of SP in pregnant women (276).

3.1.3.2 Efficacy indicator of dihyrdoartemisinin and piperaquine (DHA/PQ) in the treatment of malaria

In antimalarial therapy with DHA-PQ, study endpoints to determine the efficacy of drugs may be primary endpoints or secondary endpoints. Primary endpoints include

measuring outcomes such as: early treatment failure which may be manifested as poor treatment prognosis between the start and day 3 of treatment, late clinical failure measured as fever and parasitaemia between the 4^{th} and 42^{nd} day of commencing therapy, late parasitological failure observed as any recurrence of parasitaemia between the 4^{th} and 42^{nd} day but without fever, while adequate clinical and parasitological response indicates there is not parasitaemia or fever for 42 days after starting therapy. For the secondary outcomes, several outcomes are considered, which include but are not limited to haemoglobin level changes, occurrence of gametocytes and the correlation of day 7 concentrations of piperaquine and primary outcome measures above (279). Some studies have demonstrated that a significant determination of treatment failure following the use of DHA-PQ in patients with malaria is a piperaquine day 7 concentration level lower than 30 ng/ml and day 7 concentrations below this level are said to be associated with recurrent infection. Hence a day 7 plasma concentration of piperaquine is a good surrogate for clinical efficacy of DHA-PQ (279, 280).

3.1.4 HIV and malaria co-infection in pregnancy

Infectious diseases such as HIV are prevalent in malaria endemic regions (281, 282). Pregnant women with HIV and malaria coinfection are more vulnerable to all the complications of malaria in pregnancy such as anaemia, placental parasitaemia and low foetal birth weights (283). It has also been reported that there is higher incidence of anaemia and low foetal birth weights in malaria and HIV coinfected pregnant women than in pregnant women with either of the infections alone. As malaria may increase HIV viral load, there is higher risk of mother to child HIV transmission in pregnant women who carry both infections (284).

The implication of malaria and HIV co-infection in pregnant women suggests that some DDIs between drugs used to treat both infections are likely because of the potential for many antiretroviral (ART) drugs to elicit (DDIs) on common cytochrome P450 isozymes (CYP P450), e.g. 3A4 (285-287). Hence, the potential for a DDI to occur is a significant cause for concern when treating this population. The reduced systemic concentration of DHA-PQ, due to co-administration with efavirenz in HIV infected pregnant women, has been demonstrated in a recent study which showed that in Ugandan pregnant women, $AUC_{0\text{-}8hr}$ and $AUC_{0\text{-}21d}$ of piperaquine was 50% and 40% lower

respectively when DHA-PQ was co-administered with efavirenz compared to when DHA-PQ was taken alone (288).

In Mali, the effect of co-administration of nevirapine on the pharmacokinetics of quinine was studied in seven pregnant women (289). In this study, it was reported that nevirapine, a CYP3A4 inducer, might have been responsible for the lower plasma concentration of quinine and higher concentration of its metabolites in the six of the pregnant women who were co-administered these drugs compared with the one patient who did not have this combination of drugs. The overall effect of the DDI observed in the pregnant women was such that the systemic concentration of quinine was lower than the therapeutic range in half of the subjects involved in the DDI study (289). Very few DDI studies are likely to be granted approval in pregnant women for ethical reasons, but a systemic review of data involving DDI between ARV drugs and AMT further accentuated the likelihood of a range of such DDIs (290).

3.1.5 PBPK modelling in pregnancy

During pregnancy, many physiological changes occur in the body of the pregnant woman which potentially alter the pharmacokinetics of drugs (291). Studies have revealed the impact of pregnancy on the efficacy of different drugs. Colbers *et al* (2015) demonstrated that the exposure to darunavir was reduced during pregnancy in an open label, non-randomised study involving HIV infected pregnant women (292). Similarly, Olagunju *et al* (2015) showed that in the 44 pregnant and postpartum women recruited for their study, there was a reduction in the overall efavirenz exposure in pregnant women compared to the postpartum women (293). Kreitchmann *et al* (2013) showed that an increase in Atazanavir/ritonavir dose to 400/100 mg in second and third trimester of pregnancy was able to counteract the impact of reduced systemic exposure to atazanavir apparent with a 300/100mg dose (294). The impact of ineffective or unsafe drug concentrations during pregnancy is not only on the mother but also on the unborn foetus, for example in the case of prevention of mother to child HIV transmission during ARV therapy (291), therefore, the alteration of ADME during pregnancy may be directly caused by pregnancy induced physiological changes.

3.1.5.1 Physiological changes affecting pharmacokinetic processes during pregnancy

3.1.5.1.1 Plasma/ blood volume

Pregnancy induced changes to the cardiovascular system result in an increase of plasma volume throughout pregnancy. Increase in cardiac output during pregnancy starts at as early as gestational week 6, stabilises at around 16 weeks but continues to increase gradually until the end of pregnancy resulting in up to 50 % higher maternal blood volumes in pregnant women when compared to non-pregnant women. These blood/plasma volume changes have obvious pharmacokinetic implications. The volume of distribution of hydrophilic drugs increases with an increase in plasma/blood volumes potentially requiring an increase in the loading dose of such a drug so that the therapeutic concentration can be achieved during pregnancy because an increase in volume of distribution of the drug into extracellular space due to overall increase in total body water may lead to a decrease in plasma concentration. Similarly, during pregnancy, there is a 4 kg increase in body fat and this may potentially increase the volume of distribution of lipophilic drugs (295, 296).

3.1.5.1.2 Protein binding

The concentration of the major plasma proteins involved in drug binding, human serum albumin (HSA) and alpha 1- acidic glycoprotein (AGP) have been reported to decrease during pregnancy. Abduljali *et al* (2015) reported that at around the third trimester, HSA concentration is decreased by 31 % while AAG is reduced by 19 %, the consequence of which is an increase in amount of free drug available for both distribution and clearance leading to overall systemic drug exposure reduction as a result of pregnancy (291, 297).

3.1.5.1.3 Hepatic enzyme activity

It is known that hepatic enzyme activities may increase or decrease during pregnancy. The mechanism behind the changes is thought to be due to an increase in the levels of some hormones, such as progesterone, oestradiol and growth hormones during pregnancy (298). The extent of changes in hepatic enzyme activities due to pregnancy has been demonstrated in the Fotoupolous *et al* (2009) study where they showed clearance of lamotrigine was increase by 197, 236 and 248 % at first, second and third trimesters of pregnancy (299). During pregnancy, the metabolic enzymatic activities of CYP

isoenzymes 3A4, 2C9, 2D6 and the uridine diphosphate glucuronosyltransferase (UGT) isoenzymes UGT 1A1 and 1A4 has been shown to increase, implying that metabolism of drugs that are substrates of these enzymes will be increased and consequently resulting in lower drug concentrations of these substrates in pregnant subjects. Conversely, the metabolic activities of CYP isoenzymes 1A2 and 2C19 are decreased during pregnancy implying a reduced metabolism of drug substrates of these and a resultant increase in systemic exposure of the drug in pregnant subjects (300).

3.1.6 Physiological consideration of antimalarial therapies in pregnancy

In the section, the impact body weight and blood biochemistry might have in the AMT will be discussed. Firstly, the body weight used in this context to infer body composition can affect mainly the volume of distribution of a drugs as highly lipophilic drug will have altered volume of distribution in obese subjects compared to subjects with normal weights (301). Secondly, as discussed, pregnancy can alter the blood biochemistry, for example, serum albumin concentration which is said to also affect the distribution of drugs that are highly bound to it. This effect is further confounded in disease states such as malaria whereby HSA levels are reduced as a result of the infection (302, 303). Also, the haematocrit levels which is the percentage of red blood cell in whole blood volume is particularly important in studying drugs that might have high affinity to red blood cells. This is because changes in the haematocrit level can alter the distribution of drugs into the plasma for a drug that is highly bound to red blood cells (304).

Physiological and biochemical parameters may vary across ethnic groups and in disease states. For instance, the age-weight distributions in malaria endemic regions have been shown to differ greatly from average global weight-for-age distributions (283). Also, Goselle *et al* (2007) and Silamut *et al* (1999) (264, 305) studied the effect of malaria parasitaemia has on the levels of plasma proteins. Goselle *et al* (2007) revealed that in Nigerian subjects, serum albumin level is reduced in subjects with malaria compared to those without malaria, while Silamut *et al* (1999) showed that in Thai patients who had malaria, there was increase in AAG levels but they returned to almost half of what they were in the infected state after the patients had recovered from the infection. Newton *et al* (2013) reported that the haematocrit levels of nearly a thousand subjects in Thailand and found that the average level was 37 (range 6–56) % in a population of 60 % male – compared to normal haematocrit levels of 37-48% in men and 42-52% in women (306).

In pregnant women, changes to body physiology that may or may not significantly affect the pharmacokinetics of drugs. The effect of pregnancy on the PK of drugs is difficult to assess clinically due to ethical constraints, more so, in pregnancy several physiological and biochemical changes are happening simultaneously, and it might be difficult to determine which in particular is implicated in the alteration of the pharmacokinetics of a drug. Therefore, the use of the mechanistic approaches in PBPK modelling may proffer a holistic understanding of what physiological or biochemical factors or parameters might influence the pharmacokinetics of drugs during pregnancy.

3.1.7 The importance of PBPK modelling in pregnancy antimalarial drug research

Antimalarial clinical research aimed at addressing PK issues associated with antimalarial therapy like DDIs is not only ethically difficult but also very expensive. When studying the pharmacokinetics of antimalarial drugs in pregnancy, the effect of each physiological changes described earlier in a clinical setting may be difficult to ascertain. But PBPK modelling utilises virtual patients in whom there has been an extensive and robust validation of their capability to imitate real pharmacokinetic scenarios, therefore, studying how individual physiological variables may impact drug in such a manner that other cofounding factors are controlled, is feasible. Also, PBPK modelling has been successfully applied in many studies to describe the pharmacokinetics of drugs in pregnancy (134, 307, 308) hence there is an increasing confidence in the use of PBPK modelling to assess safety and efficacy of drugs in pregnancy, with a clear application of this technique to antimalarial agents during gestation.

3.2 Aims and objective

3.2.1 Aim

The aim of this study was to investigate the impact of changes in PQ plasma concentrations in the absence and presence of ARV-mediated DDIs in pregnant population groups from three malaria-endemic geographical regions (Thailand, Papua New Guinea and Sudan), such that changes in maternal physiology, biochemical and haematology were incorporated into the design of the population group.

3.2.2 Objectives

1. To develop and validate a PBPK model for PQ in non-pregnant and pregnant women
2. To simulated PQ concentration time profiles in adapted virtual pregnant women and non-pregnant population groups.
3. To simulate and validate ARV mediated DDI with efavirenz and ritonavir in pregnant and non-pregnant women
4. To determine the impact of human albumin levels on the PQ day 7 concentrations
5. To study the impact of gestational weeks on the pharmacokinetics of PQ.

3.3 Methods

All population based PBPK modelling was conducted using the virtual clinical trials simulator Simcyp® (Simcyp Ltd, a Certara company, Sheffield, UK, Version 16) using either a pre-validated in built "Healthy Volunteer" population group, a "Pregnancy" group, or an adapted "Pregnancy" population group. The adaptation of population group was done based on age for weight relationships and blood biochemistry peculiar to the population groups of interest. In all cases, population variability was accounted for by the inclusion of a variability metric (% coefficient variability) having been established from public health data bases such as the US National health and Nutrition Examination Survey (https://www.cdc.gov/nchs/nhanes/).

3.3.1 Study design

A four-stage stepwise approach was employed for model development.

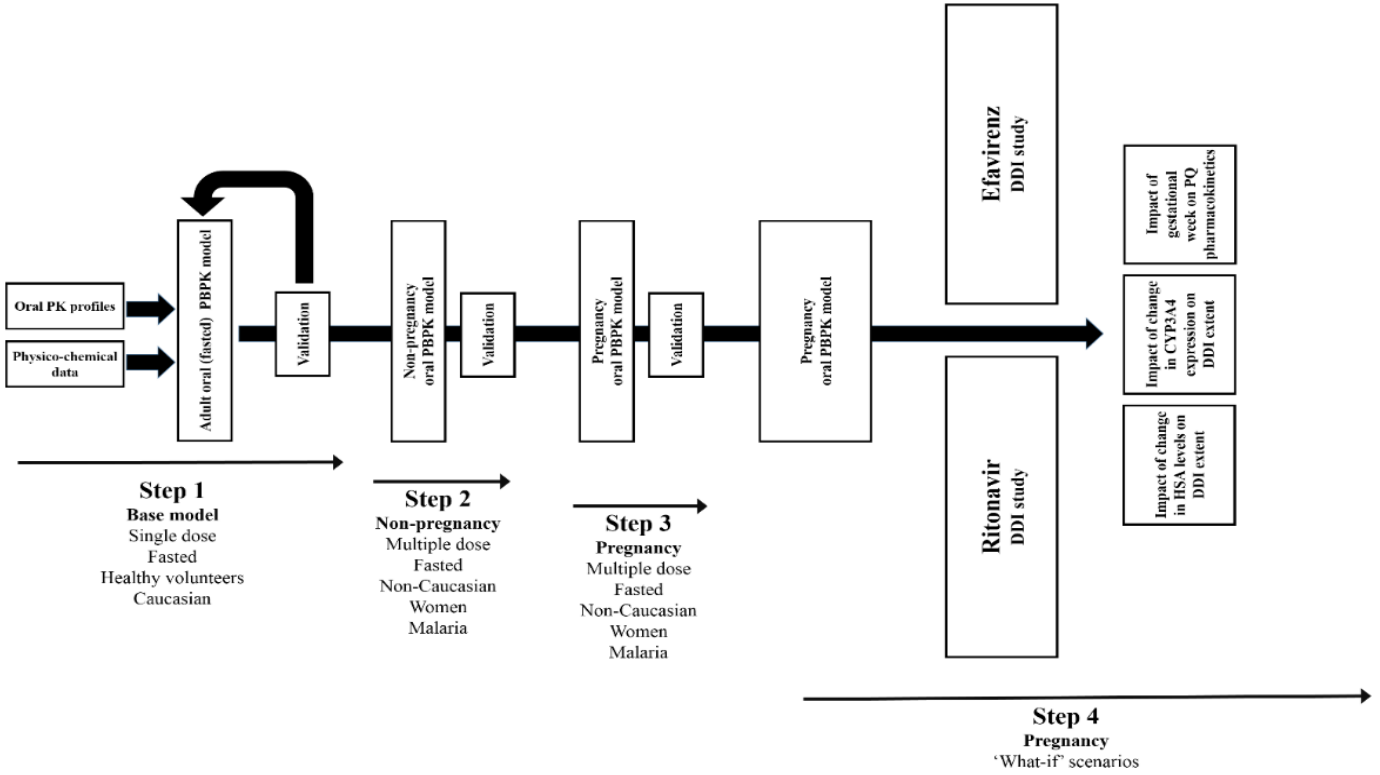

Figure 3.1: Diagrammatic representation of the work flow process of model development for the simulation of piperaquine pharmacokinetics in non-pregnant and pregnant women.

3.3.1.1 Step 1: Base model development and validation

Piperaquine physicochemical properties were obtained from the literature to create a drug compound file which was used to develop a model with the aim to recover the absorption, distribution and the elimination phases of the concentration time profiles observed from clinical studies and to simulate its maximum concentration (C_{max}), area under the curve (*AUC*) and day 7 concentration under different dosing schedules. Where some model parameters were not available in published studies, these were either predicted from the molecular descriptors of piperaquine or calculated from a clinical *in vivo* parameter when available using the Simcyp® retrograde calculator (see section 2.3.1.1). Some model parameters were optimised using the Weighted Least Square (WLS) approach and the Nelder-Mead minimisation method on Simcyp® to produce parameters with better certainty, and which best recovered published clinical drug profiles. The parameters used to develop the base model are illustrated in Table 3.1

The piperaquine model was developed and validated from two studies of PQ dosed in fasted Caucasian healthy volunteers (309, 310). Given the high lipophilicity and expected wide-spread tissue distribution of PQ, a full PBPK model was employed for all model simulations. As a result of a lack of published *in vitro* Caco-2 permeability measurements, molecular descriptors (hydrogen bond acceptors: HBA; polar surface area: PSA) were used to estimate the absorption rate constant (k_a) (see equation 43 and equation 44).

$$K_a = \frac{2 \times P_{eff}}{R} \qquad (44)$$

where P_{eff} is the effective gut wall permeability and R the intestinal radius

The k_a and fraction of dose absorbed (f_a) were then used to simulate the absorption phase using a first-order absorption model. This resulted in an initial estimate of 4.6 h^{-1} and 0.99 for k_a and f_a respectively, however this was unable to capture an appropriate t_{max} for piperaquine (~6 hours) (309, 310). A single dose study in healthy volunteers has reported k_a of 0.93 h^{-1} (311), and was better able to capture an appropriate t_{max}. These parameters were further estimated using a Weighted Least square fitting algorithm and a Nelder mead minimisation method to single dose fasted profiles reported by Sim *et al*

(2005) (310), yielding a final parameter estimate of 0.45 h^{-1} for k_a and 0.5 for f_a. Visual predictive checks identified that the absorption kinetics were still inadequately predicted, therefore, to account for the wide variability in PQ concentration around the expected t_{max} in reported clinical studies, the CV of k_a and fa were set at 50 %. This was better able to capture the range of data points within the 5^{th} – 95^{th} percentiles in our predictions. For all simulation, we assumed that the PQP:PQ was 57.5 % and hence all dosing regimens reporting PQP were appropriately scaled to reflect the PQ base (100, 310).

To recover the general shape of the distribution and elimination phases of the plasma-concentration time profiles, the volume of distribution (V_{ss}) was estimated from published clinical data through empirically fixing the global tissue-partition coefficient *Kp* scaler to yield a V_{ss} of 823 L/kg, the mean of 4 reported V_{ss} from clinical studies (310, 312-314).

The availability of *in vitro* metabolic clearance data is limited for piperaquine with CYP3A4 identified as the major metabolic pathway and CYP2B6 playing a minor role (315). It was therefore assumed that the major pathway would be CYP3A4 and an intrinsic clearance (CL_{int}) was estimated using the retrograde calculation (see section 2.3.1.1) with a fixed CL_{oral} of 69.3 mL/min, the mean of 3 reported *CL/F* (and assuming F~1) (310, 313, 314), with CYP3A4 as the major isozyme and allocated 99 % of the total clearance (8.18 µL/min/pmol) with CYP2B6 allocated 1 % (0.37 µL/min/pmol) (315). Final estimates of CL_{int} and *Kp*, for single dose healthy Caucasian subjects, were obtained from optimisation using datasets from Ahmed *et al* (2008) (309), yielding $CLint_{3A4}$: 3.08 µL/min/pmol, $CLint_{2B6}$: 0.13 µL/min/pmol and *Kp* scalar: 13 (V_{ss}: 820.5 L/kg).

Table 3.1: Input base model parameters values and predicted PBPK values used in the simulation of piperaquine.

Parameters	Piperaquine
Compound type	Diprotic base
Molecular weight (g/mol)	535.51[316]
Log P	6.2 [317]
Fu	0.014 [318]
pKa 1	8.6 [317]
pKa 2	6.5 [317]
B/P	0.90 [318]
Vss (L/kg)	63.2[a]
k_a (h^{-1})	4.6[b]
F_a	0.99[b]
Kp scalar	1
CL_{po} (mL/min)	69.3[c]
$CLint_{3A4}$ (µL/min/pmol)	8.18[d]
$CLint_{2B6}$ (µL/min/pmol)	0.37[d]
Absorption model	First-Order
Distribution model	Full

[a] Vss values was predicted on Simcyp® based on a default *Kp* scalar value of 1. [b] k_a and f_a were estimated from molecular descriptor – *PSA* 38.7 and *HBD* of 0 (PubChem). [c] CL_{po} was obtained by finding the average of three reported *CL/F* assuming *F*~1 (310, 313, 314).[d] CL_{intCYP} was based on a retrograde calculation, described in Step 1, with f_a fixed at 0.5 and F_G assumed = 1. Assumption that fm_{cyp} of 0.99 and 0.01 for CYP3A4A and CYP2B6 respectively was made. f_u: unbound fraction; *B/P*: blood-to-plasma ratio; *Vss*: steady state volume of distribution; k_a: absorption rate constant; f_a: fraction dose absorbed; CL_{po}: oral clearance; CL_{int}: *in vitro* intrinsic clearance.

3.3.1.2 Adaptation of age-weight relationships and blood biochemistry parameters in non-Caucasian females

The 'Healthy Volunteer' (HV) population group within Simcyp® was adapted to address the differences in patient demographics (primarily body weight) and biochemistry (haematocrit/plasma proteins) between healthy-subjects and malaria-subjects. A custom age-body weight relationship was developed for studies based on the publication of growth references for malaria-endemic countries (283). Median age-weight reference charts were used to establish polynomial mathematical relationships for age and weight using TableCurve 2D (Systat Software, San Jose, CA, USA), which were applied within

the population 'demographics' section of Simcyp® to create user-defined age-weight relationships and, unless otherwise specified within clinical studies, were applied to an age range of 18-30 year olds for non-pregnant and pregnant female subjects only.

In malaria population groups, it has been reported that a reduction in HSA is commonly detected (319), often coupled with a 3-4 fold increase in AAG (320). To create a Malaria-type population group, we identified haematocrit, HSA and AAG levels in the 3 population groups (Table 3.2) and revised these within our Simcyp® population group.

3.3.1.3 Step 2: Simulation and validation of PQ in non-pregnant malaria population groups

To assess the predictive performance of the model in non-Caucasian non-complicated malaria population groups, four studies where PQ was dosed to non-pregnant females in Thailand (281, 313), Papua New Guinea (282) and Sudan (321) were used. Tarning *et al* 2008 (322) was excluded from this study due to the difficulty in obtaining individual data points for the study duration. Using the adapted subject population groups, each of the studies mentioned were simulated such that the demographic patient data in the actual clinical studies were maintained when possible during the simulation. Ten virtual trials involving 10 virtual subjects were implemented during the simulation.

Table 3.2: Malaria population versus healthy Caucasian blood biochemistry

Biochemistry	Caucasian [a]	Sudan	Thai	PNG	Uganda
Haematocrit (%)	M: 43 F: 38	M: 38.6 F: 40 (323)	37 (306)	35.78 [c]	31.8 (324)
AAG (g/L)	M: 0.811 F: 0.791	1.55 [b]	1.55 (325)	1.55 [b]	1.55[d]
HSA (g/L)	M: 34-50 F: 38-49	45.3 (326)	33.7 (306)	33.7 [d]	45.3[d]

[a] Default values within Simcyp® North European Caucasian and Healthy Volunteer population groups. M: male; F: female. [b] Assumed to be equivalent to Thai patients.[c] Calculated from haemoglobin (11.8 g/dL)reported in Benjanmin *et al*, 2015(282) and assuming the following relationship: haematocrit = 5.62 + 2.60 * haemoglobin reported in Senn *et al.* 2010 (327). [d] Value was assumed to be equivalent to Thai patient based on a similar range reported in children in Rosale *et al*, 2000 (328). We assumed the 'worst-case' scenario and selected the lowest HSA value. [d] Assumed to be equivalent to that of the Sudanese population group.

3.3.1.4 Step 3: Simulation and validation of PQ model in pregnant malaria population groups

The predictive performance of the model in non-Caucasian pregnant women with uncomplicated malaria population groups was assessed using four studies where PQ was dosed to pregnant females in Thailand (281, 313), Papua New Guinea (282) and Sudan (321). The corresponding adapted population groups were used during each simulation and the simulation involved 10 virtual subjects in 10 virtual trials and the demographic characteristics of the actual clinical study was maintained wherever possible during the simulation.

3.3.1.5 Step 4: 'What-If' scenarios

3.3.1.5.1 Efavirenz/Ritonavir-mediated drug-drug interactions

To assess 'What-If' scenarios (Figure 3.1), case studies were included, in order to demonstrate the impact of possible drug-drug interactions (DDIs) mediated by efavirenz (EFV) or ritonavir (RTV); the former was selected due to the potential for CYP3A4 induction and the latter for its CYP3A4 inhibitory effects. A recently published clinical study (329) that demonstrated a DDI between EFV and PQ in pregnancy was used to validate the ability of the PBPK model to predict DDIs, however, as there was no clinical data available for DDIs in between PQ and RTV in pregnancy, a successful simulation of DDI between PQ and EFV was assumed to mean successful simulation of PQ and RTV. It should be noted that this age-weight relationship was based on non-HIV co-infected subjects and therefore may not fully represent the age-weight distributions for co-infected subjects, however the simulated weight range for this population group, 43.9 kg to 78.3 kg (median: 56.2 kg), was within the range reported by Kajubi *et al* (2017) for subjects around gestational week 28 (329). Hematocrit was fixed at 37.9 % in non-pregnant females and 31.7% in pregnant females (324) with AAG/HSA assumed to be equivalent to that of the Sudanese population group (Table 3.2). Model predictions for HIV-uninfected non-pregnant (malaria) females and HIV uninfected pregnant (malaria) females in an adapted Ugandan female population were validated with the corresponding observed data as reported by Kajubi *et al* (2017) (329).

3.3.1.5.2 Human serum albumin study

Human serum albumin (HSA) concentrations were set at 20 g/L and 50 g/L within population groups, to mimic the reduction in serum albumin reported at different stages

of malaria infection, with 20 g/L representing severe malaria (330). The Simcyp® 'Pregnancy' population includes a description for alterations in HSA during pregnancy and the baseline initial HSA concentration was fixed at the aforementioned concentrations.

3.3.1.5.3 Gestational week

The impact of gestation week on PQ pharmacokinetics during EFV/RTV-mediated DDI was assessed at weeks 10, 20 and 30 for all population groups.

3.3.2 Predictive performance

Although no uniform criterion has been accepted for defining an 'optimal' predictive performance range, a prediction to within 2-fold of the observed data is generally accepted in this context (227) and was employed as our criterion for C_{max} and AUC comparisons to those clinically reported. For EFV/RTV DDI simulation, as the clinical efficacy of PQ is determined by its day-7 concentration (post-first dose) of 30 ng/mL (280), the impact of a DDI on PQ pharmacokinetics was assessed by direct analysis of the day-7 concentration.

3.3.3 Data analysis

Unless otherwise stated, all simulations of plasma concentration-time profiles were presented as arithmetic mean and 5 - 95th percentiles. Reported concentration-time profiles from clinical studies were digitally retrieved using the WebPlotDigitizer v3.10 (http://arohatgi.info/WebPlotDigitizer/) (229) and superimposed onto simulated profiles for visual predictive checks. Where applicable, statistical analysis was conducted using paired t-tests or one-way ANOVA with a $p < 0.05$ indicating statistical significance.

3.4 Results

3.4.1 Step 1a: Base model development

The base model developed using drug physicochemical data obtained from published studies (Table 3.3) resulted in a concentration time profile which did not adequately recover the clinically reported concentration time profiles (Figure 3.2). The initial model development for healthy volunteer (HV) (Caucasian) subjects focussed on addressing model validation to recover appropriate absorption kinetics coupled with an appropriate prediction of steady state volume of distribution (V_{ss}) and CYP3A4 and CYP2C8-mediated metabolic clearance.

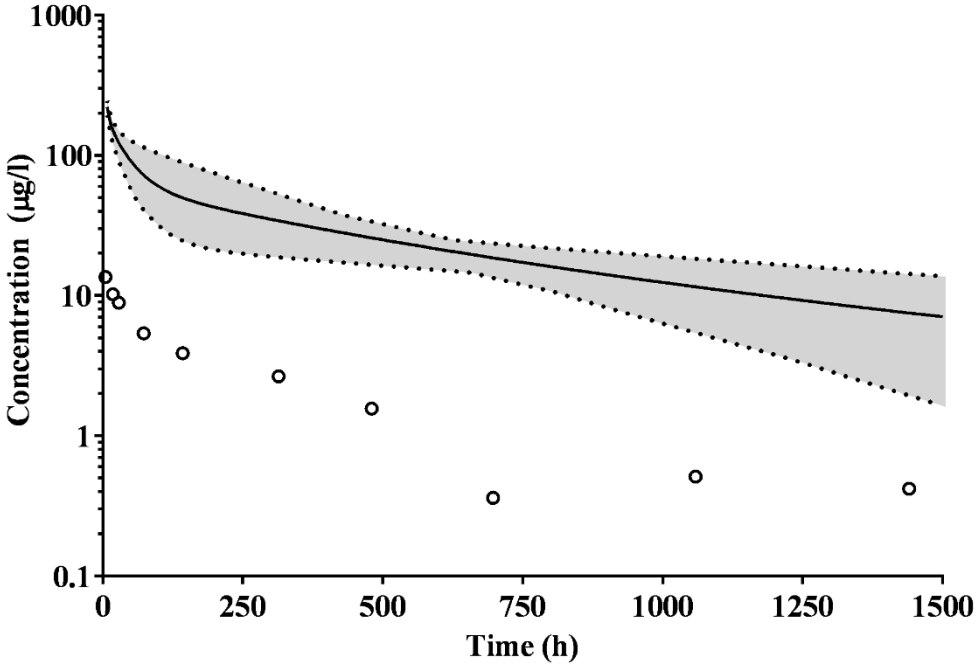

Figure 3.2: The simulated plasma fasted single-dose concentration-time profile of 500mg piperaquine in healthy-volunteers using the base model

Simulation of PQ plasma concentration-time profiles following a single oral dose of 500 mg PQP to 100 healthy volunteers using the base model. Observed data were obtained from Ahmed *et al* (2008) (309). Insert graphs illustrate plasma concentration profiles in the first 24-hours post-dosing. Open circles are observed mean points. Solid lines represent population mean prediction with dashed lines representing the 5th and 95th percentiles of prediction.

Table 3.3: Parameter values for the optimised model and predicted PBPK values used in the simulation of piperaquine.

Parameters	Piperaquine	Notes
Compound type	Diprotic base	
Molecular weight (g/mol)	535.51[316]	
Log P	6.2 [317]	
Fu	0.014 [318]	
pKa 1	8.6 [317]	
pKa 2	6.5 [317]	
B/P	0.90 [318]	
Vss (L/kg)	947[a]	Final optimised
k_a (h^{-1})	0.50	50 % CV
Fa	0.45	50 % CV
Kp scalar	15	Final optimised
CL_{po} (L/min)	69.3[b]	
$CLint_{3A4}$ (µL/min/pmol) [f]	3.08[c]	Final optimised
$CLint_{2B6}$ (µL/min/pmol) [f]	0.13[c]	Final optimised
Absorption model	First-Order	
Distribution model	Full	

[a] An appropriate Kp scalar was identified during base-model development (Step 1) and further empirically optimised using multi-dose studies described in Step 2. Final V_{ss} estimates are within the range reported for PQ (322, 331, 332). [b] CL_{po} was obtained by finding the average of three reported *CL/F* assuming F~1 (310, 313, 314).[c] $CLint_{CYP}$ was based on a retrograde calculation, described in Step 1, with f_a fixed at 0.5 and F_G assumed = 1. Final estimates were obtained through parameter estimation assuming an *fmcyp* of 0.99 and 0.01 for CYP3A4A and CYP2B6 respectively, using multi-dose studies described in Step 2. f_u: unbound fraction; *B/P*: blood-to-plasma ratio; V_{ss}: steady state volume of distribution; *ka*: absorption rate constant; *fa*: fraction dose absorbed; CL_{po}: oral clearance; CL_{int}: *in vitro* intrinsic clearance.

3.4.2 Step 1b: Optimised model for piperaquine in healthy volunteers (Caucasian)

The resultant model was found to be appropriate to capture C_{max} and t_{max} and resulted in a broadly consistent simulated C_{max} (21.5 ng/mL ± 9.2 ng/mL), t_{max} (5.3 hours) and AUC ($AUC_{0\text{-}24}$: 384.2 ng h/mL ± 145.9 ng h/mL; $AUC_{0\text{-}last}$: 3207.3 ng h/mL ± 1121 ng h/mL) when compared to Ahmed *et al* (309) (C_{max}: 41.6 ng/mL ± 29.5 µg/L; t_{max}: 4.0 hours; $AUC_{0\text{-}24}$: 393 ng h/mL ± 149 ng h/mL; $AUC_{0\text{-}last}$: 2312 ng h/mL ± 790 ng h/mL) (Figure 3.2) and Sim *et al* (310) (C_{max} [range]: 21.0 µg/L [14-31.4 µg/L]; t_{max}: 6.8 hours [2.1-11.5 hours]; $AUC_{0\text{-}last}$: 2818 µg h/L [1566-5070 µg h/L]) for a 500 mg PQP dose (Figure 3.3).

For a higher 1500 mg PQP dose, PK parameters consistent with those reported in Ahmed *et al* (309) were predicted. In this study, C_{max} (76.1 ng/mL ± 69 ng/mL), t_{max} (5.1 hours) and AUC ($AUC_{0\text{-}24}$: 1243 ng h/mL ± 193.8 ng h/mL; $AUC_{0\text{-}last}$: 9065 ng h/mL ± 1299 ng h/mL) were simulated when compared to Ahmed *et al* (309) (C_{max}: 147 ng/mL ± 110 µg/L; t_{max}: 2.5 hours; $AUC_{0\text{-}24}$: 1418 ng h/mL ± 775 ng h/mL; $AUC_{0\text{-}t}$: 6399 ng h/mL ± 2067 ng h/mL) (Figure 3.4). These predictions implied successful model development in HV population groups for fasted single dose studies only.

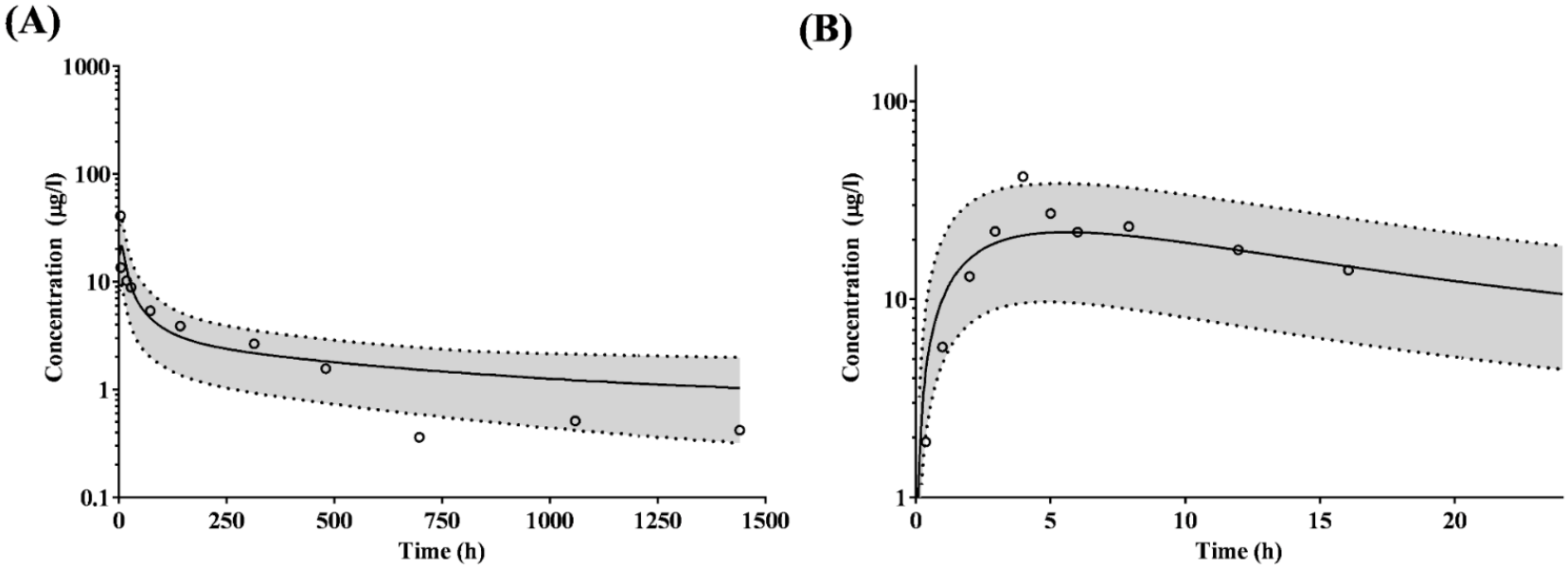

Figure 3.3: The simulated plasma fasted single-dose concentration-time profile of 500mg piperaquine in healthy-volunteers using the optimised model

Simulation of PQ plasma concentration-time profile following a single oral dose of 500 mg PQP (open circles are observed mean points) to healthy volunteers (n=6). Observed data was obtained from Ahmed *et al* (2008) (309). (A) plasma concentration profiles during the simulated study period, (B) plasma concentration profiles in the first 24-hours post-dosing. Solid lines represent population mean prediction with dashed lines representing the 5^{th} and 95^{th} percentiles of prediction.

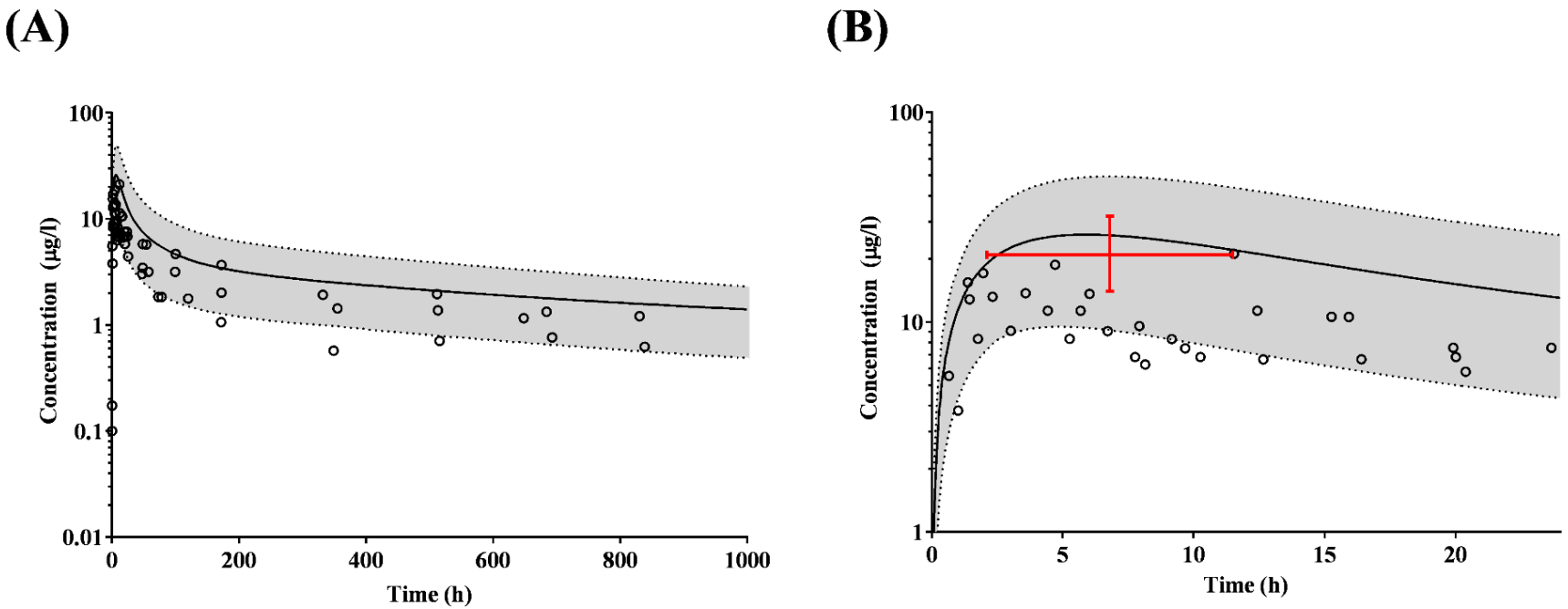

Figure 3.4: The simulated plasma fasted single-dose concentration-time profile of 500mg piperaquine in healthy-volunteers using the optimised model.

Simulation of the PQ plasma concentration-time profile following a single oral dose of 500 mg PQP to healthy volunteers (n=8). Observed data is represented by open circles and represents the 3 individual subject concentration-time points only that were reported by Sim *et al* (2005)(310) out of a total study size of 8 subject. (A) plasma concentration profiles during the simulated study period, (B) plasma concentration profiles in the first 24-hours post-dosing. Errors bars indicate reported range of C_{max} (vertical red line) or t_{max} (horizontal red line) values.

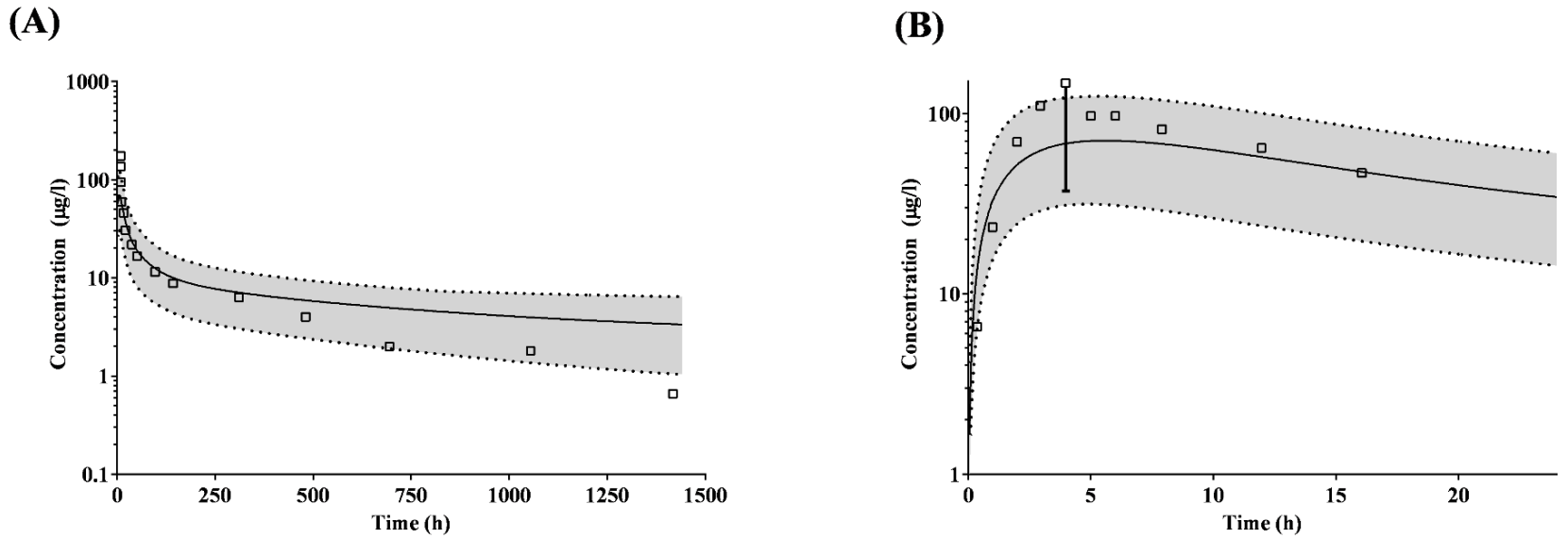

Figure 3.5: The simulated plasma fasted single-dose concentration-time profile of 1500mg piperaquine in healthy-volunteers using optimised model

Simulation of the PQ plasma concentration-time profile following a single oral dose of 1500 mg PQP (open squares are observed mean points) to healthy volunteers (n=6). Observed data were obtained from Ahmed *et al* (2008) (309). (A) plasma concentration profiles during the simulated study period, (B) plasma concentration profiles in the first 24-hours post-dosing. Solid lines represent population mean prediction with dashed lines representing the 5^{th} and 95^{th} percentiles of prediction. Errors bars indicate lower SD at C_{max} for observed data.

3.4.3 Adaptation of age-weight relationship and blood biochemistry for non-Caucasian females

The following equations were used to adapt the age-weight relationships already in-built into Simcyp®. See section 3.3.1.2 for details on how the equations were derived.

3.4.3.1.1 Thai females:

The equation below was implemented on Simcyp® to derive an age-weight relationship was reflective of ideal age-weight relations in the Thai female population group

$$Body\ weight = (6.03+0.197*age^2+0.0012*age^4)/(1+0.00127*age^2+0.0000255*age^4) \quad (45)$$

It should be noted that the growth references charts published by Hayes *et al* (283), cover age range from 0-25 years of age. Although minimal changes are expected between 20-60 years of age, this model was applied to 20-50 year olds only, and this gave a mean (± SD) body weight of 49.65 ± 7.13 kg which was similar to the ranges reported in clinical studies (333), compared to the 'Healthy Volunteer' population (66.99 ± 14.41 kg) (simulated using a 10x10 trial design).

3.4.3.1.2 Papua New Guinea females:

The equation below was implemented on Simcyp® to derive an age-weight relationship that was reflective of ideal age-weight relations in the Papua New Guinea (PNG) female population group.

$$Body\ weight = 3.53+((age*2.92)+(-0.48*age^2)+(0.022*age^3))/((1+-0.084*age)+(-0.0014*age^2)+(0.00025*age^3)) \quad (46)$$

For the PNG population group, age-weight data was not collated by Hayes *et al* (2015) (283) for this region, however the closest country (Solomon Islands) gives a similar weight range for 18-30 year old females as the range reported by Benjamin *et al* (2015) (282) (54.7 ± 7.2 kg), compared to the 'Healthy Volunteer' population group (66.67 ± 13.68 kg) for 18-30 year old females. As a result the Solomon Islands was used as a surrogate for age-weight distribution, resulting in a final weight range of 58.32 ± 12.2 kg.

3.4.3.1.3 Sudanese females:

The equation below was implemented on Simcyp® to derive an age-weight relationship was reflective of ideal age-weight relations in the Sudan female population group.

$$Body\ weight = (1.94+2.627*age^{0.5})+(-1.7086*age)+(0.245*age^{1.5}))/(1+(-0.658*age^{0.5})+(0.157*age)+(-0.017*age^{1.5})+(0.00088*age^{2})) \quad (47)$$

Age-weight data was not collated by Hayes *et al* (2015) (283) for Sudan, however the age-weight charts for Chad were used as a surrogate as these best matched the median body weight (53 kg) reported for the media age (21 years) in the reported study by Hoglund *et al* (2012) (321). The simulated weight range for this population group (matching age-ranges to Hoglund *et al* (2012) (321)) was under-predicted and the range was better recapitulated following an increase in the % CV assigned to the variability in body weight for female to 20 % (53.2 kg ± 14.46 kg).

3.4.3.1.4 Ugandan females:

The equation below was implemented on Simcyp® to derive an age-weight relationship that was reflective of ideal age-weight relations in the Ugandan female population group.

$$Body\ weight = (2.759+(2.3*age) + (-0.344*age^{2}) + (0.014*age^{3})) / (1+(-0.094*age) + (0.000398*age^{2}) + (0.000148*age^{3})). \quad (48)$$

It should be noted that this age-weight relationship was based on non-HIV co-infected subjects and therefore may not fully represent the age-weight distributions for co-infected subjects, however the simulated weight range for this population group, 43.9 kg to 78.3 kg (median: 56.2 kg), was within the range reported by Kajubi *et al* (2017) for subjects around gestational week 28 (329).

The age-weight relationships between healthy Caucasian and non-Caucasian population groups involved in the study was found to be significantly different (Figure 3.6-3.7).

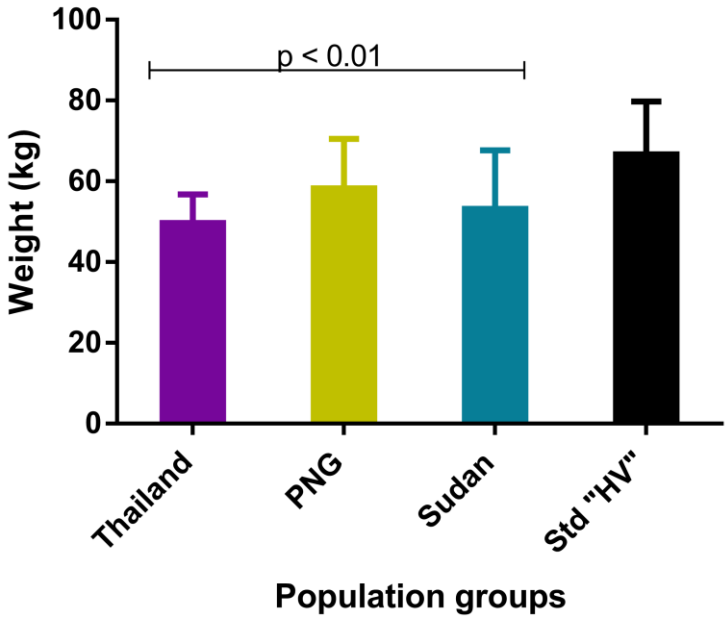

Figure 3.6: Weight comparisons between 25 years old female population groups based on Hayes et al study (283).

Statistical comparison between weight of 25-year-old adults across three population groups. $p < 0.01$: significant difference between three non- Caucasian population groups compared to healthy Caucasian population as represented on Simcyp®. Std "HV": Simcyp® health volunteer population. PNG: Papua New Guinea.

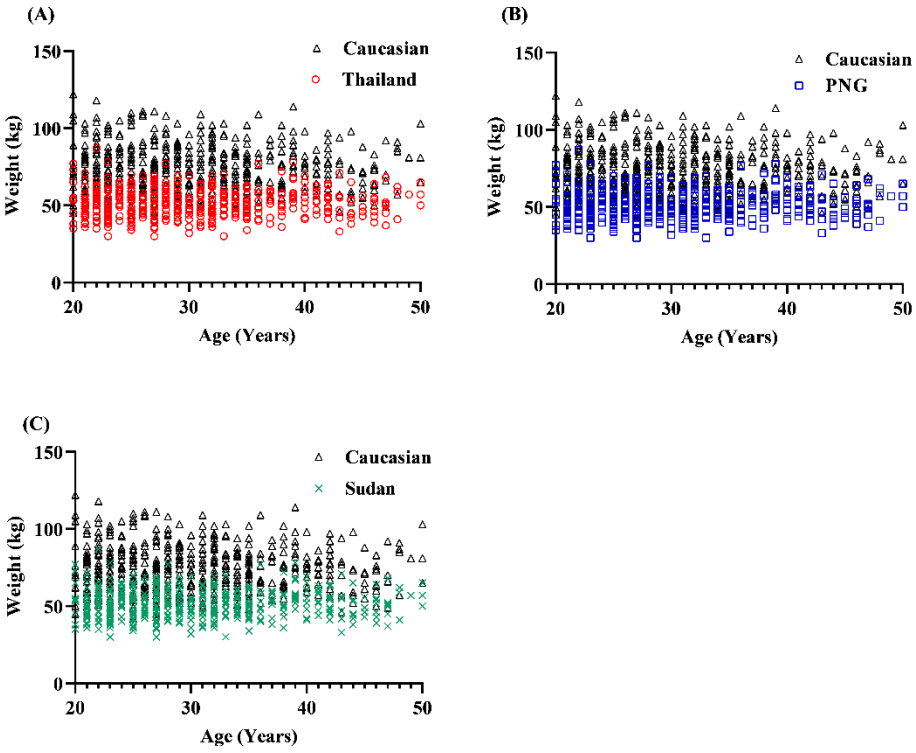

Figure 3.7: Age-weight relationship between Caucasian and subjects from three of population groups.

Age-weight relationship of three population groups in malaria endemic regions compared to Simcyp® age-weight relationships in healthy Caucasian populations. Body weight was compared between three non-Caucasian virtual populations groups and healthy Caucasian subjects within Simcyp®. Simulated non-Caucasian subjects had body weight adjusted based on the polynomial equations obtained from Hayes *et al* (2015). Comparison size was five hundred subjects between 20 year and 50 years of age. Black triangles represent Healthy Caucasian population, red circle represent Thailand population (A), blue squares represent PNG population (B) and green cross represent Sudanese population (C).

Step 2: Validation of PQ model in non-Caucasian, non-pregnant malaria population groups

To assess the predictive performance in multi-dose studies, three-population groups were developed for Thailand, Papua New Guinea and Sudan females based on published clinical studies within these groups, under conditions of standard multi-dose regimens (10 mg/kg PQ base once daily for 3 days).

For all population groups, the majority of predicted parameters (Table 3.4) fell within 2-3-fold of the reported metrics (Table 3.5). Simulated concentration time profiles adequately recovered the concentration time points reported for the Thailand population groups in the Rijken *et al* (2011) (Figure 3.8) (313) and Tarning *et al* (2012) (281) (Figure 3.9) studies, the PNG population groups in Benjamin *et al* (2015) (282) (Figure 3.10) and the Sudan population groups in Hoglund *et al* (2012) (321) (Figure 3.11).

Notable however, for the Thailand population group, the predicted increase in median C_{max} following each dose was only moderately correlated with that reported by Rijken *et al* (2011) (313) (Figure 3.8). However, the clinical end-point marker of successful antimalarial therapy (day 7 concentration) (280) were all simulated (Table 3.4) to within 2-fold of the reported clinical measures (Table 3.5), in addition to day 14 and day 28 concentrations.

Furthermore, the model predictions were also able to capture the differences in day 7 concentration across population groups, despite similar dosing strategies, e.g. Thai 24.74 ng/mL (4.42-64.93 ng/mL) *vs.* Sudanese 34.0 ng/mL (6.8-86.7 ng/mL) population groups. A one-way ANOVA indicated statistical differences in the median day 7 concentrations, when comparing all 4 predicted population studies, with the Sudanese population group demonstrating a statistically higher median C_{max} ($p = 0.0415$) compared to the other population groups. This highlighted the successful creation of sub-population groups.

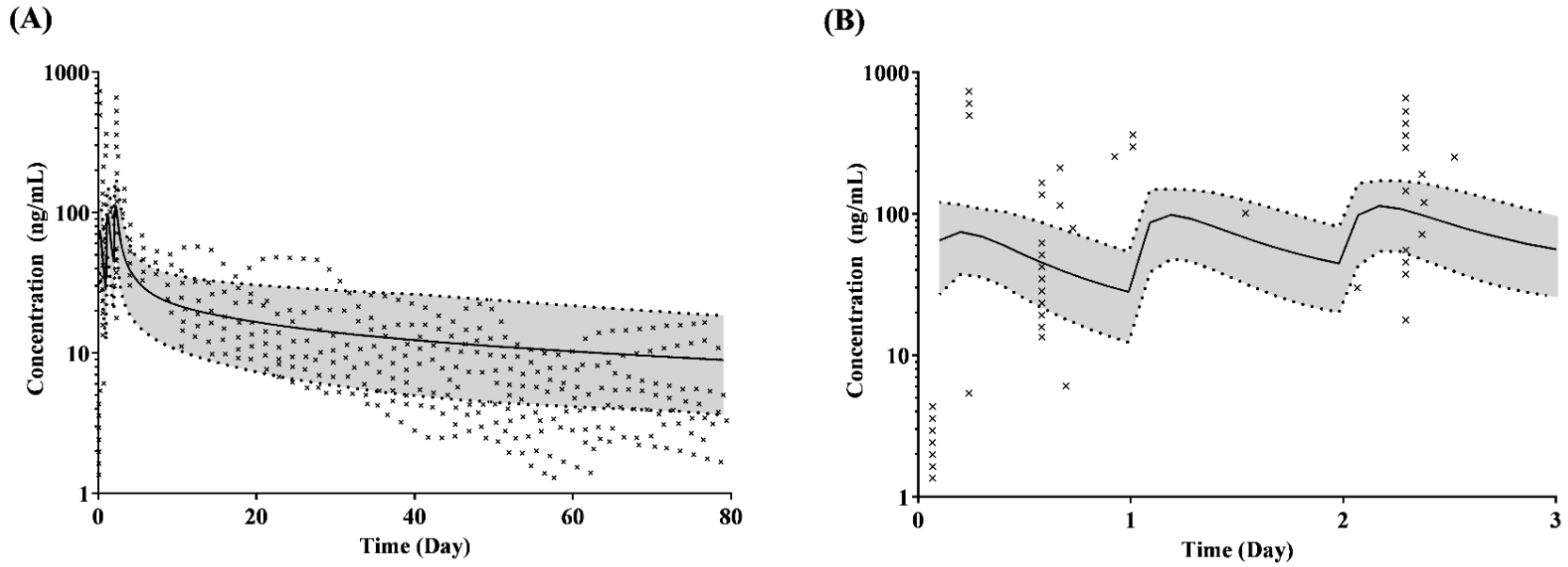

Figure 3.8: The simulated plasma fasted multi-dose concentration-time profile of piperaquine in non-pregnant adapted Thailand malaria-female subjects.

Multidose simulations of PQ (10 mg/kg base once daily for 3 days) were conducted on virtual Thailand malaria-non-pregnant female population groups as detailed in Rijken *et al*, (2011) (313), adapted from the 'Healthy Volunteer' population group with Simcyp® with adaptations to the age-weight relationships and blood biochemistry and matching (where possible) the clinical trial design (subject numbers and age range) within Simcyp®. Crosses indicate observed data obtained from reported individual subject plasma concentration-time profile lines. The solid lines represent population median predictions with the dashed lines/shaded area representing the 5^{th} and 95^{th} percentiles of prediction. (A) the concentration time profile throughout the study period as reported in referenced study, (B) plasma concentration profiles in the first three days post-dosing.

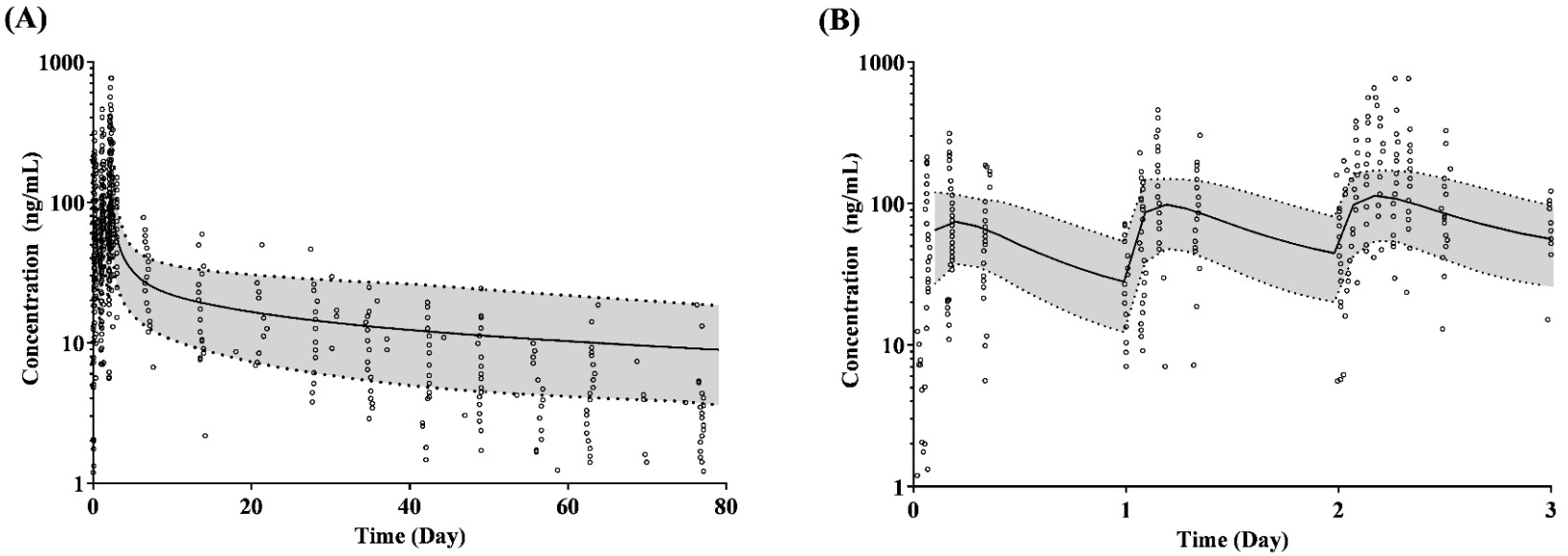

Figure 3.9: The simulated plasma fasted multi-dose concentration-time profile of piperaquine in non-pregnant adapted Thailand malaria-female subjects.

Multidose simulations of PQ (10 mg/kg base once daily for 3 days) were conducted on virtual Thailand malaria-non-pregnant female population groups as detailed in Tarning *et al* (2012) (281), adapted from the 'Healthy Volunteer' population group with Simcyp® with adaptations to the age-weight relationships and blood biochemistry and matching (where possible) the clinical trial design (subject numbers and age range) within Simcyp®. Open circles indicate observed data obtained from reported individual subject plasma concentration-time profile lines. The solid line represent population median predictions with the dashed lines/shaded area representing the 5^{th} and 95^{th} percentiles of prediction. (A) the concentration time profile reported throughout the study period as reported in referenced study, (B) plasma concentration profiles in the first three days post-dosing.

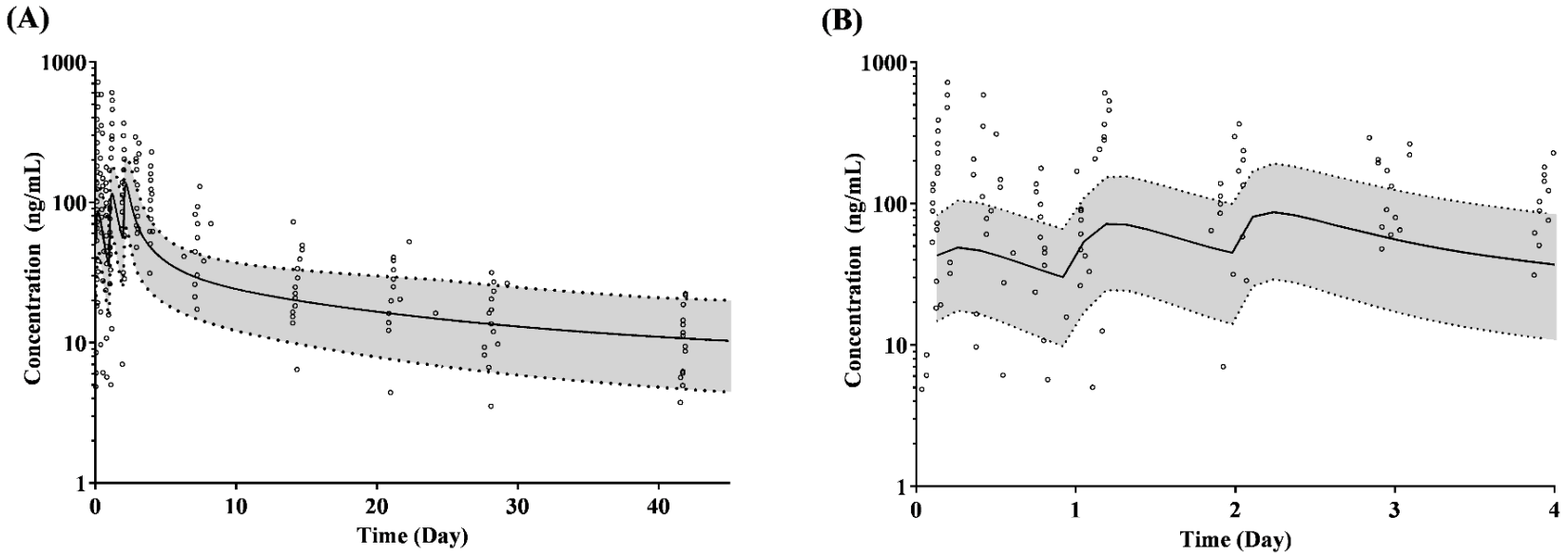

Figure 3.10: The simulated plasma fasted multi-dose concentration-time profile of piperaquine in non-pregnant adapted Papua New Guinea (PNG) malaria-female subjects.

Multidose simulations of PQ (10 mg/kg base once daily for 3 days) were conducted on virtual PNG malaria-non-pregnant female population groups as detailed in Benjamin *et al* (2015) (282), adapted from the 'Healthy Volunteer' population group with Simcyp® with adaptations to the age-weight relationships and blood biochemistry and matching (where possible) the clinical trial design (subject numbers and age range) within Simcyp®. Open circles indicate observed data obtained from reported individual subject plasma concentration-time profile lines. The solid lines represent population median predictions with the dashed line/shaded area representing the 5^{th} and 95^{th} percentiles of prediction. (A) the concentration time profile reported throughout the study period as reported in referenced study, (B) plasma concentration profiles in the first four days post-dosing.

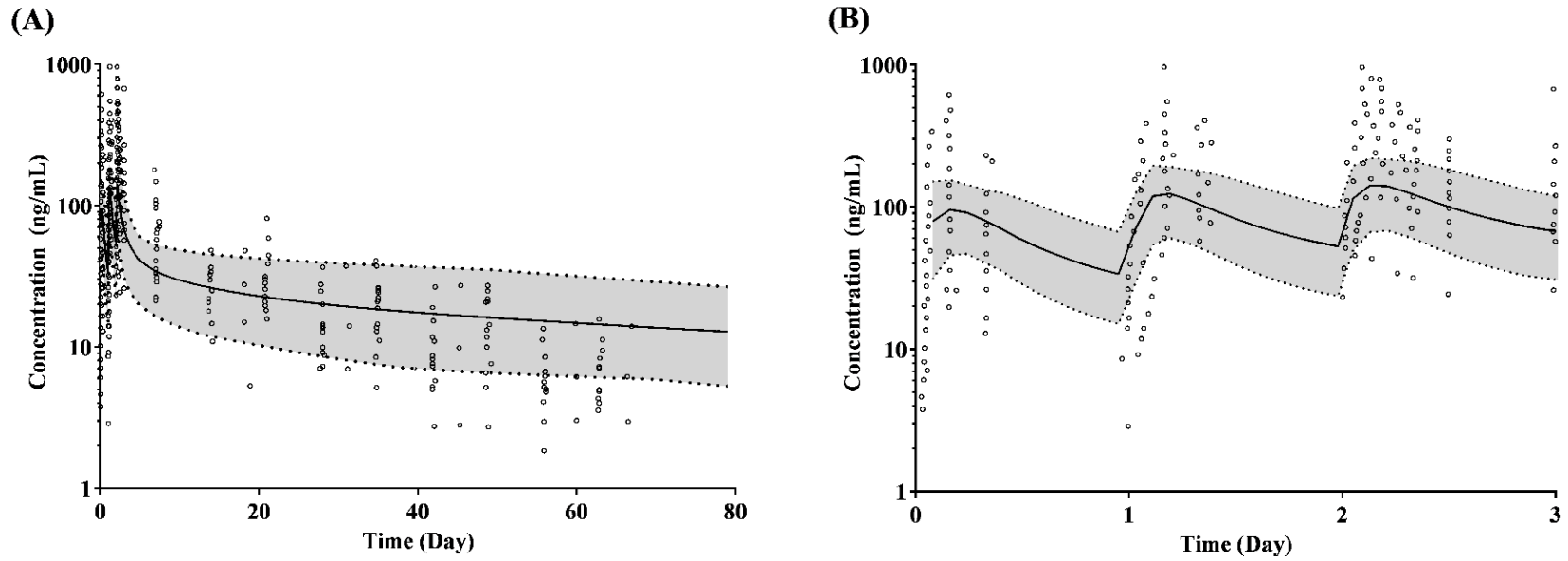

Figure 3.11: The simulated plasma fasted multi-dose concentration-time profile of piperaquine in non-pregnant adapted Sudan malaria-female subjects.

Multidose simulations of PQ (10 mg/kg base once daily for 3 days) were conducted on virtual Sudan malaria-non-pregnant female population groups as detailed in Hoglund *et al* (2012) (321), adapted from the 'Healthy Volunteer' population group with Simcyp® with adaptations to the age-weight relationships and blood biochemistry and matching (where possible) the clinical trial design (subject numbers and age range) within Simcyp®. The open circles indicate observed data obtained from reported individual subject plasma concentration-time profile lines. The solid lines represent population median predictions with the dashed line/shaded area representing the 5^{th} and 95^{th} percentiles of prediction. (A) plasma concentration time profile throughout the study period, (B) plasma concentration profiles in the first three days post-dosing.

Table 3.4: Simulated PQ pharmacokinetics in non-Caucasian non-pregnant females

	Thailand		PNG	Sudan
	Rijken Median (range)	Tarning Median (range)	Benjamin Median (range)	Hoglund Median (range)
C_{max} 1st (ng/mL)	66.1 (17.2-182)	64.6 (18.7-189)	87.7 (20.8-216)	92.2 (25.11-262)
C_{max} 2nd (ng/mL)	85.3 (21.23-242)	88.2 (23.74-252)	116 (25.8-292)	117 (30.71-338)
C_{max} 3rd (ng/mL)	98.5 (23.9-281)	99.2 (24.2-285)	135 (29.3-343)	135 (34.51-389)
T_{max} 1st (h)	4.8 (2.9-6.5)	4.8 (2.8-6.1)	4.7 (2.9-6.5)	3.8 (2.2-5.0)
T_{max} 2st (h)	4.6 (2.6-6.0)	4.6 (2.5-6.3)	4.7 (2.7-6.1)	3.6 (2.2-4.8)
T_{max} 3st (h)	4.6 (2.6-7.6)	4.6 (2.7-7.2)	4.4 (2.7-6.1)	3.6 (2.2-4.8)
AUC_{0-24} (ng/mL.h)	998 (240-2831)	993 (248-2825)	1372(297-3467)	1261 (318-3679)
AUC_{24-48} (ng/mL.h)	1409 (324-4075)	1429 (332-4108)	1968 (405-5064)	1790 (436-5254)
AUC_{48-72} (ng/mL.h)	1712 (384-4946)	1762 (381-4995)	2378 (479-6176)	2194 (521-6384)
$AUC_{0-\infty}$ (ng/mL.h)			21715 (4463-53646)	35201 (304-74181)
Day 7 Conc. (ng/mL)	24.7 (4.42-64.9)	25.1 (4.21-65.1)	29.2 (5.31-80.9)	34.0 (6.8-86.7)
Day 14 Conc. (ng/mL)	17.0 (3.17-41.6)	16.8 (3.22-42.9)	18.8 (3.67-49.9)	24.2 (5.3-54.9)
Day 28 Conc. (ng/mL)	12.0 (2.34-26.3)	11.6 (2.23-27.3)	11.70 (2.05-26.8)	17.5 (4.02-38.7)
Half-life (d)	27.3 (21.3-40.9)	28.5 (20.8-39.8)	18.3 (16.1-23.6)	32.1 (21.6-43.3)

Table 3.5: Literature reported PQ pharmacokinetics in non-Caucasian non-pregnant females

	Thailand		PNG	Sudan
	Rijken	Tarning	Benjamin	Hoglund
	Median (range)	Median (IQR)	Median (range)	Median (range)
C_{max} 1st (ng/mL)		216 (139–276)		102 (40.6-235)
C_{max} 2nd (ng/mL)	71.6 (10.1–239)			
C_{max} 3rd (ng/mL)	136 (13.6–393)			
T_{max} (h)	245 (53.4–798)			
T_{max} 1st (h)		3.04 (2.36–4.13)		1.48 (0.887-4.18)
T_{max} 2st (h)				
T_{max} 3st (h)				
AUC_{0-24} (ng/mL.h)	869 (157–2940)			
AUC_{24-48} (ng/mL.h)	1710 (167–4740)			
AUC_{48-72} (ng/mL.h)	2750 (500–8280)			
$AUC_{0-\infty}$ (ng/mL.h)	24100 (2750–60900)	23400 (17400–35100)	35644 (29546–39541)	38000 (12400–100000)
Day 7 Conc. (ng/mL)	25.9 (6.80–56.6)	22.7 (17.6–32.8)		
Day 14 Conc. (ng/mL)	16.7 (2.24–59.2)			55.4 (16.6-146)
Day 28 Conc. (ng/mL)	9.17 (5.14–47.6)	10.3 (8.06–14.9)		15.4 (4.85-38.6)
Half-life (d)[a]	8.88-24.9	16.2-19.4	15.9	19.1-25.8

[a] Half-life is reported as a range or median

3.4.4 Step 3: Validation of PQ model in non-Caucasian, pregnant malaria population groups

The PBPK model was further adapted to evaluate PQ pharmacokinetics in non-Caucasian pregnant population groups (Figure 3.12-3.15). For all population groups, the majority of predicted parameters (Table 3.6) fell within 2-fold of the reported metrics (Table 3.7), with predictions of the median day 7, 14 and 28 concentrations all simulated to with 2-fold of the reported clinical measures (Table 3.7). These predicted point markers were not significantly different from those for non-pregnant subjects ($p > 0.05$) (Tables 3.4-3.5). Also, to investigate any difference in the concentration time profile and pharmacokinetic parameters of PQ at different stages of pregnancy, the concentration time profile at different gestational ages was compared and found to be largely similar throughout pregnancy (Figure 3.16).

A one-way ANOVA indicated statistical differences in the median day 7 concentrations, when comparing all 4 predicted population studies, with the Sudanese population group demonstrating a statistically higher median C_{max} ($p = 0.0392$) compared to the other population groups (Table 3.6). However, when comparing non-pregnant to pregnant population groups, no significant difference in the median day 7 concentration was identified for each population. Further, predicted half-life in pregnancy population groups were significantly different ($p < 0.01$ for all population groups) from those in non-pregnant population groups (Table 3.4). This highlighted the successful creation of sub-population group.

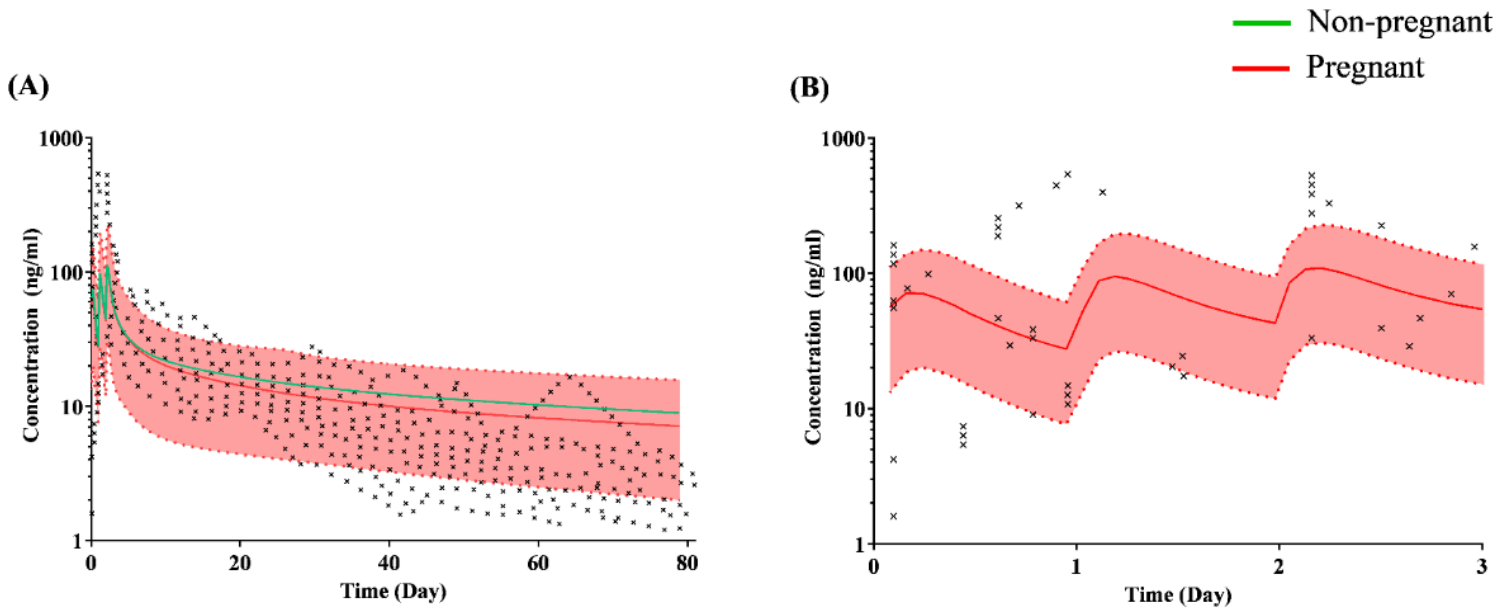

Figure 3.12: The simulated plasma fasted multi-dose concentration-time profile of piperaquine in adapted Thailand pregnant malaria subjects

Multidose simulations of PQ (10 mg/kg base once daily for 3 days) were conducted on virtual pregnant women from Thailand with malaria as detailed in Rijken *et al*, 2011 (313), adapted from the 'Healthy Volunteer' population group with Simcyp® with adaptations to the age-weight relationships and blood biochemistry and matching (where possible) the clinical trial design (subject numbers and age range) within Simcyp®. (A) the concentration time profile reported throughout the study period (B) plasma concentration profiles in the first three days post-dosing. Solid lines (green: non-pregnant [for comparison]; red: pregnant) represent population median predictions with the dashed lines/shaded area representing the 5^{th} and 95^{th} percentiles of prediction. Crosses indicate observed data obtained from reported individual subject plasma concentration-time profile lines.

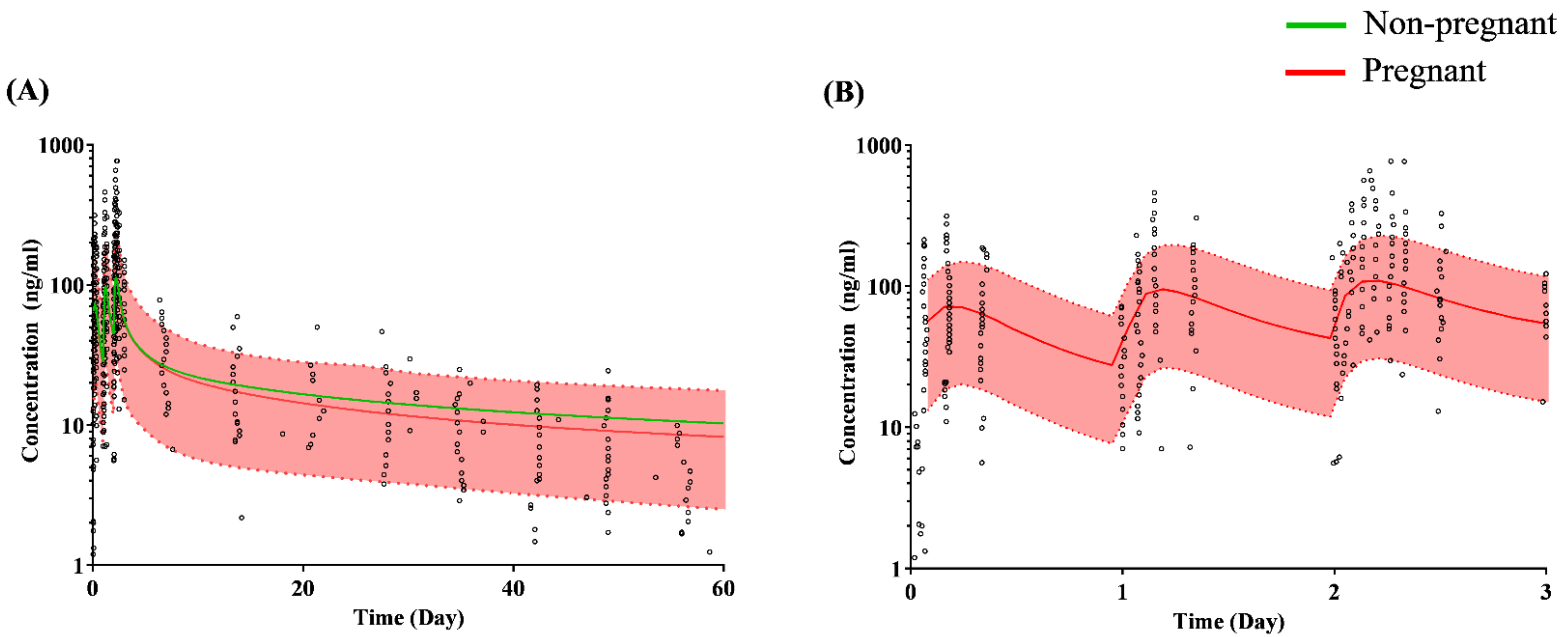

Figure 3.13: The simulated plasma fasted multi-dose concentration-time profile of piperaquine in pregnant adapted Thailand malaria-female subjects.

Multidose simulations of PQ (10 mg/kg base once daily for 3 days) were conducted on virtual pregnant women from Thailand with malaria as detailed in Tarning *et al*., 2012 (281), adapted from the 'Healthy Volunteer' population group with Simcyp® with adaptations to the age-weight relationships and blood biochemistry and matching (where possible) the clinical trial design (subject numbers and age range) within Simcyp®. (A) illustrates the concentration time profile reported throughout the study period study, (B) plasma concentration profiles in the first three days post-dosing. Solid lines (green: non-pregnant [for comparison]; red: Open circles indicate observed data obtained from reported individual subject plasma concentration-time profile lines.

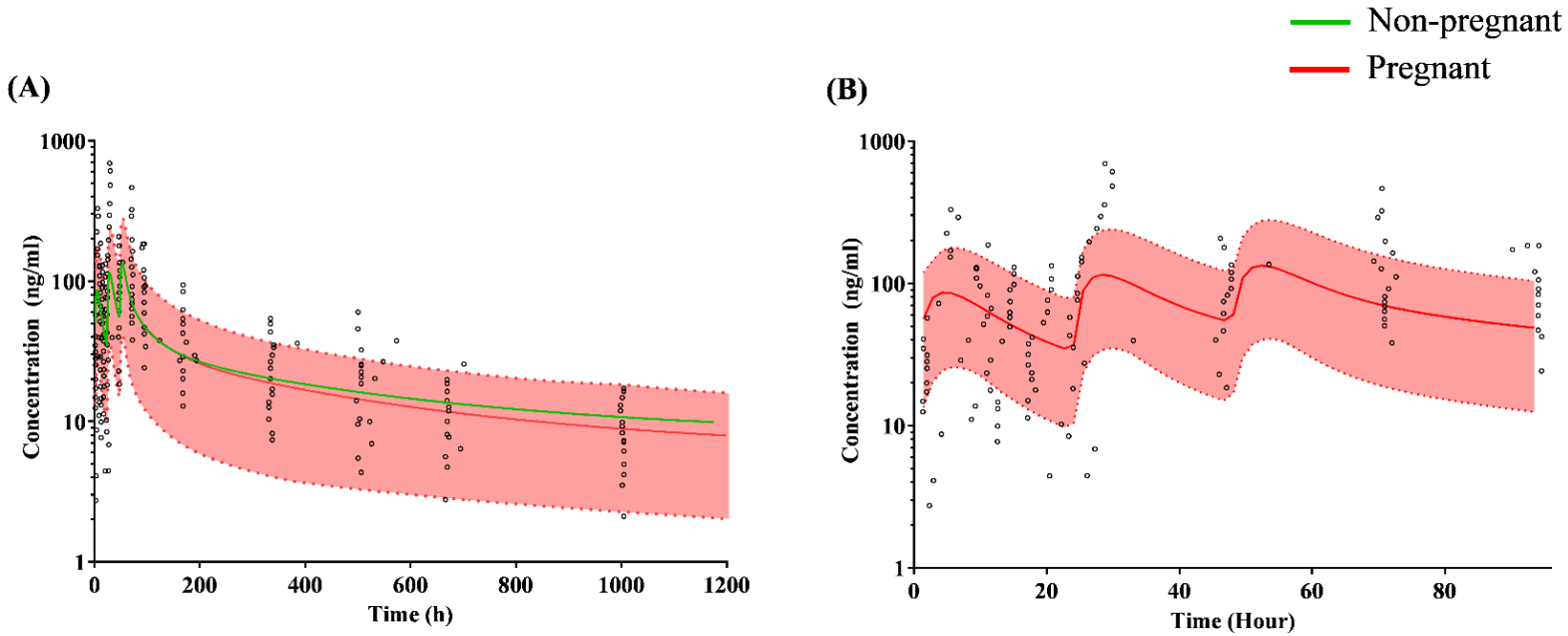

Figure 3.14: The simulated plasma fasted multi-dose concentration-time profile of piperaquine pregnant adapted Papua New Guinea (PNG) malaria-female subjects.

Multidose simulations of PQ (10 mg/kg base once daily for 3 days) were conducted on virtual pregnant women from PNG with malaria as detailed in Benjamin *et al*, 2015 (282), adapted from the 'Healthy Volunteer' population group with Simcyp® with adaptations to the age-weight relationships and blood biochemistry and matching (where possible) the clinical trial design (subject numbers and age range) within Simcyp®. (A) illustrates the concentration time profile reported throughout the study period, (B) plasma concentration profiles in the first four days post-dosing. Solid lines (green: non-pregnant [for comparison]; red: Open circles indicate observed data obtained from reported individual subject plasma concentration-time profile lines.

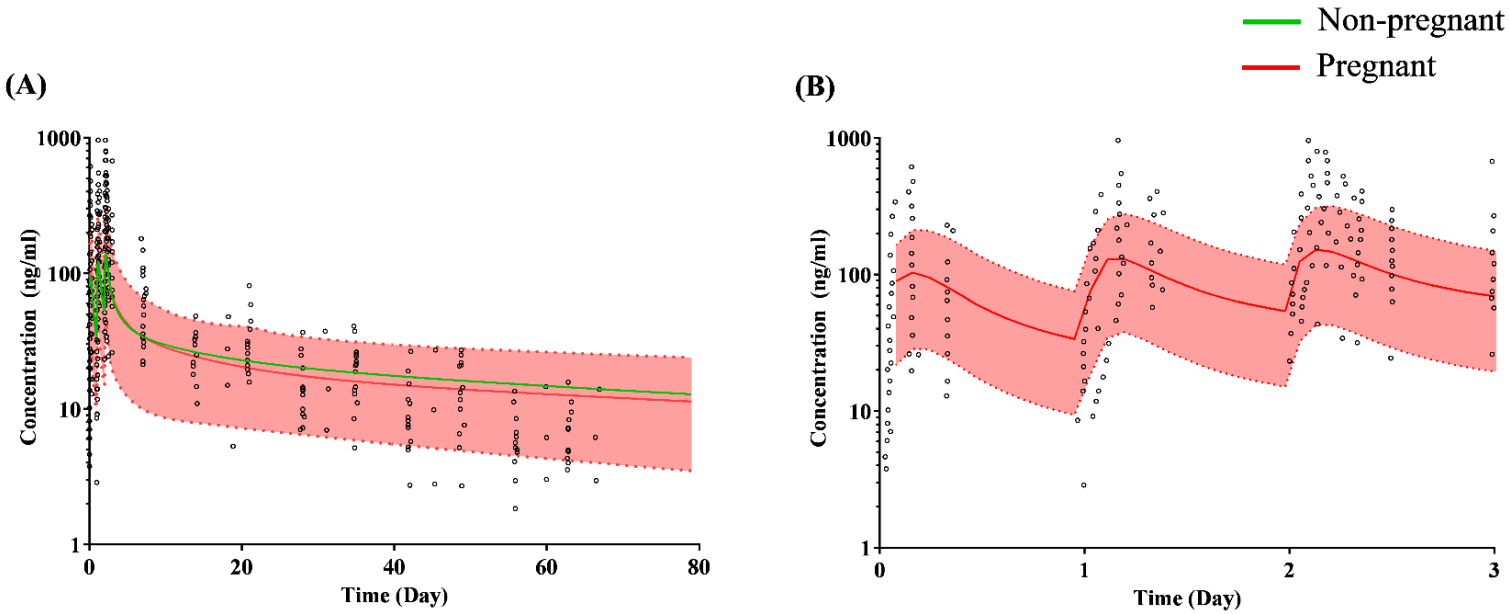

Figure 3.15: The simulated plasma fasted multi-dose concentration-time profile of piperaquine in pregnant adapted Sudan malaria-female subjects.

Multidose simulations of PQ (10 mg/kg base once daily for 3 days) were conducted on virtual Sudan malaria-pregnant female population as detailed in Hoglund *et al*., 2012 (321), adapted from the 'Healthy Volunteer' population group with Simcyp® with adaptations to the age-weight relationships and blood biochemistry and matching (where possible) the clinical trial design (subject numbers and age range) within Simcyp®. (A) illustrates the concentration time profile reported throughout the study period, (B) plasma concentration profiles in the first three days post-dosing. Solid lines (green: non-pregnant [for comparison]; red: Open circles indicate observed data obtained from reported individual subject plasma concentration-time profile lines.

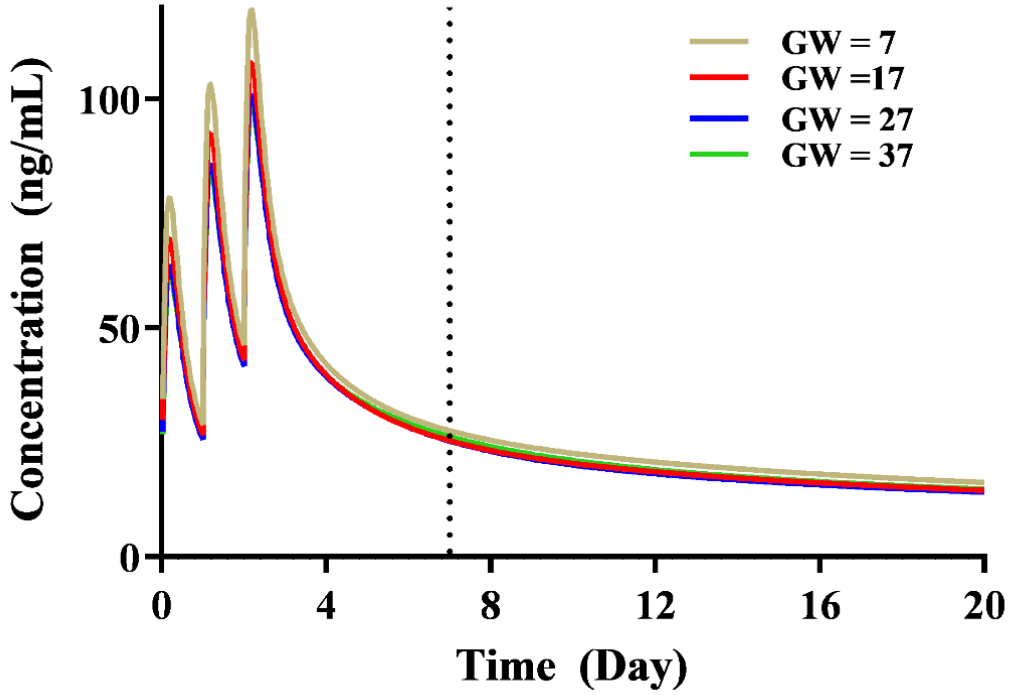

Figure 3.16: Simulated median PQ plasma concentration-time profiles during gestation

Multi-dose simulations of PQ (10mg/kg base once daily for 3 days) for simulations in a representative population group (Thai) (n=30) across gestational weeks 7 to 37. The dashed line represents the day-7 concentration determination point. The Thailand population was chosen as a representative of the other population groups as the same pattern of pharmacokinetics is expected for all three population groups.

Table 3.6: Simulated piperaquine pharmacokinetics in non-Caucasian pregnant females

	Thailand		PNG	Sudan
	Rijken Median (range)	Tarning Median (range)	Benjamin Median (range)	Hoglund Median (range)
C_{max} 1st (ng/mL)	70.4 (33.5-153)	72.4 (31.9-168)	89.5 (38.2-175)	92.9 (41.0-202)
C_{max} 2nd (ng/mL)	90.5 (46-205)	86.2 (50.6-214)	118 (25.8-238)	117 (55.6-263)
C_{max} 3rd (ng/mL)	103 (53.9-237)	109 (53.54-264)	137 (62-277)	132 (65.3-303)
T_{max} 1st (h)	4.8 (2.9-7.7)	4.6 (3.1-7.9)	5.1 (2.9-8.2)	4.3 (2.6-6.9)
T_{max} 2st (h)	4.6 (2.9-6.9)	4.9 (2.9-7.0)	4.8 (2.9-7.2)	4.1 (2.6-6.5)
T_{max} 3st (h)	4.6 (2.9-6.9)	4.8 (2.8-7.1)	4.6 (2.9-6.9)	4.1 (2.6-6.2)
AUC_{0-24} (ng/mL.h)	1036 (565-2429)	1135 (537-2532)	1399 (681-2850)	1249 (112-2974)
AUC_{24-48} (ng/mL.h)	1450 (770-3482)	1424 (779-3599)	2002 (938-4127)	1745 (932-4229)
AUC_{48-72} (ng/mL.h)	1736 (913-4196)	1811 (965-4202)	2408 (1110-4977)	2425 (1114-5108)
$AUC_{0-\infty}$ (ng/mL.h)			21633 (8383-42238)	30067 (15267-84201)
Day 7 Conc. (ng/mL)	25.9 (10.9-52.6)	24.2 (11-53.1)	29.6 (12.2-57.7)	34.0 (15.1-70.6)
Day 14 Conc. (ng/mL)	19.1 (7.88-39.5)	19.9 (8.24-40.1)	20.2 (7.89-38.8)	26.1 (11.3-56.5)
Day 28 Conc. (ng/mL)	14.4 (5.63-31.2)	15.1 (5.91-39.9)	13.6 (4.82-27.2)	20.1 (7.94-45.6)
Half-life (d)	19.4 (18.7-35.4)	19.9 (18.7-35.7)	26.3 (16.7-39.2)	24.7 (14.9-27.2)

Table 3.7: Literature reported piperaquine pharmacokinetics in non-Caucasian pregnant females

	Thailand		PNG	Sudan
	Rijken	Tarning	Benjamin	Hoglund
	Median (range)	Median (IQR)	Median (range)	Median (range)
C_{max} 1st (ng/mL)		291 (194–362)		185 (109–363)
C_{max} 2nd (ng/mL)	138 (39.3–328)			
C_{max} 3rd (ng/mL)	201 (58.2–455)			
T_{max} (h)	309 (138–575)			
T_{max} 1st (h)		3.14 (2.84–3.84)		3.07 (1.65-4.64)
T_{max} 2st (h)				
T_{max} 3st (h)				
AUC_{0-24} (ng/mL.h)	1480 (506–3270)			
AUC_{24-48} (ng/mL.h)	2400 (734–4400)			
AUC_{48-72} (ng/mL.h)	3660 (1160–5010)			
$AUC_{0-\infty}$ (ng/mL.h)	29200 (11600–41800)	27400 (21000–32400)	23721 (21481–27951)	42700 (27100–68700)
Day 7 Conc. (ng/mL)	31.8 (13.3–80.2)	28.8 (23.6–34.6)		60.7 (40.1-103)
Day 14 Conc. (ng/mL)	19.5 (7.76–49.3)			
Day 28 Conc. (ng/mL)	10.7 (3.70–31.4)	10.3 (9.18–14.4)		16.1(9.68-26.8)
Half-life (d)[a]	4.78-39.9	22-26.1	20.3	20.9-33.3

[a] Half-life is reported as a range or median

3.4.5 Step 4: 'What-If' scenarios

3.4.5.1 Validation of DDI simulation between piperaquine and efavirenz in pregnancy

To evaluate and validate the impact of ARV on PQ systemic exposure, the only known study (to-date) which investigated the impact of ARV (efavirenz) on PQ systemic exposure in Ugandan pregnant women (329) was replicated, following creation of a Uganda pregnancy-malaria population group where EFV was orally dosed at 600 mg once daily. Model predictions for HIV-uninfected non-pregnant (malaria) females (Figure 3.17A) and HIV uninfected pregnant (malaria) females (Figure 3.17B) demonstrated the successful development of a Uganda population group with model predictions within the range reported by Kajubi *et al* (2017) (329) (Table 3.8), showing a predictions of day 7, 14 and 21 concentrations to within 2-fold of the reported concentrations. Concentrations for HIV-infected pregnant (malaria) females (Figure 3.17C) were slightly over-predicted (Table 3.8) in terminal elimination phases, and this may be a result of physiological alternatives during HIV-infection which were not explicitly incorporated into our 'Malaria' population group. Comparison of all three profiles (Figure 3.17D) showed that the HIV-infected pregnant (malaria) subjects had the lowest piperaquine exposure relatively. Further, in all simulations the C_{max} per dosing day was under-predicted. As simulations were run under fasted-conditions, this under-prediction may be attributed to the reported clinical studies not restricting food intake during the study period.

The predicated day 7, 14 and 21 PQ concentrations were all within 2-fold of that reported by Kajubi *et al* (2017) (329), with a similar approximate 50 % decrease in the predicted mean day 7 concentrations (No EFV: 20.5 ng/mL; EFV: 9.2 ng/mL) (Table 3.8). Furthermore, our predicted $AUC_{0\text{-}21}$ was within 2-fold of that reported by Kajubi *et al* (2017) (this study: 0.51; Kajubi: 0.62).

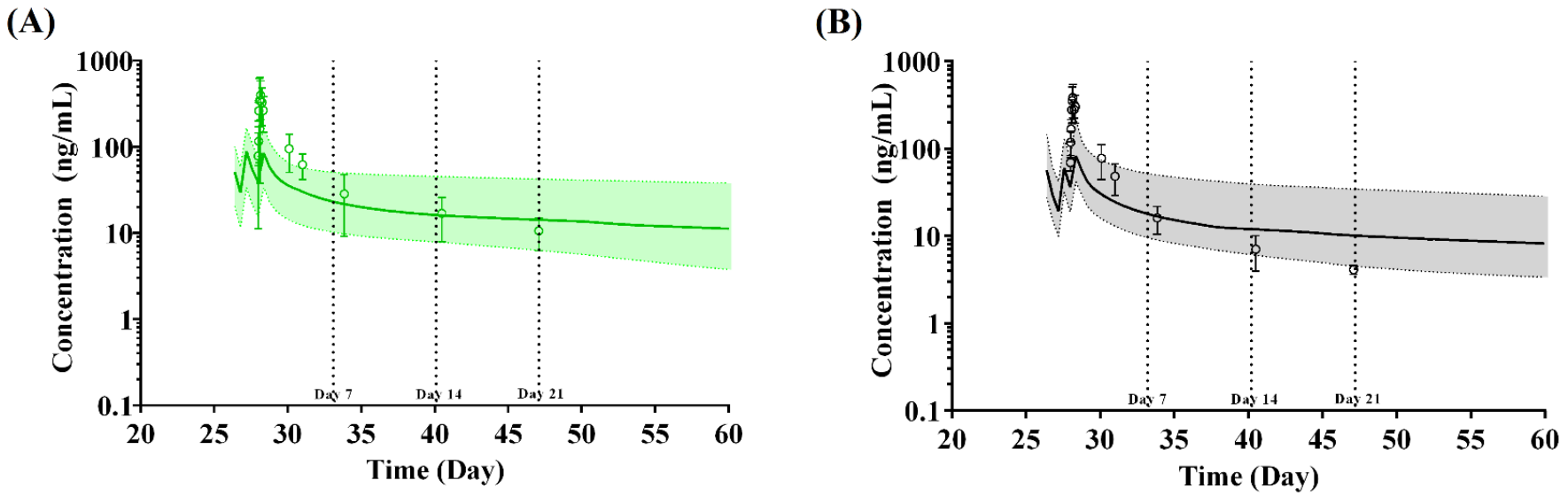

Figure 3.17 : Simulated plasma concentration-time profile of piperaquine in pregnant women in the presence of interaction with efavirenz.

Multi-dose simulations of PQ (960 mg PQP once daily for 3 days) were conducted in (A) HIV-uninfected non-pregnant (malaria) females; (B) HIV uninfected pregnant (malaria) females. PQ dosing was started on day 25 of a once daily dosing of efavirenz which was simulated over 60 days. Solid lines represent median with shaded areas representing 5^{th}-95^{th} percentile range. Open circles represent observed median data points with error bars indicted SD.

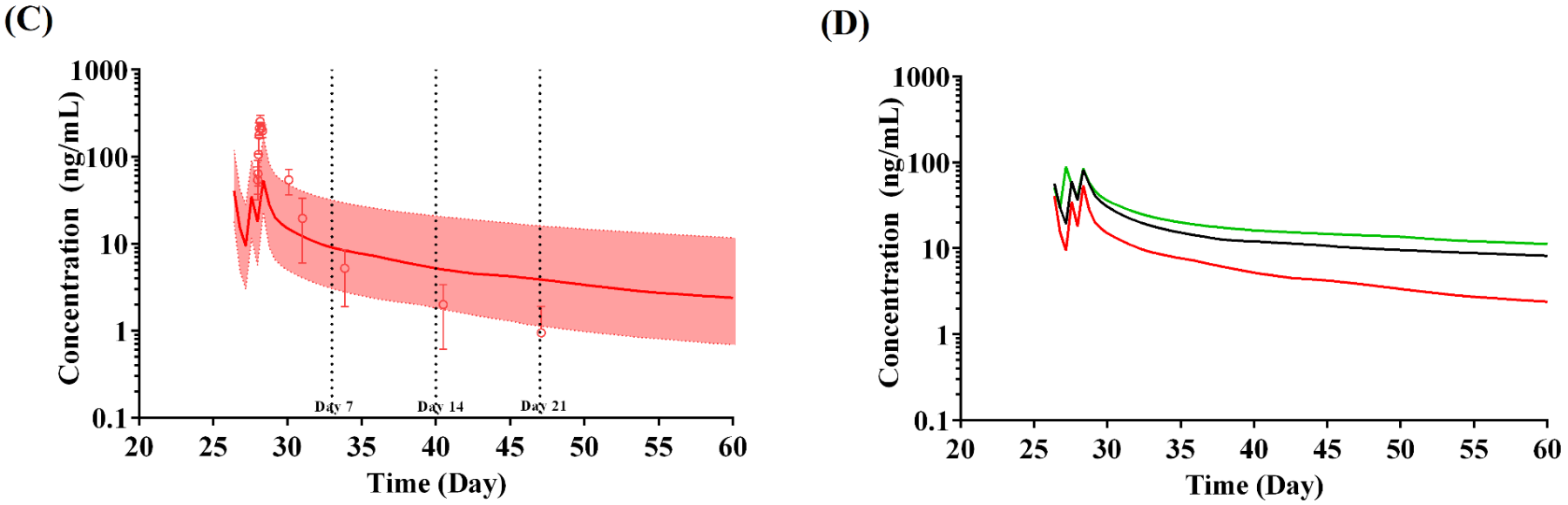

Figure 3.17 (cont.): Simulated plasma concentration-time profile of piperaquine in pregnant women in the presence of interaction with efavirenz.

Multi-dose simulations of PQ (960 mg PQP once daily for 3 days) were conducted in (C) HIV-infected pregnant (malaria) females treated with EFV from day 1 to day 60; (D) Comparison of median plasma concentration-time profiles for the three simulated groups. PQ dosing was started on day 25 of a once daily dosing of efavirenz for which was simulated over 60 days. Solid lines represent median with shaded areas representing 5^{th}-95^{th} percentile range. Open circles represent observed median data point with error bars indicted SD.

Table 3.8: Predicted and observed day 7, 14 and 21 piperaquine concentrations in the absence and presence of a EFV-mediated DDI

	During Pregnancy		Non-Pregnant
	HIV-uninfected (no EFV)	HIV-infected (EFV)	HIV-uninfected (no EFV)
Observed C_{d7} (ng/mL)	30.5 (25.9-36)	15.1 (13-17.6)	39 (32.3-47.2)
Predicted C_{d7} (ng/mL)	20.5 (9.1-54.3)	9.2 (3.1-33.4)	23.7 (9.9-51.2)
Observed C_{d14} (ng/mL)	15 (12.4-18.1)	6.67 (5.44-8.19)	22.6 (18.7-27.3)
Predicted C_{d14} (ng/mL)	11.9 (8.2-16.3)	5.2 (1.25-22.1)	16.5 (7.1-44.9)
Observed C_{d21} (ng/mL)	11.8 (5.7-39)	3.75 (2.77-5.08)	14.5 (12.2-17.1)
Predicted C_{d21} (ng/mL)	10.1 (4.2-32.5)	3.47 (1-15.8)	14.2 (6.2-41.2)

Data represents median (range). EFV: efavirenz.

3.4.5.2 The impact of change in HSA on the extent of ART-DDIs

In all population groups (absence and presence of a DDI), simulations were conducted in 100 virtual subjects. An increase in HSA from 20 g/L to 50 g/L significantly increased the median day 7 (total) plasma concentration of PQ (Figure 3.18-3.20). This was associated with a significant increase in the number of subjects with a day 7 concentration > 30 ng/mL in the absence of an ART (Thailand: 8 to 45, $p = 0.007$ (Figure 3.18); PNG: 11 to 53, $p = 0.00009$ (Figure 3.19); Sudan: 9 to 49, $p = 0.0006$) (Figure 3.20), and in the presence of EFV (Thailand: 7 to 48, $p = 0.006$ (Figure 3.18); PNG: 4 to 24, $p = 0.0003$ (Figure 3.19); Sudan: 1 to 16, $p = 0.0005$ (Figure 3.20)) or RTV (Thailand: 41 to 80, $p = 0.0009$ (Figure 3.18); PNG: 49 to 85, $p = 0.0008$ (Figure 3.19); Sudan: 47 to 80, $p = 0.00003$(Figure 3.20)).

Additionally, the presence of EFV or RTV significantly reduced or increased, respectively, the day 7 PQ concentration across all population groups, however the overall impact of the HSA were broadly similar under different DDI conditions (Figure 3.18-20). This resulted in a similar number of subjects attaining a day 7 concentration ≥ 30 ng/mL except for the Sudanese population with a EFV-mediated DDI, where a statistically significant difference in the median day 7 concentration across the three population groups was identified (one-way ANOVA, $p = 0.0023$)

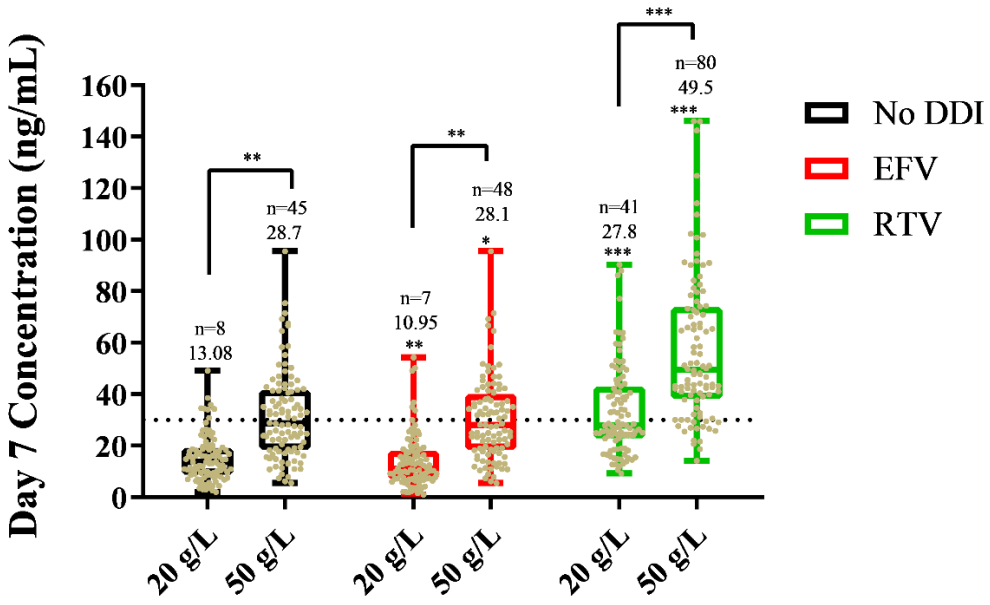

Figure 3.18: The impact of changes in human serum albumin concentrations on the piperaquine median day 7 concentration in the absence and presence of an EFZ or RTV-mediated DDI

Multi-dose simulations of PQP (10 mg/kg base once daily for 3 days) were conducted 100 pregnant women from Thailand with malaria. The human serum albumin concentration was fixed at 20 g/L or 50 g/L. EFV (600 mg once daily) (red bars) or RTV (100 mg twice daily) (green bars) were orally dosed throughout the simulation time period (30 days) with piperaquine dosed on days 10, 11 and 12. Dashed lines indicate the 30 ng/mL clinical efficacy cut-off. Numbers above the box and whisker are median values and the number (n) of subjects with a predicted concentration of over 30 ng/mL is indicated. Vertical drop-lines indicated statistical comparisons between 20g/L or 50 g/L simulations. Asterisks above the maximum bar indicate statistical significance when compared to black (no DDI) simulations. ** $p \leq 0.01$; *** $p \leq 0.001$.

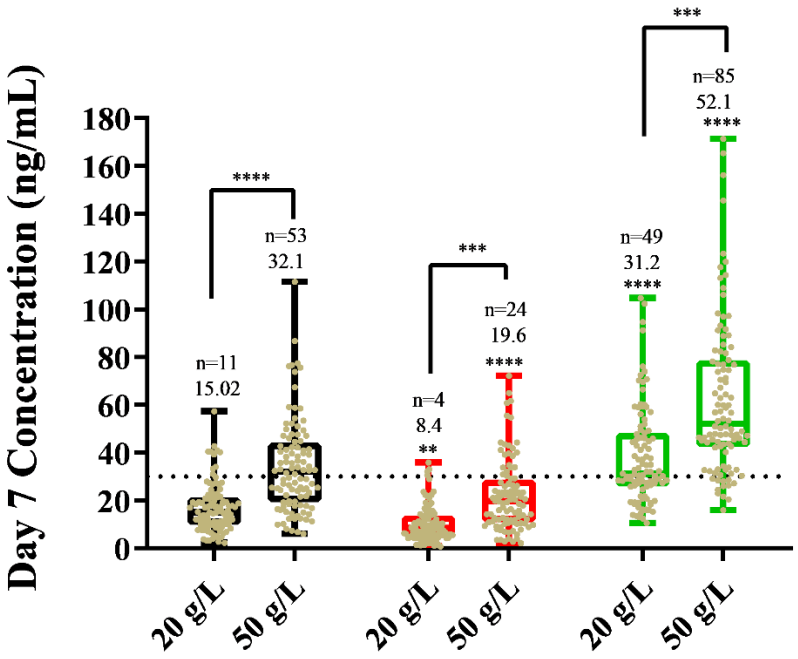

Figure 3.19: The impact of changes in human serum albumin concentrations on the piperaquine median day 7 concentration in the absence and presence of an EFZ or RTV-mediated DDI

Multi-dose simulations of PQP (10 mg/kg base once daily for 3 days) were conducted in 100 pregnant women from PNG with malaria. The human serum albumin concentration was fixed at 20 g/L or 50 g/L. EFV (600 mg once daily) (red bars) or RTV (100 mg twice daily) (green bars) were orally dosed throughout the simulation time period (30 days) with piperaquine dosed on days 10, 11 and 12. Dashed lines indicate the 30 ng/mL clinical efficacy cut-off. Numbers above the box and whisker are median values and the number (n) of subjects with a predicted concentration of over 30 ng/mL is indicated. Vertical drop-lines indicated statistical comparisons between 20g/L or 50 g/L simulations. Asterisks above the maximum bar indicate statistical significance when compared to black (no DDI) simulations. *** $p \leq 0.001$; **** $p \leq 0.0001$.

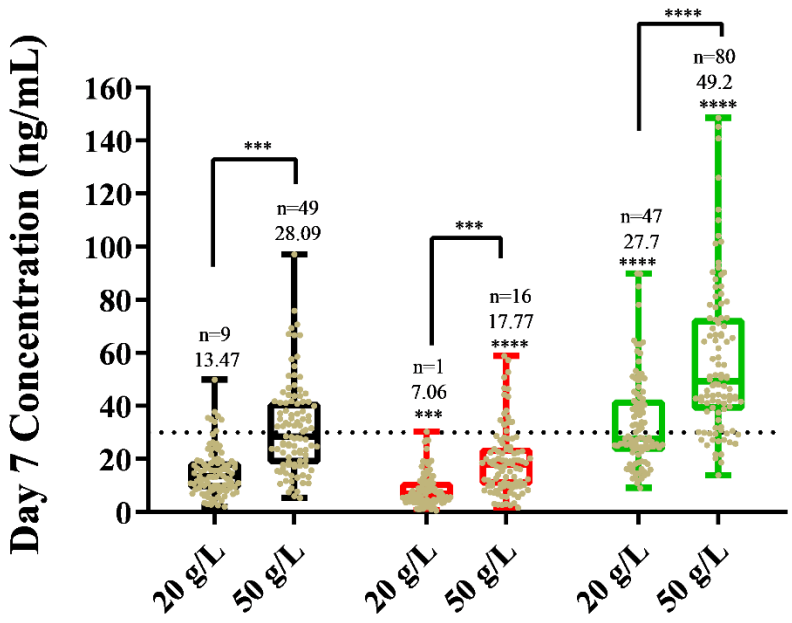

Figure 3.20: The impact of changes in human serum albumin concentrations on the piperaquine median day 7 concentration in the absence and presence of an EFZ or RTV-mediated DDI

Multi-dose simulations of PQP (10 mg/kg base once daily for 3 days) were conducted on 100 Sudan pregnant female with malaria. The human serum albumin concentration was fixed at 20 g/L or 50 g/L. EFV (600 mg once daily) (red bars) or RTV (100 mg twice daily) (green bars) were orally dosed throughout the simulation time period (30 days) with piperaquine dosed on days 10, 11 and 12. Dashed lines indicate the 30 ng/mL clinical efficacy cut-off. Numbers above the box and whisker are median values and the number (n) of subjects with a predicted concentration of over 30 ng/mL is indicated. Vertical drop-lines indicated statistical comparisons between 20g/L or 50 g/L simulation. Asterisks above the maximum bar indicate statistical significance when compared to black (no DDI) simulations. *** $p \leq 0.001$; **** $p \leq 0.0001$.

3.4.5.3 The impact of gestation on the extent of an ART-mediated DDI

In the absence of ART-mediated DDIs, the median predicted day 7 concentration was broadly consistent across all gestational weeks investigated (Thailand: 20.2-21.2 ng/mL; PNG: 22.5-23.5 ng/mL); Sudan: 25.1-26.2 ng/mL) and demonstrated no significant difference across gestational weeks within the same population group (Figure 3.21-3.23).

In the presence of EFV, a significant decrease in PQ day 7 concentrations ($p < 0.0001$) was simulated across all gestational weeks within each population group (Thailand: 9.8-11.3 ng/mL; PNG: 13.2-21.5 ng/mL; Sudan: 15.4-18.3 ng/mL), except for gestational week 40 with the PNG population group (Figure 3.21-23). In the presence of RTV, a significant increase in PQ concentrations ($p < 0.0001$) was simulated across all gestational weeks within each population group (Thailand: 34.2-37.9 ng/mL; PNG: 40.7-42.2 ng/mL; Sudan: 41.3-46.1 ng/mL). Furthermore, a trend in increasing median day 7 concentration with increasing gestational week was observed for all population groups, although this was not statistically significant (Figure 3.21-3.23).

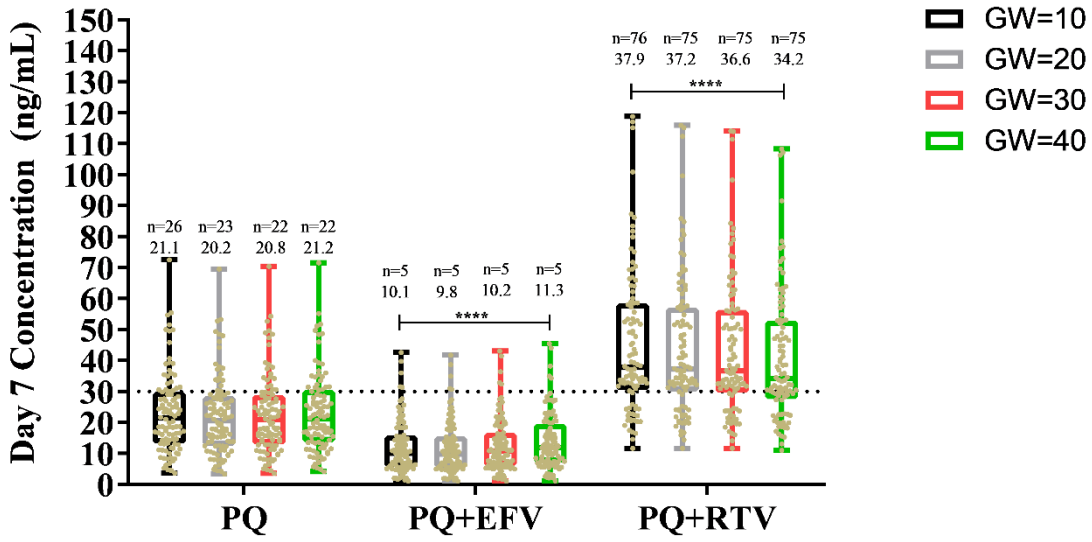

Figure 3.21: The impact of changes in gestational week on median day 7 PQ concentration in the absence and presence of a DDI mediated by EFZ (induction) or RTV (inhibition).

Multidose simulations of PQP (10 mg/kg base once daily for 3 days) were conducted on 100 Thailand pregnant female with malaria (over gestational weeks (GW) 10, 20, 30 and 40. Interaction perpetrators – EFV (600 mg once daily) or RTV (100 mg twice daily) were co-administered) were orally dosed throughout the simulation time period (30 days) with PQ dosed on days 10, 11 and 12. Box and whisker plots represent minimal, 25th percentile, median, 75th percentile and maximum values. Dashed lines indicate the 30 ng/mL clinical efficacy cut-off. Numbers above the box and whisker are median values and the number (n) of subjects with a predicted concentration of over 30 ng/mL is indicated. Horizontal drop-lines indicate statistical comparisons between each GW in the absence and presence of the ART. **** $p \leq 0.0001$.

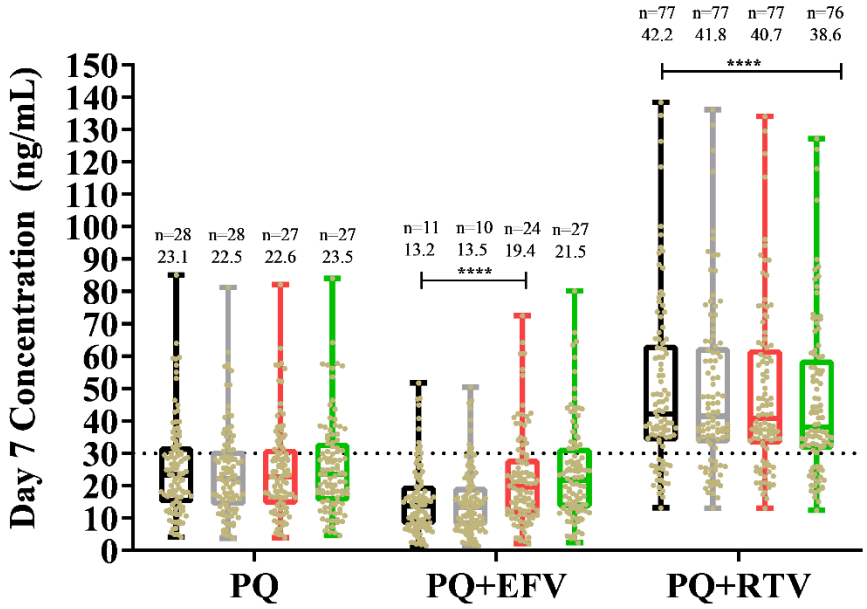

Figure 3.22: The impact of changes in gestational week on median day 7 PQ concentration in the absence and presence of a DDI mediated by EFZ (induction) or RTV (inhibition).

Multidose simulations of PQP (10 mg/kg base once daily for 3 days) were conducted on 100 PNG pregnant female with malaria (over gestational weeks (GW) 10, 20, 30 and 40. Interaction perpetrators – EFV (600 mg once daily) or RTV (100 mg twice daily) were co-administered) were orally dosed throughout the simulation time period (30 days) with PQ dosed on days 10, 11 and 12. Box and whisker plots represent minimal, 25th percentile, median, 75th percentile and maximum values. Dashed lines indicate the 30 ng/mL clinical efficacy cut-off. Numbers above the box and whisker are median values and the number (n) of subjects with a predicted concentration of over 30 ng/mL is indicated. Horizontal drop-lines indicate statistical comparisons between each GW in the absence and presence of the ART. **** $p \leq 0.0001$.

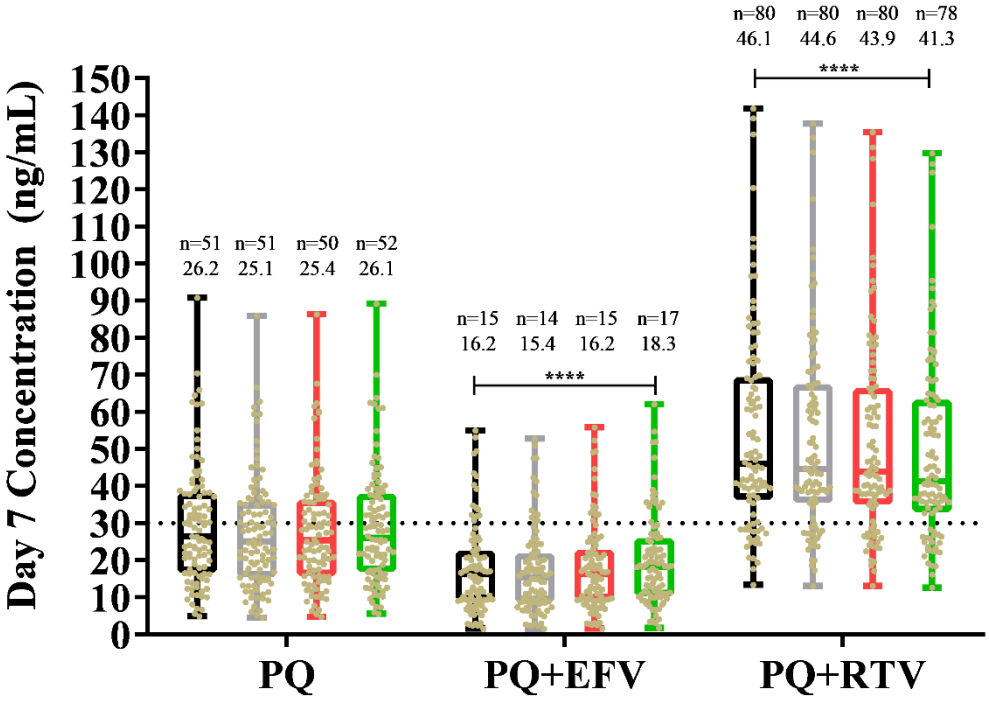

Figure 3.23: The impact of changes in gestational week on median day 7 PQ concentration in the absence and presence of a DDI mediated by EFZ (induction) or RTV (inhibition).

Multidose simulations of PQP (10 mg/kg base once daily for 3 days) were conducted on 100 Sudan pregnant female with malaria (over gestational weeks (GW) 10, 20, 30 and 40. Interaction perpetrators – EFV (600 mg once daily) or RTV (100 mg twice daily) were co-administered) were orally dosed throughout the simulation time period (30 days) with PQ dosed on days 10, 11 and 12. Box and whisker plots represent minimal, 25th percentile, median, 75th percentile and maximum values. Dashed lines indicate the 30 ng/mL clinical efficacy cut-off. Numbers above the box and whisker are median values and the number (n) of subjects with a predicted concentration of over 30 ng/mL is indicated. Horizontal drop-lines indicate statistical comparisons between each GW in the absence and presence of the ART. **** $p \leq 0.0001$.

3.4.5.4 The changes in clearances and AUCs in the presence and absence of interaction across gestational weeks.

Using the Thailand population as a representative population group, the possibility of changes in oral/hepatic clearance and AUC during gestation was simulated. There was a statistical difference (p<0.0001) between the oral clearance estimates in the presence and absence of an interaction (Figure 3.24), similarly, there was a statistical difference (p<0.0001) between the hepatic clearance estimates in the presence and absence of an interaction (Figure 3.24). However, when clearance and AUC comparisons in the presence or absence of interaction was made to identify any difference across the gestational weeks, there was no statistical difference. Further, the AUC from the last dose to the end of simulation in the absence of interaction was similar throughout pregnancy as there was no significant difference between the estimated parameters. As expected, the AUC ratio between aforementioned AUC estimates the in the absence and presence of interaction with EFV and RTV was below 1 and above 1 respectively but was largely consistent throughout gestational weeks (Figure 3.25). The impact of HSA on the hepatic clearance during pregnancy is summarised in Table 3.9 which showed that hepatic clearance was consistently higher in patients with severe malaria compared with healthy patients in the presence or absence of DDIs.

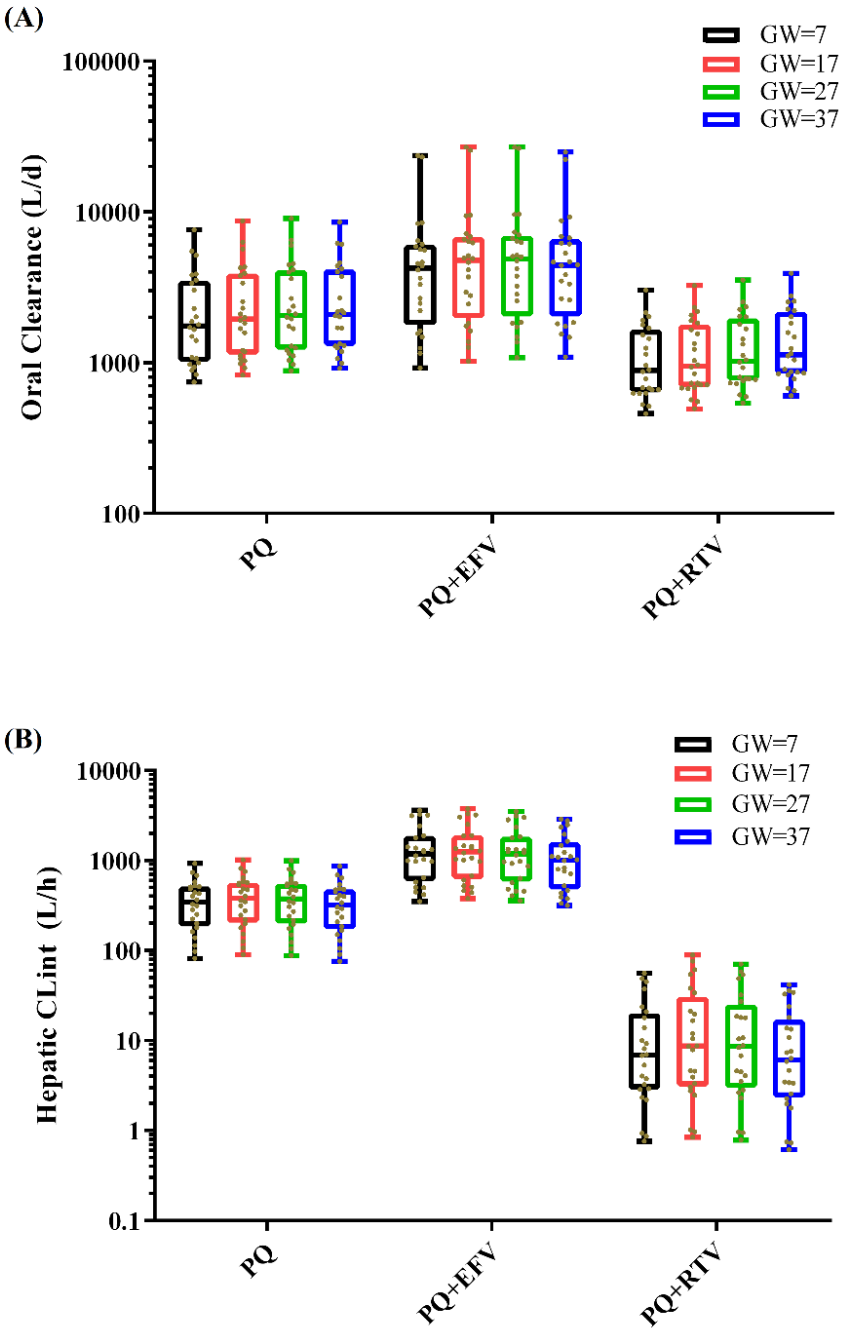

Figure 3.24: Variation in intrinsic hepatic and oral clearance parameters in the absence and presence of ART-mediated DDIs

Comparison of the oral clearance (A) and hepatic intrinsic clearance (B) of piperaquine in pregnant representative Thailand subjects administered piperaquine alone and in combination with efavirenz or ritonavir. GW: gestational weeks. The simulation was done in twenty five subjects per GW.

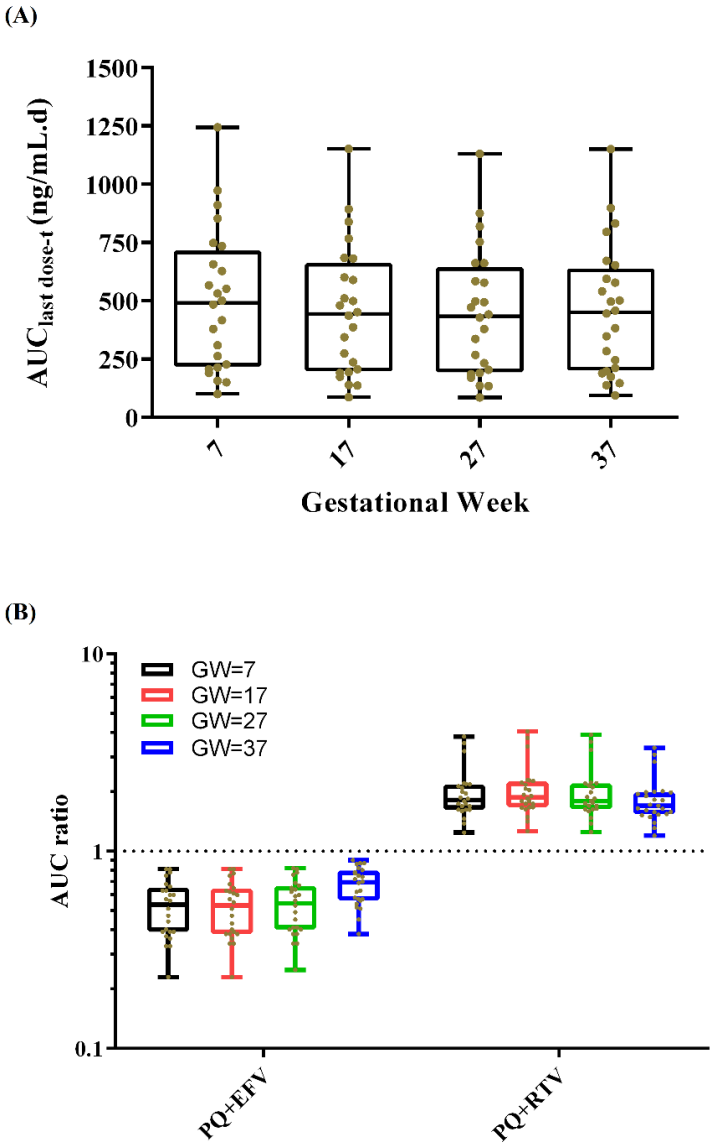

Figure 3.25: Variation in AUC (A) and AUC_{ratio} (B) in the absence and presence of ART-mediated DDIs

The AUC between the last dose of piperaquine administered and the specified gestation weeks (A), and AUC ratios (B) of piperaquine alone and in the presence of interaction with efavirenz or ritonavir in pregnant representative Thailand subjects. GW: gestational weeks. The simulation was done in twenty-five subjects per GW.

Table 3.9: Impact of changes in human serum albumin on hepatic clearance in the absence and presence of a efavirenz or ritonavir mediated drug-drug interaction for a representative population group (Thailand non-pregnant).

	No DDI			Efavirenz			Ritonavir		
	Healthy	20 g/L [a]	50 g/L [a]	Healthy	20 g/L	50 g/L	Healthy	20 g/L	50 g/L
CL_h (L/h)	8.4 ± 4.5	16.2 ± 6.9	7.1 ± 3.8	33.9 ± 10.9	46.9 ± 10.3	29.9 ± 9.4	2.6 ± 1.3	5.1 ± 2.4	1.9 ± 0.9
fu_{plasma}	0.0139 ± 0.0014	0.0368 ± 0.0037	0.0135 ± 0.0013	0.0138 ± 0.0016	0.0375 ± 0.0032	0.0136 ± 0.0014	0.0137 ± 0.0016	0.0381 ± 0.0031	0.0138 ± 0.0014
HSA (g/L) [b]	45.3 ± 4.5	16.7 ± 1.7	46.8 ± 4.7	45.7 ± 4.7	16.6 ± 1.7	47 ± 4.6	45.2 ± 4.6	16.9 ± 1.7	47.2 ± 4.6

[a] Pre-defined fixed mean human serum albumin (HSA) concentration.

[b] Simcyp® simulated population median HSA concentration

Data represented as median ± standard deviation

Healthy: Healthy Volunteer population group; CL_H: hepatic clearance; fu_{plasma}: unbound fraction in plasma; HSA: human serum albumin.

3.5 Discussion

The treatment of malaria in special populations, such as pregnant women and young children, is complicated by the 'moving-target' nature of such population groups and their associated reduced immune function with which to resist the individual impact and spread of malaria. Attempting to address the problem of antimalaria treatments in malaria endemic areas requires careful consideration of the disease pathophysiology in those population groups which may in turn impact upon the efficacy endpoint of the antimalarial treatment. With the aid of PBPK modelling techniques, these factors can be investigated separately to suggest the effect specific impacts can make on antimalarial therapy clinically. Hence, the applied 4-stage workflow model (Figure 3.1) was aimed at developing and validating a PBPK model to assess the pharmacokinetics of PQ during pregnancy, as well as under conditions of altered serum albumin (mimicking severe malaria), and during potential DDIs; these were mediated by common ARTs available for use in pregnant women (efavirenz and ritonavir).

3.5.1 Model development

Despite the advantages of PBPK/mechanistic modelling, the application of modelling approaches to the prediction of plasma concentration profiles has largely been based around systems-parameters derived from Caucasian healthy subjects. The base model development in step 1 followed this similar approach, but only to identify and optimise parameters for single dose PQ studies. A common feature of many antimalarials is the large variability in absorption kinetic processes, represented by a highly variable C_{max}, and it was important to capture this, where possible (49, 310, 314, 334). To this end, in the absence of appropriate *in vitro* Caco-2 derived passive permeability (P_{app}) measures for PQ, we applied a first-order absorption model with final estimates of 0.50 for f_a and 0.45 h^{-1} for k_a which were able to recover the C_{max} and t_{max} compared to the single-dose studies (Figure 3.3-3.5). However, to capture the range of reported values (e.g. C_{max}: 14-31.5 µg/L and t_{max}: 2.1-11.7 h) a 50 % CV was applied. It should be noted that an inclusion of a transit absorption model, such as the Simcyp® ADAM module, may improve predictions (281) but the lack of appropriate *in vitro* permeability measures makes this less attractive over a first order model. The development of the base model was successful for single dose studies.

Malaria is endemic in developing countries and this is reflected by the availability of reported clinical studies we identified where PQ was administrated to pregnant and non-pregnant women from studies conducted with subjects from Thailand (281, 313), Sudan (321) and Papua New Guinea (282). Application of the 'Healthy-Volunteer' population group to simulate PQ pharmacokinetics would not be appropriate given the difference in adult age across these geographic regions (335) and therefore custom age-weight relationships (283) were generated for each population group to develop non-pregnant and pregnant populations from these regions, which incorporated alterations in blood parameters (haematocrit, human serum albumin and alpha-1-acidic glycoprotein) (Table 3.2). Changes in haematological biochemistry are also common in malaria and it plays a major role in pathogenesis (336-338). From a pharmacokinetic perspective, such changes are likely impact upon the blood:plasma ratio, but more importantly the unbound fraction, a key driver for the prediction of clearance, Vss and the DDIs.

The development of appropriate systems-based population groups, specific to the study design is important and highlighted by the stark differences in body weights compared to the 'Healthy Volunteer' population. Using the customised age-weight relationships for malaria population body weight for Thai (49.7 ± 7.1 kg), PNG (58.3 ± 12.2 kg) and Sudan (53.2 kg ± 14.5 kg) were generally consistent and significant difference ($p < 0.01$) from a standard 'Healthy Volunteer' population group giving an average weight of 66.7 ± 13.1 kg (Figure 3.6). Also, Figure 3.7 illustrates the distribution of age-weight relationships between healthy Caucasians and the three non-Caucasian population groups. As dosing for many AMT is based on body weight, this may have a direct effect on the dose administered and the resultant determination of endpoint concentrations (339, 340), particularly considering dosing in many developing countries is based on age as a surrogate for body weight, in situations where weight facilities are unavailable.

Further, the inclusion of potential alterations in biochemistry- based changes during pregnancy or because of a disease state are important if they are thought to directly impact upon the resultant pharmacokinetics of AMT. Haematological alterations are common in malaria and a marker of the severity of malaria is often determined from changes in serum albumin. Equally, albumin binding is a direct driver for the free fraction of drugs, and any alterations in this may directly impact upon drug distribution and metabolic pathways.

Indeed, the stark difference in HSA in Sudanese (45.5 g/L) and Thai (33.7 g/L) individuals illustrates this difference across population groups (Table 3.2).

3.5.2 Model simulations and validation.

For the three population groups developed, model predictions of key pharmacokinetic metrics were within 2-fold of those reported and illustrate the successful prediction of PQ in non-pregnant (Table 3.4-3.5) (Figure 3.8-3.11) and pregnant women (Table 3.6-3.7; Figure 3.12-3.15). Notably, no significant differences in key pharmacokinetic parameters, including day 7 concentrations, were observed between non-pregnant or pregnant population groups, suggesting the systemic exposure of PQ is relatively unchanged between the two groups and concurs with other reports of unchanged PQ pharmacokinetics in non-pregnant and pregnant populations (281, 313, 341). However, model predictions were less successful at predicting the interindividual variability in the range of C_{max} for population groups for each dosing period (Figure 3.8-3.15). This may be partially due to poor control of food intake during the trial study, e.g. Tarning *et al* (2012) (281), but may also be a feature of the sparse collection points around the expected C_{max} for each dosing day compared to the much richer collection over the longer elimination phases (281). Further, the larger predicted C_{max} for each dosing period could be a result of the splanchnic blood flow (as a result of increased cardiac output) seen in pregnancy (342), and which is altered using 'Pregnancy' population groups in Simcyp®, and hence represents a slight increase in the bioavailability of PQ (281).

3.5.3 Drug-drug interaction predictability of the model

During pregnancy, the activity of CYP3A4 is also known to increase (343), directly impacting upon the metabolic clearance of any CYP3A4 substrates. In our simulations, increasing gestational week had a noticeable impact of the terminal elimination of the PQ (Figure 3.15A), as quantified by a decrease in the terminal elimination half-life of PQ during pregnancy populations (Table 3.6) compared to non-pregnancy populations (Table 3.4).

Having established a working PBPK for PQ in pregnant females, the importance of the risk of DDIs was next assessed. The only existing study assessing the risk of DDI with PQ and antiretroviral (efavirenz) was recently published by Kajubi *et al* (329), and

demonstrated a 40% reduction in $AUC_{0\text{-}21d}$ along with a 50 % reduction in day-7 concentrations, highlighting the potential risk EFV-mediated DDIs pose, and our model was able to recapitulate these changes (Figure 3.17A-D). As EFV is known to induce CYP3A4, the reduction in AUC and day-7 concentration is likely to be a result of this effect (344). Further, this effect would be augmented by the induction of CYP3A4 itself during pregnancy, as noted for other drugs (295, 342), and therefore would likely reduce day-7 concentrations below the clinical efficacy end-point of 30 ng/mL (280). Indeed, our model simulation demonstrated the impact of this in non-pregnant, pregnant and pregnant +EFV populations, demonstrating the additive effect of EFV-mediated DDI and pregnancy-related induction of CYP3A4 expression (Figure 3.17A-D).

3.5.4 The impact of blood biochemistry on the PQ pharmacokinetics when co-administered with DDI perpetrators during pregnancy.

Although pregnancy has been associated with a reduction in haematological parameters, e.g. human serum albumin (decrease by 1% at week 8 and 12% at week 32 (345)), the impact of such changes on the pharmacokinetics of highly bound drugs is not well characterised in malaria infected subjects. Further, as demonstrated by the development of specific populations, the overall haematological levels are often reduced in such populations. It has also been speculated that *P. falciparum* plays a major role in proteolysis of albumin (346, 347). Further, previous reports have demonstrated alteration in fu_{plasma} for quinine (348) and halofantrine (349) during the progression of malaria. In attempting to assess the impact of potential changes in human serum, albumin on the overall extent of ARV-mediated DDIs (via assessing change in PQ day 7 concentration), we set the HSA concentration to 20 g/L (severe malaria) and 50 g/L (healthy subjects). In all cases (absence and presence of an ARV) and in all population groups, the change from 20 g/L to 50 g/L had a direct impact on day 7 concentrations, leading to a statistically significant increase (Figure 3.18-3.20). For all population groups developed, the reduction in HSA to 20 g/L, generally resulted in a statistically significant increase in PQ fu_{plasma} ($p < 0.001$) which subsequently propagated to an increase in the hepatic clearance ($p < 0.001$), when compared to compared to healthy volunteer population groups. This trend was also demonstrated under conditions of efavirenz/ritonavir exposure when compared to non-DDI studies (see Table 3.9 for representative illustration in the Thailand non-pregnant population). The impact of this combined reduction in baseline HSA

concentration in malaria population coupled with the pregnancy-related reduction in HSA is important considering as it can directly impact upon the elimination of the drug.

As expected, the impacts of EFV and RTV on day 7 concentrations were in-line with their function as CYP3A4 inducer (EFV) and inhibitors (RTV) resulting in a direct effect on day-7 concentration (Figure 3.21-3.23). A reduction in AMT concentrations as a result of induction will lead to parasite recrudescence, as has been demonstrated for lumefantrine (350, 351), dihydroartemisinin (180) and piperaquine (329). Further, piperaquine is known to prolong QTc in a concentrations dependant manner (352), and increased concentrations following inhibition of metabolic clearance may potentially lead to QTc prolongation, as demonstrated with an adapted 2-day treatment with DHA-PQ (353).

3.5.5 The impact of gestational weeks on the pharmacokinetic of PQ when co-administered with DDI perpetrators during pregnancy.

Physiological changes during gestation can result in significant changes in plasma volume, CYP expression and cardiac output (295, 342), it would therefore be expected that significant changes in the pharmacokinetics would occur during pregnancy. We explored the impact of gestation on the predicted day-7 concentrations in the three pregnancy population groups.

In all three populations, the baseline median day 7 concentration was consistent across all population groups and with increasing GW, approximately 20-26 ng/mL, with no significant differences when GW increased (Figure 3.21-3.23). Given the long half-life of PQ, the impact of gestation on day 7 concentrations may not be significantly noticeable. However, CYP3A4 activity is thought to increase during pregnancy, reaching a peak at approximately week 20-24 (354-356). When considering the Thai population as an example, at baseline, GW20 corresponded with the lowest median day-7 concentration and highest hepatic *CLint* (week 17-27) (Figure 3.24B). However, the impact of this may be negligible given the long half-life and large volume of distribution of PQ (282, 313, 324, 341).

3.5.6 The impact of pregnancy on the AUC and clearance of PQ in the presence of interaction

When ARVs were concomitantly dosed with PQ, statistically significant decreases (efavirenz) or increases (ritonavir) in PQ median day-7 concentrations were predicted, in-line with the role of EFV and RTV as inducer/inhibitors of CYP3A4 expression. Surprisingly, there were no significant difference across GW for either ARV, suggesting the magnitude of the DDI would be similar, irrespective of the gestation period of the mother. Further, when considering the Thai population as an example, although each ARV resulted in a significant change in the hepatic *CLint* in the absence of ARV and presence of ARV, no significant differences across gestational weeks were simulated (Figure 3.24B). Similarly, although each ARV resulted in a significant change in the oral CL in the absence of ARV and presence of ARV, no significant differences across gestational weeks were simulated (Figure 3.24A). The resultant AUC_{ratio} (last dose-to-end) in the presence of EFV was consistent across GW 7 to 27 but increased to 0.72 at GW 37 (Figure 3.25A-B). Similarly, inhibition results in an AUC_{ratio} across GW 7 to 27 which decreased to 1.64 at GW 37 (Figure 3.25A-B).

3.5.7 Population variation impact on the PQ pharmacokinetics in pregnant women.

The median day 7 concentration in the absence and presence of an ARV-mediated DDI was consistently higher in the Sudanese population compared to Thai and PNG populations, and this can be attributed to the lower body-weight corrected doses administered to Thai subjects (Table 3.9) coupled with the higher HSA concentrations in Sudanese populations (Table 3.9). Thus, although the impact of ARV on PQ pharmacokinetics in pregnancy may lead to treatment failure or an increase in the adverse effects, the overall effect and magnitude of the DDI during pregnancy is largely minimal, with little change in day-7 concentrations.

It should be noted that in the population groups developed, only the age-weight relationships and haematological parameters were the changes reflecting changes observed predominantly in malaria-infected subjects. Genetic polymorphisms in CYP2B6 are common (357-359) and may impact upon the clearance of EFV and hence its ability to elicit a DDI, and CYP2B6 population-based polymorphic changes were not incorporated into our customised population groups. Further, changes in the abundance

of CYP-isozymes across population groups have also not been incorporated and this may enable better predictions of the terminal elimination phases for PQ across population groups (360). It should also be noted that only one previous study reported PQ metabolic pathways (315) and our assumption of the fraction metabolised by CYP3A4 and CYP2B6 of 0.99 and 0.01, alongside parameter estimated CLint, may be optimised at a later date with *in vitro* metabolic clearance data to enhance the application of the model, when such data becomes available.

3.5.8 Study challenges

The complexity of diseases states which can present differently depending upon the disease progress, as is common with malaria and HIV (361), would dictate that the developed population groups should address these different stages of disease progression. Finally, the studies used for validation utilised two DHA-PQ combination formulation regimens, Eurartesim® (Sigma-Tau, Rome, Italy) or Artekin® (Holleykin Pharmaceutical Co., Guangzhou, China). However only Eurartesim® has gained Good Manufacturing Practice compliance, having being developed without the Medicines for Malaria Venture (MMV) (362). Therefore, batch-to-batch variability in the manufacture of the Artekin® fixed-dose combination tablet, may lead to variability in disintegration/dissolution process resulting in altered absorption kinetics and this should be considered in the context of further validation of the absorption kinetics of the model development. Finally, estimates of PQ *in vitro* Caco-2 permeability are currently lacking and therefore this precludes the application of the Simcyp® Advanced Dissolution, Absorption and Metabolism (ADAM) model, to appropriately model the biopharmaceutic processes in greater mechanistic detail. The modelling of the absorption phase of PQ pharmacokinetics may therefore be improved when such information becomes available. In the ADAM model, more complex processes occurring during the absorption of drug molecules from the gut are accounted for. This might involve the simulation of the absorption of drugs from immediate release and modified or controlled release dosage forms or the simulation of the metabolic and transporter DDIs in the small intestine. The ADAM model therefore enables credible simulation of gut absorption, transport, metabolism and interaction (115).

3.6 Conclusion

The present PBPK model provides the ability to mechanistically predict the pharmacokinetics of PQ in non-pregnant and pregnant women, whilst also considering possible population differences in malaria-HIV co-infected subjects. The present model demonstrated that PQ pharmacokinetics in pregnancy was relatively unchanged, compared to non-pregnant women and that the impact of ART-mediated DDIs can significantly alter the PQ pharmacokinetics, the magnitude of which was generally consistent across GW. Further adaptions of the model presented are warranted and would require further detailed collation of relevant physiological and biochemical alterations common to HIV/malaria patients and which would further enhance the clinical application of the proposed model.

CHAPTER 4

PBPK optimisation of chloroquine dosing for the treatment of Zika Virus disease during pregnancy

Disclaimer

Elements of this chapter have been published as follows:

Olusola Olafuyi, Raj K.S Badhan. Dose Optimization of Chloroquine by Pharmacokinetic Modelling during Pregnancy for the Treatment of Zika Virus Infection. **Journal of Pharmaceutical Sciences**. 2019 Jan;108 (1):661-673

DOI: 10.1016/j.xphs.2018.10.056

4.1 Introduction

First isolated in an infected Ugandan monkey in 1947 (363) Zika virus (ZIKV), is a single stranded RNA *Flavivirus* transmitted to its host via bites from various *Aedes* species mosquito and is similar to the dengue virus (364). An epidemic of the disease broke out in Yap Island in 2007 and was later known to have been reported in French Polynesia between 2013 and 2014 and was followed by a spread to the parts of the Americas around 2015 (363, 365) . With cases reported in recent times in several countries across the world, the spread of ZIKV disease may now be referred to as a pandemic (363). In 2014, cases of Zika virus infection were found in countries from Africa, Asia, the Americas and the Pacific (365), while currently the Pan American Health Organisation (PAHO) and the World Health Organisation (WHO) report that aside from the states within the USA where there are cases autochthonous cases of ZIKV disease, 48 other Central and South American countries have now become affected by the transmission of the disease. There have been a total of 3720 cases of congenital syndrome associated with the infection (48). During the epidemic in Brazil in 2015, there were about 440,000-1,300,000 estimated cases as at December 2015 (366). Due to the non-specific and asymptomatic nature of the infection, a detailed worldwide prevalence has proved difficult to report, however, the Centers for Disease Control and Prevention (CDC) also report that excluding congenital disease cases, between January 2015 and May 2018, there had been 5700 symptomatic cases of ZIKV disease in the USA and 37,229 cases in US territories (367). ZIKV has an incubation period thought to be between three and 12 days. A key symptom of the disease is a maculopapular rash in the face, palm, sole and trunk which is expected to be seen within seven days of infection and infection may last for weeks. Other symptoms of the disease include fever, joint pain, conjunctivitis and retroocular headache and usually resolve in one week (368-370).

4.1.1 Health implications of Zika virus disease

Though ZIKV may be a mild infection owing to the fact that in about 80 % of cases, the disease results in no hospitalisation or deaths, an acute inflammatory polyradiculoneuropathy known as Guillian-Barre syndrome, is a complication and can consequently cause weakness and reduced reflexes in victims (368, 370). Another rather disturbing fact about the infection is its ability to cross the placenta and bring about congenital anomalies such as microcephaly and other ophthalmologic abnormalities in the foetus. In Brazil, an unusual spike in the incidence of microcephaly by early 2016 was

reported involving 270 confirmed cases of microcephaly in the foetus and this was thought to be attributed to the outbreak Zika virus at around mid-2015 (371, 372).

Twenty seven out of 35 infants born with microcephaly involved in a Brazilian study exhibited severe microcephaly. Findings in the study revealed that all 35 mothers in the study had habited to different extents, areas where cases of ZIKV had been existent during their pregnancy and all their infants had not tested positive for any other congenital infection (366). ZIKV RNA was found to be present in the placenta and foetal tissue as well as the amniotic fluid of mothers with new-borns during the outbreak of the disease in Brazil (366, 372). Therefore, a major concern for ZIKV virus disease has over time drifted toward the foetus as these are more prone to the consequences of the disease.

4.1.2 Treatment options of Zika virus disease

Presently, work is underway to develop new vaccines or treatment for ZIKV disease as there are currently none. The potential for new and already existing pharmacological agents to be used to treat or prevent ZIKV disease is being explored. For instance, interferon (IFN) have been studied by various groups for their effectiveness in treating ZIKV. Contreras *et al* (2016), showed via a ZIKV cultivated *in vitro* cell culture system that IFN-a, IFN b and IFNy inhibit viral replication (373), also another group of researchers demonstrated that ZIKV growth is inhibited in trophoblastic and non-trophoblastic cells when the production of IFN-gamma 1 is stimulated (374). Nanchangmycin, a polyether originating from the Streptomyces nanchangensis was screened and found to inhibit ZIKV replication abilities, however further research is required to further validate its clinical efficacy (375).

Another potential anti-ZIKV agent, Obatoclax, a broad spectrum antiviral agent with probable antineoplastic properties, has been shown to prevent the endosomal fusion of ZIKV in *in vitro* systems and may be considered as a prophylactic option for ZIKV (376). A natural product, Cavinafungin has also recently been found to possess an inhibitory effect against the ZIKV due to its ability to inhibit the endoplasmic reticulum signal peptides of the host in *in vitro* systems (377). Similarly, 25-hydroxycholesterol has been discovered to inhibit ZIKV entry into the host in a mouse and rhesus macaque study (378). Cial *et al* (2017) demonstrated that other agents like ribavirin and favipiravir reduce ZIKV induced cell death (379). There are tens of other agents which have been

studied in *in vitro* or in *in vivo* mouse models but the major concern about them are their safety in humans and in pregnancy (380).

4.1.3 Chloroquine as a potential anti-Zika virus agent

In a study by Delvecchio *et al* (2016), it was demonstrated that the antimalarial agent chloroquine provides protection to the human brain microvascular endothelial and neural stem cells in addition to mouse neurospheres by inhibition of the ZIKV (381). Chloroquine is potentially an efficacious inhibitor of the ZIKV disease, this potential coupled with the fact that its safety profile as an antimalarial and anti-rheumatoid arthritis agent is widely documented makes it stands out as a good candidate for repurposing in the prevention of ZIKV disease.

Chloroquine (CQ) was first developed for the treatment of different forms of malaria but is currently recommended for the treatment of *Plasmodium vivax* malaria infection due to wide-spread resistance by the common *Plasmodium falciparum* malaria. In addition to it antimalarial benefits, it has been used as a suppressant of autoimmune disorders like rheumatoid arthritis (RA) and systemic lupus erythematosus (SLE) (382). CQ is almost totally absorbed following oral administration. A study showed that in the fasted condition and in subjects who took the drug orally, 89% of the drug was absorbed (383). There is conflicting data about the effect of food on oral absorption. While one study suggests that gastrointestinal absorption of CQ is not altered in the presence of food (384), another study reports that maximum concentration (C_{max}) and exposure (area under the curve (AUC)) of CQ were significantly higher following administration of 600 mg of CQ to 7 healthy volunteers who had received a standard breakfast (385). A separate study suggested that the intake of CQ with local Sudanese beverages decreased the C_{max} and AUC of CQ phosphate administered to the subjects in the study. The author of this study explained that the acidic beverages might have ionised CQ in the gut thereby reducing its absorption (386).

It is worthy of note that oral absorption can show between 30-100% variability among subjects and this might be influenced by certain health conditions, for example in cases of malnutrition (387-389). CQ is well distributed in the body and its plasma steady state volume of distribution (V_{ss}) has been reported to be between 204 and 800 L/kg (390) with plasma protein binding of about 60% (391). With a long half-life of about 20-60 days

(383), CQ is both renally and hepatically excreted from the body with both routes contributing equally to its excretion. An average of 55% is excreted unchanged in the urine while CYP *2C8*, 3A4 and *2D6* are the main metabolising pathways in the liver (392).

4.1.4 Chloroquine safety during pregnancy

Though the efficacy of chloroquine for the treatment of malaria is now mainly acknowledged for *vivax* malaria due to development of resistance to the *falciparum* strains, its safety profiles remains satisfactory in pregnant and non-pregnant subjects at doses used for malaria, SLE and RA. The use of chloroquine as an oral antimalarial dates as far back as 1984 (393), and in 1985, Wolfe *et al* (1985) demonstrated that there was no significant teratogenic consequences of chloroquine used by pregnant women to their foetus (394). They showed that among the 169 births from women who had received 300 mg weekly of chloroquine for malaria during their pregnancy, there was no significant difference in birth defects between these women and those who has not received, the treatment. Infants born to the majority of pregnant women with RA and SLE who received, in their first trimester up to 250 daily doses of CQ for long periods of time prior to and during pregnancy or a 500 mg daily dose for up to three days during early pregnancy, did not develop adverse conditions due the use of CQ in their mothers (35). Another study showed that compared to pregnant women who received quinine treatment during pregnancy, there was no significant difference in the mean gestational age; stillbirths and rates of abortion in 130 pregnant women who received 25 mg/kg of CQ for three days in their first trimester of treatment for vivax malaria during pregnancy (395). Similarly, in 634 Thai pregnant women, treatment of malaria vivax with 25 mg/kg CQ for three days resulted in no foetal anomalies in infants born to them (396).

In this current study, a pharmacokinetic modelling approach will be used to estimate the level of exposure following current dosage regimens of CQ to the foetus while a prospective approach to assess dosage regimen options that will ensure adequate foetal exposure will be explored.

4.2 Aims and objectives

4.2.1 Aims

The aim of this chapter was to use PBPK techniques to optimise the dosing of oral chloroquine for the treatment of ZIKV disease in pregnant women.

4.2.2 Objectives

1. To develop and validate a PBPK model for CQ in non-pregnant and pregnant women.
2. To determine an effective and safe systemic concentration of CQ for prevention of ZIKV.
3. To propose a dosing schedule of CQ for the treatment of ZIKV disease in pregnant women.
4. To determine the impact of different stages of pregnancy on the attainment of safe and therapeutic concentrations of CQ for the treatment of ZIKV disease in pregnant women
5. To determine the appropriate length of administration of CQ to produce the required exposure to ensure protection against ZIKV disease in pregnant women.

4.3 Methods

The virtual clinical trial simulator Simcyp® (Simcyp® Ltd, a Certara company, Sheffield, UK, Version 17) was used to create all the population based PBPK models used in this study through the implementation of a pre-validated 'Healthy Volunteer' (HV) population. For simulations requiring the use of pregnant subjects, we utilised the Simcyp® 'Pregnancy' population group (297, 307, 397), which incorporates gestational-phase dependant physiological changes associated with pregnancy that may alter the pharmacokinetics of drugs such as a change in blood volume and organ/tissue blood flows; change in enzyme/protein expressions (297, 398-402).

A 3-stage workflow model was utilised and is detailed in Figure 4.1. We adopted a robust validation approach utilising 16 clinical studies for CQ, a summary of which is described in Table 4.1 and Table 4.2. Further, unless otherwise stated, population sizes used in validation steps simulations and those utilised within Steps 3 included a 10x10 trial design with 100 subjects

4.3.1 Study design

Three stages of model development and validation were followed as depicted below

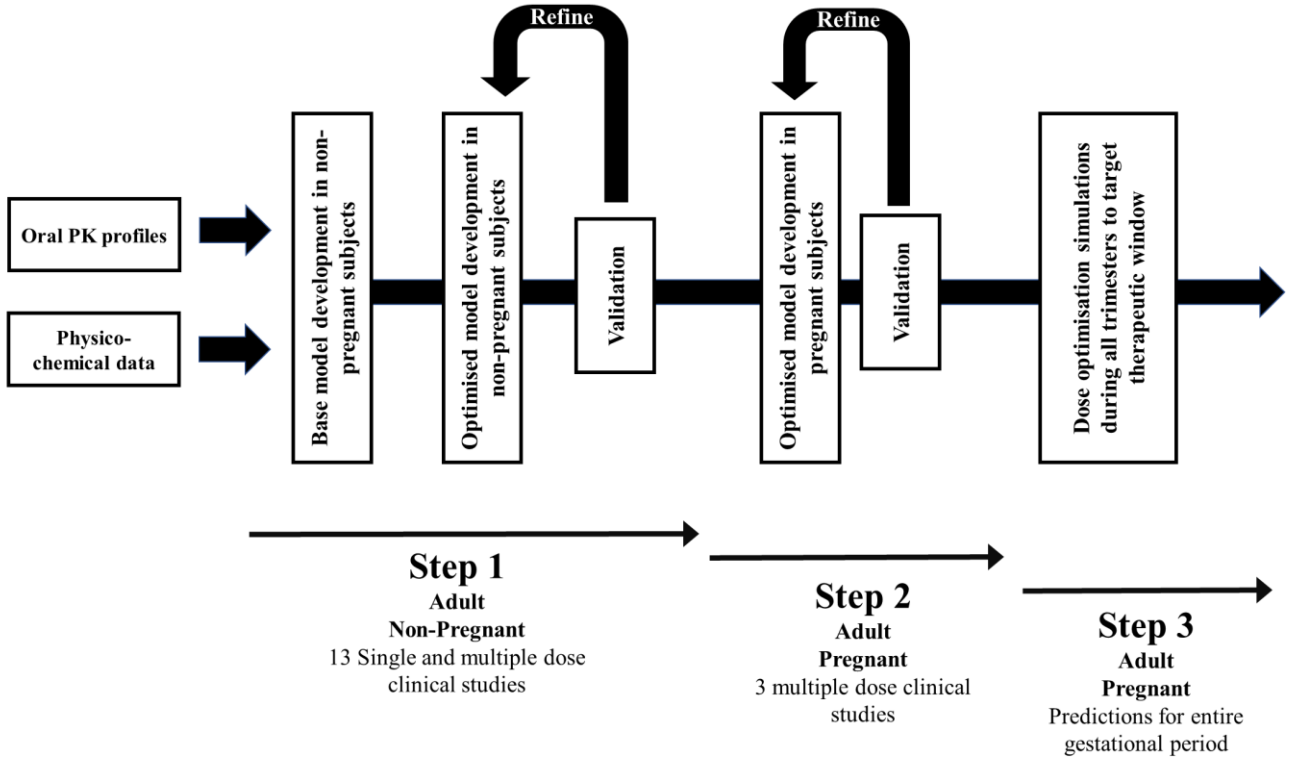

Figure 4.1: A workflow of the processes involved in the development and validation of the chloroquine model and optimisation of CQ dosing for Zika virus disease

4.3.1.1 Step 1: Development and validation of the base model of CQ in non-pregnant Caucasian

CQ physicochemical parameters were obtained from published studies. Where some model parameters where not available in published studies, these were either predicted from the molecular descriptors of chloroquine or back calculated from a clinical *in vivo* parameter when available using the Simcyp® retrograde calculator (section 2.3.1.1). In the process of model development and validation of a CQ model the model was optimised to adequately recover the general shape of the plasma concentration-time profiles and accurately predict pharmacokinetic parameters of CQ in non-pregnant populations. Where the initial model did not appropriately recover pharmacokinetic phases and parameters as reported in clinical studies, a parameter estimation methodology was employed on Simcyp® with the Weighted Least Square (WLS) approach and the Nelder-Mead minimisation method. To determine the effect of final optimised parameter on the final predicted outcomes, a sensitivity analysis was done.

Model development utilised a total of 13 clinical studies reporting CQ pharmacokinetics across a range of Caucasian and non-Caucasian population groups (Table 4.1). These studies incorporated both single and multiple dose studies for CQ model development and validation. All modelling was conducted within the Simcyp® Simulator (Version 17).

Table 4.1: Summary of single and multiple dose studies used in the validation of CQ pharmacokinetics in non-pregnant subjects

Study	N	Ethnic group	Age (Years)	Weight (kg)	Gender (M/F)	Dosing regimen	Sampling matrix
Mzayek *et al* (2007)(403)	24	Mixed*	28.7 ± 5.3	75.8 ± 18.6	M, F	600 mg (single oral)	Blood
Gustaffson *et al* (1983)(404)	11	Caucasian	20 – 36	65 - 91	M	300 mg (single oral)	Plasma
Najmi *et al* (2008)(405)	10	Pakistani	33.5	66	M	600 mg (single oral)	Plasma
Höglund *et al* (2016)(406)	75	Thai	17 – 52	NR	M, F	10 and 5 mg/kg at 0 and 6–12 h on day 0, and 5 mg/kg each on day 1 and day 2	Plasma
Karunajeewa *et al* (2010)(407)	30	Papuan	25.5 ± 8.9	51.8 ± 5.5	F	450 mg once daily for 3 days	Plasma
Tanariya e*t al* (1995)(408)	57	Thai	26.4 ± 8.7	56.4 ± 7.1	M, F	600 mg initially, followed by 300 mg at hours 6, 24 and 48 hours)	Blood
Na-Bangchang *et al* (1994)(409)	7	Thai	18 – 35	45 – 68	M	600 mg initially, followed by 300 mg at hours 6, 24 and 48 hours)	Blood
Chukwuani *et al* (2004)(410)	5	Nigerian	23 – 37	56 – 66	F	600 mg (single oral)	Plasma
Lee *et al* (2008)(411)	13	Thai	29 (15 - 40)	46 ± 4.9	F	10, 10, and 5 mg/kg given at 0, 24, and 48 hours	Blood
Bustos *et al* (2002)(412)	11	Filipino	35 (13 - 63)	60 (40-63)	M, F	10 and 5 mg/kg at 0 and 6 hours on day 0, and 5 mg/kg each on day 1 and day 2	Plasma
Wetsteyn *et al* (1995)(413)	5	Caucasian	41	64 ± 10	M, F	300 mg weekly for 3 weeks	Plasma
Frisk-Holmberg *et al* (1984)(414)	5	Caucasian	37 - 42	72 ± 8	M, F	150 mg (single oral); 300 mg (single oral); 600 mg (single oral) given to each subject on 3 separate occasions	Blood
Walker *et al* (1987)(413)	8	Nigerian	19 – 55	53 – 66	M, F	600 mg (single oral)	Plasma

Data represented as: range, median (range) or mean ± SD. *: Caucasian and Black American, N: number of subjects

4.3.1.2 Step 2: Development and validation of a CQ model in pregnant subjects

For simulations involving pregnant women, the non-pregnant CQ model was revised to incorporate a full PBPK distribution model, which allows for consideration of gestation-phase dependant changes in maternal physiology (398, 399, 401, 402) for pharmacokinetic modelling studies (297, 307, 397). To recover the distribution phase profile, an appropriate volume of distribution (V_{ss}) was empirically fixed at the mean of the range reported in literature studies utilising pregnant subjects (407, 411, 415), following by parameter estimation using a Weighted Least Square (WLS) method and the Nelder-Mead minimisation approach. This optimised CQ model was subsequently validated utilising three clinical studies, details of which can be found in Table 4.2.

Table 4.2: Summary of single and multiple dose studies used in the validation of CQ pharmacokinetics in pregnant subjects

Study	Number of subjects	Ethnic group	Age (Years)	Weight (kg)	Gestation (Weeks)	Dosing regimen	Concentration matrix
Karunajeewa *et al* 2010(407)	30	Papuan	26.0 ± 5.9	54.0 ± 6.4	NR	450 mg once daily for 3 days	Plasma
Lee *et al* 2008(411)	12	Thai	25 (15 - 37)	49.5 ± 5.6	20 -32	10, 10, and 5 mg/kg given at 0, 24, and 48 hours	Blood
Fakeye *et al*, 2002(415)	4	Nigerian	30 ± 2.3	60.3 ± 8.9		10, 10, and 5 mg/kg given at 0, 24, and 48 hours	Plasma

Data represented as: range, mean (range) or mean ± SD

4.3.1.3 Adaptation of the age-weight relationships for non-Caucasian groups

The age-weight relationships in the non-Caucasian subjects were adapted from Caucasian subjects to reflect the difference in weight for age between these population groups as it has been reported that there is a significant difference between the weight for age in Caucasians and those of non-Caucasians (252) and this might therefore have significant impact on the Vss. In this study, the CQ model validation was condcuted with clinical data reported from various ethnic groups such as: Americans, Caucasians, Filipinos, Nigerians, Pakistani, Papuans and Thais. For the Americans and Caucasians, the healthy Caucasian population groups inbuilt into Simcyp® were used while for the non-Caucasian groups a representative age-weight relationship peculiar to the non-Caucasian ethnic group were built from the Hayes *et al* (2015) study using TableCurve 2D (Systat Software, San Jose, CA, USA).

4.3.1.4 Step 3: Identification of a suitable CQ prophylactic dose regimen for ZIKV

In order to propose a plasma therapeutic window for CQ which could be used to identify an optimal dosing regimen against ZIKV, we utilised reported *in vitro* and *in vivo* concentrations for the inhibition of ZIKV uptake into cells. Delvecchio *et al*. (2016) reported a CQ EC_{50} for the inhibition of ZIKV uptake within Vero cells, human brain microvascular endothelial cells (hBMEC) and human neural stem cells (hNSC) being within the range of 9-15 µM (381). Further, in ZIKV-infected interferon signalling-deficient AG129 mice, Shiryaev *et al* (2017) (416), reported that CQ extended their lifespan and confirmed that concentrations up to 40 µM were able to reduce ZIKV uptake in primary human foetal neural progenitor cells (NPCs) (with 90 % inhibition at 6 µM). In other studies, the correlation between brain and plasma concentrations has been identified, with a suggested 10-to-30-fold greater brain concentration compared to plasma concentrations for CQ (417, 418) and a 4-to-30-fold difference for the CQ analogue hydroxychloroquine (390), highlighting the ability of CQ to adequately partition into brain tissue.

Furthermore, in the study reported by Shiryaev *et al* (2017) (416), doses of 30 mg/kg were used in their ZIKV-infected interferon signalling-deficient AG129 mice to demonstrate uptake inhibition. This dose was similar to that used in arthritic patients where 5 mg/kg CQ salt was administered daily for one week which resulted in CQ plasma concentrations of 10 µM (419). A total dose of about 30 mg/kg would be achieved in humans, which would comparable to doses used in the study by Shiryaev *et al* (2017) (416), suggesting that such plasma concentrations are attainable using similar dosing regimens employed for existing therapeutic indications for CQ.

Therefore, in order to define a therapeutic window for CQ, we assumed that the target brain concentration of a maximum of 40 µM was required and to theoretically achieve this concentration in the human brain, a plasma concentration of less than an average of at least 20-fold of the brain concentration may be required, that is, approximately 2 µM. This was defined as the upper plasma therapeutic window. Given that concentrations in excess of 6 µM have been reported to prevent ZIKV uptake in brain derived cells, we set the lower plasma therapeutic window at 20-fold less, that is 0.3 µM. Therefore a plasma concentration therapeutic range of 0.3 µM to 2 µM was assumed in this study.

To identify an appropriate dosing regimen to target this therapeutic window, plasma concentration-time profiles for CQ were simulated in 100 pregnant subjects (during the entire gestational phase of 280 days) using the validated CQ model at doses used for the prophylaxis of malaria and RA, i.e. 150 mg-300 mg weekly or 150 mg daily, respectively. During this optimisation phase, the dose regimen which was able to maintain trough plasma concentrations above the lower limit of the plasma therapeutic window was identified as the optimal predicted dosing regimen.

4.3.2 Predictive performance

There are currently no universally agreed measures of predictive performance range when comparing observed data to predicted data in PBPK pharmacokinetic studies, however, a 2- fold prediction of observed data is largely accepted (420-422).

4.3.3 Visual Predictive Checks

Model predictions were compared to existing clinical studies using visual predictive checking (VPC), an approach described at the 2012 FDA Pediatric Advisory Committee (US Food and Drug Administration, 2012) (228). In brief, the predictability of the simulations was confirmed by comparing the predicted 5^{th} and 95^{th} percentiles of predicted concentration–time profiles with the observed data for any validation data sets. When the predicted data points overlapped with those from the observed data sets, which should (normally) contain a measure of spread of observed plasma concentration data (e.g., a standard deviation for each mean concentration point), the prediction was assumed to be valid.

4.3.4 Data analysis

Retrospective clinical data used for VPC were extracted using WebPlotDigitizer v.3.10 (http://arohatgi.info/WebPlotDigitizer/) (229). Where applicable, statistical analysis was conducted using paired t-tests with a $p < 0.05$ indicating statistical significance.

4.4 Results

4.4.1 Step 1a: Development of base model in non- pregnant subjects

The validity of the initial base model was assessed using a 300 mg single dose CQ study (383) in order to visualise the segment(s) of the concentration time profile that differed from published profiles. The model failed to recover the absorption kinetics of CQ and poorly predicted the distribution and elimination kinetics of CQ in a healthy Caucasian population (Figure 4.2).

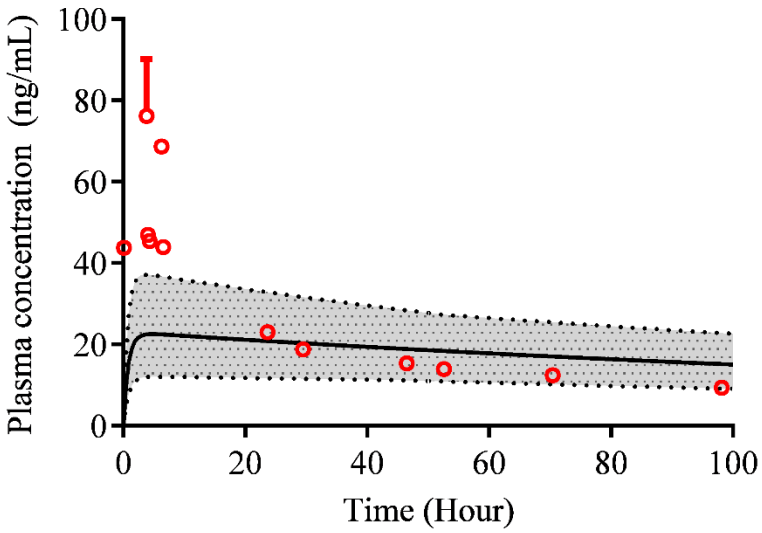

Figure 4.2: Concentration time profile of single dose CQ using the base model

Simulation of plasma concentration time profile of CQ following the administration of a single oral 300 mg dose using the base model according to the Lars *et al* study (383). Solid line represents the population means prediction and the dash lines bordering the shaded portion represent the 5^{th} and 95^{th} percentiles of prediction. He mean observed plasma concentration is represented by solid red circles while the red solid error bar represents the standard deviation of maximum plasma concentration.

4.4.2 Step 1b: Optimisation of base model in non- pregnant subjects

To recover the shape of the absorption phase, a first order absorption model was utilised to identify appropriate maximum plasma/blood concentrations (C_{max}) and time to reach the C_{max} (t_{max}). Clinically reported absorption rate constants (k_a) and fraction absorbed (f_a) values were selected with k_a reported in literature as ranging from 0.27 to 3.4 h^{-1} and f_a reported as 0.9. These were empirically fixed (with k_a fixed as the mean of the reported range), and subsequently optimised by parameter estimation methodology implementing a Weighted Least Square (WLS) approach and the Nelder-Mead minimisation method to arrive at parameters which appropriately recovered the absorption phase (f_a: 0.8; k_a: 1.2 h^{-1}) (Table 4.3), and were within the range reported from clinical studies (385, 423, 424).

The volume of distribution at steady-state (V_{ss}) was estimated by a similar methodology as that applied for the absorption phase, with V_{ss} reported in clinical studies as ranging from 100 L/kg to 1000 L/kg (390, 407, 425), and empirically fixed as the mean of this range prior to parameter estimation. As the reported V_{ss} was large, a minimal PBPK model was utilised with the incorporation of a 'single adjusting compartment' (SAC) to capture the correct distribution phases of the plasma concentration-time profile. Final parameter estimates of 125 L/kg for the central compartment (V_{ss}) and 52.9 L/kg for the SAC (V_{sac}) were able to appropriately recover the distribution phase of the profile. It should be noted that this was achieved following the incorporation of a change in the mean dispersion parameter applied to the central compartment (i.e. the coefficient of variation), which was adjusted from the Simcyp® default of 30 % to a revised 40 %.

Finally, the rates of metabolite formation, V_{max} and Michaelis-Menten constants (K_m) for CYPs 2D6, 3A4 and 2C8 elimination pathways were obtained from a literature reported study (426) using recombinant P450 systems. However, to achieve satisfactory recovery of the elimination phase, the Inter-System Extrapolation Factor (ISEF) for scaling recombinant cytochrome (CYP) P450 enzymes from *in vitro* kinetic parameters were estimated for all three metabolism pathways. In addition, CQ elimination has contributions from both hepatic and renal pathways, with the latter contribution approximately 30-50 % of the total clearance of CQ (404, 427). Therefore, a renal clearance parameter was estimated based on an empirically fixed mean estimate.

Parameter sensitivity analysis was subsequently conducted on ISEF for CYP2D6 and CYP3A4 (the two isozymes requiring significant changes in ISEF). When conducted over a range of 0.2-2, there was minimal sensitivity of *CL*, C_{max} and AUC to changes in ISEF (Figure 4.3) confirming appropriate estimates of ISEF for CYP2D6 and CYP3A4.

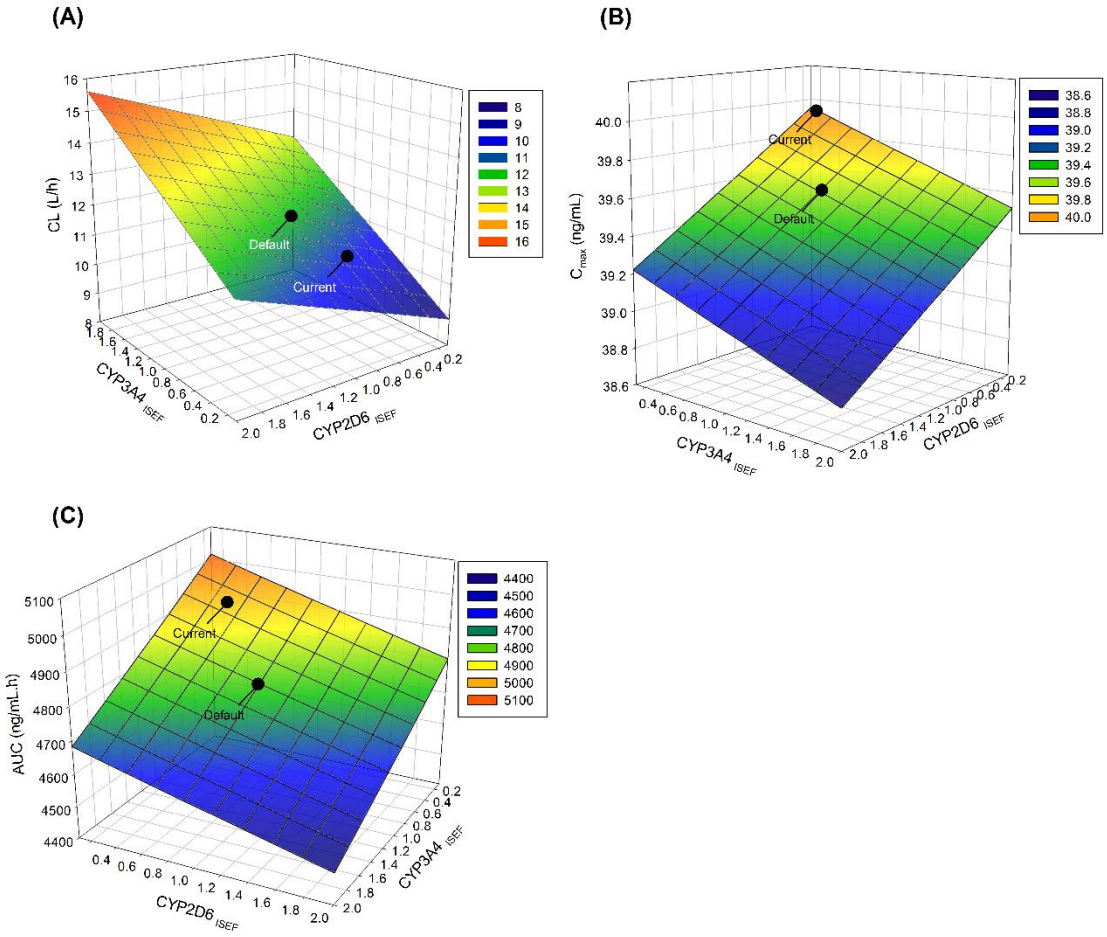

Figure 4.3: Sensitivity analysis of CYP3A4 and CYP2D6 ISEF

Sensitivity analysis of (A) clearance, (B) first dose C_{max} and (C) AUC following alterations in CYP3A4 and CYP2D6 ISEF (over a range of 0.2-2) for non-pregnant adults. Current optimised model estimates (CYP3A4 ISEF = 0.42 and CYP2D6 = 0.5) and default estimates (ISEF = 1) are illustrated.

Following the optimisation of the model, the final model predicted C_{max}, AUC and t_{max} were within 2-fold of the reported parameters across all thirteen published single and multiple dose clinical studies in Caucasian and non-Caucasian subjects (Table 4.4). Further, as demonstrated in Figures 4.4-4.7, the model was able to appropriately recover the plasma concentration-time profiles.

Mzayek *et al* (2007) (403) demonstrated a wide variability in the absorption phase of the reported plasma concentration-time profiles (Figure 4.5A), and the optimised model developed was able to recover this, with resultant predicted pharmacokinetic parameters within 2-fold of those reported (Table 4.4). Further, for the Walker *et al* (1987) (428) study, the terminal elimination phase was slightly over predicted (Figure 4.5D), however, the resultant AUC predicted by the model was within 2-fold of that reported (Table 4.4).

The wide inter-individual variation observed on the predicted concentration time profiles were perhaps due to the population size used during the virtual clinical trial simulations compared to the actual studies which involved few subjects (see Table 4. 1)

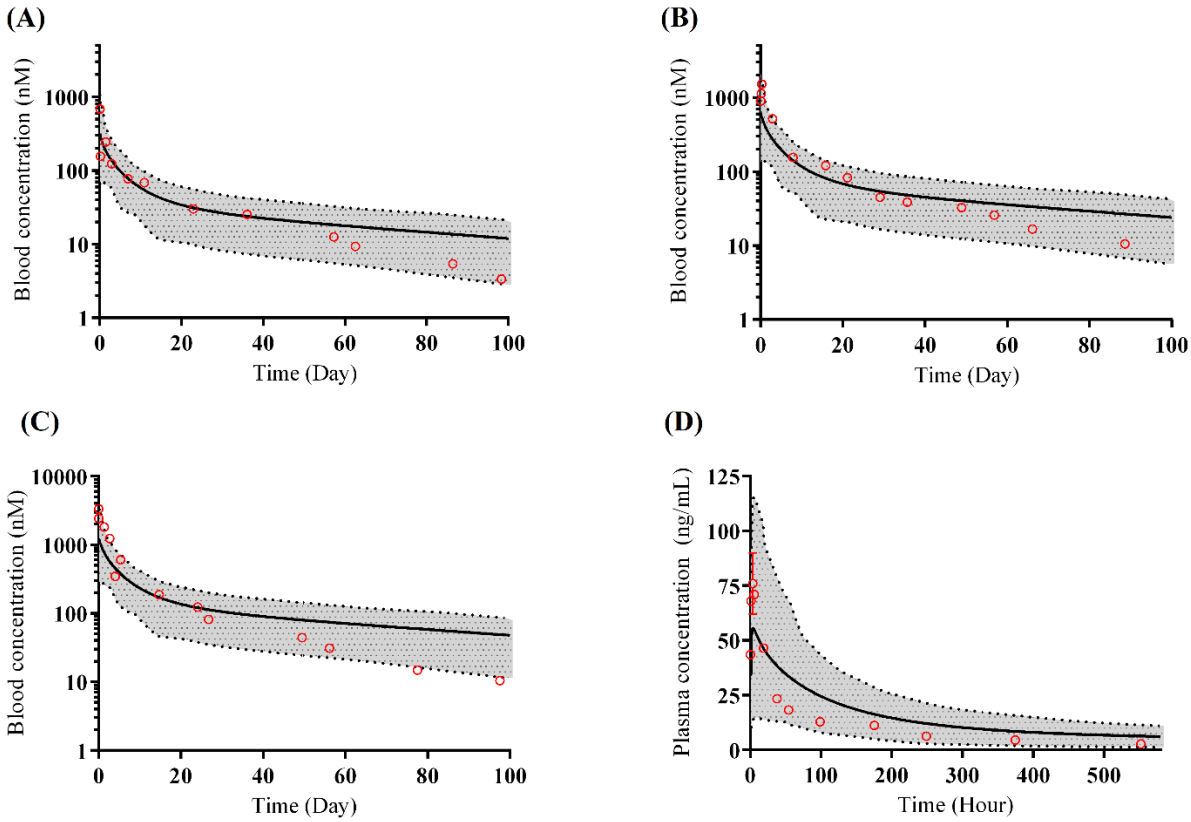

Figure 4.4: Simulated blood or plasma concentration-time profiles of single dose CQ in non-pregnant subjects

Simulated blood or plasma concentrations for CQ following single dose studies in healthy Caucasian subjects. (A): Frisk-Holmberg et al – 150mg; (B): Frisk-Holmberg *et al*– 300mg; (C): Frisk-Holmberg *et al* – 600mg; (D): Gustaffson *et al*. Solid lines represent mean predicted concentration-time profile with dotted lines representing the 5^{th} and 95^{th} percentile range. Open red circles represent observed clinical data from each study. For the Frisk-Holmberg *et al* studies, individual observed data were reported in the original studies. Where presented, error bars indicate standard deviation.

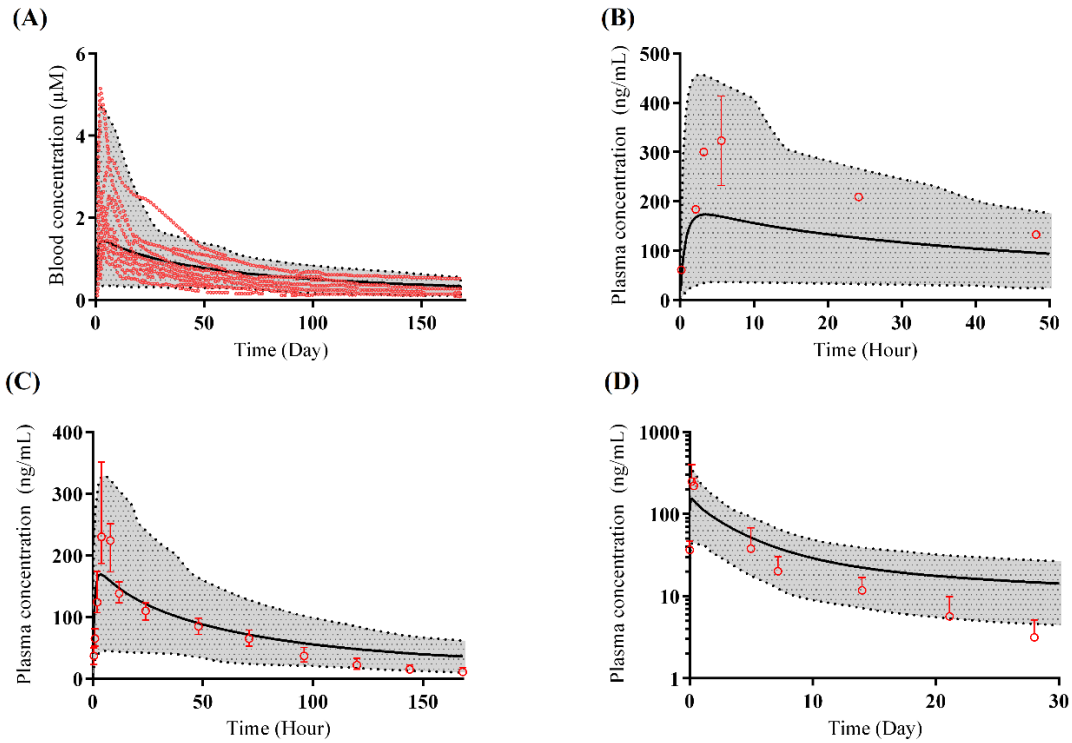

Figure 4.5: Simulated blood or plasma concentration-time profiles of single dose CQ in non-pregnant subjects

Simulated blood or plasma concentrations for CQ following single dose studies in non-Caucasian subjects except (A) involving Caucasian healthy volunteers. (A): Mzayek *et al*; (B): Chukwuani *et al*; (C): Najmi *et al*; (D): Walker *et al*. Solid lines represent mean predicted concentration-time profiles with dotted lines representing the 5^{th} and 95^{th} percentile range. Open red circles represent observed clinical data from each study. For the Mzayek *et al* study, red circles indicate data extracted from complete plasma concentration profile 'lines' for individual subjects rather than discrete time-points. Where presented, error bars indicate standard deviation.

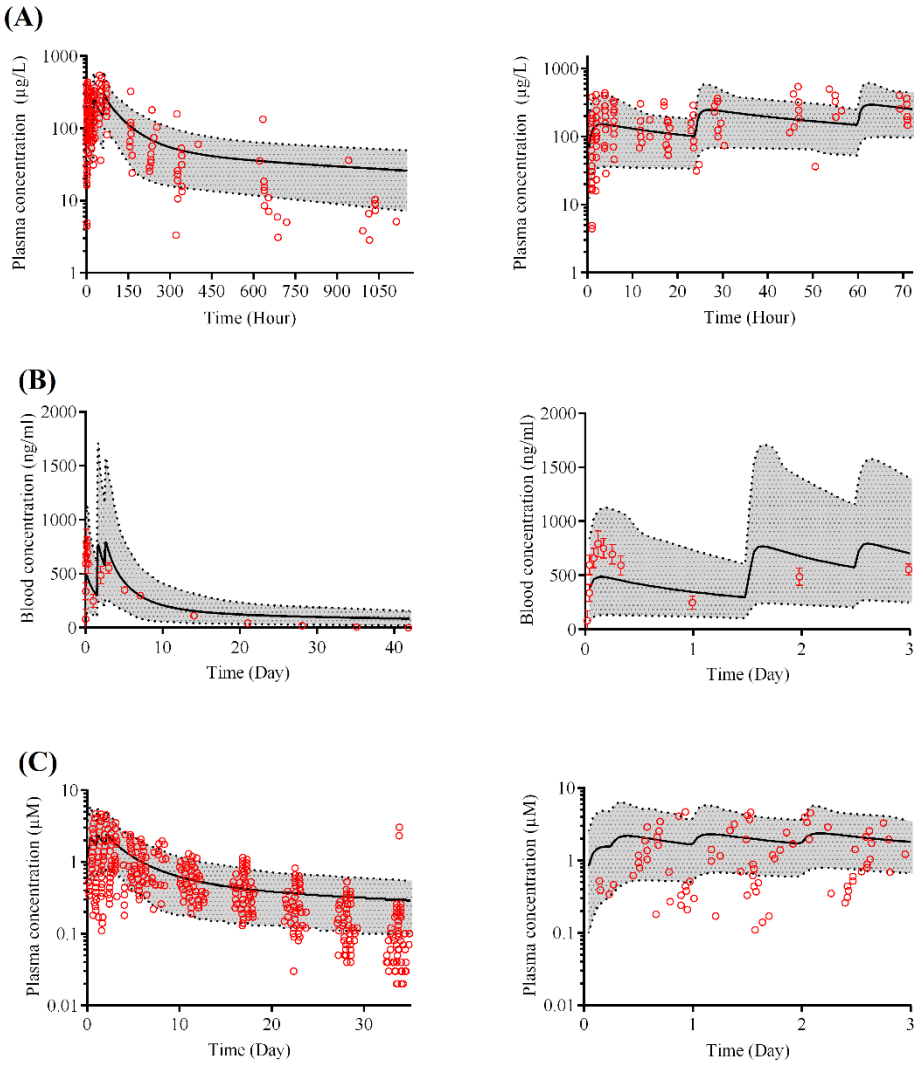

Figure 4.6: Simulated blood or plasma concentration-time profiles of multiple dose CQ in non-pregnant subjects

Simulated mean blood or plasma concentrations for CQ following multi- dose studies in non-Caucasian subjects. (A): Karunjeewaa *et al*; (B): Lee *et al*; (C): Hoglund *et al*. Solid lines represent mean predicted concentration-time profiles with dotted lines representing the 5th and 95th percentile range. Open red circles represent observed clinical data from each study. Error bars indicate standard deviation in Lee *et al* while Individual plasma or blood concentration data points are represented by open red circles in the Karunajeewa and Hoglund studies. Left-hand side panels indicate simulations for the total study duration and right-hand side panels illustrate the first three dosing days.

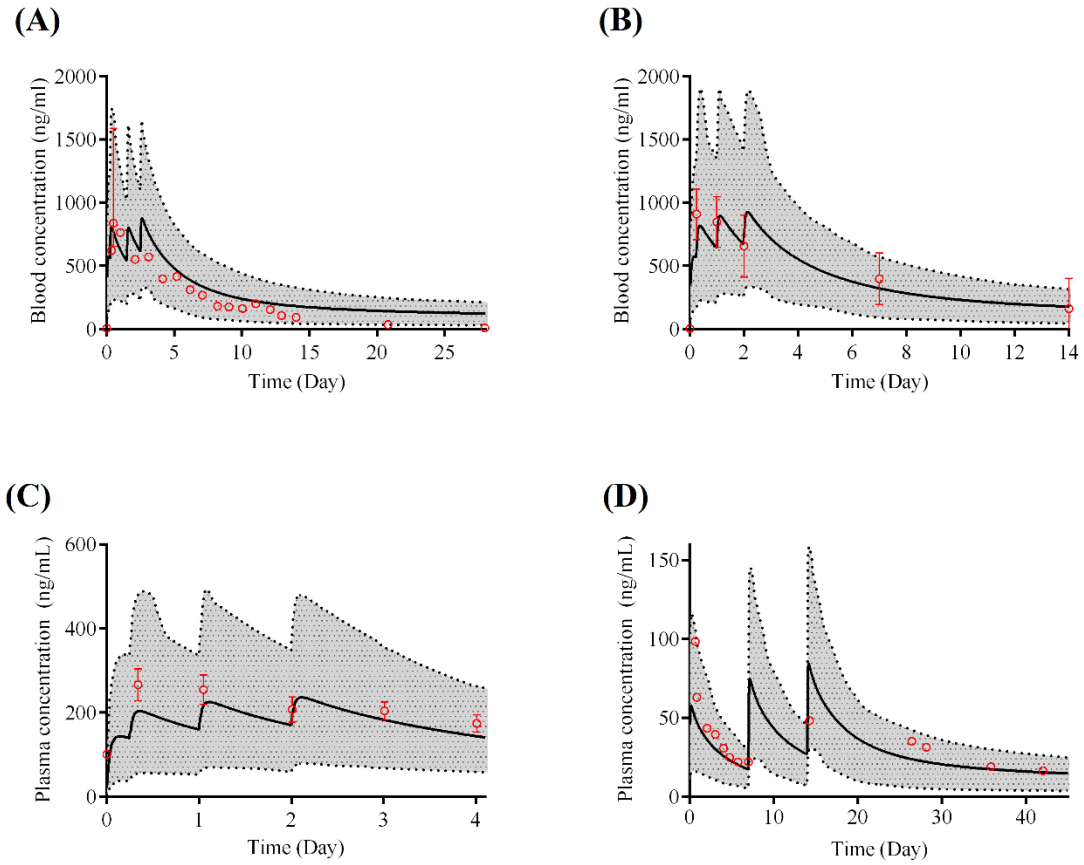

Figure 4.7: Simulated blood or plasma concentration-time profiles of multiple dose CQ in non-pregnant subjects

Simulated mean blood or plasma concentrations for CQ following multi- dose studies in non-Caucasian subjects (D: healthy Caucasian subjects). (A): Na-Bangchang *et al*; (B): Tanariya *et al*; (C): Bustos *et al*; (D); Wetsteyn *et al*. Solid lines represent mean predicted concentration-time profile with dotted lines representing 5^{th} and 95^{th} percentile range. Open red circles represent observed clinical data from each study. Error bars indicate standard deviation in the Na-Bangchang; Tanariya; Bustos and Wetsteyn studies.

4.4.3 Step 2: Development and validation of an optimised model of CQ in pregnant subjects

Following the optimisation of the CQ model developed for non-pregnant subjects, a CQ pregnancy model was developed and the parameter estimates for the final optimised pregnancy model are detailed in Table 4.3.

Simulation and validation of the pregnancy model for CQ was conducted using the clinical studies summarised in Table 4.2 while ensuring gestational weeks reported in the clinical studies matched (where possible) those in the pregnancy group simulated in the current study. Subsequently, the model was able to satisfactorily predict the plasma concentration-time profiles of CQ in pregnant women (Figures 4.8) with all pharmacokinetic parameters predicted to within 2-fold of those reported in clinical studies (Table 4.4).

Table 4.3: Model parameter values for base and optimised model of CQ in non-pregnant and pregnant subjects

Parameter	Optimised model (non-pregnant)	Optimised model (pregnant)
Compound type	Diprotic base [429]	Diprotic base [429]
Molecular weight (g/mol)	319.9 [316]	319.9 [316]
log P	4.72 [430]	4.72 [430]
Fu	0.55 [431]	0.55 [431]
pKa 1	10.1 [430]	10.1 [430]
pKa 2	8.38 [430]	8.38 [430]
Vss (L/kg)	125 (CV: 40 %) [b]	130[b]
Vsac (L/kg)	52.9 [b]	-
Q (L/h)	5 [b]	-
Kp scalar	-	3.35 [c]
Fa	0.8 [d]	0.8 [d]
k_a (h^{-1})	1.2 [d]	0.5 [d]
Solubility (mg/mL)	0.0175 [316]	0.0175 [316]
$Vmax_{2D6}$ (pmol/min/pmol)	2.10 [426]	2.10 [426]
$Vmax_{3A4}$ (pmol/min/pmol)	2.94 [426]	2.94 [426]
$Vmax_{2C8}$ (pmol/min/pmol)	8.33 [426]	8.33 [426]
Km_{2D6} (µM)	19.5 [426]	19.5 [426]
Km_{3A4} (µM)	294 [426]	294 [426]
Km_{2C8} (µM)	111 [426]	111 [426]
Fumic	0.13 [e]	0.13 [e]
ISEF CYP2D6	0.5 [f]	0.8 [f]
ISEF CYP3A4	0.42 [f]	0.7 [f]
ISEF CYP2C8	1.1 [f]	1.6 [f]
Cl_{renal} (L/h)	4.6 [g]	5.5 [g]
Absorption model	first order	first order
Distribution model	minimal PBPK	full PBPK

[a]Simcyp® mechanistic prediction; [b] parameter estimated using a minimal PBPK model with a single adjusting compartment (SAC); [c] an appropriate Kp scalar was empirically optimised for a full PBPK model in pregnancy; [d] parameter estimated using a first order absorption kinetic model; [e] parameter estimated; [f] parameter estimated for use in optimisation of clearance kinetics; [g] parameter estimated. logP: the logarithm of the n-octanol:buffer partition coefficient; fu: unbound fraction; B/P: blood-to-plasma ratio; Vss: steady state volume of distribution; Vsac: volume of single adjusting compartment; Q: blood flow to the single adjusting compartment; ka: absorption rate constant; Kp scalar: scalar applied to all predicted tissue partition values fa: fraction dose absorbed; ka: absorption rate constant; Vmax: maximum rate of metabolite formation; Km: Michaelis-Menten constant; fumic: fraction of unbound drug in the invitro microsomal incubation; ISEF: Intersystem extrapolation factor for scaling CYP *in vitro* kinetic data; CLrenal: renal clearance.

Table 4.4: Summary of predicted and observed pharmacokinetic parameters of for CQ

		C_{max}		t_{max} (h)		AUC	
		Predicted	Observed	Predicted	Observed	Predicted	Observed
Caucasian Single Dose	Gustafsson [a, e]	56.8 ± 23.8	76 ± 14	4.9 ± 2.6	3.6 ± 2.0	9315 ± 3951	6111 ± 1315
	Mzayek [b, f *]	1.4 (0.3 – 6.1)	1.8 (1.3-5.2)	4.2 (1.5 – 7.1)	3.0 (1.0-8.0)	112 (31.5 - 225)	90 (48.9-212
	Frisk (150 mg dose) [b, i]	0.11	NR	5.2 ± 2.4	NR	3.14 ± 1.3	2.54 ± 0.55
	Frisk (300 mg dose) [b, i]	0.94	NR	5.2 ± 2.4	NR	6.28 ± 2.5	6.19 ± 1.39
	Frisk (600 mg dose) [b, i]	1.9 ± 7.4	NR	5.2 ± 2.4	NR	12.6 ± 5.1	11.6 ± 2.4
Non-Caucasian Single Dose	Chukwuani [a, e]	177 ± 170	391 ± 91	4.7 ± 2.4	5.6 ± 0.8	7408 ± 4622	10820 ± 2714
	Najmi [c, g,**]	172 ± 166	201 ± 15	4.6 ± 2.3	6.10 ± 0.66	12775 ± 5835	10827 ± 1340
	Walker [a, e]	159 ± 149	374 ± 56	4.8 ± 2.4	5 ± 3	25865 ± 10608	18609 ± 4254
Non-Caucasian Multi Dose	Karunajeewa [c, g,**]	297 (79.1-769)	376 [#]	-	-	57014 (11218-112760)	47892 (43486-53746)
	Na-Bangchang [a, j.***]	883 (266-2306)	838 (656-1587)	-	-	167 (35.4-315)	122 (103-182)
	Bustos [a, k,**]	166 (63.47-336)	285 (186-422)	-	-	2189 (525-4760)	2299 (1149 -39908)
	Lee [a, e,**]	836 (244-3006)	700 (403 - 1625) [##]	-	-	189024 (47160 - 334210)	134087 (62940 - 229695)
	Hoglund [b, I,**]	2.7 (2.04)	NR	3.8	NR	24.2 (10.3)	NR
	Tanariya [a, k,**]	994 (666)	NR	4.3	NR	7897 (3245)	NR

Caucasian Multi Dose	Wetsteyn [d, l,**]	85.6 (56.1)	NR	3.6	NR	1429 (590)	NR
Pregnant	Fakeye [a, e]	124 ± 56.0	204 ± 135	4.6 ± 1.68	2	2114 ± 38.3	NR
	Karunjeewa [d, h,**]	145 (53.4-240)	296**	-	-	38585 (14236-65641)	35750 (31343-39729)
	Lee [a, e,**]	482 (167-921)	960 (297-1835)	3.84 (2.4-4.8)	3 (1.5- 8)	156 847 (54768-349488)	122216 (74145-269600)

Units for C_{max} are as follows: [a] ng/mL; [b] µM; [c] mg/L; [d] µg/L; Units for AUC are as follows: [e] ng/mL.h; [f] µM.h; [g] mg/L.h; [h] µg/L.h; [i] µM.day; [j] µg/mL.h ; [k] ng/mL.Day; [l] µg/L.Day. Unless otherwise stated, data represent means ± SD or median (range). * Data represents median (range); ** $AUC_{0-\infty}$ (AUC calculated from the start of the study and extrapolated to infinity); *** AUC_{0-28d}: AUC calculated 28 days period only; **** AUC_{0-48d}: AUC calculated 48 days period only. # No SD or median was reported; ## C_{max} reported for the first dose only

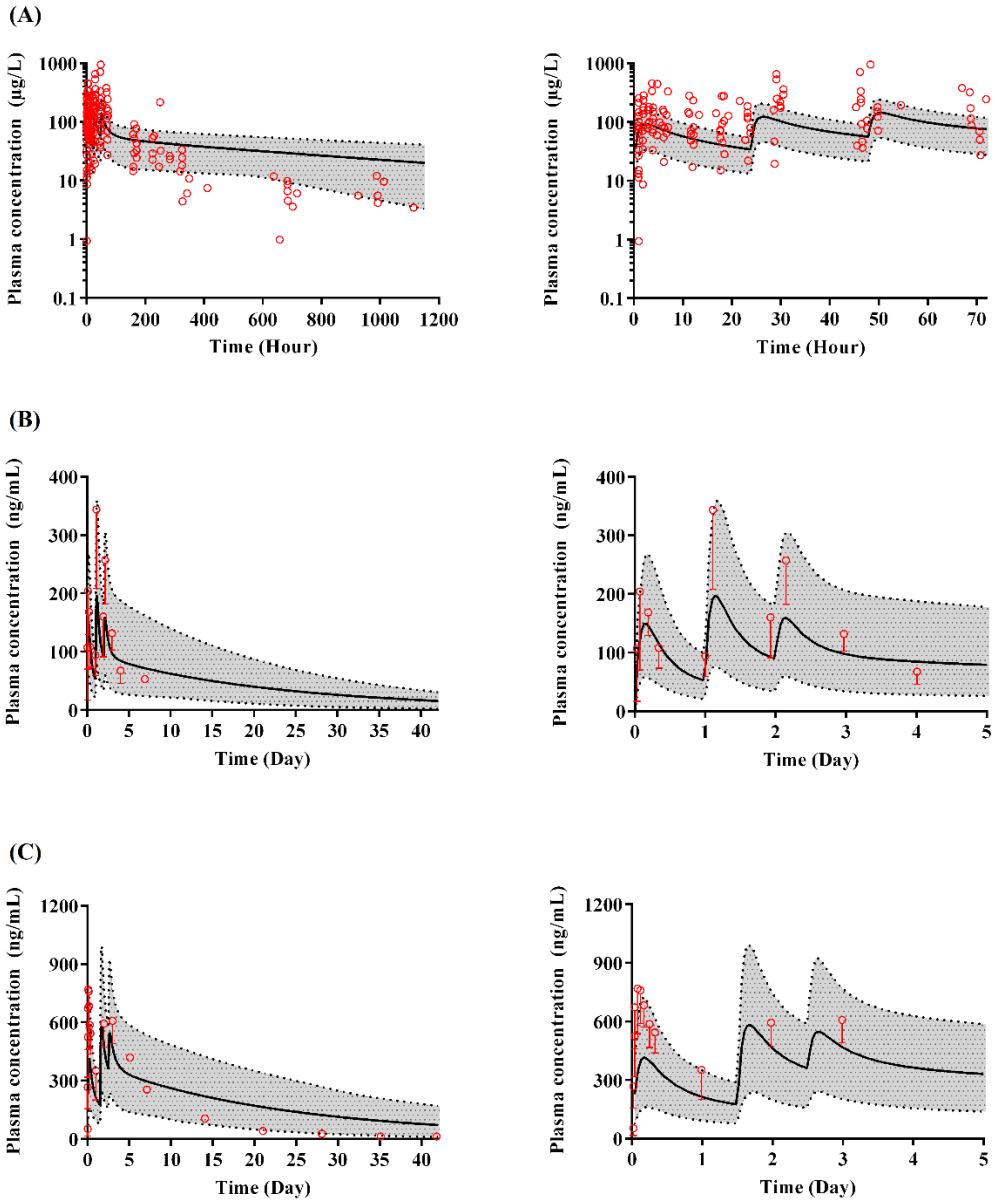

Figure 4.8: Simulated plasma concentration-time profiles of multiple dose CQ in pregnant subjects

Simulated mean plasma concentrations for CQ following multidose studies in pregnant subjects. (A): Karunjeewa *et al*; (B): Fakeye *et al*; (C): Lee *et al*. Solid lines represent mean predicted plasma concentration-time profiles with dotted lines the representing 5th and 95th percentile range. Open red circles represent observed clinical data from each study. Error bars indicate standard deviation. Left-hand side panels indicate simulations for the total study duration and right-hand side panels illustrate the dosing period only.

4.4.4 Adaptation of the age-weight relationships for non-Caucasian groups

The following mathematical expressions of age-weight distribution showed were inputted into Simcyp® in order to adapt its Caucasian age-weight relationships to the appropriate population groups

4.4.4.1 Filipinos and Papuans

Due to geographical locations, the age-weight relationship for Filipinos and Papuans were assumed to be similar and the age weight relationship was shown below:

Adult males:

$$Body\ weight = (6.0000871 + (1.8363904*age) + (-0.28876641*age^2) + (0.011482471*age^3)) / (1 + (-0.06584622*age) + (-0.0016572488*age^2) + (0.00016955778*age^3)) \quad (49)$$

Adult females:

$$Body\ weight = (6.03 + 0.197*age^2 + 0.0012*age^4) / (1+0.00127*age^2 + 0.0000255*age^4) \quad (50)$$

4.4.4.2 Nigerians

Adult males:

$$Body\ weight = (3.1190351 + (2.7547707*age^{0.5})+(-1.9861521*age) +(0.29731577*age^{1.5}))/(1+(-0.63494158*age^{0.5})+(0.15239313*age)+(-0.017751472*age^{1.5})+(0.0010549434*age^2) \quad (51)$$

Adult females:

$$Body\ weight = (3.9015149 + (0.280026178*age^{0.5}) + (-0.92347063*age) + (0.16145376*age^{1.5})) / (1 + (-0.75349793*age^{0.5}) + (0.2157188*age) + (-0.028738874*age^{1.5}) + (0.0016167479*age^2)) \quad (52)$$

4.4.4.3 Pakistani and Thais

Due to geographical locations, the age-weight relationship for Pakistani and Thais were assumed to be similar and the age weight relationship is shown below:

Adult males:

$$Body\ weight = 33.46 + (-0.3569*age^2) + (0.001522*age^4) / (1 + (-0.00755*age^2) + (2.78x10 - 5*age^4) + (-1.07x10\text{-}9*age^6)) \quad (53)$$

Adult Females:

$$Body\ weight = -920.66 + (-188.63*age) + (22.48*age^{1.5}) + (-0.999*age^2) + (700.23*age^{0.5}) \quad (54)$$

4.4.5 Step 3: Identification of a CQ prophylactic dosing regimen for ZIKV during pregnancy

In order to identify a dosing regimen appropriate for maintaining maternal plasma (and foetal exposure) levels, such that a sufficient concentration would be achieved to prevent foetal ZIKA brain endocytosis, standard CQ dosing regimens commonly used for malaria, RA and SLE (150 mg or 300 mg weekly, and 150 mg or 300 mg daily, respectively), were simulated during the first trimester.

For malaria prophylaxis doses, 150 mg and 300 mg weekly, the simulated plasma concentration-time profiles did not achieve the lower target therapeutic limit until the end of trimester 1 (Figure 4.9) and were not considered for further optimisation.

For doses used in RA and SLE, with a 150 mg daily dose the mean trough plasma-concentration did not reach the lower limit of 0.3 µM until 12 days post first dose (Figure 4.10) when 96 % of subjects achieved a trough concentration in excess of the lower therapeutic window (Table 4.5). At steady-state, a C_{max} of 0.9 ± 0.4 µM was achieved. For the 300 mg daily dose, the trough plasma-concentration doubled (Table 4.5) (Figure 4.11), with a shortening of the time taken to reach the target plasma concentration to 5 days (Table 4.5). However, the mean steady-state C_{max} was 1.8 ± 0.8 µM with 59 % of subject demonstrating a peak plasma-concentration in excess of 2 µM (Table 4.5).

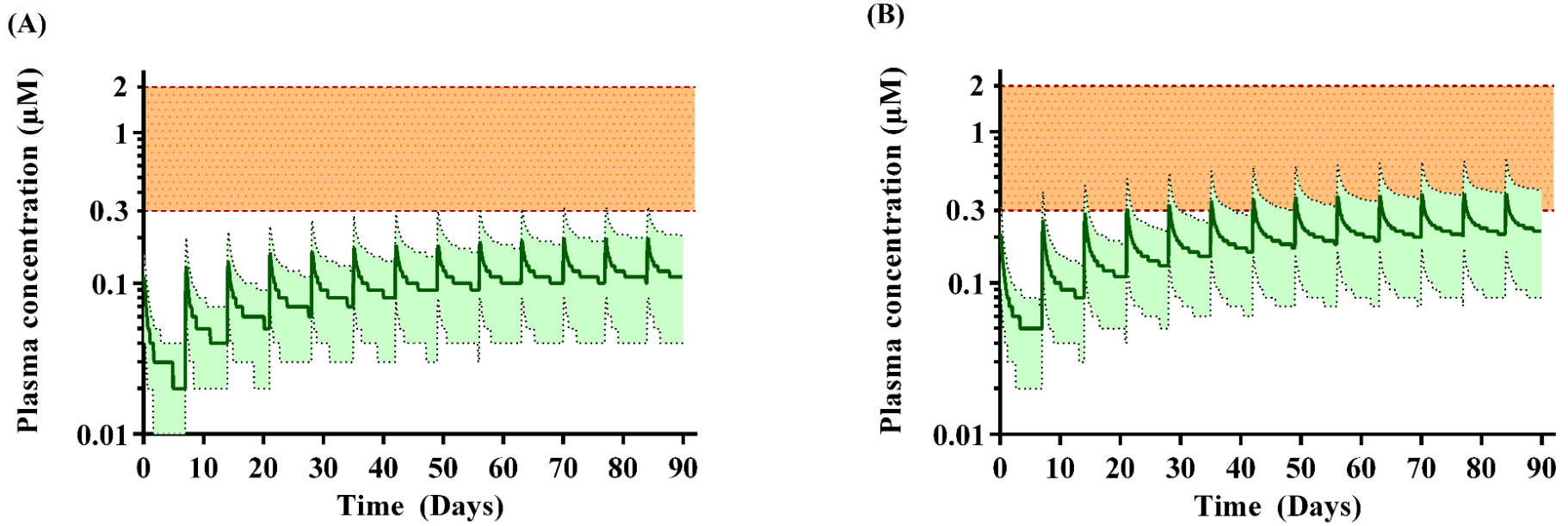

Figure 4.9: Simulated plasma concentration-time profiles for CQ dosed once weekly during the first trimester.

Simulated CQ plasma concentration-time profiles during trimester 1 for: (A) a 150 mg weekly dose; (B) a 300 mg weekly dose. Dark green lines indicate mean plasma concentration-time profiles; light green shaded area bordered by the dashed lines indicate the area within the 5th and 95th percentile of predicted mean plasma concentration-time profiles; light brown shaded areas represent the proposed therapeutic range of CQ for ZIKV (0.3-2 µM).

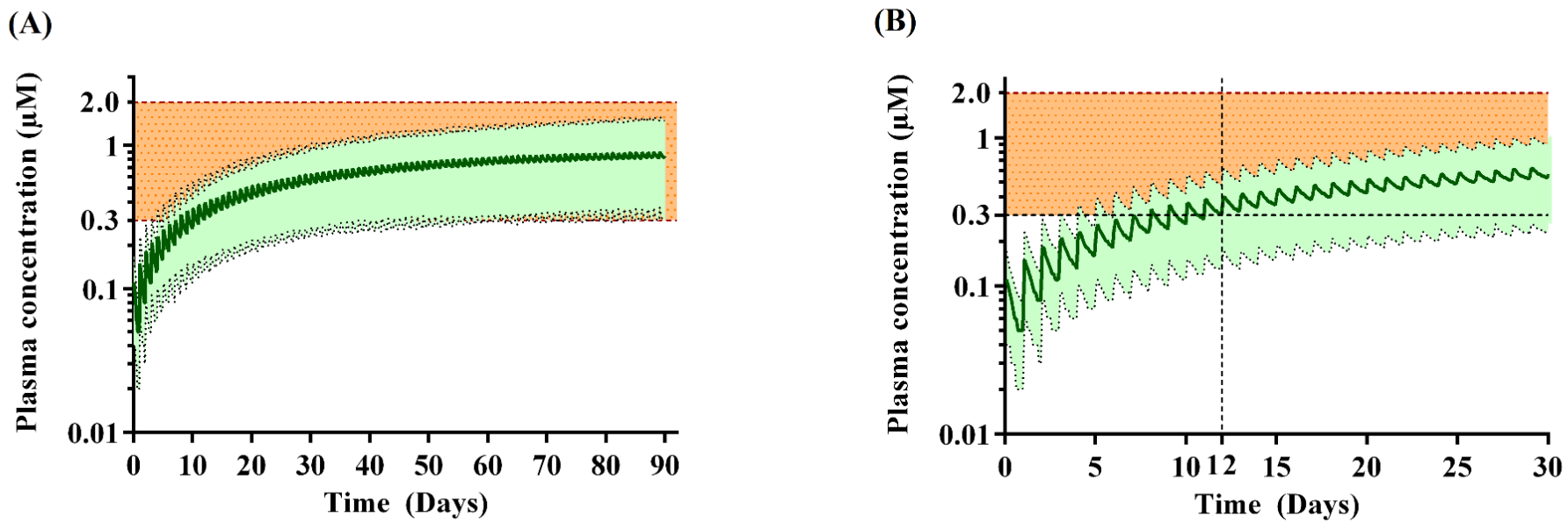

Figure 4.10: Simulated plasma concentration-time profiles for CQ dosed at 150 mg daily during the first trimester.

Simulated CQ plasma concentration-time profiles during trimester 1 for a 150 mg daily dose. (A) indicates simulations for the first trimester and (B) illustrate the dosing for thirty days. Dark green lines indicate mean plasma concentration-time profiles; light green shaded area bordered by the dashed lines indicate the area within the 5th and 95th percentile of predicted mean plasma concentration-time profiles; light brown shaded area represents the proposed therapeutic range of CQ for ZIKV (0.3-2 µM); dashed vertical lines indicates the time at which trough concentrations are maintained above the lower therapeutic window.

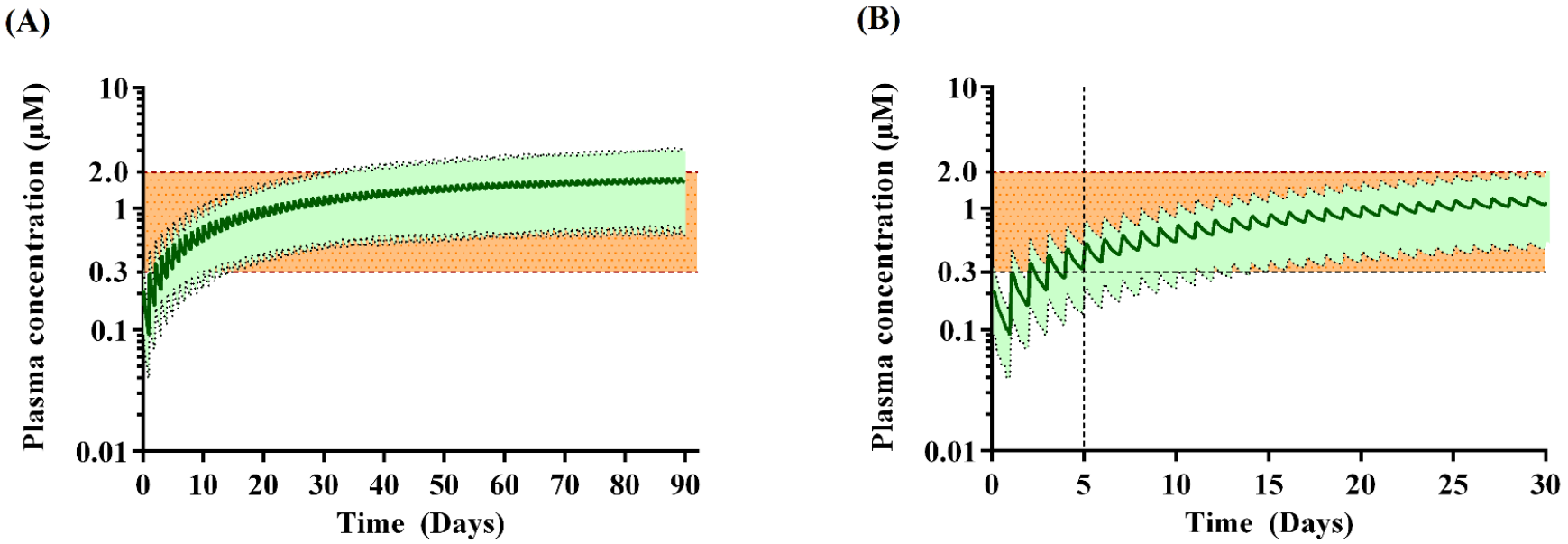

Figure 4.11: Simulated plasma concentration-time profiles for CQ dosed at 300 mg daily during the first trimester.

Simulated CQ plasma concentration-time profiles during trimester 1 for a 300 mg daily dose. (A) indicate simulations for the first trimester and (B) illustrate the dosing for thirty days. Dark green lines indicate mean plasma concentration-time profiles; light green shaded areas bordered by the dashed lines indicate the area within the 5^{th} and 95^{th} percentile of predicted mean plasma concentration-time profiles; light brown shaded area represents the proposed therapeutic range of CQ for ZIKV (0.3-2 µM); dashed vertical lines indicates the time at which trough concentrations are maintained above the lower therapeutic window.

Dose optimisation was considered to identify an appropriate dosing regimen for trimester 1 to (i) achieve rapid attainment of the lower plasma therapeutic window and (ii) to maintain this concentration for the longest duration possible. The dosing regimen identified was a loading dose of 600 mg on day 1 followed by 300 mg for 2 days and subsequently 150 mg daily during trimester 1 (Figure 4.12). Under this regimen, the time taken for trough plasma concentrations to be maintained within the therapeutic window shortened by six days (Figure 4.12) (Table 4.5) compared to a 150 mg daily dose (Figure 4.10) (Table 4.5). Further, only 1 % of subjects achieved a plasma concentration above the upper therapeutic limit of 2 µM (Table 4.5).

Table 4.5: Simulated steady-state pharmacokinetic parameters of CQ during pregnancy

Dose (mg)	C_{max} (µM)	tmax (h)	AUC (µM.h)	Time to lower window [a] (days)	Percentage of subjects with C_{min} > 0.3 µM at SS [b]	Percentage of subjects with C_{max} < 2 µM at SS [c]
150	0.9 ± 0.4	2.4 ± 0.5	21.8 ± 9.4	12	96	99
300	1.8 ± 0.8	2.4 ± 0.5	43.9 ± 18.7	5	99	59
Optimised	0.9 ± 0.4	2.4 ± 0.5	48.8 ± 30.9	6	96	99

Data represents mean ± standard deviation. [a] Time taken for mean trough plasma concentrations to be maintained above 0.3 µM; [b] Percentage of subjects with trough plasma concentrations above 0.3 µM at steady-state; [c] Percentage of subjects with peak plasma concentrations below 2 µM at steady-state. AUC was calculated for the final dosing day.

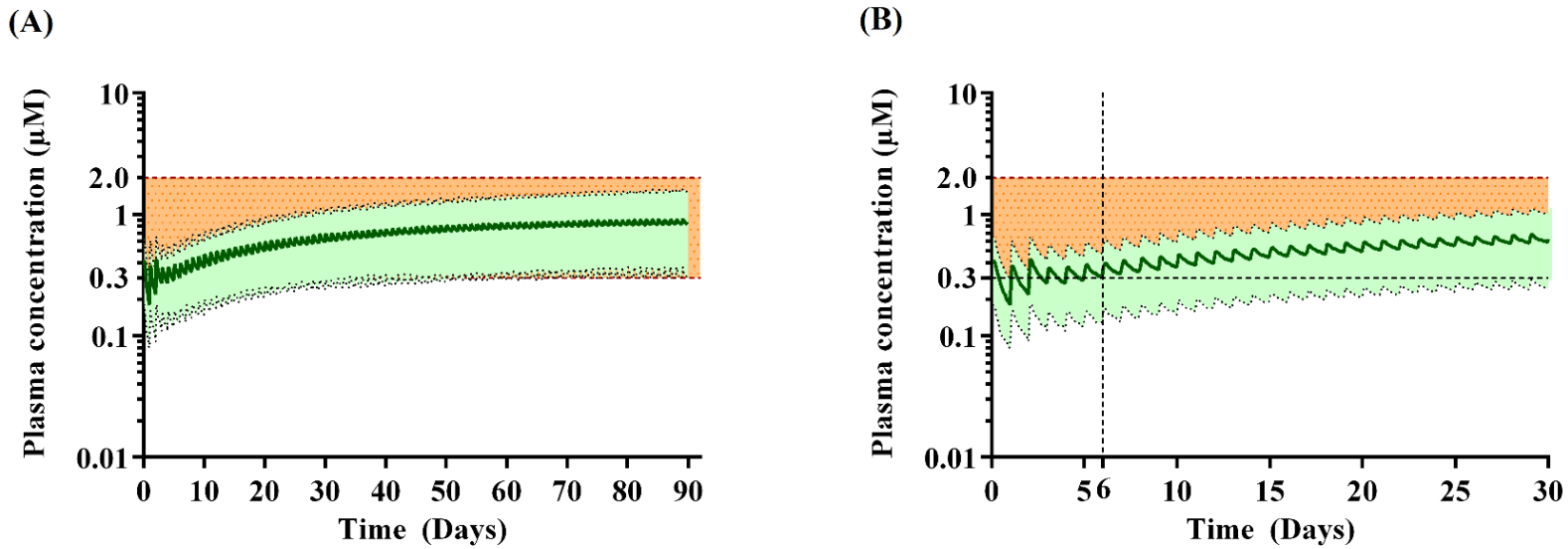

Figure 4.12: Simulated plasma concentration-time profiles for CQ dosed at optimised dose during the first trimester.

Simulated CQ plasma concentration-time profiles during trimester 1 for an optimised CQ dose: a loading dose of 600 mg on day 1 followed by 300 mg for 2 days and subsequently 150 mg daily during trimester). (A) indicates simulations for the first trimester and (B) illustrates dosing for thirty days. Dark green lines indicate mean plasma concentration-time profiles; light green shaded area bordered by the dashed lines indicate the area within the 5^{th} and 95^{th} percentile of predicted mean plasma concentration-time profiles; light brown shaded areas represent the proposed therapeutic range of CQ for ZIKV (0.3-2 µM); dashed vertical lines indicates the time at which trough concentrations are maintained above the lower therapeutic window.

Subsequently, the impact of initiating the optimal dosing regimen at the start of each trimester on the pharmacokinetics of CQ was assessed. CQ pharmacokinetics were simulated for each trimester period. In comparison to the results from trimester 1, dosing this optimal regimen during either trimester 2 or 3 resulted in a progressive and statistically significant decrease ($p < 0.001$) in AUC, from 20.9 ± 9.6 µM.h to 11.8 ± 4.8 µM.h (calculated on the final day of the trimester) (Figure 4.13) with an increase in the time to reach target trough plasma concentration from 6 days for trimester 1 to 35 days for trimester 3 (Table 4.6) (Figure 4.13). Further, at trimester 3, only 79 % of subjects achieved a trough plasma concentration above the lower therapeutic limit (Table 4.6).

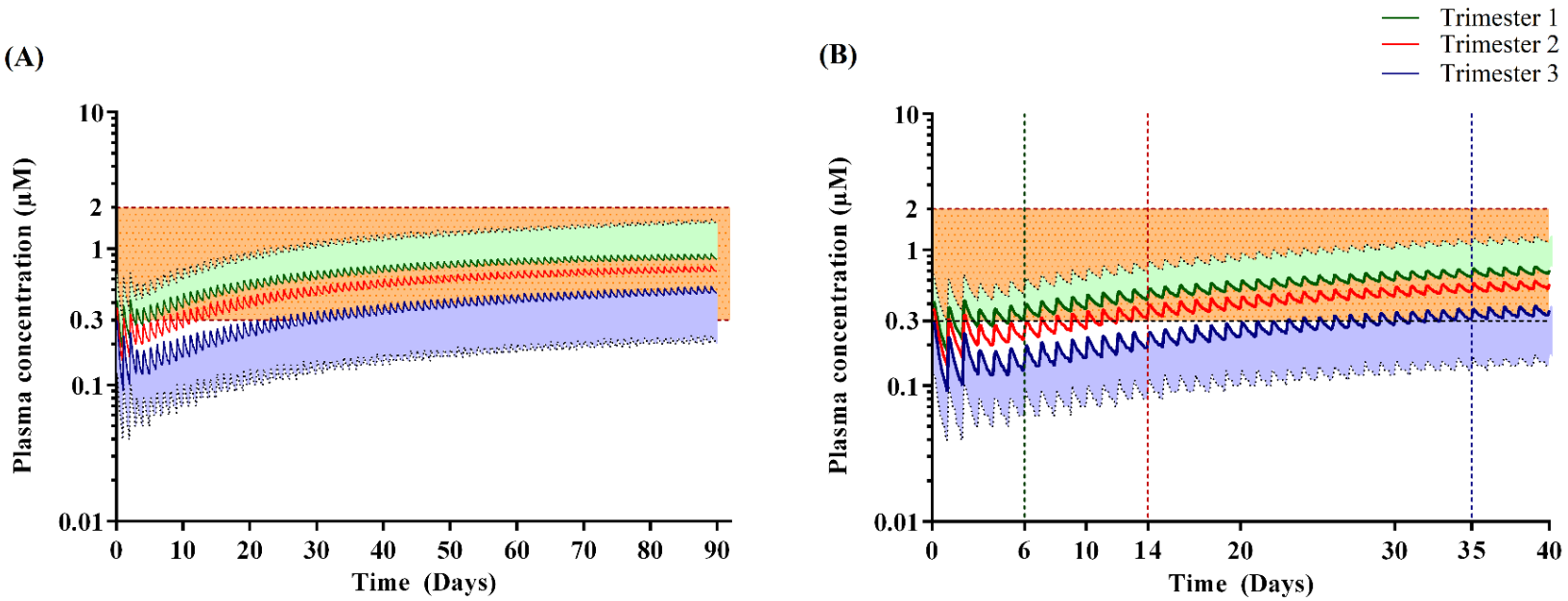

Figure 4.13: Simulated plasma concentration-time profiles for optimised CQ dosed during each trimester

Simulated CQ plasma concentration-time profile utilising the optimised dosing regimen, during each trimester. (A) Simulated profiles for the entire duration of each trimester; (B) Simulated profiles for the first 40 days of each trimester. Dark green, red and blue lines indicate mean plasma concentration-time profiles during the 1st, 2nd and 3rd trimesters respectively; lighter shaded areas indicate the area within the 95th and 5th percentile of the predicted mean plasma concentration-time profiles during trimester 1 (upper, light green) and trimester 3 (lower, light blue); light brown shaded area represents the proposed plasma therapeutic window of CQ for ZIKV (0.3-2 µM); dashed vertical lines indicates the time at which trough concentrations are maintained above the lower therapeutic window.

Table 4.6: Steady-state pharmacokinetic parameters of the optimised CQ regimen during pregnancy

Trimester	C_{max} (µM)	tmax (h)	AUC (µM.h)	Time to lower window [a] (days)	Percentage of subjects with C_{min} > 0.3 µM at SS [b]	Percentage of subjects with C_{max} < 2 µM at SS [b]
1	0.92 ± 0.41	2.2 ± 0.5	21.8 ± 9.6	6	96	99
2	0.75 ± 0.32	2.2 ± 0.5	17 ± 7.2	14	93	100
3	0.53 ± 0.21	2.6 ± 0.7	11.8 ± 4.8	35	79	100

Data represents mean ± standard deviation. [a] Time taken for mean trough plasma concentrations to be maintained above 0.3 µM; [b] Percentage of subjects with trough plasma concentrations above 0.3 µM at steady-state; [c] Percentage of subjects with peak plasma concentrations below 2 µM at steady-state. AUC was calculated for the final dosing day.

Finally, to identify an appropriate CQ dosing regimen for the entire duration of pregnancy, CQ treatment was extended from the end of the first trimester to the end of the second trimester. During trimester 1 (days 1 to 84), the predicted mean plasma concentration was maintained above the lower therapeutic window (Figure 4.14) with a steady-state C_{max} of 0.92 ± 0.41 ng/mL (Table 4.7). Assuming CQ was halted at the end of trimester 1, mean plasma concentrations reached the lower therapeutic window on day 150 with 95 % of subjects possessing a trough plasma concentration above the lower therapeutic window (Table 4.7). When dosing was continued throughout trimester 2 (Figure 4.15), steady-state plasma concentrations were maintained with a C_{max} of 0.92 ± 0.41 ng/mL (Table 4.7) until the end of trimester 2 (day 168), at which point CQ was halted. Mean plasma concentrations reached the lower therapeutic window on day 279 with 94 % of subjects possessing a trough plasma concentration above the lower therapeutic window and 5 % of subjects possessing a peak plasma concentration below the lower therapeutic window (Table 4.7).

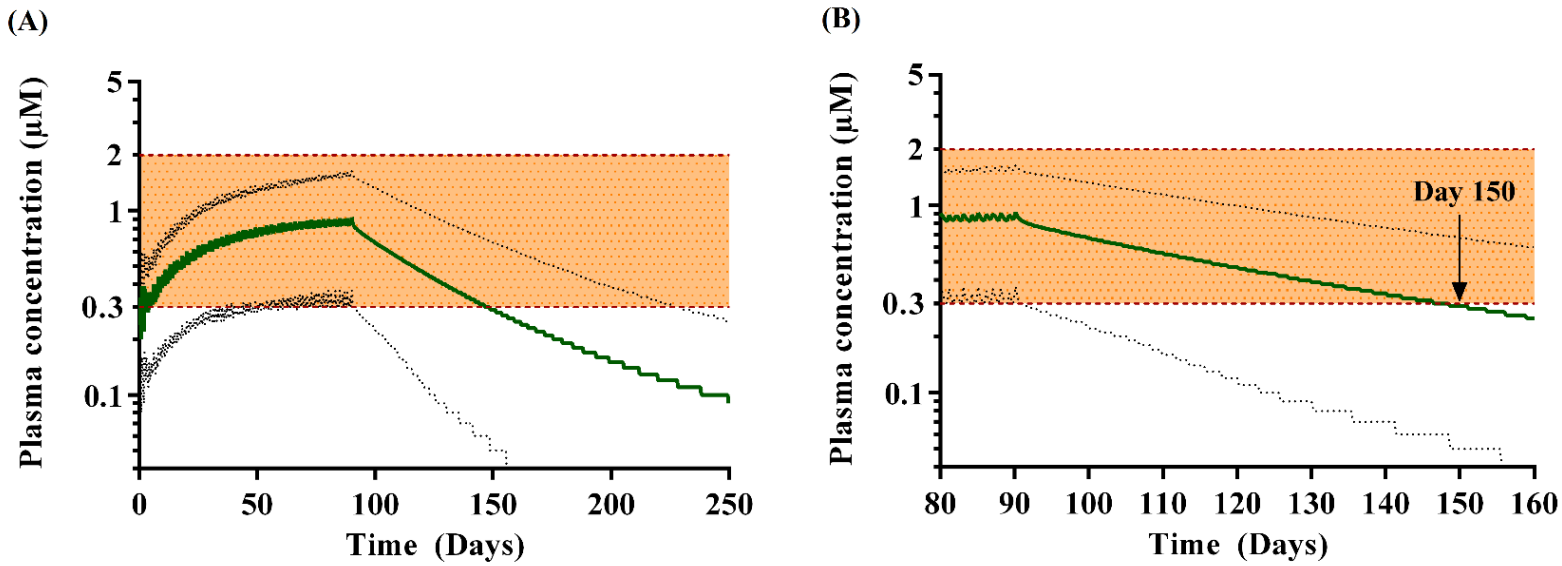

Figure 4.14: Simulated plasma concentration-time profiles for optimised CQ dosed during trimester 1

Simulated CQ plasma concentration-time profile utilising the optimised dosing regimen during trimester 1. (A) indicates the entire duration of gestation (day 0 to 280) and (B) indicate periods from the end of the trimester to the point at which mean trough plasma concentrations fall below the lower therapeutic window. Dosing schedule is Day 1:600 mg; Day 2 and 3: 300 mg and 150 mg to end of 1st trimester. Dark green lines indicate mean plasma concentration-time profiles during the study period with transparent area bordered by dashed line indicating the area within the 95th and 5th percentile of the predicted mean plasma concentration-time profiles; light brown shaded areas represent the therapeutic range of CQ proposed to be effective against ZIKV. The times at which the mean trough plasma concentrations fall below the lower therapeutic window are indicated by the arrows.

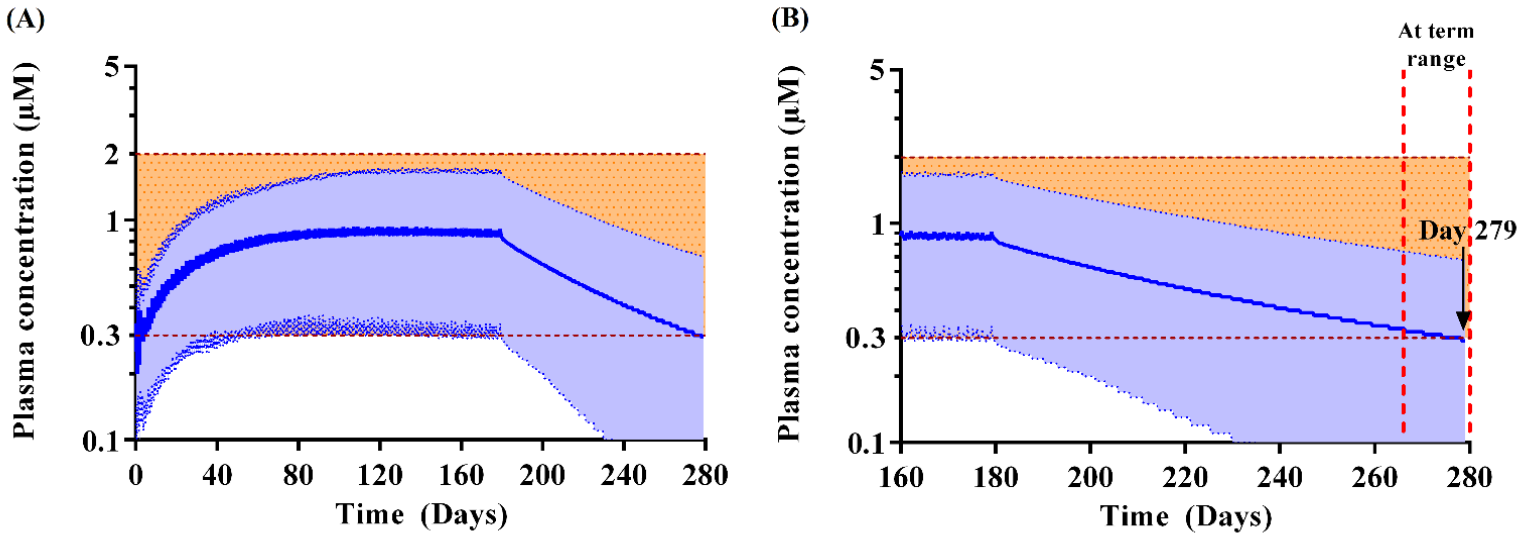

Figure 4.15: Simulated plasma concentration-time profiles for optimised CQ dosed during trimester 2

Simulated CQ plasma concentration-time profile utilising the optimised dosing regimen throughout trimester 1 and 2. (A) indicates the entire duration of gestation (day 0 to 280) and (B) indicates period from the end of the trimester to the point at which mean trough plasma concentrations fall below the lower therapeutic window. Dosing schedule is Day 1:600 mg; Day 2 and 3: 300 mg and 150 mg to end of 2nd trimester. Dark blue lines indicate mean plasma concentration-time profiles during the study period with light blue area bordered by dashed line indicating the area within the 95th and 5th percentile of the predicted mean plasma concentration-time profiles; light brown shaded area represent the therapeutic range of CQ proposed to be effective against ZIKV. The time at which the mean trough plasma concentrations fall below the lower therapeutic window is indicated by the arrows. Red dashed lines indicate the 'at term' phase.

Table 4.7: Steady-state pharmacokinetic parameters of the optimised CQ regimen during pregnancy

	Trimester	
	1	1 and 2 *
C_{max} (µM)	0.92 ± 0.41	0.92 ± 0.41
t_{max} (h)	2.2 ± 0.5	2.2 ± 0.5
AUC (µM.h)	20.9 ± 9.6	21.0 ± 9.5
Time to increase to lower window [a] (Days)	6	6
Subjects with C_{min} above window (%) [b]	67	65
Time to decrease to lower window [c] (Days)	150	279
Subjects with C_{min} above window (%) [b]	95	94
Subjects with C_{max} below window (%) [d]	1	5

Data represents mean ± standard deviation from the final dose. * C_{max}, tmax and AUC collected on the final dosing day. [a] Time taken for mean concentrations to be reach 0.3 µM; [b] Percentage of subjects with trough plasma concentrations above 0.3 µM; AUC was calculated for the final dosing day; [c] Time taken for mean plasma concentrations to decrease to 0.3 µM; [d] Percentage of subjects with peak plasma concentrations below 0.3 µM.

4.5 Discussion

The Zika virus (ZIKV) is an infectious disease that began spreading at an alarming and unprecedented way in the early part of the current decade, and its spread has been classified as a pandemic (363). Perhaps alarmingly (and importantly) a prominent feature of ZIKV which gained much publicity was the foetal and neurological consequences on infants born to infected mothers, and which primarily exhibited as microcephaly and Guillian-Barr syndrome. Although no current treatment options are available for the prevention of the spread of ZIKV, the opportunity for repurposing existing treatments towards ZIKV exists for the antimalarial drug chloroquine (CQ). This study addressed the potential to repurpose CQ for use in ZIKV, with a focus on developing potential dosing regimens for use in pregnancy.

4.5.1 Model development and validation

During model development and validation (Step 1), model performance depends largely upon the certainty of model input parameters describing CQ absorption, distribution and metabolism and elimination (ADME) (142). When using literature reported pharmacokinetic parameters for absorption (k_a), distribution (V_{ss}) and elimination (clearance), the model performance was poor. This may be, in part, due to the wide variability reported for these parameters, for instance, k_a has been reported in different studies as 1.8 h^{-1} (0.27-3.4 h^{-1}) (424); 1.19 h^{-1} ± 1.44 h^{-1} (423) and 0.51 h^{-1} ± 0.11 h^{-1} (385) and V_{ss} has been reported as 204-800 L/kg (390); 128 L/kg (112-137 L/kg) (407) and 100-1000 L/kg (425). Further, the reported V_{ss} of CQ depends on whether they were estimated based on the plasma concentration or blood concentrations, particularly given that CQ has a high blood-to-plasma partitioning ratio of >5:1, therefore the blood V_{ss} is likely to differ from that of the plasma V_{ss} by up to 10-fold (432, 433). Therefore, we utilised a parameter estimation approach with the application of Weighted Least Square (WLS) and the Nelder-Mead minimisation, final optimised parameter value were obtained (Table 4.3), and this model was used for subsequently validation purposes.

The application of this optimised model with retrospective clinical studies conducted in Caucasian subjects (403, 414, 434) resulted in model predictions of pharmacokinetic parameters to within 2-fold of these reports (Table 4.4), with VPCs confirming appropriate predictions of the plasma concentration-time profiles for each study (Figure 4.4, 4.5A, 4.7D).

In non-Caucasian subjects, physiological parameters, such as body-weight, vary significantly from typical Caucasian subjects and these differences may alter the pharmacokinetics of the drugs (283). We have previously demonstrated the impact of this in Thai (145, 435), Sudanese and Papua New Guinea (145), Ugandan (436) and Malaysians (437) population groups, and these alterations were made to the Simcyp® HV population groups as explained above. Following these revision, in all single and multidose simulations involving Caucasians and non-Caucasian subjects, plasma concentration-time profiles and resultant pharmacokinetic parameters were well predicted (Figure 4.4 – 4.7) and within 2-fold of the reported parameters (Table 4.4) (406-409, 411-413).

Having successfully validated a non-pregnant model in Caucasian and non-Caucasian subjects, the model was extended to pregnant subjects. The non-pregnant model was adapted by the inclusion of a full PBPK distribution model, which enables the consideration of gestational-age related alterations in maternal physiology. This is important considering that physiological alterations such as blood volume, tissue perfusion, plasma protein binding (398, 399, 401, 402) and CYP450 metabolic capacity (400) can occur. One strength of PBPK modelling is in its ability to incorporate these changes into predictive modelling approaches (297). When using this pregnancy model, key pharmacokinetic parameters were predicted to within 2-fold of the reported clinical parameters (Table 4.4), with plasma concentration-time profiles well recovered for all studies (Figure 4.8) (407, 411, 415). The altered blood volumes, blood flows and albumin binding capacity expected in pregnancy led to a reduction in the overall exposure of CQ in pregnant subjects compared to non-pregnant subjects (Table 4.4), and a similar decrease in exposure (AUC) and associated C_{max} has been reported in studies where CQ was used in pregnant subjects (407, 411, 415).

4.5.2 Considerations for CQ dosing for ZIKV disease in pregnancy

Current dose regimens for CQ use in antimalarial prophylaxis, RA and SLE treatment were next examined to determine the ability of these regimens to drive steady state concentrations within the proposed therapeutic window for ZIKV disease. With a malaria prophylactic weekly CQ dose of 150 mg and 300 mg administered to pregnant subjects during the first trimester, the proposed therapeutic range for ZIKV was not achieved (Figure 4.9). However, when CQ doses commonly used for SLE, that is, 150

mg daily (Figure 4.10) or 300 mg daily (Figure 4.11) was administered, the 150 mg daily dose achieved a satisfactory mean steady-state C_{max} (Table 4.5) within the proposed therapeutic window for ZIKV (Figure 4.10), and attained the lower therapeutic window on day 12 (Table 4.5). However, despite the higher daily dose of 300 mg achieving the target lower therapeutic limit after 5 days, this regimen was not selected as a result of peak plasma concentrations exceeding the upper therapeutic window (Figure 4.11) (Table 4.5).

4.5.3 Optimisation of CQ dosing for ZIKV in pregnancy

Based upon the 150 mg daily dose regimen, an optimal dosing regimen was derived to reduce the time taken for trough concentration of CQ to fall within the therapeutic range proposed, and consisted of: (i) an initial loading dose of 600 mg on day 1; (ii) 300 mg daily on day 2 and 3; (iii) 150 mg daily thereafter (Figure 4.12). This dosing regimen attained the target lower limit within 6 days with the majority of subjects, 96 %, possessing trough plasma concentrations within the lower therapeutic window (Table 4.5). In order to improve the clinical plausibility of the optimised dose, the optimised dose was adapted from doses used for malaria treatment (600 mg at 0 hour, 6 hours, 24 hours and 36 hours) (406, 408, 409, 412) and SLE/RA prophylaxis (long-term 150 mg daily dose) (35) because there is sufficient evidence to show at these doses, CQ administration is safe for both mother and foetus (35) (394).

Having identified an optimal dosing regimen, we next assessed its application at different trimesters, and when comparing starting in trimester 1 to trimester 3, identified a concurrent decrease in C_{max} and AUC (Table 4.6) (Figure 4.13A), which resulted in an increased in the time take to achieve trough plasma concentrations at the lower limit of the therapeutic window (Figure 4.13B) (Table 4.6). It is important to achieve the C_{min} as quickly and safely as possible to prevent progression of infection. The physiological changes during pregnancy, primarily alterations in the body weight, plasma proteins and plasma volume (438-442), will drive this decrease in exposure as gestation progresses.

Finally, when assessing the optimised dosing regimen for its use throughout pregnancy, we first considered dosing through trimester 1 only (Figure 4.14), which resulted in mean plasma concentrations decreasing below the lower window at 150 days

gestation (Figure 4.14) where 95 % of subjects possessed trough plasma concentrations above the lower window (Table 4.7).

On extension of this optimised dosing regimen throughout trimester 2 (Figure 4.15), mean plasma concentrations were maintained within the therapeutic window until day 279 (40 weeks), which exceeded the start of the 'at term' phase, commencing from week 38 onwards (Figure 4.15), and where 94 % of subjects possessed trough plasma concentrations above the lower therapeutic window (Table 4.7).

In summary, we have identified a possible therapeutic range that would be capable of proving sufficient plasma exposure for the duration of the gestational period to potentially limit ZIKV uptake into the developing foetus. However, this study is not without limitations.

4.5.4 Safety of chloroquine dosing at high doses in pregnancy

In relation to the dosing regimen proposed, chloroquine has been in use for at least 50 years, having been introduced as an alternative to quinine (443, 444). Its use in pregnancy has therefore been examined by various groups for safety and efficacy with little reported concerns. At doses proposed in this simulation, Klinger *et al* (2001)(445) reported no ophthalmic abnormalities in children born followed the maternal use of CQ during a mean duration of 7.2 months of gestation for doses of up to 332 mg daily. In a further study by Rukaria-Kaumbutho *et al* (1996) (446), at doses of 25 mg/kg achieved over 3 days administration, no safety concerns were identified in births at term. Further, a review by Nosten *et al* (2006) (447) identified 755 cases of first trimester exposure to chloroquine with no significant abortion risk or foetal risk. Finally, a study by Wolfe and Cordero (1985) (394) examined a cohort of 168 births to women treated with 300 mg CQ once weekly for the duration of pregnancy and identified no significant increase in the proportion of birth defects when compared to a control group who were not treated with CQ. Therefore, the proposed dosing regimen would provide a level of exposure similar to those reported in existing studies of CQ in pregnant women.

4.5.5 Study limitations

An obvious limitation to our work is the current inability to accurately predict the pharmacokinetics of CQ in the foetus. Only two clinical studies have reported CQ as

being able to reach the foetus through sampling cord blood (448, 449), but foetal drug levels were not recorded. However, the reported foetal: maternal concentration ratio was reported to be near unity, suggesting overall foetal exposure would be similar to that within the mother. Therefore, we assumed that the driving force for overall foetal exposure would be the maternal plasma concentration, which was used as a measure of the 'target' concentration within the foetus also. It further goes without saying that this assumption would therefore need to also consider the gestational-related changes in foetal physiology. However, the placenta plays a vital ADME role in controlling delivery of xenobiotics to the foetus, and given the similarity in exposure of CQ between both the mother and foetus (448, 449), the Simcyp® pregnancy model incorporated these key gestation related changes in anthropometric features of the mother and the foetus (implemented as a pooled feto-placental compartment within Simcyp®) (297, 307, 397).

Recently Abduljalil *et al* (2018) (450) collated foetal biometry and tissue composition data which may drive future studies to better describe and drive, from a mechanistic pharmacokinetic viewpoint, the development of a more appropriate and detailed foetal PBPK model which could predict overall foetal CQ brain exposure, however without CQ foetal tissue sampling data, any validation of such prediction would be difficult.

Our modelling approach utilised a 'worst-case' scenario in deriving a possible plasma therapeutic window for CQ. Our upper and lower plasma concentrations, 2 µM and 0.3 µM respectively, were based on assuming that a 10-to-30-fold greater brain concentration existing when compared to plasma concentrations for CQ (417, 418). We utilised the average of this range, a 20-fold lower plasma concentration compared to reported range of inhibitory concentration of 6-40 µM (381, 416). Whilst not being able to directly verify human foetal brain concentrations, our range of predicted peak plasma concentrations (0.1-1.88 µM) for the final optimised dosing regimen in pregnant subjects spanned this range and would potentially provide an overall peak brain exposure of 18.8 µM to 56.4 µM. This is assuming that CQ is capable of partitioning across the blood-brain barrier (BBB), with reports suggesting the BBB does not provide a permeability barrier to CQ (418). However, it is known that the foetal BBB develops from gestational week 8 with tight junction formation by week 18 (451). Therefore, further

characterisation of the role of the foetal BBB is warranted to estimate the likely CQ foetal brain exposure.

4.6 Conclusion

With the CQ model developed in this study, a CQ dose of 600 mg on day one, followed by 2 days treatment of 300 mg daily and thereafter 150 mg daily from day 3 until the end of trimester 2 would provide a plasma concentration within the range of 0.3-2 µM, potentially providing protection against ZIKV throughout pregnancy. Though the results from this study are subject to clinical confirmation, it serves as a guide for future clinical studies.

CHAPTER 5
Conclusion and future work

5.1 Conclusions

This thesis has demonstrated that the PBPK modelling approach is a powerful and evolving technique that may be used to understand the pharmacokinetic of antimalarials and address antimalaria drug therapy problems in special populations. To avoid the threat of DDI induced sub-therapeutic antimalarial concentrations which might lead to antimalarial drug resistance or the risk of drug toxicities, and to explore the potential of current antimalaria therapies for repurposing in other infectious diseases, this thesis demonstrates that PBPK modelling and simulations is a valuable tool and its potential to address this drug related therapies challenges is fast evolving.

In Chapter 2, a PBPK model for AL was successfully developed. The model performed well in the prediction of the pharmacokinetics of AL first in adult healthy volunteers and then in children. The model also performed well in the prediction of DDIs with a CYP inhibitor (ketoconazole) and inducer (rifampicin) in adults. The satisfactory performance of the model led to a further prediction of the DDI predictions between AL and rifampicin in children to address the AL dosing therapy limitations in children with tuberculosis and co-infected with malaria. Dosing optimisation of standard AL was suggested if they are to be used concomitantly with rifampicin in children. A 2/12 mg/kg of AL over a period of seven days when a patient is co-administered a rifampicin based anti-tuberculosis medication was proposed. Though this result is subject to clinical verification, it could serve as a guide to planning a clinical trial involving the DDI between AL and rifampicin based anti-TB treatment.

In Chapter 3, a PBPK model was developed that was used to mechanistically predict the pharmacokinetics of PQ in non-pregnant and pregnant women in which the population differences in malaria-HIV co-infected subjects was incorporated. We were able to show using the model that PQ pharmacokinetics in pregnancy is consistent and was relatively unchanged compared to non-pregnant women and that the impact of ART-mediated DDIs can significantly change the PQ pharmacokinetics, the magnitude of which was generally consistent across GW. The model required further adaptions to include data which detailed the relevant physiological and biochemical alterations common to HIV/malaria patients and which would further enhance the clinical application of the proposed model.

In Chapter 4, the potential to use PBPK modelling techniques to repurpose chloroquine for ZIKV treatment was explored. The CQ model developed in this study was developed and robustly validated and with the model, a CQ dose of 600 mg on day one, followed by 2 days treatment of 300 mg daily and thereafter 150 mg daily from day 3 until the end of trimester 2 would provide a plasma concentration within the range of 0.3-2 µM, potentially providing protection against ZIKV throughout pregnancy. Though the results from this study are subject to clinical confirmation, they serve as a guide for future clinical studies.

The thesis clearly demonstrates that PBPK modelling and simulation can be used to understand the pharmacokinetics of antimalarial agents in special populations. An understanding of which is required to improve existing antimalaria drug therapy, especially in the case of DDI in children or pregnant women or enhance the processes of development of new antimalarial agents in these groups.

5.2 Future work

The usefulness of PBPK in addressing drug related problems that may have been identified at early stages or translational phases of drug development in special populations demonstrated throughout this work is conspicuous. During this project, some aspects of antimalarial therapy which require more elaborate research have been identified. Some of such areas are:

5.2.1 Diseases specific physiological or biochemical changes that may affect the pharmacokinetics of antimalarials in special populations

Alteration in physiological and biochemical characteristics can affect the pharmacokinetics of antimalarials as demonstrated in this research. This research did not explore the effect of diseases common in malaria endemic areas, such as HIV/AIDS, on the body biochemistry or physiology and how this might affect the treatment of malaria in infected subjects. Therefore, in the future, the impact of disease specific physiological and biochemical changes on the pharmacokinetics of antimalarials in special population will be evaluated.

5.2.2 Modelling the effects of ethnic factors (e.g. polymorphisms) on the pharmacokinetic of antimalarials in special populations

Ethnic variation in the polymorphism of CYP enzymes and transport proteins can impact on the pharmacokinetics of certain antimalarials for example amodiaquine. Amodiaquine is metabolised by CYP2C8 which exhibits four polymorphic alleles which occur at varying frequencies in malaria endemic population groups (452). Since amodiaquine might be dosed to subjects across different ethnic groups, the significance of an alteration in its pharmacokinetics across ethnic population groups is yet to be evaluated. This is therefore another area of potential antimalarial research.

5.2.3 Development of models capable of predicting the pharmacokinetics of antimalarials in the foetus during pregnancy and in breastmilk after pregnancy

There is some suggestion that the foetus might be expose to malarial infection from its infected mother. Despite the robust data available on the pharmacokinetics of antimalarials in pregnant women, there is not much known about the changes in drug

disposition in the foetus. During the write up of this thesis, a few studies have provided an insight into the maternal to foetal transfer of drugs using a PBPK model (453, 454) but none of these models have been validated for antimalarial drugs, also the limitations of these studies lies in their ability to assess the maternal to infant drug transfer through the milk. Therefore, a PBPK model capable of predicting the pharmacokinetics of antimalarials in the foetus during pregnancy and in the infant during breastfeeding will be developed.

References

1. Gomes M. Economic and Demographic-Research on Malaria - a Review of the Evidence. Soc Sci Med. 1993;37(9):1093-108.
2. World Health Organisation WHO. Malaria: Fact sheets 2016 [updated January Available from: http://www.who.int/mediacentre/factsheets/fs094/en/.
3. World Health Organisation WHO. Number of malaria cases : Global Health Observatory (GHO) data 2015 [Available from: http://www.who.int/gho/malaria/epidemic/cases/en/.
4. Centers for Disease Control and Prevention CDC. About Malaria: Biology 2016 [updated March 1; cited 2016 14th June]. Available from: https://www.cdc.gov/malaria/about/biology/index.html.
5. Gupta S, Snow RW, Donnelly CA, Marsh K, Newbold C. Immunity to non-cerebral severe malaria is acquired after one or two infections. Nat Med. 1999;5(3):340-3.
6. Trape JF, Rogier C. Combating malaria morbidity and mortality by reducing transmission. Parasitol Today. 1996;12(6):236-40.
7. Carter R, Mendis KN. Evolutionary and historical aspects of the burden of malaria. Clin Microbiol Rev. 2002;15(4):564-94.
8. Jeffery GM. Epidemiological significance of repeated infections with homologous and heterologous strains and species of Plasmodium. Bull World Health Organ. 1966;35(6):873-82.
9. Mendis KN, David PH, Carter R. Antigenic polymorphism in malaria: is it an important mechanism for immune evasion? Immunol Today. 1991;12(3):A34-7.
10. Powell RD, Mcnamara JV, Rieckman.Kh. Clinical Aspects of Acquisition of Immunity to Falciparum Malaria. P Helm Soc Wash. 1972;39(Nov):51-66.
11. Baird JK. Host Age as a Determinant of Naturally Acquired-Immunity to Plasmodium-Falciparum. Parasitol Today. 1995;11(3):105-11.
12. Baird JK, Jones TR, Danudirgo EW, Annis BA, Bangs MJ, Basri H, et al. Age-Dependent Acquired Protection against Plasmodium-Falciparum in People Having 2 Years Exposure to Hyperendemic Malaria. Am J Trop Med Hyg. 1991;45(1):65-76.
13. Lengeler C. Insecticide-treated bed nets and curtains for preventing malaria. Cochrane Database Syst Rev. 2004(2):CD000363.
14. Pluess B, Tanser FC, Lengeler C, Sharp BL. Indoor residual spraying for preventing malaria. Cochrane Db Syst Rev. 2010(4).
15. Sinclair D, Zani B, Donegan S, Olliaro P, Garner P. Artemisinin-based combination therapy for treating uncomplicated malaria. Cochrane Database Syst Rev. 2009(3):CD007483.
16. Wongsrichanalai C, Barcus MJ, Muth S, Sutamihardja A, Wernsdorfer WH. A review of malaria diagnostic tools: Microscopy and rapid diagnostic test (RDT). Am J Trop Med Hyg. 2007;77(6):119-27.
17. White MT, Conteh L, Cibulskis R, Ghani AC. Costs and cost-effectiveness of malaria control interventions - a systematic review. Malaria J. 2011;10.
18. Wotodjo AN, Richard V, Boyer S, Doucoure S, Diagne N, Toure-Balde A, et al. The implication of long-lasting insecticide-treated net use in the resurgence of malaria morbidity in a Senegal malaria endemic village in 2010-2011. Parasite Vector. 2015;8.
19. Okoyo C, Mwandawiro C, Kihara J, Simiyu E, Gitonga CW, Noor AM, et al. Comparing insecticide-treated bed net use to Plasmodium falciparum infection among schoolchildren living near Lake Victoria, Kenya. Malaria J. 2015;14.
20. Iwuafor AA, Egwuatu CC, Nnachi AU, Ita IO, Ogban GI, Akujobi CN, et al. Malaria Parasitaemia and the use of insecticide-treated nets (INTs) for malaria control amongst under-5 year old children in Calabar, Nigeria. Bmc Infect Dis. 2016;16.
21. Yukich JO, Bennett A, Albertini A, Incardona S, Moonga H, Chisha Z, et al. Reductions in Artemisinin-Based Combination Therapy Consumption after the Nationwide Scale up of Routine Malaria Rapid Diagnostic Testing in Zambia. Am J Trop Med Hyg. 2012;87(3):437-46.

22. Murray CK, Gasser RA, Magill AJ, Miller RS. Update on rapid diagnostic testing for malaria. Clinical Microbiology Reviews. 2008;21(1):97-+.
23. West PA, Protopopoff N, Wright A, Kivaju Z, Tigererwa R, Mosha FW, et al. Enhanced Protection against Malaria by Indoor Residual Spraying in Addition to Insecticide Treated Nets: Is It Dependent on Transmission Intensity or Net Usage? Plos One. 2015;10(3).
24. Kim D, Fedak K, Kramer R. Reduction of malaria prevalence by indoor residual spraying: a meta-regression analysis. Am J Trop Med Hyg. 2012;87(1):117-24.
25. Matangila JR, Mitashi P, da Luz RAI, Lutumba PT, Van Geertruyden JP. Efficacy and safety of intermittent preventive treatment for malaria in schoolchildren: a systematic review. Malaria J. 2015;14.
26. World Health Organisation WHO. Malaria: Intermittent preventive treatment in pregnancy (IPTp) 2016 [updated 20 March 2016. Available from: http://www.who.int/malaria/areas/preventive_therapies/pregnancy/en/.
27. Harrington WE, Fried M, Duffy PE. Defending the Use of Sulfadoxine-Pyrimethamine for Intermittent Preventive Treatment for Malaria in Pregnancy: A Short-Sighted Strategy. J Infect Dis. 2016;213(3):496-7.
28. Gutman J, Taylor S, Meshnick SR, Ter Kuile FO. Reply to Harrington et al. J Infect Dis. 2016;213(3):497-8.
29. Hill J, Hoyt J, Achieng F, Ouma P, L'lanziva A, Kariuki S, et al. User and Provider Acceptability of Intermittent Screening and Treatment and Intermittent Preventive Treatment with Dihydroartemisinin-Piperaquine to Prevent Malaria in Pregnancy in Western Kenya. Plos One. 2016;11(3).
30. Harrison N. In celebration of the Jesuit's powder: a history of malaria treatment. Lancet Infect Dis. 2015;15(10):1143-.
31. Faurant C. From Bark to Weed: The History of Artemisinin. Parasite. 2011;18(3):215-8.
32. Organisation WH. Guideline for the treatment of malaria. 3rd ed. Geneva, Switzerland: WHO Press, World Health Organisation 2015.
33. Payne D. Spread of Chloroquine Resistance in Plasmodium-Falciparum. Parasitol Today. 1987;3(8):241-6.
34. Snow RW, Trape JF, Marsh K. The past, present and future of childhood malaria mortality in Africa. Trends Parasitol. 2001;17(12):593-7.
35. Levy M, Buskila D, Gladman DD, Urowitz MB, Koren G. Pregnancy outcome following first trimester exposure to chloroquine. Am J Perinatol. 1991;8(3):174-8.
36. Le Bras J, Durand R. The mechanisms of resistance to antimalarial drugs in Plasmodium falciparum. Fundam Clin Pharmacol. 2003;17(2):147-53.
37. Schlitzer M. Malaria chemotherapeutics part I: History of antimalarial drug development, currently used therapeutics, and drugs in clinical development. ChemMedChem. 2007;2(7):944-86.
38. Farooq U, Mahajan RC. Drug resistance in malaria. J Vector Borne Dis. 2004;41(3-4):45-53.
39. Krudsood S, Patel SN, Tangpukdee N, Thanachartwet W, Leowattana W, Pornpininworakij K, et al. Efficacy of atovaquone-proguanil for treatment of acute multidrug-resistant Plasmodium falciparum malaria in Thailand. Am J Trop Med Hyg. 2007;76(4):655-8.
40. Cottrell G, Musset L, Hubert V, Le Bras J, Clain J, Atovaquone-Proguanil Treatment Failure Study G. Emergence of resistance to atovaquone-proguanil in malaria parasites: insights from computational modeling and clinical case reports. Antimicrob Agents Chemother. 2014;58(8):4504-14.
41. van den Broek IV, Gatkoi T, Lowoko B, Nzila A, Ochong E, Keus K. Chloroquine, sulfadoxine-pyrimethamine and amodiaquine efficacy for the treatment of uncomplicated Plasmodium falciparum malaria in Upper Nile, south Sudan. Trans R Soc Trop Med Hyg. 2003;97(2):229-35.

42. Pitmang SL, Thacher TD, Madaki JK, Egah DZ, Fischer PR. Comparison of sulfadoxine-pyrimethamine with and without chloroquine for uncomplicated malaria in Nigeria. Am J Trop Med Hyg. 2005;72(3):263-6.
43. Basco LK, Same-Ekobo A, Ngane VF, Ndounga M, Metoh T, Ringwald P, et al. Therapeutic efficacy of sulfadoxine-pyrimethamine, amodiaquine and the sulfadoxine-pyrimethamine-amodiaquine combination against uncomplicated Plasmodium falciparum malaria in young children in Cameroon. Bull World Health Organ. 2002;80(7):538-45.
44. Thapar MM, Ashton M, Lindegardh N, Bergqvist Y, Nivelius S, Johansson I, et al. Time-dependent pharmacokinetics and drug metabolism of atovaquone plus proguanil (Malarone) when taken as chemoprophylaxis. Eur J Clin Pharmacol. 2002;58(1):19-27.
45. Weidekamm E, Plozza-Nottebrock H, Forgo I, Dubach UC. Plasma concentrations in pyrimethamine and sulfadoxine and evaluation of pharmacokinetic data by computerized curve fitting. Bull World Health Organ. 1982;60(1):115-22.
46. Cui L, Su XZ. Discovery, mechanisms of action and combination therapy of artemisinin. Expert Rev Anti Infect Ther. 2009;7(8):999-1013.
47. Sinclair D, Donegan S, Isba R, Lalloo DG. Artesunate versus quinine for treating severe malaria. Cochrane Database Syst Rev. 2012(6):CD005967.
48. Pan American Health Organisation PAHO, World Health Organisation WHO. ZIka cumulative cases
49. Borrmann S, Sallas WM, Machevo S, Gonzalez R, Bjorkman A, Martensson A, et al. The effect of food consumption on lumefantrine bioavailability in African children receiving artemether-lumefantrine crushed or dispersible tablets (Coartem) for acute uncomplicated Plasmodium falciparum malaria. Trop Med Int Health. 2010;15(4):434-41.
50. Byakika-Kibwika P, Lamorde M, Mayanja-Kizza H, Merry C, Colebunders B, Van Geertruyden JP. Update on the efficacy, effectiveness and safety of artemether-lumefantrine combination therapy for treatment of uncomplicated malaria. Ther Clin Risk Manag. 2010;6:11-20.
51. Mwesigwa J, Parikh S, McGee B, German P, Drysdale T, Kalyango JN, et al. Pharmacokinetics of artemether-lumefantrine and artesunate-amodiaquine in children in Kampala, Uganda. Antimicrob Agents Chemother. 2010;54(1):52-9.
52. Ezzet F, van Vugt M, Nosten F, Looareesuwan S, White NJ. Pharmacokinetics and pharmacodynamics of lumefantrine (benflumetol) in acute falciparum malaria. Antimicrob Agents Chemother. 2000;44(3):697-704.
53. Basco LK, Ringwald P. In vitro activities of piperaquine and other 4-aminoquinolines against clinical isolates of Plasmodium falciparum in Cameroon. Antimicrob Agents Chemother. 2003;47(4):1391-4.
54. Janssens B, van Herp M, Goubert L, Chan S, Uong S, Nong S, et al. A randomized open study to assess the efficacy and tolerability of dihydroartemisinin-piperaquine for the treatment of uncomplicated falciparum malaria in Cambodia. Trop Med Int Health. 2007;12(2):251-9.
55. Kakar Q, Sheikh S, Ahmed I, Khan MA, Jamil M, ElMohammady H, et al. Efficacy of artemisinin-based combination therapies for the treatment of falciparum malaria in Pakistan (2007-2015): In vivo response and dhfr and dhps mutations. Acta Trop. 2016;164:17-22.
56. Amaratunga C, Lim P, Suon S, Sreng S, Mao S, Sopha C, et al. Dihydroartemisinin-piperaquine resistance in Plasmodium falciparum malaria in Cambodia: a multisite prospective cohort study. Lancet Infect Dis. 2016;16(3):357-65.
57. Gobbi F, Buonfrate D, Menegon M, Lunardi G, Angheben A, Severini C, et al. Failure of dihydroartemisinin-piperaquine treatment of uncomplicated Plasmodium falciparum malaria in a traveller coming from Ethiopia. Malar J. 2016;15(1):525.
58. Pasay CJ, Rockett R, Sekuloski S, Griffin P, Marquart L, Peatey C, et al. Piperaquine Monotherapy of Drug-Susceptible Plasmodium falciparum Infection Results in Rapid Clearance of Parasitemia but Is Followed by the Appearance of Gametocytemia. J Infect Dis. 2016;214(1):105-13.

59. Gonzalez R, Hellgren U, Greenwood B, Menendez C. Mefloquine safety and tolerability in pregnancy: a systematic literature review. Malar J. 2014;13:75.
60. Lee SJ, Ter Kuile FO, Price RN, Luxemburger C, Nosten F. Adverse effects of mefloquine for the treatment of uncomplicated malaria in Thailand: A pooled analysis of 19, 850 individual patients. Plos One. 2017;12(2):e0168780.
61. Schlagenhauf P, Adamcova M, Regep L, Schaerer MT, Rhein HG. The position of mefloquine as a 21st century malaria chemoprophylaxis. Malar J. 2010;9:357.
62. Olliaro P, Mussano P. Amodiaquine for treating malaria. Cochrane Database Syst Rev. 2003(2):CD000016.
63. Mandi G, Mockenhaupt FP, Coulibaly B, Meissner P, Muller O. Efficacy of amodiaquine in the treatment of uncomplicated falciparum malaria in young children of rural north-western Burkina Faso. Malar J. 2008;7:58.
64. Assi SB, Aba YT, Yavo JC, Nguessan AF, Tchiekoi NB, San KM, et al. Safety of a fixed-dose combination of artesunate and amodiaquine for the treatment of uncomplicated Plasmodium falciparum malaria in real-life conditions of use in Cote d'Ivoire. Malar J. 2017;16(1):8.
65. Blasco B, Leroy D, Fidock DA. Antimalarial drug resistance: linking Plasmodium falciparum parasite biology to the clinic. Nat Med. 2017;23(8):917-28.
66. White NJ, Pongtavornpinyo W, Maude RJ, Saralamba S, Aguas R, Stepniewska K, et al. Hyperparasitaemia and low dosing are an important source of anti-malarial drug resistance. Malaria J. 2009;8.
67. White NJ. Antimalarial drug resistance. J Clin Invest. 2004;113(8):1084-92.
68. Fan JH, de Lannoy IAM. Pharmacokinetics. Biochem Pharmacol. 2014;87(1):93-120.
69. Urso R, Blardi P, Giorgi G. A short introduction to pharmacokinetics. Eur Rev Med Pharmacol Sci. 2002;6(2-3):33-44.
70. Benet LZ, Zia-Amirhosseini P. Basic principles of pharmacokinetics. Toxicol Pathol. 1995;23(2):115-23.
71. Benet LZ. Pharmacokinetic Parameters - Which Are Necessary to Define a Drug Substance. Eur J Respir Dis. 1984;65:45-61.
72. Pang KS, Rowland M. Hepatic clearance of drugs. III. Additional experimental evidence supporting the "well-stirred" model, using metabolite (MEGX) generated from lidocaine under varying hepatic blood flow rates and linear conditions in the perfused rat liver in situ preparation. J Pharmacokinet Biopharm. 1977;5(6):681-99.
73. Pang KS, Rowland M. Hepatic clearance of drugs. II. Experimental evidence for acceptance of the "well-stirred" model over the "parallel tube" model using lidocaine in the perfused rat liver in situ preparation. J Pharmacokinet Biopharm. 1977;5(6):655-80.
74. Pang KS, Rowland M. Hepatic clearance of drugs. I. Theoretical considerations of a "well-stirred" model and a "parallel tube" model. Influence of hepatic blood flow, plasma and blood cell binding, and the hepatocellular enzymatic activity on hepatic drug clearance. J Pharmacokinet Biopharm. 1977;5(6):625-53.
75. Taft DR. Pharmacology: Principles and practice. Hacker M, II WSM, Bachmann KA, editors. Burlington MA 01803, USA: Elsevier; 2009.
76. Markl D, Zeitler JA. A Review of Disintegration Mechanisms and Measurement Techniques. Pharm Res. 2017;34(5):890-917.
77. Noyes AA, Whitney WR. The rate of solution of solid substances in their own solutions. . Journal of American Chemistry Society. 1897;19:930-4.
78. Gavhane YN, Yadav AV. Loss of orally administered drugs in GI tract. Saudi Pharm J. 2012;20(4):331-44.
79. Karlsson J, Ungell A, Grasjo J, Artursson P. Paracellular drug transport across intestinal epithelia: influence of charge and induced water flux. Eur J Pharm Sci. 1999;9(1):47-56.
80. Lennernas H. Does Fluid-Flow across the Intestinal-Mucosa Affect Quantitative Oral-Drug Absorption - Is It Time for a Reevaluation. Pharmaceut Res. 1995;12(11):1573-82.
81. Lipinski CA. Drug-like properties and the causes of poor solubility and poor permeability. J Pharmacol Toxicol Methods. 2000;44(1):235-49.

82. Urso R, Blardi P, G G. A short introduction to pharmacokinetics. European Review for Medical and Pharmacological Sciences. 2002;6(2-3):33-44.
83. Schmidt S, Gonzalez D, Derendorf H. Significance of Protein Binding in Pharmacokinetics and Pharmacodynamics. J Pharm Sci-Us. 2010;99(3):1107-22.
84. Nebert DW, Russell DW. Clinical importance of the cytochromes P450. Lancet. 2002;360(9340):1155-62.
85. Gan J, Ma S, Zhang D. Non-cytochrome P450-mediated bioactivation and its toxicological relevance. Drug Metab Rev. 2016:1-29.
86. Jhajra S, Varkhede N R, Ahire D S, Naik B V, Bhagwat P, Paliwal J, et al. Extrahepatic Drug-Metabolizing Enzymes and Their Significance. Drug Metabolism and Interactions. 2012;6:1-97.
87. Krishna DR, Klotz U. Extrahepatic Metabolism of Drugs in Humans. Clin Pharmacokinet. 1994;26(2):144-60.
88. Zanger UM, Schwab M. Cytochrome P450 enzymes in drug metabolism: Regulation of gene expression, enzyme activities, and impact of genetic variation. Pharmacol Therapeut. 2013;138(1):103-41.
89. Glatt H. Sulfotransferases in the bioactivation of xenobiotics. Chem Biol Interact. 2000;129:141-70.
90. Ritter JK. Roles of glucuronidation and UDP-glucuronosyltransferases in xenobiotic bioactivation reactions. Chem-Biol Interact. 2000;129(1-2):171-93.
91. Chiba K, Trevor A, Castagnoli N, Jr. Metabolism of the neurotoxic tertiary amine, MPTP, by brain monoamine oxidase. Biochem Biophys Res Commun. 1984;120(2):574-8.
92. Khan AA, Rahmani AH, Aldebasi YH, Aly SM. Biochemical and pathological studies on peroxidases -an updated review. Glob J Health Sci. 2014;6(5):87-98.
93. Krueger SK, Williams DE. Mammalian flavin-containing monooxygenases: structure/function, genetic polymorphisms and role in drug metabolism. Pharmacol Ther. 2005;106(3):357-87.
94. Pryde DC, Dalvie D, Hu QY, Jones P, Obach RS, Tran TD. Aldehyde Oxidase: An Enzyme of Emerging Importance in Drug Discovery. J Med Chem. 2010;53(24):8441-60.
95. Walsh JS, Reese MJ, Thurmond LM. The metabolic activation of abacavir by human liver cytosol and expressed human alcohol dehydrogenase isozymes. Chem Biol Interact. 2002;142(1-2):135-54.
96. O'Brien PJ. Molecular mechanisms of quinone cytotoxicity. Chem Biol Interact. 1991;80(1):1-41.
97. Dresser MJ, Leabman MK, Giacomini KM. Transporters involved in the elimination of drugs in the kidney: Organic anion transporters and organic cation transporters. J Pharm Sci-Us. 2001;90(4):397-421.
98. Moore BR, Benjamin JM, Salman S, Griffin S, Ginny E, Page-Sharp M, et al. Effect of coadministered fat on the tolerability, safety, and pharmacokinetic properties of dihydroartemisinin-piperaquine in Papua New Guinean children with uncomplicated malaria. Antimicrob Agents Chemother. 2014;58(10):5784-94.
99. Tarning J, Ashley EA, Lindegardh N, Stepniewska K, Phaiphun L, Day NP, et al. Population pharmacokinetics of piperaquine after two different treatment regimens with dihydroartemisinin-piperaquine in patients with Plasmodium falciparum malaria in Thailand. Antimicrob Agents Chemother. 2008;52(3):1052-61.
100. Salman S, Page-Sharp M, Batty KT, Kose K, Griffin S, Siba PM, et al. Pharmacokinetic comparison of two piperaquine-containing artemisinin combination therapies in Papua New Guinean children with uncomplicated malaria. Antimicrob Agents Chemother. 2012;56(6):3288-97.
101. Gabrielsson J, Weiner D. Non-compartmental analysis. Methods Mol Biol. 2012;929:377-89.
102. Administration USDoHaHSFaD. Guidance for industry - population pharmacokinetics. USA; 1999.

103. Kiang TK, Sherwin CM, Spigarelli MG, Ensom MH. Fundamentals of Population Pharmacokinetic Modelling : Modelling and Software. Clin Pharmacokinet. 2012;51(8):515-25.
104. Ali AM, Penny MA, Smith TA, Workman L, Sasi P, Adjei GO, et al. Population Pharmacokinetics of the Antimalarial Amodiaquine: a Pooled Analysis To Optimize Dosing. Antimicrob Agents Chemother. 2018;62(10).
105. Reuter SE, Upton RN, Evans AM, Navaratnam V, Olliaro PL. Population pharmacokinetics of orally administered mefloquine in healthy volunteers and patients with uncomplicated Plasmodium falciparum malaria. J Antimicrob Chemother. 2015;70(3):868-76.
106. Hoglund RM, Workman L, Edstein MD, Thanh NX, Quang NN, Zongo I, et al. Population Pharmacokinetic Properties of Piperaquine in Falciparum Malaria: An Individual Participant Data Meta-Analysis. PLoS Med. 2017;14(1):e1002212.
107. Badhan RKS. Physiologically based pharmacokinetic modelling in drug delivery. Defang O, Smith SC, editors. United Kingdom: John Wiley & Sons, Ltd; 2015.
108. Huang SM, Rowland M. The role of physiologically based pharmacokinetic modeling in regulatory review. Clinical pharmacology and therapeutics. 2012;91(3):542-9.
109. Jones H, Rowland-Yeo K. Basic concepts in physiologically based pharmacokinetic modeling in drug discovery and development. CPT Pharmacometrics Syst Pharmacol. 2013;2:e63.
110. Khalil F, Laer S. Physiologically Based Pharmacokinetic Modeling: Methodology, Applications, and Limitations with a Focus on Its Role in Pediatric Drug Development. Journal of Biomedicine and Biotechnology. 2011:13.
111. Lin W, Heimbach T, Jain JP, Awasthi R, Hamed K, Sunkara G, et al. A Physiologically Based Pharmacokinetic Model to Describe Artemether Pharmacokinetics in Adult and Pediatric Patients. J Pharm Sci. 2016;105(10):3205-13.
112. Johnson TN, Cleary Y, Parrott N, Reigner B, Smith JR, Toovey S. Development of a physiologically based pharmacokinetic model for mefloquine and its application alongside a clinical effectiveness model to select an optimal dose for prevention of malaria in young Caucasian children. Brit J Clin Pharmaco. 2019;85(1):100-13.
113. Barrett JS, Alberighi OD, Laer S, Meibohm B. Physiologically Based Pharmacokinetic (PBPK) Modeling in Children. Clinical Pharmacology & Therapeutics. 2012;92(1):40-9.
114. Miyagi SJ, Long-Boyle JR. Predicting Pediatric Drug Disposition - Present and Future Directions of Pediatric Physiologically-Based Pharmacokinetics. Drug Metabolism Letters.9(1):1-8.
115. Certara®, biosimulator, informatics) mbdda. Simcyp Simulator. 14.0.93.0 ed. 100 Overlook Center, Suite 101, Princeton, NJ 08540 USA: Certara USA, Inc.
116. Abduljalil K, Furness P, Johnson TN, Rostami-Hodjegan A, Soltani H. Anatomical, Physiological and Metabolic Changes with Gestational Age during Normal Pregnancy A Database for Parameters Required in Physiologically Based Pharmacokinetic Modelling. Clinical Pharmacokinetics. 2012;51(6):365-96.
117. Price PS, Conolly RB, Chaisson CF, Gross EA, Young JS, Mathis ET, et al. Modeling interindividual variation in physiological factors used in PBPK models of humans. Crit Rev Toxicol. 2003;33(5):469-503.
118. Thompson CM, Johns DO, Sonawane B, Barton HA, Hattis D, Tardif R, et al. Database for Physiologically Based Pharmacokinetic (PBPK) Modeling: Physiological Data for Healthy and Health-Impaired Elderly. J Toxicol Env Heal B. 2009;12(1):1-24.
119. Brown RP, Delp MD, Lindstedt SL, Rhomberg LR, Beliles RP. Physiological parameter values for physiologically based pharmacokinetic models. Toxicol Ind Health. 1997;13(4):407-84.
120. Nestorov IA, Aarons LJ, Arundel PA, Rowland M. Lumping of whole-body physiologically based pharmacokinetic models. J Pharmacokinet Biop. 1998;26(1):21-46.
121. Brünner E. Reaktionsgeschwindigkeit in heterogenen systemen. Z Phys Chem. 1904;47:56-102.
122. Nernst W. Theorie der reaktionsgeschwindigkeit in heterogenen systemen. Z Phys Chem. 1904;47:52-5.

123. Costa P, Sousa Lobo JM. Modeling and comparison of dissolution profiles. European Journal of Pharmaceutical Sciences. 2001;13(2):123-33.
124. Neuhoff S, Gaohua L, Burt H, Jamei M, Li L, Geoffrey T, et al. Accounting for Transporters in Renal Clearance: Towards a Mechanistic Kidney Model (Mech KiM). Y. S, B. S, editors. New York, NY: Springer
125. Rodgers T, Leahy D, Rowland M. Physiologically based pharmacokinetic modeling 1: Predicting the tissue distribution of moderate-to-strong bases. J Pharm Sci-Us. 2005;94(6):1259-76.
126. Rodgers T, Rowland M. Mechanistic approaches to volume of distribution predictions: Understanding the processes. Pharmaceut Res. 2007;24(5):918-33.
127. Mentre F, Mallet A. Handling covariates in population pharmacokinetics. Int J Biomed Comput. 1994;36(1-2):25-33.
128. Huisinga W, Solms A, Fronton L, Pilari S. Modeling interindividual variability in physiologically based pharmacokinetics and its link to mechanistic covariate modeling. CPT Pharmacometrics Syst Pharmacol. 2012;1:e4.
129. Dahiya RS. Application of PBPK models in personalized healthcare. Journal of Pharmacokinet Exp Ther. 2016;1(1):e004.
130. Khalil F, Laer S. Physiologically Based Pharmacokinetic Models in the Prediction of Oral Drug Exposure Over the Entire Pediatric Age Range-Sotalol as a Model Drug. Aaps J. 2014;16(2):226-39.
131. Walsh C, Bonner JJ, Johnson TN, Neuhoff S, Ghazaly EA, Gribben JG, et al. Development of a physiologically based pharmacokinetic model of actinomycin D in children with cancer. Brit J Clin Pharmaco. 2016;81(5):989-98.
132. Batchelor H, Appleton R, Hawcutt DB. Comparing paediatric intravenous phenytoin doses using physiologically based pharmacokinetic (PBPK) modelling software. Seizure-Eur J Epilep. 2015;33:8-12.
133. Mendes MD, Hirt D, Urien S, Valade E, Bouazza N, Foissac F, et al. Physiologically-based pharmacokinetic modeling of renally excreted antiretroviral drugs in pregnant women. Brit J Clin Pharmaco. 2015;80(5):1031-41.
134. Alqahtani S, Kaddoumi A. Development of Physiologically Based Pharmacokinetic/Pharmacodynamic Model for Indomethacin Disposition in Pregnancy. Plos One. 2015;10(10).
135. Li J, Guo HF, Liu C, Zhong ZY, Liu L, Liu XD. Prediction of Drug Disposition in Diabetic Patients by Means of a Physiologically Based Pharmacokinetic Model. Clinical Pharmacokinetics. 2015;54(2):179-93.
136. Zhao P, Vieira MDT, Grillo JA, Song PF, Wu TC, Zheng JH, et al. Evaluation of Exposure Change of Nonrenally Eliminated Drugs in Patients With Chronic Kidney Disease Using Physiologically Based Pharmacokinetic Modeling and Simulation. J Clin Pharmacol. 2012;52:91s-108s.
137. Polasek TM, Patel F, Jensen BP, Sorich MJ, Wiese MD, Doogue MP. Predicted metabolic drug clearance with increasing adult age. Brit J Clin Pharmaco. 2013;75(4):1019-28.
138. Kuepfer L, Niederalt C, Wendl T, Schlender JF, Willmann S, Lippert J, et al. Applied Concepts in PBPK Modeling: How to Build a PBPK/PD Model. Cpt-Pharmacomet Syst. 2016;5(10):516-31.
139. European Medicines Agency, Use CfMPfH. Guideline on the reporting of physiologically based pharmacokinetic (PBPK) modelling and simulation. UK; 2018.
140. Leong R, Vieira ML, Zhao P, Mulugeta Y, Lee CS, Huang SM, et al. Regulatory experience with physiologically based pharmacokinetic modeling for pediatric drug trials. Clinical pharmacology and therapeutics. 2012;91(5):926-31.
141. Zhao P, Zhang L, Grillo JA, Liu Q, Bullock JM, Moon YJ, et al. Applications of physiologically based pharmacokinetic (PBPK) modeling and simulation during regulatory review. Clinical pharmacology and therapeutics. 2011;89(2):259-67.

142. Zhuang X, Lu C. PBPK modeling and simulation in drug research and development. Acta Pharm Sin B. 2016;6(5):430-40.
143. Suri A, Chapel S, Lu C, Venkatakrishnan K. Physiologically Based and Population PK Modeling in Optimizing Drug Development: A Predict-Learn-Confirm Analysis. Clinical Pharmacology & Therapeutics. 2015;98(3):336-44.
144. Olafuyi O, Badhan RKS. Dose Optimization of Chloroquine by Pharmacokinetic Modeling During Pregnancy for the Treatment of Zika Virus Infection. J Pharm Sci. 2018.
145. Olafuyi O, Coleman M, Badhan RKS. The application of physiologically based pharmacokinetic modelling to assess the impact of antiretroviral-mediated drug-drug interactions on piperaquine antimalarial therapy during pregnancy. Biopharm Drug Dispos. 2017;38(8):464-78.
146. Olafuyi O, Coleman M, Badhan RKS. Development of a paediatric physiologically based pharmacokinetic model to assess the impact of drug-drug interactions in tuberculosis co-infected malaria subjects: A case study with artemether-lumefantrine and the CYP3A4-inducer rifampicin. Eur J Pharm Sci. 2017;106:20-33.
147. Batchelor HK, Marriott JF. Paediatric pharmacokinetics: key considerations. Brit J Clin Pharmaco. 2015;79(3):395-404.
148. Johnson TN, Tanner MS, Taylor CJ, Tucker GT. Enterocytic CYP3A4 in a paediatric population: developmental changes and the effect of coeliac disease and cystic fibrosis. Br J Clin Pharmacol. 2001;51(5):451-60.
149. Salem F, Johnson TN, Barter ZE, Leeder JS, Rostami-Hodjegan A. Age Related Changes in Fractional Elimination Pathways for Drugs: Assessing the Impact of Variable Ontogeny on Metabolic Drug-Drug Interactions. J Clin Pharmacol. 2013;53(8):857-65.
150. Feng B, Varma MV. Evaluation and Quantitative Prediction of Renal Transporter-Mediated Drug-Drug Interactions. J Clin Pharmacol. 2016;56 Suppl 7:S110-21.
151. Johansson S, Lofberg B, Aunes M, Lunde H, Frison L, Edvardsson N, et al. In Silico Predictions and In Vivo Results of Drug-Drug Interactions by Ketoconazole and Verapamil on AZD1305, a Combined Ion Channel Blocker and a Sensitive CYP3A4 Substrate. Clin Pharmacol Drug Dev. 2016;5(5):364-73.
152. Mehlotra RK, Henry-Halldin CN, Zimmerman PA. Application of pharmacogenomics to malaria: a holistic approach for successful chemotherapy. Pharmacogenomics. 2009;10(3):435-49.
153. World Health Organisation WHO. Malaria in children under five 2016 [updated April 6, 2016; cited 2016 29th September]. Available from: http://www.who.int/malaria/areas/high_risk_groups/children/en/.
154. Doolan DL, Dobano C, Baird JK. Acquired Immunity to Malaria. Clinical Microbiology Reviews. 2009;22(1):13-36.
155. Ezeamama AE, Spiegelman D, Hertzmark E, Bosch RJ, Manji KP, Duggan C, et al. HIV Infection and the Incidence of Malaria Among HIV-Exposed Children from Tanzania. J Infect Dis. 2012;205(10):1486-94.
156. Idro R, Marsh K, John CC, Newton CR. Cerebral malaria: mechanisms of brain injury and strategies for improved neurocognitive outcome. Pediatr Res. 2010;68(4):267-74.
157. Riley EM, Wagner GE, Ofori MF, Wheeler JG, Akanmori BD, Tetteh K, et al. Lack of association between maternal antibody and protection of African infants from malaria infection. Infect Immun. 2000;68(10):5856-63.
158. Kassim OO, Ako-Anai KA, Torimiro SE, Hollowell GP, Okoye VC, Martin SK. Inhibitory factors in breastmilk, maternal and infant sera against in vitro growth of Plasmodium falciparum malaria parasite. J Trop Pediatr. 2000;46(2):92-6.
159. Ogouyemi-Hounto A, Damien G, Deme AB, Ndam NT, Assohou C, Tchonlin D, et al. Lack of artemisinin resistance in Plasmodium falciparum in northwest Benin after 10 years of use of artemisinin-based combination therapy. Parasite. 2016;23.
160. Davis TME, Moore BR, Salman S, Page-Sharp M, Batty KT, Manning L. Use of quantitative pharmacology tools to improve malaria treatments. Expert Rev Clin Phar. 2016;9(2):303-16.

161. Amaratunga C, Lim P, Suon S, Sreng S, Mao S, Sopha C, et al. Dihydroartemisinin-piperaquine resistance in Plasmodium falciparum malaria in Cambodia: a multisite prospective cohort study. Lancet Infect Dis. 2016;16(3):357-65.
162. Adjei A, Narh-Bana S, Amu A, Kukula V, Nagai RA, Owusu-Agyei S, et al. Treatment outcomes in a safety observational study of dihydroartemisinin/piperaquine (Eurartesim (R)) in the treatment of uncomplicated malaria at public health facilities in four African countries. Malaria J. 2016;15.
163. Dorkenoo AM, Yehadji D, Agbo YM, Layibo Y, Agbeko F, Adjeloh P, et al. Therapeutic efficacy trial of artemisinin-based combination therapy for the treatment of uncomplicated malaria and investigation of mutations in k13 propeller domain in Togo, 2012-2013. Malaria J. 2016;15.
164. Sowunmi A, Akano K, Ayede AI, Ntadom G, Adewoye EO, Fatunmbi B, et al. Therapeutic efficacy and effects of artesunate-amodiaquine and artemether-lumefantrine on malaria-associated anaemia in Nigerian children aged two years and under. Infect Dis Poverty. 2016;5.
165. World Health Organisation WHO. Guidelines for the treatment of malaria. Geneva: World Health Organization; 2015.
166. Falade C, Makanga M, Premji Z, Ortmann CE, Stockmeyer M, de Palacios PI. Efficacy and safety of artemether-lumefantrine (Coartem) tablets (six-dose regimen) in African infants and children with acute, uncomplicated falciparum malaria. Trans R Soc Trop Med Hyg. 2005;99(6):459-67.
167. Makanga M, Premji Z, Falade C, Karbwang J, Mueller EA, Andriano K, et al. Efficacy and safety of the six-dose regimen of artemether-lumefantrine in pediatrics with uncomplicated Plasmodium falciparum malaria: a pooled analysis of individual patient data. Am J Trop Med Hyg. 2006;74(6):991-8.
168. Achan J, Tibenderana JK, Kyabayinze D, Wabwire Mangen F, Kamya MR, Dorsey G, et al. Effectiveness of quinine versus artemether-lumefantrine for treating uncomplicated falciparum malaria in Ugandan children: randomised trial. BMJ. 2009;339:b2763.
169. Faucher JF, Aubouy A, Adeothy A, Cottrell G, Doritchamou J, Gourmel B, et al. Comparison of sulfadoxine-pyrimethamine, unsupervised artemether-lumefantrine, and unsupervised artesunate-amodiaquine fixed-dose formulation for uncomplicated plasmodium falciparum malaria in Benin: a randomized effectiveness noninferiority trial. J Infect Dis. 2009;200(1):57-65.
170. Coartem®: Novartis Pharma; 2016 [Available from: http://www.coartem.com/content/nigeria/coartem.html.
171. Djimde A, Lefevre G. Understanding the pharmacokinetics of Coartem. Malar J. 2009;8 Suppl 1:S4.
172. Ezzet F, Mull R, Karbwang J. Population pharmacokinetics and therapeutic response of CGP 56697 (artemether+benflumetol) in malaria patients. Brit J Clin Pharmaco. 1998;46(6):553-61.
173. Piola P, Fogg C, Bajunirwe F, Biraro S, Grandesso F, Ruzagira E, et al. Supervised versus unsupervised intake of six-dose artemether-lumefantrine for treatment of acute, uncomplicated Plasmodium falciparum malaria in Mbarara, Uganda: a randomised trial. The Lancet. 2005;365(9469):1467-73.
174. WorldWide Antimalarial Resistance WAR. Artemether-lumefantrine treatment of uncomplicated Plasmodium falciparum malaria: a systematic review and meta-analysis of day 7 lumefantrine concentrations and therapeutic response using individual patient data. Bmc Med. 2015;13.
175. World Health Organisation WHO. Global tuberculosis report WHO; 2016.
176. Niemi M, Backman JT, Fromm MF, Neuvonen PJ, Kivistö KT. Pharmacokinetic interactions with rifampicin: Clinical relevance. Clinical Pharmacokinetics. 2003;42(9):819-50.
177. FDA. Drug Development and Drug Interactions: Table of Substrates, Inhibitors and Inducers. 2006 [cited 2016 5th September]. Available from:

http://www.fda.gov/Drugs/DevelopmentApprovalProcess/DevelopmentResources/DrugInteractionsLabeling/ucm093664.htm#4.
178. Wen X, Wang JS, Neuvonen PJ, Backman JT. Isoniazid is a mechanism-based inhibitor of cytochrome P450 1A2, 2A6, 2C19 and 3A4 isoforms in human liver microsomes. Eur J Clin Pharmacol. 2002;57(11):799-804.
179. Valadas E, Gomes A, Sutre A, Brilha S, Wete A, Hänscheid T, et al. Tuberculosis with malaria or HIV co-infection in a large hospital in Luanda, Angola2013.
180. Lamorde M, Byakika-Kibwika P, Mayito J, Nabukeera L, Ryan M, Hanpithakpong W, et al. Lower artemether, dihydroartemisinin and lumefantrine concentrations during rifampicin-based tuberculosis treatment. Aids. 2013;27(6):961-5.
181. Norvartis. Coartem: International Package Leaflet 2012 [Available from: http://www.coartem.com/downloads/Coartem-IPL-DEC-2012.pdf.
182. Parikh S, Kajubi R, Huang L, Ssebuliba J, Kiconco S, Gao Q, et al. Antiretroviral Choice for HIV Impacts Antimalarial Exposure and Treatment Outcomes in Ugandan Children. Clin Infect Dis. 2016;63(3):414-22.
183. Huang L, Gao Q, Aweeka F. ART Choice Impacts Antimalarial Exposure and Treatment Outcomes in Ugandan Children. In Abstracts of the Annual Conference on Retroviruses and Opportunistic Infections, Seattle, Washington, , USA, February 23–26 2015;Abstract 513.
184. Gasasira AF, Kamya MR, Achan J, Mebrahtu T, Kalyango JN, Ruel T, et al. High risk of neutropenia in HIV-infected children following treatment with artesunate plus amodiaquine for uncomplicated malaria in Uganda. Clin Infect Dis. 2008;46(7):985-91.
185. Laventhal N, Tarini BA, Lantos J. Ethical Issues in Neonatal and Pediatric Clinical Trials. Pediatric Clinics of North America. 2012;59(5):1205-20.
186. Kimland E, Odlind V. Off-label drug use in pediatric patients. Clinical pharmacology and therapeutics. 2012;91(5):796-801.
187. EMA. Clinical investigation of medicinal products in the paediatric population. ICH Topic E11. 2001 [Available from: http://www.ema.europa.eu/docs/en_GB/document_library/Scientific_guideline/2009/09/WC500002926.pdf.
188. Strolin Benedetti M, Whomsley R, Baltes EL. Differences in absorption, distribution, metabolism and excretion of xenobiotics between the paediatric and adult populations. Expert Opin Drug Metab Toxicol. 2005;1(3):447-71.
189. Jong Gt. Pediatric Development: Physiology. Enzymes, Drug Metabolism, Pharmacokinetics and Pharmacodynamics2014. 9-23 p.
190. Jong Gt. Pediatric Development: Physiology. Enzymes, Drug Metabolism, Pharmacokinetics and Pharmacodynamics. In: Bar-Shalom D, Rose K, editors. Pediatric Formulations: A Roadmap. New York, NY: Springer New York; 2014. p. 9-23.
191. Ahmad I, Nemet D, Eliakim A, Koeppel R, Grochow D, Coussens M, et al. Body composition and its components in preterm and term newborns: A cross-sectional, multimodal investigation. Am J Hum Biol. 2010;22(1):69-75.
192. Ellis KJ, Shypailo RJ, Abrams SA, Wong WW. The reference child and adolescent models of body composition. A contemporary comparison. Ann N Y Acad Sci. 2000;904:374-82.
193. Fomon SJ, Nelson SE. Body composition of the male and female reference infants. Annu Rev Nutr. 2002;22:1-17.
194. . !!! INVALID CITATION !!! {Rylance, 1981 #193;Alcorn, 2003 #194;Jong, 2014 #442}.
195. Alcorn J, McNamara PJ. Pharmacokinetics in the newborn. Advanced Drug Delivery Reviews. 2003;55(5):667-86.
196. Kearns GL A-RS, Alander SW, Blowey DL, Leeder JS, Kauffman RE. Developmental pharmacology drug disposition, action, and therapy in infants and children. N Engl J Med. 2003;349(12):1157-67.
197. Huang NN, High RH. Comparison of serum levels following the administration of oral and parenteral preparations of penicillin to infants and children of various age groups. J Pediatr. 1953;42(6):657-8.

198. Windorfe.A, Kuenzer W, Urbanek R. Influence Of Age On Activity Of Acetylsalicylic Acid Esterase And Protein-Salicylate Binding. European Journal of Clinical Pharmacology. 1974;7(3):227-31.
199. Ehrnebo M, Agurell S, Jalling B, Boreus LO. AGE DIFFERENCES IN DRUG BINDING BY PLASMA PROTEINS - STUDIES ON HUMAN FOETUSES, NEONATES AND ADULTS. European Journal of Clinical Pharmacology. 1971;3(4):189-&.
200. Hines RN. The ontogeny of drug metabolism enzymes and implications for adverse drug events. Pharmacol Ther. 2008;118(2):250-67.
201. Bartelink IH, Rademaker CM, Schobben AF, van den Anker JN. Guidelines on paediatric dosing on the basis of developmental physiology and pharmacokinetic considerations. Clin Pharmacokinet. 2006;45(11):1077-97.
202. Salem F, Johnson TN, Barter ZE, Leeder JS, Rostami-Hodjegan A. Age related changes in fractional elimination pathways for drugs: assessing the impact of variable ontogeny on metabolic drug-drug interactions. J Clin Pharmacol. 2013;53(8):857-65.
203. Salem F, Rostami-Hodjegan A, Johnson TN. Do children have the same vulnerability to metabolic drug-drug interactions as adults? A critical analysis of the literature. J Clin Pharmacol. 2013;53(5):559-66.
204. Johnson TN, Zhou D, Bui KH. Development of physiologically based pharmacokinetic model to evaluate the relative systemic exposure to quetiapine after administration of IR and XR formulations to adults, children and adolescents. Biopharm Drug Dispos. 2014;35(6):341-52.
205. Johnson TN, Rostami-Hodjegan A, Tucker GT. Prediction of the clearance of eleven drugs and associated variability in neonates, infants and children. Clinical Pharmacokinetics. 2006;45(9):931-56.
206. Johnson TN, Thomson M. Intestinal metabolism and transport of drugs in children: the effects of age and disease. J Pediatr Gastroenterol Nutr. 2008;47(1):3-10.
207. Small BG, Wendt B, Jamei M, Johnson TN. Prediction of liver volume - a population-based approach to meta-analysis of paediatric, adult and geriatric populations - an update. Biopharm Drug Dispos. 2017;38(4):290-300.
208. White NJ, van Vugt M, Ezzet FD. Clinical Pharmacokinetics and Pharmacodynamics of Artemether-Lumefantrine. Clinical Pharmacokinetics. 1999;37(2):105-25.
209. Wishart DS, Knox C, Guo AC, Shrivastava S, Hassanali M, Stothard P, et al. DrugBank: a comprehensive resource for in silico drug discovery and exploration. Nucleic acids research. 2006;34(Database issue):D668-72.
210. Avery MA, Bonk JD, Chong WK, Mehrotra S, Miller R, Milhous W, et al. Structure-activity relationships of the antimalarial agent artemisinin. 2. Effect of heteroatom substitution at O-11: synthesis and bioassay of N-alkyl-11-aza-9-desmethylartemisinins. J Med Chem. 1995;38(26):5038-44.
211. Huang LS, Li XH, Marzan F, Lizak PS, Aweeka FT. Determination of lumefantrine in small-volume human plasma by LC-MS/MS: using a deuterated lumefantrine to overcome matrix effect and ionization saturation. Bioanalysis. 2012;4(2):157-66.
212. Colussi D, Parisot C, Legay F, Lefèvre G. Binding of artemether and lumefantrine to plasma proteins and erythrocytes. European Journal of Pharmaceutical Sciences. 1999;9(1):9-16.
213. Zaloumis S, Humberstone A, Charman SA, Price RN, Moehrle J, Gamo-Benito J, et al. Assessing the utility of an anti-malarial pharmacokinetic-pharmacodynamic model for aiding drug clinical development. Malar J. 2012;11:303.
214. NCBI. PubChem Compound Database 2017 [Available from: https://pubchem.ncbi.nlm.nih.gov/compound/68911.
215. Kotila OA, Olaniyi OO, Adegoke AO, Babalola CP. Experimental determination of the physicochemical properties of lumefantrine. African journal of medicine and medical sciences. 2013;42(3):209-14.

216. Siccardi M, Olagunju A, Seden K, Ebrahimjee F, Rannard S, Back D, et al. Use of a physiologically-based pharmacokinetic model to simulate artemether dose adjustment for overcoming the drug-drug interaction with efavirenz. In Silico Pharmacol. 2013;1:4.
217. Winiwarter S, Bonham NM, Ax F, Hallberg A, Lennernas H, Karlen A. Correlation of human jejunal permeability (in vivo) of drugs with experimentally and theoretically derived parameters. A multivariate data analysis approach. J Med Chem. 1998;41(25):4939-49.
218. Musther H, Gill KL, Chetty M, Rostami-Hodjegan A, Rowland M, Jamei M. Are Physiologically Based Pharmacokinetic Models Reporting the Right C(max)? Central Venous Versus Peripheral Sampling Site. Aaps J. 2015;17(5):1268-79.
219. Proctor NJ, Tucker GT, Rostami-Hodjegan A. Predicting drug clearance from recombinantly expressed CYPs: intersystem extrapolation factors. Xenobiotica. 2004;34(2):151-78.
220. Lefevre G, Carpenter P, Souppart C, Schmidli H, McClean M, Stypinski D. Pharmacokinetics and electrocardiographic pharmacodynamics of artemether-lumefantrine (Riamet (R)) with concomitant administration of ketoconazole in healthy subjects. Brit J Clin Pharmaco. 2002;54(5):485-92.
221. Ashley EA, Stepniewska K, Lindegardh N, McGready R, Annerberg A, Hutagalung R, et al. Pharmacokinetic study of artemether-lumefantrine given once daily for the treatment of uncomplicated multidrug-resistant falciparum malaria. Trop Med Int Health. 2007;12(2):201-8.
222. Dennison TJ, Smith JC, Badhan RK, Mohammed AR. Fixed-dose combination orally disintegrating tablets to treat cardiovascular disease: formulation, in vitro characterization and physiologically based pharmacokinetic modeling to assess bioavailability. Drug design, development and therapy. 2017;11:811-26.
223. George M, Shewade DG, Kumar SV, Adithan C. Effect of anti-tuberculosis therapy on polymorphic drug metabolizing enzyme CYP2C9 using phenytoin as a probe drug. Indian journal of pharmacology. 2012;44(4):485-8.
224. Kay L, Kampmann JP, Svendsen TL, Vergman B, Hansen JE, Skovsted L, et al. Influence of rifampicin and isoniazid on the kinetics of phenytoin. Brit J Clin Pharmaco. 1985;20(4):323-6.
225. Wanwimolruk S, Kang W, Coville P, Viriyayudhakorn S, Thitiarchakul S. Marked enhancement by rifampicin and lack of effect of isoniazid on the elimination of quinine in man. Brit J Clin Pharmaco. 1995;40(1):87-91.
226. Lamorde M, Byakika-Kibwika P, Mayito J, Nabukeera L, Ryan M, Hanpithakpong W, et al. Lower artemether, dihydroartemisinin and lumefantrine concentrations during rifampicin-based tuberculosis treatment. Aids. 2013;27:961-5.
227. Sager JE, Yu J, Ragueneau-Majlessi I, Isoherranen N. Physiologically Based Pharmacokinetic (PBPK) Modeling and Simulation Approaches: A Systematic Review of Published Models, Applications, and Model Verification. Drug Metabolism and Disposition. 2015;43(11):1823-37.
228. Administration UFaD. Summary Minutes of the Advisory Committee for Pharmaceutical Science and Clinical Pharmacology 2012 [Available from: https://wayback.archive-it.org/7993/20170403224110/https://www.fda.gov/AdvisoryCommittees/CommitteesMeetingMaterials/Drugs/AdvisoryCommitteeforPharmaceuticalScienceandClinicalPharmacology/ucm286697.htm.
229. Rohatgi AW. Version 3.4. 2014. 2014.
230. Lefevre G, Bhad P, Jain JP, Kalluri S, Cheng Y, Dave H, et al. Evaluation of two novel tablet formulations of artemether-lumefantrine (Coartem (R)) for bioequivalence in a randomized, open-label, two-period study. Malaria J. 2013;12.
231. Lefevre G, Carpenter P, Souppart C, Schmidli H, McClean M, Stypinski D. Pharmacokinetics and electrocardiographic pharmacodynamics of artemether-lumefantrine (Riamet) with concomitant administration of ketoconazole in healthy subjects. Br J Clin Pharmacol. 2002;54(5):485-92.
232. Gaohua L, Wedagedera J, Small BG, Almond L, Romero K, Hermann D, et al. Development of a Multicompartment Permeability-Limited Lung PBPK Model and Its Application

in Predicting Pulmonary Pharmacokinetics of Antituberculosis Drugs. CPT: Pharmacometrics & Systems Pharmacology. 2015;4(10):605-13.
233. Djimde AA, Tekete M, Abdulla S, Lyimo J, Bassat Q, Mandomando I, et al. Pharmacokinetic and Pharmacodynamic Characteristics of a New Pediatric Formulation of Artemether-Lumefantrine in African Children with Uncomplicated Plasmodium falciparum Malaria (vol 55, pg 3994, 2011). Antimicrob Agents Ch. 2012;56(10):5429-.
234. Bassat Q, Gonzalez R, Machevo S, Nahum A, Lyimo J, Maiga H, et al. Similar efficacy and safety of artemether-lumefantrine (Coartem (R)) in African infants and children with uncomplicated falciparum malaria across different body weight ranges. Malaria J. 2011;10.
235. Hietala SF, Martensson A, Ngasala B, Dahlstrom S, Lindegardh N, Annerberg A, et al. Population pharmacokinetics and pharmacodynamics of artemether and lumefantrine during combination treatment in children with uncomplicated falciparum malaria in Tanzania. Antimicrob Agents Chemother. 2010;54(11):4780-8.
236. Mayxay M, Khanthavong M, Lindegardh N, Keola S, Barends M, Pongvongsa T, et al. Randomized comparison of chloroquine plus sulfadoxine-pyrimethamine versus artesunate plus mefloquine versus artemether-lumefantrine in the treatment of uncomplicated falciparum malaria in the Lao People's Democratic Republic. Clin Infect Dis. 2004;39(8):1139-47.
237. Schramm B, Valeh P, Baudin E, Mazinda CS, Smith R, Pinoges L, et al. Efficacy of artesunate-amodiaquine and artemether-lumefantrine fixed-dose combinations for the treatment of uncomplicated Plasmodium falciparum malaria among children aged six to 59 months in Nimba County, Liberia: an open-label randomized non-inferiority trial. Malaria J. 2013;12(1):251.
238. Ngasala BE, Malmberg M, Carlsson AM, Ferreira PE, Petzold MG, Blessborn D, et al. Effectiveness of artemether-lumefantrine provided by community health workers in under-five children with uncomplicated malaria in rural Tanzania: an open label prospective study. Malaria J. 2011;10(1):64.
239. Borrmann S, Sallas WM, Machevo S, González R, Björkman A, Mårtensson A, et al. The effect of food consumption on lumefantrine bioavailability in African children receiving artemether–lumefantrine crushed or dispersible tablets (Coartem®) for acute uncomplicated Plasmodium falciparum malaria. Tropical Medicine & International Health. 2010;15(4):434-41.
240. Checchi F, Piola P, Fogg C, Bajunirwe F, Biraro S, Grandesso F, et al. Supervised versus unsupervised antimalarial treatment with six-dose artemether-lumefantrine: pharmacokinetic and dosage-related findings from a clinical trial in Uganda. Malaria J. 2006;5(1):59.
241. Salman S, Page-Sharp M, Griffin S, Kose K, Siba PM, Ilett KF, et al. Population Pharmacokinetics of Artemether, Lumefantrine, and Their Respective Metabolites in Papua New Guinean Children with Uncomplicated Malaria. Antimicrob Agents Ch. 2011;55(11):5306-13.
242. Tchaparian E, Sambol NC, Arinaitwe E, McCormack SA, Bigira V, Wanzira H, et al. Population Pharmacokinetics and Pharmacodynamics of Lumefantrine in Young Ugandan Children Treated With Artemether-Lumefantrine for Uncomplicated Malaria. J Infect Dis. 2016;214(8):1243-51.
243. Ezzet F, van Vugt M, Nosten F, Looareesuwan S, White NJ. Pharmacokinetics and pharmacodynamics of lumefantrine (benflumetol) in acute falciparum malaria. Antimicrob Agents Ch. 2000;44(3):697-704.
244. Bindschedler M, Lefevre G, Degan P, Sioufi A. Comparison of the cardiac effects of the antimalarials co-artemether and halofantrine in healthy participants. Am J Trop Med Hyg. 2002;66(3):293-8.
245. Huisinga W, Solms A, Fronton L, Pilari S. Modeling Interindividual Variability in Physiologically Based Pharmacokinetics and Its Link to Mechanistic Covariate Modeling. CPT: Pharmacometrics & Systems Pharmacology. 2012;1(9):e4.
246. McLeay SC, Morrish GA, Kirkpatrick CM, Green B. The relationship between drug clearance and body size: systematic review and meta-analysis of the literature published from 2000 to 2007. Clin Pharmacokinet. 2012;51(5):319-30.

247. Obach RS, Baxter JG, Liston TE, Silber BM, Jones BC, MacIntyre F, et al. The prediction of human pharmacokinetic parameters from preclinical and in vitro metabolism data. The Journal of pharmacology and experimental therapeutics. 1997;283(1):46-58.
248. Sager JE, Yu J, Ragueneau-Majlessi I, Isoherranen N. Physiologically Based Pharmacokinetic (PBPK) Modeling and Simulation Approaches: A Systematic Review of Published Models, Applications, and Model Verification. Drug metabolism and disposition: the biological fate of chemicals. 2015;43(11):1823-37.
249. Pahlman I, Edholm M, Kankaanranta S, Odell M-L. Pharmacokinetics of Susalimod, a Highly Biliary-excreted Sulphasalazine Analogue, in Various Species. Nonpredictable Human Clearance by Allometric Scaling. Pharmacy and Pharmacology Communications. 1998;4(10):493-8.
250. Lave T, Portmann R, Schenker G, Gianni A, Guenzi A, Girometta MA, et al. Interspecies pharmacokinetic comparisons and allometric scaling of napsagatran, a low molecular weight thrombin inhibitor. The Journal of pharmacy and pharmacology. 1999;51(1):85-91.
251. Johnson TN. The problems in scaling adult drug doses to children. Archives of disease in childhood. 2008;93(3):207-11.
252. Hayes DJ, van Buuren S, ter Kuile FO, Stasinopoulos DM, Rigby RA, Terlouw DJ. Developing regional weight-for-age growth references for malaria-endemic countries to optimize age-based dosing of antimalarials. Bulletin of the World Health Organization. 2015;93(2):74-83.
253. Edginton AN, Willmann S. Physiology-based versus allometric scaling of clearance in children: a comparison. Age [years]. 2006;10:100.
254. Jamei M. Recent Advances in Development and Application of Physiologically-Based Pharmacokinetic (PBPK) Models: a Transition from Academic Curiosity to Regulatory Acceptance. Current pharmacology reports. 2016;2:161-9.
255. Rowland M, Peck C, Tucker G. Physiologically-based pharmacokinetics in drug development and regulatory science. Annual review of pharmacology and toxicology. 2011;51:45-73.
256. Zhao P, Rowland M, Huang SM. Best practice in the use of physiologically based pharmacokinetic modeling and simulation to address clinical pharmacology regulatory questions. Clinical pharmacology and therapeutics. 2012;92(1):17-20.
257. Wagner C, Zhao P, Pan Y, Hsu V, Grillo J, Huang SM, et al. Application of Physiologically Based Pharmacokinetic (PBPK) Modeling to Support Dose Selection: Report of an FDA Public Workshop on PBPK. CPT: Pharmacometrics & Systems Pharmacology. 2015;4(4):226-30.
258. Leong R, Vieira MLT, Zhao P, Mulugeta Y, Lee CS, Huang SM, et al. Regulatory Experience With Physiologically Based Pharmacokinetic Modeling for Pediatric Drug Trials. Clinical Pharmacology & Therapeutics. 2012;91(5):926-31.
259. Yoshida K, Budha N, Jin JY. Impact of Physiologically Based Pharmacokinetic Models on Regulatory Reviews and Product Labels: Frequent Utilization in the Field of Oncology. Clinical Pharmacology & Therapeutics. 2017;101(5):597-602.
260. Worldwide Antimalarial Resistance Network ALDISG. The effect of dose on the antimalarial efficacy of artemether–lumefantrine: a systematic review and pooled analysis of individual patient data. The Lancet Infectious Diseases. 2015;15(6):692-702.
261. Palumbo P, Violari A, Lindsey JC, Hughes M, Jean-Philippe P, Mofenson L. NVP–-based ART among HIV+ infants in resource limited settings: the IMPAACT1060 trial. 8th Conference on Retroviruses and Opportunistic Infections; 27/02/2011; Boston2011.
262. Hoglund RM, Byakika-Kibwika P, Lamorde M, Merry C, Ashton M, Hanpithakpong W, et al. Artemether-lumefantrine co-administration with antiretrovirals: population pharmacokinetics and dosing implications. Brit J Clin Pharmaco. 2015;79(4):636-49.
263. Wanwimolruk S, Denton JR. Plasma Protein Binding of Quinine: Binding to Human Serum Albumin, α1-Acid Glycoprotein and Plasma from Patients with Malaria. Journal of Pharmacy and Pharmacology. 1992;44(10):806-11.

264. Silamut K, Molunto P, Ho M, Davis TM, White NJ. Alpha 1-acid glycoprotein (orosomucoid) and plasma protein binding of quinine in falciparum malaria. Brit J Clin Pharmaco. 1991;32(3):311-5.
265. William T, Menon J, Rajahram G, Chan L, Ma G, Donaldson S, et al. Severe Plasmodium knowlesi Malaria in a Tertiary Care Hospital, Sabah, Malaysia. Emerging Infectious Diseases. 2011;17(7):1248-55.
266. Bruxvoort K, Goodman C, Kachur SP, Schellenberg D. How Patients Take Malaria Treatment: A Systematic Review of the Literature on Adherence to Antimalarial Drugs. Plos One. 2014;9(1):e84555.
267. du Plessis LH, Govender K, Denti P, Wiesner L. In vivo efficacy and bioavailability of lumefantrine: Evaluating the application of Pheroid technology. European journal of pharmaceutics and biopharmaceutics : official journal of Arbeitsgemeinschaft fur Pharmazeutische Verfahrenstechnik eV. 2015;97(Pt A):68-77.
268. Das D, Grais RF, Okiro EA, Stepniewska K, Mansoor R, van der Kam S, et al. Complex interactions between malaria and malnutrition: a systematic literature review. Bmc Med. 2018;16.
269. National Library of Medicine. Bethesda (MD)2017 [Available from: ClinicalTrials.gov.
270. Schantz-Dunn J, Nour NM. Malaria and pregnancy: a global health perspective. Rev Obstet Gynecol. 2009;2(3):186-92.
271. Consortium M. The challenges 2017 [Available from: http://www.malariaconsortium.org/pages/malaria_challenges.htm.
272. Murray CK, Bennett JW. Rapid Diagnosis of Malaria. Interdisciplinary Perspectives on Infectious Diseases. 2009;2009:415953.
273. van Eijk AM, Hill J, Noor AM, Snow RW, ter Kuile FO. Prevalence of malaria infection in pregnant women compared with children for tracking malaria transmission in sub-Saharan Africa: a systematic review and meta-analysis. Lancet Glob Health. 2015;3(10):e617-28.
274. Nosten F, McGready R, d'Alessandro U, Bonell A, Verhoeff F, Menendez C, et al. Antimalarial drugs in pregnancy: a review. Curr Drug Saf. 2006;1(1):1-15.
275. Kayentao K, Garner P, van Eijk AM, Naidoo I, Roper C, Mulokozi A, et al. Intermittent preventive therapy for malaria during pregnancy using 2 vs 3 or more doses of sulfadoxine-pyrimethamine and risk of low birth weight in Africa: systematic review and meta-analysis. JAMA. 2013;309(6):594-604.
276. Kakuru A, Jagannathan P, Muhindo MK, Natureeba P, Awori P, Nakalembe M, et al. Dihydroartemisinin-Piperaquine for the Prevention of Malaria in Pregnancy. N Engl J Med. 2016;374(10):928-39.
277. Desai M, Gutman J, L'Lanziva A, Otieno K, Juma E, Kariuki S, et al. Intermittent screening and treatment or intermittent preventive treatment with dihydroartemisinin-piperaquine versus intermittent preventive treatment with sulfadoxine-pyrimethamine for the control of malaria during pregnancy in western Kenya: an open-label, three-group, randomised controlled superiority trial. Lancet. 2015;386(10012):2507-19.
278. Poespoprodjo JR, Fobia W, Kenangalem E, Lampah DA, Sugiarto P, Tjitra E, et al. Dihydroartemisinin-piperaquine treatment of multidrug resistant falciparum and vivax malaria in pregnancy. Plos One. 2014;9(1):e84976.
279. Zongo I, Some FA, Somda SA, Parikh S, Rouamba N, Rosenthal PJ, et al. Efficacy and day 7 plasma piperaquine concentrations in African children treated for uncomplicated malaria with dihydroartemisinin-piperaquine. Plos One. 2014;9(8):e103200.
280. Price RN, Hasugian AR, Ratcliff A, Siswantoro H, Purba HL, Kenangalem E, et al. Clinical and pharmacological determinants of the therapeutic response to dihydroartemisinin-piperaquine for drug-resistant malaria. Antimicrob Agents Chemother. 2007;51(11):4090-7.
281. Tarning J, Rijken MJ, McGready R, Phyo AP, Hanpithakpong W, Day NP, et al. Population pharmacokinetics of dihydroartemisinin and piperaquine in pregnant and nonpregnant women with uncomplicated malaria. Antimicrob Agents Chemother. 2012;56(4):1997-2007.

282. Benjamin JM, Moore BR, Salman S, Page-Sharp M, Tawat S, Yadi G, et al. Population pharmacokinetics, tolerability, and safety of dihydroartemisinin-piperaquine and sulfadoxine-pyrimethamine-piperaquine in pregnant and nonpregnant Papua New Guinean women. Antimicrob Agents Chemother. 2015;59(7):4260-71.
283. Hayes DJ, van Buuren S, ter Kuile FO, Stasinopoulos DM, Rigby RA, Terlouw DJ. Developing regional weight-for-age growth references for malaria-endemic countries to optimize age-based dosing of antimalarials. Bull World Health Organ. 2015;93(2):74-83.
284. Brentlinger PE, Behrens CB, Micek MA. Challenges in the concurrent management of malaria and HIV in pregnancy in sub-Saharan Africa. Lancet Infect Dis. 2006;6(2):100-11.
285. Fichtenbaum CJ, Gerber JG. Interactions between antiretroviral drugs and drugs used for the therapy of the metabolic complications encountered during HIV infection. Clin Pharmacokinet. 2002;41(14):1195-211.
286. Renjifo B, van Wyk J, Salem AH, Bow D, Ng J, Norton M. Pharmacokinetic enhancement in HIV antiretroviral therapy: a comparison of ritonavir and cobicistat. AIDS reviews. 2015;17(1):37-46.
287. Horita Y, Doi N. Comparative study of the effects of antituberculosis drugs and antiretroviral drugs on cytochrome P450 3A4 and P-glycoprotein. Antimicrob Agents Chemother. 2014;58(6):3168-76.
288. Kajubi R, Huang L, Jagannathan P, Chamankhah N, Were M, Ruel T, et al. Antiretroviral therapy with efavirenz accentuates pregnancy-associated reduction of dihydroartemisinin-piperaquine exposure during malaria chemoprevention. Clinical pharmacology and therapeutics. 2017;102(3):520-8.
289. Kayentao K, Guirou EA, Doumbo OK, Venkatesan M, Plowe CV, Parsons TL, et al. Preliminary study of quinine pharmacokinetics in pregnant women with malaria-HIV co-infection. Am J Trop Med Hyg. 2014;90(3):530-4.
290. Seden K, Gibbons S, Marzolini C, Schapiro JM, Burger DM, Back DJ, et al. Development of an evidence evaluation and synthesis system for drug-drug interactions, and its application to a systematic review of HIV and malaria co-infection. Plos One. 2017;12(3):e0173509.
291. Ban Ke A, Greupink R, Abduljal K. Drug Dosing in Pregnant Women: Challenges and Opportunities in Using Physiologically Based Pharmacokinetic Modeling and Simulations. CPT Pharmacometrics Syst Pharmacol. 2018;7(2):103-10.
292. Colbers A, Molto J, Ivanovic J, Kabeya K, Hawkins D, Gingelmaier A, et al. Pharmacokinetics of total and unbound darunavir in HIV-1-infected pregnant women. J Antimicrob Chemother. 2015;70(2):534-42.
293. Olagunju A, Bolaji O, Amara A, Else L, Okafor O, Adejuyigbe E, et al. Pharmacogenetics of pregnancy-induced changes in efavirenz pharmacokinetics. Clinical pharmacology and therapeutics. 2015;97(3):298-306.
294. Kreitchmann R, Best BM, Wang J, Stek A, Caparelli E, Watts DH, et al. Pharmacokinetics of an increased atazanavir dose with and without tenofovir during the third trimester of pregnancy. J Acquir Immune Defic Syndr. 2013;63(1):59-66.
295. Costantine MM. Physiologic and pharmacokinetic changes in pregnancy. Front Pharmacol. 2014;5:65.
296. Feghali M, Venkataramanan R, Caritis S. Pharmacokinetics of drugs in pregnancy. Semin Perinatol. 2015;39(7):512-9.
297. Abduljalil K, Furness P, Johnson TN, Rostami-Hodjegan A, Soltani H. Anatomical, physiological and metabolic changes with gestational age during normal pregnancy: a database for parameters required in physiologically based pharmacokinetic modelling. Clin Pharmacokinet. 2012;51(6):365-96.
298. Jeong H. Altered drug metabolism during pregnancy: hormonal regulation of drug-metabolizing enzymes. Expert Opin Drug Metab Toxicol. 2010;6(6):689-99.
299. Fotopoulou C, Kretz R, Bauer S, Schefold JC, Schmitz B, Dudenhausen JW, et al. Prospectively assessed changes in lamotrigine-concentration in women with epilepsy during pregnancy, lactation and the neonatal period. Epilepsy Res. 2009;85(1):60-4.

300. Ke AB, Rostami-Hodjegan A, Zhao P, Unadkat JD. Pharmacometrics in pregnancy: An unmet need. Annual review of pharmacology and toxicology. 2014;54:53-69.
301. Hanley MJ, Abernethy DR, Greenblatt DJ. Effect of obesity on the pharmacokinetics of drugs in humans. Clin Pharmacokinet. 2010;49(2):71-87.
302. Shimoda M, Kokue E, Hayama T, Vree TB. Effect of albumin distribution. A simulation analysis of the effect of altered albumin distribution on the apparent volume of distribution and apparent elimination rate constant of drugs. Pharm Weekbl Sci. 1989;11(3):87-91.
303. Schmidt S, Gonzalez D, Derendorf H. Significance of protein binding in pharmacokinetics and pharmacodynamics. J Pharm Sci. 2010;99(3):1107-22.
304. van Erp NP, van Herpen CM, de Wit D, Willemsen A, Burger DM, Huitema AD, et al. A Semi-Physiological Population Model to Quantify the Effect of Hematocrit on Everolimus Pharmacokinetics and Pharmacodynamics in Cancer Patients. Clin Pharmacokinet. 2016;55(11):1447-56.
305. Goselle NO. Albumin Level Among HIV/AIDS-Patients in Jos, Nigeria. J Med Sci. 2007;7(7):1187-91.
306. Newton PN, Stepniewska K, Dondorp A, Silamut K, Chierakul W, Krishna S, et al. Prognostic indicators in adults hospitalized with falciparum malaria in Western Thailand. Malar J. 2013;12:229.
307. Gaohua L, Abduljalil K, Jamei M, Johnson TN, Rostami-Hodjegan A. A pregnancy physiologically based pharmacokinetic (p-PBPK) model for disposition of drugs metabolized by CYP1A2, CYP2D6 and CYP3A4. Br J Clin Pharmacol. 2012;74(5):873-85.
308. Sharma RP, Schuhmacher M, Kumar V. The development of a pregnancy PBPK Model for Bisphenol A and its evaluation with the available biomonitoring data. Sci Total Environ. 2018;624:55-68.
309. Ahmed T, Sharma P, Gautam A, Varshney B, Kothari M, Ganguly S, et al. Safety, tolerability, and single- and multiple-dose pharmacokinetics of piperaquine phosphate in healthy subjects. J Clin Pharmacol. 2008;48(2):166-75.
310. Sim IK, Davis TM, Ilett KF. Effects of a high-fat meal on the relative oral bioavailability of piperaquine. Antimicrob Agents Chemother. 2005;49(6):2407-11.
311. Staehli Hodel EM, Guidi M, Zanolari B, Mercier T, Duong S, Kabanywanyi AM, et al. Population pharmacokinetics of mefloquine, piperaquine and artemether-lumefantrine in Cambodian and Tanzanian malaria patients. Malar J. 2013;12(1):235.
312. Liu C, Zhang R, Hong X, Huang T, Mi S, Wang N. Pharmacokinetics of piperaquine after single and multiple oral administrations in healthy volunteers. Yakugaku zasshi : Journal of the Pharmaceutical Society of Japan. 2007;127(10):1709-14.
313. Rijken MJ, McGready R, Phyo AP, Lindegardh N, Tarning J, Laochan N, et al. Pharmacokinetics of dihydroartemisinin and piperaquine in pregnant and nonpregnant women with uncomplicated falciparum malaria. Antimicrob Agents Chemother. 2011;55(12):5500-6.
314. Tarning J, Lindegardh N, Lwin KM, Annerberg A, Kiricharoen L, Ashley E, et al. Population pharmacokinetic assessment of the effect of food on piperaquine bioavailability in patients with uncomplicated malaria. Antimicrob Agents Chemother. 2014;58(4):2052-8.
315. Lee TM, Huang L, Johnson MK, Lizak P, Kroetz D, Aweeka F, et al. In vitro metabolism of piperaquine is primarily mediated by CYP3A4. Xenobiotica. 2012;42(11):1088-95.
316. NCBI. 2017 [cited 2017 1st February]. PubChem Compound Database]. Available from: https://pubchem.ncbi.nlm.nih.gov/compound/122262.
317. Kjellin LL, Dorsey G, Rosenthal PJ, Aweeka F, Huang L. Determination of the antimalarial drug piperaquine in small volume pediatric plasma samples by LC–MS/MS. Bioanalysis. 2014;6(23):3081-9.
318. Zaloumis S, Humberstone A, Charman SA, Price RN, Moehrle J, Gamo-Benito J, et al. Assessing the utility of an anti-malarial pharmacokinetic-pharmacodynamic model for aiding drug clinical development. Malar J. 2012;11(1):303.

319. Kwena AW, J.; Mambo, F. Possible Biochemical Markers in Plasmodium falciparum Malaria Infected Children with or without Malnutrition at Webuye and Eldoret, Western Kenya. Advances in Bioresearch. 2012;3(2):49-54.
320. Friedman MJ. Control of malaria virulence by alpha 1-acid glycoprotein (orosomucoid), an acute-phase (inflammatory) reactant. Proceedings of the National Academy of Sciences of the United States of America. 1983;80(17):5421-4.
321. Hoglund RM, Adam I, Hanpithakpong W, Ashton M, Lindegardh N, Day NP, et al. A population pharmacokinetic model of piperaquine in pregnant and non-pregnant women with uncomplicated Plasmodium falciparum malaria in Sudan. Malar J. 2012;11:398.
322. Tarning J, Ashley EA, Lindegardh N, Stepniewska K, Phaiphun L, Day NPJ, et al. Population Pharmacokinetics of Piperaquine after Two Different Treatment Regimens with Dihydroartemisinin-Piperaquine in Patients with Plasmodium falciparum Malaria in Thailand. Antimicrob Agents Ch. 2008;52(3):1052-61.
323. Othman AA. Estimation of Complete Blood Count and Platelet Indices In Sudanese patients with Malaria. Sudan University Of Science And Technology: Sudan University; 2014.
324. Tarning J, Kloprogge F, Dhorda M, Jullien V, Nosten F, White NJ, et al. Pharmacokinetic properties of artemether, dihydroartemisinin, lumefantrine, and quinine in pregnant women with uncomplicated plasmodium falciparum malaria in Uganda. Antimicrob Agents Chemother. 2013;57(10):5096-103.
325. Silamut K, Molunto P, Ho M, Davis TM, White NJ. Alpha 1-acid glycoprotein (orosomucoid) and plasma protein binding of quinine in falciparum malaria. British journal of clinical pharmacology. 1991;32(3):311-5.
326. Abdagalil ME, N. Effect of falciparum malaria on some plasma proteins in males: With special reference to the levels of testosterone and cortisol. African Journal of Biochemistry Research. 2009;3(11):349-55.
327. Senn N, Maraga S, Sie A, Rogerson SJ, Reeder JC, Siba P, et al. Population hemoglobin mean and anemia prevalence in Papua New Guinea: new metrics for defining malaria endemicity? Plos One. 2010;5(2):e9375.
328. Rosales FJ, Topping JD, Smith JE, Shankar AH, Ross AC. Relation of serum retinol to acute phase proteins and malarial morbidity in Papua New Guinea children. The American journal of clinical nutrition. 2000;71(6):1582-8.
329. Kajubi R, Huang L, Jagannathan P, Chamankhah N, Were M, Ruel T, et al. Antiretroviral therapy with efavirenz accentuates pregnancy-associated reduction of dihydroartemisinin-piperaquine exposure during malaria chemoprevention. Clin Pharmacol Ther. 2017:n/a-n/a.
330. Sagaki P, Thanachartwet V, Desakorn V, Sahassananda D, Chamnanchanunt S, Chierakul W, et al. Clinical factors for severity of Plasmodium falciparum malaria in hospitalized adults in Thailand. Plos One. 2013;8(8):e71503.
331. Hung TY, Davis TM, Ilett KF, Karunajeewa H, Hewitt S, Denis MB, et al. Population pharmacokinetics of piperaquine in adults and children with uncomplicated falciparum or vivax malaria. Brit J Clin Pharmaco. 2004;57(3):253-62.
332. Tarning J, Lindegårdh N, Annerberg A, Singtoroj T, Day NPJ, Ashton M, et al. Pitfalls in Estimating Piperaquine Elimination. Antimicrob Agents Ch. 2005;49(12):5127-8.
333. . !!! INVALID CITATION !!! (13, 35, 42).
334. White NJ. Pharmacokinetic and pharmacodynamic considerations in antimalarial dose optimization. Antimicrob Agents Chemother. 2013;57(12):5792-807.
335. Walpole SC, Prieto-Merino D, Edwards P, Cleland J, Stevens G, Roberts I. The weight of nations: an estimation of adult human biomass. BMC public health. 2012;12:439.
336. Bakhubaira S. Hematological Parameters in Severe Complicated Plasmodium falciparum Malaria among Adults in Aden. Turkish journal of haematology : official journal of Turkish Society of Haematology. 2013;30(4):394-9.
337. Maina RN, Walsh D, Gaddy C, Hongo G, Waitumbi J, Otieno L, et al. Impact of Plasmodium falciparum infection on haematological parameters in children living in Western Kenya. Malar J. 2010;9 Suppl 3(Suppl 3):S4.

338. van Wolfswinkel ME, Vliegenthart-Jongbloed K, de Mendonca Melo M, Wever PC, McCall MB, Koelewijn R, et al. Predictive value of lymphocytopenia and the neutrophil-lymphocyte count ratio for severe imported malaria. Malar J. 2013;12:101.
339. Terlouw DJ, Courval JM, Kolczak MS, Rosenberg OS, Oloo AJ, Kager PA, et al. Treatment History and Treatment Dose Are Important Determinants of Sulfadoxine-Pyrimethamine Efficacy in Children with Uncomplicated Malaria in Western Kenya. The Journal of Infectious Diseases. 2003;187(3):467-76.
340. Terlouw DJ, Nahlen BL, Courval JM, Kariuki SK, Rosenberg OS, Oloo AJ, et al. Sulfadoxine-Pyrimethamine in Treatment of Malaria in Western Kenya: Increasing Resistance and Underdosing. Antimicrob Agents Ch. 2003;47(9):2929-32.
341. Adam I, Tarning J, Lindegardh N, Mahgoub H, McGready R, Nosten F. Pharmacokinetics of piperaquine in pregnant women in Sudan with uncomplicated Plasmodium falciparum malaria. Am J Trop Med Hyg. 2012;87(1):35-40.
342. Dawes M, Chowienczyk PJ. Drugs in pregnancy. Pharmacokinetics in pregnancy. Best practice & research Clinical obstetrics & gynaecology. 2001;15(6):819-26.
343. Little BB. Pharmacokinetics during pregnancy: evidence-based maternal dose formulation. Obstetrics and gynecology. 1999;93(5 Pt 2):858-68.
344. Hariparsad N, Nallani SC, Sane RS, Buckley DJ, Buckley AR, Desai PB. Induction of CYP3A4 by efavirenz in primary human hepatocytes: comparison with rifampin and phenobarbital. J Clin Pharmacol. 2004;44(11):1273-81.
345. Murphy MM, Scott JM, McPartlin JM, Fernandez-Ballart JD. The pregnancy-related decrease in fasting plasma homocysteine is not explained by folic acid supplementation, hemodilution, or a decrease in albumin in a longitudinal study. The American journal of clinical nutrition. 2002;76(3):614-9.
346. El Tahir A, Malhotra P, Chauhan VS. Uptake of proteins and degradation of human serum albumin by Plasmodium falciparum-infected human erythrocytes. Malar J. 2003;2(1):11.
347. Kolakovich KA, Gluzman IY, Duffin KL, Goldberg DE. Generation of hemoglobin peptides in the acidic digestive vacuole of Plasmodium falciparum implicates peptide transport in amino acid production. Molecular and biochemical parasitology. 1997;87(2):123-35.
348. Mansor SM, Molyneux ME, Taylor TE, Ward SA, Wirima JJ, Edwards G. Effect of Plasmodium falciparum malaria infection on the plasma concentration of alpha 1-acid glycoprotein and the binding of quinine in Malawian children. Brit J Clin Pharmaco. 1991;32(3):317-21.
349. Cenni B, Meyer J, Brandt R, Betschart B. The antimalarial drug halofantrine is bound mainly to low and high density lipoproteins in human serum. Brit J Clin Pharmaco. 1995;39(5):519-26.
350. WorldWide Antimalarial Resistance Network Lumefantrine PKPDSG. Artemether-lumefantrine treatment of uncomplicated Plasmodium falciparum malaria: a systematic review and meta-analysis of day 7 lumefantrine concentrations and therapeutic response using individual patient data. Bmc Med. 2015;13:227.
351. Huang L, Parikh S, Rosenthal PJ, Lizak P, Marzan F, Dorsey G, et al. Concomitant efavirenz reduces pharmacokinetic exposure to the antimalarial drug artemether-lumefantrine in healthy volunteers. J Acquir Immune Defic Syndr. 2012;61(3):310-6.
352. Darpo B, Ferber G, Siegl P, Laurijssens B, Macintyre F, Toovey S, et al. Evaluation of the QT effect of a combination of piperaquine and a novel anti-malarial drug candidate OZ439, for the treatment of uncomplicated malaria. Br J Clin Pharmacol. 2015;80(4):706-15.
353. Manning J, Vanachayangkul P, Lon C, Spring M, So M, Sea D, et al. Randomized, double-blind, placebo-controlled clinical trial of a two-day regimen of dihydroartemisinin-piperaquine for malaria prevention halted for concern over prolonged corrected QT interval. Antimicrob Agents Chemother. 2014;58(10):6056-67.
354. Hebert MF, Easterling TR, Kirby B, Carr DB, Buchanan ML, Rutherford T, et al. Effects of pregnancy on CYP3A and P-glycoprotein activities as measured by disposition of midazolam and

digoxin: a University of Washington specialized center of research study. Clinical pharmacology and therapeutics. 2008;84(2):248-53.
355. Hirt D, Treluyer JM, Jullien V, Firtion G, Chappuy H, Rey E, et al. Pregnancy-related effects on nelfinavir-M8 pharmacokinetics: a population study with 133 women. Antimicrob Agents Chemother. 2006;50(6):2079-86.
356. Villani P, Floridia M, Pirillo MF, Cusato M, Tamburrini E, Cavaliere AF, et al. Pharmacokinetics of nelfinavir in HIV-1-infected pregnant and nonpregnant women. Br J Clin Pharmacol. 2006;62(3):309-15.
357. To KW, Liu ST, Cheung SW, Chan DP, Chan RC, Lee SS. Pharmacokinetics of plasma efavirenz and CYP2B6 polymorphism in southern Chinese. Therapeutic drug monitoring. 2009;31(4):527-30.
358. Lang T, Klein K, Fischer J, Nussler AK, Neuhaus P, Hofmann U, et al. Extensive genetic polymorphism in the human CYP2B6 gene with impact on expression and function in human liver. Pharmacogenetics. 2001;11(5):399-415.
359. Haas DW, Gebretsadik T, Mayo G, Menon UN, Acosta EP, Shintani A, et al. Associations between CYP2B6 polymorphisms and pharmacokinetics after a single dose of nevirapine or efavirenz in African americans. J Infect Dis. 2009;199(6):872-80.
360. Bains RK. African variation at Cytochrome P450 genes: Evolutionary aspects and the implications for the treatment of infectious diseases. Evolution, Medicine, and Public Health. 2013;2013(1):118-34.
361. Wanke C, Silva M, Knox T, Forrester J, Speigelman D, Gorbach S. Weight loss and wasting remain common complications in individuals infected with human immunodeficiency virus in the era of highly active antiretroviral therapy. Clinical Infectious Diseases. 2000;31(3):803-5.
362. Ubben D, Poll EM. MMV in partnership: the Eurartesim(R) experience. Malar J. 2013;12(1):211.
363. Moghadam SRJ, Bayrami S, Moghadam SJ, Golrokhi R, Pahlaviani FG, Ahmad S, et al. Zika virus: A review of literature. Asian Pacific Journal of Tropical Biomedicine. 2016;6(12):989-94.
364. Ali A, Wahid B, Rafique S, Idrees M. Advances in research on Zika virus. Asian Pac J Trop Med. 2017;10(4):321-31.
365. World Health Organisation WHO. Zika virus 2018 [Available from: http://www.who.int/news-room/fact-sheets/detail/zika-virus.
366. European Centre for Disease Prevention and Control S. Zika virus disease epidemic: potential association with microcephaly and Guillain-Barré syndrome. (first update) 2016 [Available from: http://ecdc.europa.eu/en/publications/Publications/rapid-risk-assessment-zika-virus-first-update-jan-2016.pdf.
367. (CDC) CfDCaP. Zika Cases in the United States 2018 [Available from: https://www.cdc.gov/zika/reporting/case-counts.html.
368. Petersen E, Wilson ME, Touch S, McCloskey B, Mwaba P, Bates M, et al. Rapid Spread of Zika Virus in The Americas - Implications for Public Health Preparedness for Mass Gatherings at the 2016 Brazil Olympic Games. Int J Infect Dis. 2016;44:11-5.
369. Duffy MR, Chen TH, Hancock WT, Powers AM, Kool JL, Lanciotti RS, et al. Zika Virus Outbreak on Yap Island, Federated States of Micronesia. New Engl J Med. 2009;360(24):2536-43.
370. Ioos S, Mallet HP, Goffart IL, Gauthier V, Cardoso T, Herida M. Current Zika virus epidemiology and recent epidemics. Med Maladies Infect. 2014;44(7):302-7.
371. Olson JG, Ksiazek TG, Suhandiman, Triwibowo. Zika Virus, a Cause of Fever in Central Java, Indonesia. T Roy Soc Trop Med H. 1981;75(3):389-93.
372. Roth A, Mercier A, Lepers C, Hoy D, Duituturaga S, Benyon E, et al. Concurrent outbreaks of dengue, chikungunya and Zika virus infections - an unprecedented epidemic wave of mosquito-borne viruses in the Pacific 2012-2014. Eurosurveillance. 2014;19(41):2-9.
373. Contreras D, Arumugaswami V. Zika Virus Infectious Cell Culture System and the In Vitro Prophylactic Effect of Interferons. Jove-J Vis Exp. 2016(114).

374. Bayer A, Lennemann NJ, Ouyang YS, Bramley JC, Morosky S, Marques ETD, et al. Type III Interferons Produced by Human Placental Trophoblasts Confer Protection against Zika Virus Infection. Cell Host Microbe. 2016;19(5):705-12.
375. Rausch K, Hackett BA, Weinbren NL, Reeder SM, Sadovsky Y, Hunter CA, et al. Screening Bioactives Reveals Nanchangmycin as a Broad Spectrum Antiviral Active against Zika Virus. Cell Rep. 2017;18(3):804-15.
376. Varghese FS, Rausalu K, Hakanen M, Saul S, Kummerer BM, Susi P, et al. Obatoclax Inhibits Alphavirus Membrane Fusion by Neutralizing the Acidic Environment of Endocytic Compartments. Antimicrob Agents Ch. 2017;61(3).
377. Estoppey D, Lee CM, Janoschke M, Lee BH, Wan KF, Dong HP, et al. The Natural Product Cavinafungin Selectively Interferes with Zika and Dengue Virus Replication by Inhibition of the Host Signal Peptidase. Cell Rep. 2017;19(3):451-60.
378. Li CF, Deng YQ, Wang S, Ma F, Aliyari R, Huang XY, et al. 25-Hydroxycholesterol Protects Host against Zika Virus Infection and Its Associated Microcephaly in a Mouse Model. Immunity. 2017;46(3):446-56.
379. Cai L, Sun YJ, Song YB, Xu LK, Bei ZC, Zhang DN, et al. Viral polymerase inhibitors T-705 and T-1105 are potential inhibitors of Zika virus replication. Arch Virol. 2017;162(9):2847-53.
380. Munjal A, Khandia R, Dhama K, Sachan S, Karthik K, Tiwari R, et al. Advances in Developing Therapies to Combat Zika Virus: Current Knowledge and Future Perspectives. Front Microbiol. 2017;8.
381. Delvecchio R, Higa LM, Pezzuto P, Valadao AL, Garcez PP, Monteiro FL, et al. Chloroquine, an Endocytosis Blocking Agent, Inhibits Zika Virus Infection in Different Cell Models. Viruses-Basel. 2016;8(12).
382. Rubin M, Bernstein HN, Zvaifler NJ. Studies on the Pharmacology of Chloroquine. Recommendations for the Treatment of Chloroquine Retinopathy. Arch Ophthalmol. 1963;70:474-81.
383. Gustafsson LL, Walker O, Alvan G, Beermann B, Estevez F, Gleisner L, et al. Disposition of chloroquine in man after single intravenous and oral doses. Br J Clin Pharmacol. 1983;15(4):471-9.
384. Browning DJ. Hydroxychloroquine and chloroquine retinopathy. New York: Springer; 2014. xv, 291 pages p.
385. Tulpule A, Krishnaswamy K. Effect of food on bioavailability of chloroquine. Eur J Clin Pharmacol. 1982;23(3):271-3.
386. Mahmoud BM, Ali HM, Homeida MM, Bennett JL. Significant reduction in chloroquine bioavailability following coadministration with the Sudanese beverages Aradaib, Karkadi and Lemon. J Antimicrob Chemother. 1994;33(5):1005-9.
387. Laaksonen AL, Koskiahde V, Juva K. Dosage of antimalarial drugs for children with juvenile rheumatoid arthritis and systemic lupus erythematosus. A clinical study with determination of serum concentrations of chloroquine and hydroxychloroquine. Scand J Rheumatol. 1974;3(2):103-8.
388. Tett S, Cutler D, Day R. Antimalarials in rheumatic diseases. Baillieres Clin Rheumatol. 1990;4(3):467-89.
389. Walker O, Dawodu AH, Salako LA, Alvan G, Johnson AO. Single dose disposition of chloroquine in kwashiorkor and normal children--evidence for decreased absorption in kwashiorkor. Br J Clin Pharmacol. 1987;23(4):467-72.
390. Titus EO. Recent developments in the understanding of the pharmacokinetics and mechanism of action of chloroquine. Therapeutic drug monitoring. 1989;11(4):369-79.
391. Walker O, Birkett DJ, Alvan G, Gustafsson LL, Sjoqvist F. Characterization of chloroquine plasma protein binding in man. Br J Clin Pharmacol. 1983;15(3):375-7.
392. Verbeeck RK, Junginger HE, Midha KK, Shah VP, Barends DM. Biowaiver monographs for immediate release solid oral dosage forms based on biopharmaceutics classification system (BCS) literature data: chloroquine phosphate, chloroquine sulfate, and chloroquine hydrochloride. J Pharm Sci. 2005;94(7):1389-95.

393. Mwendera C, de Jager C, Longwe H, Phiri K, Hongoro C, Mutero CM. Malaria research and its influence on anti-malarial drug policy in Malawi: a case study. Health Res Policy Sy. 2016;14.
394. Wolfe MS, Cordero JF. Safety of Chloroquine in Chemosuppression of Malaria during Pregnancy. British Medical Journal. 1985;290(6480):1466-7.
395. McGready R, Thwai KL, Cho T, Samuel, Looareesuwan S, White NJ, et al. The effects of quinine and chloroquine antimalarial treatments in the first trimester of pregnancy. Trans R Soc Trop Med Hyg. 2002;96(2):180-4.
396. Nosten F, McGready R, Simpson JA, Thwai KL, Balkan S, Cho T, et al. Effects of Plasmodium vivax malaria in pregnancy. Lancet. 1999;354(9178):546-9.
397. Ke AB, Nallani SC, Zhao P, Rostami-Hodjegan A, Isoherranen N, Unadkat JD. A physiologically based pharmacokinetic model to predict disposition of CYP2D6 and CYP1A2 metabolized drugs in pregnant women. Drug Metab Dispos. 2013;41(4):801-13.
398. Dean M, Stock B, Patterson RJ, Levy G. Serum protein binding of drugs during and after pregnancy in humans. Clinical pharmacology and therapeutics. 1980;28(2):253-61.
399. Hytten FE, Paintin DB. Increase in plasma volume during normal pregnancy. J Obstet Gynaecol Br Emp. 1963;70:402-7.
400. Isoherranen N, Thummel KE. Drug Metabolism and Transport During Pregnancy: How Does Drug Disposition Change during Pregnancy and What Are the Mechanisms that Cause Such Changes? Drug Metabolism and Disposition. 2013;41(2):256-62.
401. Loebstein R, Lalkin A, Koren G. Pharmacokinetic changes during pregnancy and their clinical relevance. Clinical Pharmacokinetics. 1997;33(5):328-43.
402. Pirani BB, Campbell DM, MacGillivray I. Plasma volume in normal first pregnancy. J Obstet Gynaecol Br Commonw. 1973;80(10):884-7.
403. Mzayek F, Deng H, Mather FJ, Wasilevich EC, Liu H, Hadi CM, et al. Randomized dose-ranging controlled trial of AQ-13, a candidate antimalarial, and chloroquine in healthy volunteers. PLoS Clin Trials. 2007;2(1):e6.
404. Gustafsson L, Walker O, Alvan G, Beermann B, Estevez F, Gleisner L, et al. Disposition of chloroquine in man after single intravenous and oral doses. Brit J Clin Pharmaco. 1983;15(4):471-9.
405. Najmi MH, Akhtar MA. Pharmacokinetic profile of chloroquine in healthy pakistani subjects. A Journal of Army Medical & Dental Corps. 2008;58(1).
406. Hoglund R, Moussavi Y, Ruengweerayut R, Cheomung A, Abelo A, Na-Bangchang K. Population pharmacokinetics of a three-day chloroquine treatment in patients with Plasmodium vivax infection on the Thai-Myanmar border. Malar J. 2016;15:129.
407. Karunajeewa HA, Salman S, Mueller I, Baiwog F, Gomorrai S, Law I, et al. Pharmacokinetics of chloroquine and monodesethylchloroquine in pregnancy. Antimicrob Agents Chemother. 2010;54(3):1186-92.
408. Tan-ariya P, Na-Bangchang K, Tin T, Limpaibul L, Brockelman CR, Karbwang J. Clinical response and susceptibility in vitro of Plasmodium vivax to the standard regimen of chloroquine in Thailand. Trans R Soc Trop Med Hyg. 1995;89(4):426-9.
409. Na-Bangchang K, Limpaibul L, Thanavibul A, Tan-Ariya P, Karbwang J. The pharmacokinetics of chloroquine in healthy Thai subjects and patients with Plasmodium vivax malaria. Br J Clin Pharmacol. 1994;38(3):278-81.
410. Chukwuani MC, Bolaji OO, Onyeji CO, Makinde ON, Ogunbona FA. Evidence for increased metabolism of chloroquine during the early third trimester of human pregnancy. Trop Med Int Health. 2004;9(5):601-5.
411. Lee SJ, McGready R, Fernandez C, Stepniewska K, Paw MK, Viladpai-nguen SJ, et al. Chloroquine pharmacokinetics in pregnant and nonpregnant women with vivax malaria. Eur J Clin Pharmacol. 2008;64(10):987-92.
412. Bustos DG, Lazaro JE, Gay F, Pottier A, Laracas CJ, Traore B, et al. Pharmacokinetics of sequential and simultaneous treatment with the combination chloroquine and sulfadoxine-

pyrimethamine in acute uncomplicated Plasmodium falciparum malaria in the Philippines. Trop Med Int Health. 2002;7(7):584-91.
413. Wetsteyn JC, De Vries PJ, Oosterhuis B, Van Boxtel CJ. The pharmacokinetics of three multiple dose regimens of chloroquine: implications for malaria chemoprophylaxis. Br J Clin Pharmacol. 1995;39(6):696-9.
414. Frisk-Holmberg M, Bergqvist Y, Termond E, Domeij-Nyberg B. The single dose kinetics of chloroquine and its major metabolite desethylchloroquine in healthy subjects. Eur J Clin Pharmacol. 1984;26(4):521-30.
415. Fakeye TO, Fehintola FA, Ademowo OG, Walker O. Therapeutic monitoring of chloroquine in pregnant women with malaria. West Afr J Med. 2002;21(4):286-7.
416. Shiryaev SA, Mesci P, Pinto A, Fernandes I, Sheets N, Shresta S, et al. Repurposing of the anti-malaria drug chloroquine for Zika Virus treatment and prophylaxis. Sci Rep. 2017;7(1):15771.
417. Vijaykumar TS, Nath A, Chauhan A. Chloroquine mediated molecular tuning of astrocytes for enhanced permissiveness to HIV infection. Virology. 2008;381(1):1-5.
418. Adelusi SA, Salako LA. Tissue and blood concentrations of chloroquine following chronic administration in the rat. The Journal of pharmacy and pharmacology. 1982;34(11):733-5.
419. Mackenzie A. Dose refinements in long-term therapy of rheumatoid arthritis with antimalarials American Journal of Medicine. 1983;75(1A):40-5.
420. Edginton AN, Schmitt W, Willmann S. Development and evaluation of a generic physiologically based pharmacokinetic model for children. Clinical Pharmacokinetics. 2006;45(10):1013-34.
421. Ginsberg G, Hattis D, Russ A, Sonawane B. Physiologically based pharmacokinetic (PBPK) modeling of caffeine and theophylline in neonates and adults: Implications for assessing children's risks from environmental agents. Journal of Toxicology and Environmental Health-Part a-Current Issues. 2004;67(4):297-329.
422. Parrott N, Davies B, Hoffmann G, Koerner A, Lave T, Prinssen E, et al. Development of a Physiologically Based Model for Oseltamivir and Simulation of Pharmacokinetics in Neonates and Infants. Clinical Pharmacokinetics. 2011;50(9):613-23.
423. Devries PJ, Oosterhuis B, Vanboxtel CJ. Single-Dose Pharmacokinetics of Chloroquine and Its Main Metabolite in Healthy-Volunteers. Drug Invest. 1994;8(3):143-9.
424. Obua C, Ntale M, Lundblad MS, Mahindi M, Gustafsson LL, Ogwal-Okeng JW, et al. Pharmacokinetic interactions between chloroquine, sulfadoxine and pyrimethamine and their bioequivalence in a generic fixed-dose combination in healthy volunteers in Uganda. Afr Health Sci. 2006;6(2):86-92.
425. Krishna S, White NJ. Pharmacokinetics of quinine, chloroquine and amodiaquine. Clinical implications. Clin Pharmacokinet. 1996;30(4):263-99.
426. Projean D, Baune B, Farinotti R, Flinois JP, Beaune P, Taburet AM, et al. In vitro metabolism of chloroquine: identification of CYP2C8, CYP3A4, and CYP2D6 as the main isoforms catalyzing N-desethylchloroquine formation. Drug Metab Dispos. 2003;31(6):748-54.
427. Gustafsson LL, Lindström B, Grahnén A, Alván G. Chloroquine excretion following malaria prophylaxis. Brit J Clin Pharmaco. 1987;24(2):221-4.
428. Walker O, Salako LA, Alvan G, Ericsson O, Sjoqvist F. The disposition of chloroquine in healthy Nigerians after single intravenous and oral doses. Br J Clin Pharmacol. 1987;23(3):295-301.
429. Pellegrini P, Strambi A, Zipoli C, Hagg-Olofsson M, Buoncervello M, Linder S, et al. Acidic extracellular pH neutralizes the autophagy-inhibiting activity of chloroquine: implications for cancer therapies. Autophagy. 2014;10(4):562-71.
430. Warhurst DC, Craig JC, Adagu IS, Meyer DJ, Lee SY. The relationship of physico-chemical properties and structure to the differential antiplasmodial activity of the cinchona alkaloids. Malar J. 2003;2:26.
431. White NJ. Antimalarial pharmacokinetics and treatment regimens. Br J Clin Pharmacol. 1992;34(1):1-10.

432. Moore BR, Page-Sharp M, Stoney JR, Ilett KF, Jago JD, Batty KT. Pharmacokinetics, pharmacodynamics, and allometric scaling of chloroquine in a murine malaria model. Antimicrob Agents Chemother. 2011;55(8):3899-907.
433. Ducharme J, Farinotti R. Clinical pharmacokinetics and metabolism of chloroquine. Focus on recent advancements. Clin Pharmacokinet. 1996;31(4):257-74.
434. Gustafsson L, Walker O, Alvan G, Beermann B, Estevez F, Gleisner L, et al. Disposition of chloroquine in man after single intravenous and oral doses. Br J Clin Pharmacol. 1983;15(4):471-9.
435. Badhan R, Zakaria Z, Olafuyi O. The Repurposing of Ivermectin for Malaria: A Prospective Pharmacokinetics-Based Virtual Clinical Trials Assessment of Dosing Regimen Options. J Pharm Sci. 2018;107(8):2236-50.
436. Zakaria Z, Badhan RKS. The impact of CYP2B6 polymorphisms on the interactions of efavirenz with lumefantrine: Implications for paediatric antimalarial therapy. Eur J Pharm Sci. 2018;119:90-101.
437. . !!! INVALID CITATION !!! (459).
438. Costantine MM. Physiologic and pharmacokinetic changes in pregnancy. Frontiers in Pharmacology. 2014;5:65.
439. Qasqas SA, McPherson C, Frishman WH, Elkayam U. Cardiovascular pharmacotherapeutic considerations during pregnancy and lactation. Cardiology in review. 2004;12(4):201-21.
440. Hayashi M, Ueda Y, Hoshimoto K, Ota Y, Fukasawa I, Sumori K, et al. Changes in urinary excretion of six biochemical parameters in normotensive pregnancy and preeclampsia. American journal of kidney diseases : the official journal of the National Kidney Foundation. 2002;39(2):392-400.
441. Erman A, Neri A, Sharoni R, Rabinov M, Kaplan B, Rosenfeld JB, et al. Enhanced urinary albumin excretion after 35 weeks of gestation and during labour in normal pregnancy. Scandinavian journal of clinical and laboratory investigation. 1992;52(5):409-13.
442. Cheung CK, Lao T, Swaminathan R. Urinary excretion of some proteins and enzymes during normal pregnancy. Clinical chemistry. 1989;35(9):1978-80.
443. Ginsburg H. Should chloroquine be laid to rest? Acta tropica. 2005;96(1):16-23.
444. Wellems TE, Plowe CV. Chloroquine-resistant malaria. The Journal of infectious diseases. 2001;184(6):770-6.
445. Klinger G, Morad Y, Westall CA, Laskin C, Spitzer KA, Koren G, et al. Ocular toxicity and antenatal exposure to chloroquine or hydroxychloroquine for rheumatic diseases. The Lancet. 2001;358(9284):813-4.
446. Rukaria-Kaumbutho RM, Ojwang SBO, Oyieke JB. Resistance to chloroquine therapy in pregnant women with malaria parasitemia. International Journal of Gynecology & Obstetrics. 1996;53(3):235-41.
447. Francois N, Rose M, Umberto dA, Ana B, Francine V, Clara M, et al. Antimalarial Drugs in Pregnancy: A Review. Current Drug Safety. 2006;1(1):1-15.
448. Law I, Ilett KF, Hackett LP, Page-Sharp M, Baiwog F, Gomorrai S, et al. Transfer of chloroquine and desethylchloroquine across the placenta and into milk in Melanesian mothers. Brit J Clin Pharmaco. 2008;65(5):674-9.
449. Akintonwa A, Gbajumo SA, Mabadeje AF. Placental and milk transfer of chloroquine in humans. Therapeutic drug monitoring. 1988;10(2):147-9.
450. Abduljalil K, Johnson TN, Rostami-Hodjegan A. Fetal Physiologically-Based Pharmacokinetic Models: Systems Information on Fetal Biometry and Gross Composition. Clinical Pharmacokinetics. 2018;57(9):1149-71.
451. Virgintino D, Robertson D, Benagiano V, Errede M, Bertossi M, Ambrosi G, et al. Immunogold cytochemistry of the blood–brain barrier glucose transporter GLUT1 and endogenous albumin in the developing human brain11Published on the World Wide Web on 24 August 2000. Developmental Brain Research. 2000;123(1):95-101.

452. Cavaco I, Stromberg-Norklit J, Kaneko A, Msellem MI, Dahoma M, Ribeiro VL, et al. CYP2C8 polymorphism frequencies among malaria patients in Zanzibar. European Journal of Clinical Pharmacology. 2005;61(1):15-8.
453. Mendes MD, Hirt D, Vinot C, Valade E, Lui G, Pressiat C, et al. Prediction of human fetal pharmacokinetics using ex vivo human placenta perfusion studies and physiologically based models. Brit J Clin Pharmaco. 2016;81(4):646-57.
454. Zhang Z, Imperial MZ, Patilea-Vrana GI, Wedagedera J, Gaohua L, Unadkat JD. Development of a Novel Maternal-Fetal Physiologically Based Pharmacokinetic Model I: Insights into Factors that Determine Fetal Drug Exposure through Simulations and Sensitivity Analyses. Drug Metab Dispos. 2017;45(8):920-38.